UILU-ENG-72-2003

CIVIL ENGINEERING STUDIES
STRUCTURAL RESEARCH SERIES NO. 383
Illinois Cooperative Highway Research Program
Series No. 128

EFFECTS OF DIAPHRAGMS IN BRIDGES WITH PRESTRESSED CONCRETE I-SECTION GIRDERS

By
S. SITHICHAIKASEM
W. L. GAMBLE

Issued as a Documentation Report on
The Field Investigation of Prestressed
Reinforced Concrete Highway Bridges
Project IHR-93
Illinois Cooperative Highway Research Program
Phase I

Conducted by

THE STRUCTURAL RESEARCH LABORATORY
DEPARTMENT OF CIVIL ENGINEERING
ENGINEERING EXPERIMENT STATION
UNIVERSITY OF ILLINOIS

in cooperation with

THE STATE OF ILLINOIS
DIVISION OF HIGHWAYS

and

THE U.S. DEPARTMENT OF TRANSPORTATION
FEDERAL HIGHWAY ADMINISTRATION

UNIVERSITY OF ILLINOIS
URBANA, ILLINOIS

FEBRUARY 1972

UILU-ENG-72-2003

EFFECTS OF DIAPHRAGMS IN BRIDGES WITH PRESTRESSED CONCRETE I-SECTION GIRDERS

by

S. Sithichaikasem
W. L. Gamble

Issued as a Documentation Report on
The Field Investigation of Prestressed
Reinforced Concrete Highway Bridges
Project IHR-93
Illinois Cooperative Highway Research Program
Phase I

Conducted by

THE STRUCTURAL RESEARCH LABORATORY
DEPARTMENT OF CIVIL ENGINEERING
ENGINEERING EXPERIMENT STATION
UNIVERSITY OF ILLINOIS

in cooperation with

THE STATE OF ILLINOIS
DIVISION OF HIGHWAYS

and

THE U. S. DEPARTMENT OF TRANSPORTATION
FEDERAL HIGHWAY ADMINISTRATION

UNIVERSITY OF ILLINOIS
URBANA, ILLINOIS
February 1972

ABSTRACT

Sithichaikasem, S. and W. L. Gamble, "Effects of Diaphragms in Bridges with Prestressed Concrete I-Section Girders," Civil Engineering Studies, Structural Research Series No. 383, Department of Civil Engineering, University of Illinois, Urbana, 1971.

Key Words: Highway bridges, Analysis, Influence lines, Beams, Moments, Diaphragms, Truck loadings

The results of a study of the effects of the number, stiffness, and locations of diaphragms in multi-beam, simply supported, right highway bridges is presented. The parameters studied also included the relative girder stiffness, H, the ratio of girder spacing to span, b/a, the girder torsional stiffness, the girder spacing, and the location of the loads relative to the edge girders of the structure. The behavior of the bridges is evaluated for several types of loadings, including single loads and groups of loads.

The bridges studied were divided into three general categories according to the uniformity of load distribution to the girders, and design recommendations regarding diaphragm arrangements and stiffnesses made. In most structures in which the outer line of wheels can fall directly over the edge girders, diaphragms should not be used, as they will increase the controlling moment in the bridge. In other cases, diaphragms may be either helpful or harmful, and criteria are developed for design purposes.

The influence of the number of diaphragms was studied, and the effects of a single midspan diaphragm and two diaphragms located near midspan were about the same, structurally, though the cost effectiveness of the single diaphragm is better.

The current arbitrary practice of determining location and spacing of diaphragms as a function of span length alone should be changed, as many short span bridges which do not include diaphragms could benefit from them, and many longer span structures which normally contain diaphragms either receive no benefit or are harmed by them.

ACKNOWLEDGMENTS

This study was carried out as a part of the research under the Illinois Cooperative Highway Research Program, Project IHR-93, "Field Investigation of Prestressed Reinforced Concrete Highway Bridges." The work on the project was conducted by the Department of Civil Engineering, University of Illinois, in cooperation with Division of Highways, State of Illinois, and the U. S. Department of Transportation, Federal Highway Administration. At the University, the work covered by this report was carried out under the general administrative supervision of D. C. Drucker, Dean of the College of Engineering, Ross J. Martin, Director of the Engineering Experiment Station, N. M. Newmark, Head of the Department of Civil Engineering, and Ellis Danner, Director of the Illinois Cooperative Highway Research Program and Professor of Highway Engineering.

At the Division of Highways of the State of Illinois, the work was under the administrative direction of Richard H. Golterman, Chief Highway Engineer, R. D. Brown, Jr., Deputy Chief Highway Engineer, and J. E. Burke, Engineer of Research and Development.

The program of investigation has been guided by a Project Advisory Committee consisting of the following members:

Representing the Illinois Division of Highways:

J. E. Burke, Engineer of Research and Development

F. K. Jacobsen, Engineer of Bridge Research

C. E. Thunman, Jr., Engineer of Bridge and Traffic Structures, Bureau of Design

Representing the Federal Highway Administration:

Robert J. Deatrick, Assistant Bridge Engineer

Edward L. Tyk, Assistant Bridge Engineer

Representing the University of Illinois:

Narbey Khachaturian, Professor of Civil Engineering

C. P. Siess, Professor of Civil Engineering

Acknowledgment is due to Mr. R. C. Mulvey and Mr. R. Bradford, Illinois Division of Highways, who contributed materially to the guidance and progress of the program.

This investigation is directed by Dr. M. A. Sozen, Professor of Civil Engineering, as Project Supervisor. Immediate supervision of the investigation is provided by Dr. W. L. Gamble, Associate Professor of Civil Engineering, as Project Investigator.

This report has been prepared in cooperation with the U. S. Department of Transportation, Federal Highway Administration.

TABLE OF CONTENTS

Chapter | Page

LIST OF TABLES

LIST OF FIGURES

Chapter 1

INTRODUCTION

1.1 General

A slab and girder highway bridge is a very common type of structure. It consists of concrete roadway slab continuous over a number of flexible girders spanning in the direction of the traffic. The supporting girders may be steel I-beams, precast prestressed concrete or reinforced concrete cast monolithically with the slab. In the current design of precast prestressed concrete girder bridges, I-sections or box sections may be used. Most of the highway bridges in this country have been built with the intermediate diaphragms at different locations. The primary purpose of adding the diaphragms is to improve the distribution of the loads to the supporting girders.

Bridges are classified as noncomposite bridges and composite bridges. In noncomposite bridges, the slab is simply placed on the supporting girders without any connection. There are no mechanical devices to resist slip at the junction of the slab and the girders. On the other hand, in composite bridges, shear connectors, shear stirrups or shear keys are provided at the junction between the slab and the girders to prevent slip.

The design problem which is one of determining how a concentrated load or system of concentrated loads equivalent to the truck loading is distributed among the longitudinal girders of a bridge structure for various bridge geometries, properties of the girders, slab and diaphragms, as well as the locations of loads.

1.2 Previous Studies

The problem of wheel load distribution in slab and girder highway bridges has been studied for decades. Many investigators have tried in the past, with different approaches, to obtain satisfactory solutions to the problem. Various analytical methods have been used both in this country and abroad. Because of the complexity of the solutions, most of the previous studies have simplified the problem by making different assumptions. The advent of the electronic computer has reduced the number of simplifying assumptions which must be made.

There are two schools of thought in dealing with this type of structure. Those theories mentioned above may be classified into these two schools of thought as follows:

1. The first school of thought consists of methods that ignore the presence of the slab and consider the remaining structure to be of the grillage type. Pippard and Waele[1] have used this method by assuming that the transverse members are replaced by a continuous connecting system throughout the span and can resist bending transversely to the bridge without rotation of the longitudinal girders. According to this assumption, the girders have to be very stiff in torsion. Leonhardt[2] has simplified the transverse members by replacing one central beam of equivalent stiffness. The effects of torsion are neglected in this method of analysis. Hendry and Jaeger[3] replaced the transverse members by a uniformly spread medium, which may or may not cover the full length of the span.

2. The second school of thought consists of methods by which plate theory has been applied to the solution of this interconnected structure. Two distinct categories of plate theory have been applied to the slab and girder bridge.

The first category is orthotropic plate theory. In this category the actual system of discrete interconnected beams is replaced by an elastically equivalent system in which the stiffness is uniformly distributed in both directions. That is, the system is replaced by a plate having different flexural rigidities in two orthogonal directions. This theory has been described by Timoshenko.[4] Guyon[5] has applied this theory to the study of slab and girder bridge structure. Torsional stiffness is not included in Guyon's analysis. Massonet[6] has generalized Guyon's analysis by adding the torsional stiffness of the members. Morice and Little[7] have presented the numerical results of Guyon and Massonet in the form of charts.

The second category treats the structure in a more realistic manner by considering the slab to be simply supported on two opposite edges, and continuous over any number and spacing of rigid or flexible simple beams transverse to the simply supported edges. Newmark[8] first developed this method, using a moment distribution procedure. The torsional stiffness of the girders may or may not be taken into account. To simplify the complexity of the in-plane forces, the T-beam action has to be taken into account by modifying the actual stiffness of the supporting beam. By this method, Newmark and Siess[9] made an extensive study of the moments and deflections in steel I-beam bridges. Because of the small torsional stiffness of the steel I-beams and since the electronic computer was not available, the torsional restraint offered by the beams was not included. Newmark, Siess and

Penman[10] conducted laboratory tests on fifteen I-beam bridges. All structures tested were quarter-scale models of simple span right bridges. The results of tests agreed very well with the analysis. The effects of adding the diaphragms, or transverse members, on the moments in the girders have been studied by B. C. F. Wei[11] and by Siess and Veletsos.[12] Their studies have also neglected the torsion and used the distribution procedure developed by Newmark.

With the aid of the electronic computer to solve the complex structures, the investigators in the past decade and currently have been trying to analyze the slab and girder structure by including the in-plane forces as well as the bending forces. Goldberg and Leve[13] have developed a theory of prismatic folded plate structures. Their method of analysis has combined plate theory and two-dimensional theory of elasticity. It can be applied to the problem of bridge structures. Van Horn and Daryoush[14] also have considered plate theory and two-dimensional theory of elasticity in analyzing the problem of load distribution in prestressed concrete box beam bridges. But, the effects of warping and of adding the diaphragms were not included in their analysis.

If the in-plane forces are ignored in the Goldberg and VanHorn methods, and the T-beam action is taken into account by modifying the actual stiffnesses of the supporting girders as in the Newmark method, the Goldberg and Leve, and VanHorn and Daryoush methods will yield the same results as Newmark's method.

There are other techniques to analyze the problem of slab continuous over a number of flexible girders, such as a finite element developed by Gustafson,[15] an energy method by Badaruddin,[16] and others.

1.3 Object and Scope of Investigation

It was mentioned in the preceding section that the analyses of the slab and girder bridge, taking into account the effects of the intermediate diaphragms as well as the torsional stiffness of the girder, are very limited. Many analyses have been applied to particular problems and were not general enough for design purposes. In some analyses, the bridge structures have been simplified so much that the accuracy of the results may be questionable.

Because of its simplicity and economy of construction, the slab and girder bridge with precast prestressed concrete girders, either I-section or box section, has found widespread application in most highways. It has also been found that most of the bridges have been built with intermediate diaphragms. Shear stirrups were provided as shear connectors at the junctions between the slab and the girders for the purpose of insuring composite action. In most cases, the diaphragms were cast monolitically with the slab.

As mentioned previously, Wei's analysis of the effects of diaphragms in steel I-beam bridges has neglected the torsional stiffness of the beam. Neglecting the torsional stiffness of steel I-beam is quite reasonable since the torsional stiffness is very low. The torsional stiffness of a typical prestressed concrete I-beam is much greater than that of a steel beam of the same moment capacity, and the increased stiffness may have some influence on the load distribution in the beam. Increased torsional stiffness should improve the load distribution, and should be taken into account if further study shows a significant influence of the torsional stiffness.

It might be questioned whether the warping stiffness of the current standard precast prestressed concrete I-sections may also affect the load distribution. The warping stiffness is more or less dependent upon the width of the flange of the girder.

Because of the questions about the influence of the torsional stiffness parameters, an investigation of the action of this type of bridge, with the goal of the development of a better design method which is both simple and convenient appeared desirable. Instead of solving any particular problem, the main purpose of this study is to analyze a large number of bridges with the aid of the electronic computer. All essential parameters concerning the load distribution behavior are included. The span of the bridges may be varied from 25 ft to about 150 ft which are the practical range of span for this type of structure.

The behavior of the structure when the diaphragms are added is also investigated to determine whether the distribution of the loads among the supporting girders is improved. If the diaphragms do improve the load distribution, the required properties, the best location of diaphragms, the state of stress in the diaphragms must be determined. The results of this study will provide either the basis for a rational design procedure for diaphragms or for their omission.

According to the objectives mentioned above, the scope of the studies may be drawn as follows:

For a concentrated load moving on the bridges:

1. To compare the results of the present analysis to that of Newmark's moment distribution method;

2. To compute the influence coefficients for moments and deflections of the girders at various locations along the span;
3. To study the effects of varying the parameters introduced in Chapter 2 on the moments produced in the girders;
4. To compare the load distributions of a five-girder bridge and a six-girder bridge;
5. To compare the load distribution among a composite steel I-beam bridge and composite prestressed concrete bridges for both I-sections and box sections;
6. To study the effects of adding the diaphragms by varying the number as well as their locations on the girder moments.

For 4-wheel loads moving on the bridges

1. To compute the influence coefficients for maximum moments at midspan and coefficients for moment envelopes in the various girders for five-girder bridges with and without diaphragms. The spacings among the wheels are specified by AASHO;[17]
2. To compare the influence coefficients for maximum moments at midspan and moment envelopes of the composite prestressed concrete girders with I-section and box section;
3. To determine the effects of varying the parameters introduced in Chapter 2 on the influence coefficients for maximum moments at midspan and moment envelopes.

This study considers only the simple span right bridges. Typical cross-sections of the bridges are shown in Fig. 1.1.

1.4 Notation

The following notation is used throughout this study. The longitudinal direction is always taken as the direction of the girders.

A	cross-sectional area of the modified girder, the cross-section of the girder plus the slab which has a width equal to the width of the top flange
A, B, C, etc.	symbols to be used to indicate the girders or points on the slab directly over the girders as shown in Figs. 1.2 and 1.3
AB, BC, etc.	symbols to be used to indicate the longitudinal centerline of a panel of the slab as shown in Figs. 1.2 and 1.3
B^D	submatrix in the flexibility matrix of diaphragms, F_D
$B_{1,1}$, $B_{1,2}$, etc.	submatrices in the flexibility matrix of the bridge, F_B, relative to line o-o, Fig. 4.3
$B'_{1,1}$, $B'_{1,2}$, etc.	submatrices in the flexibility matrix of the bridge, F'_B, relative to line o'-o', Fig. 4.3
C	warping constant of the girder
C_G	flexibility matrix for girder due to moment
C_M	coefficient for bending moment in girder with a composite slab

C_1, C_2, etc.	flexibility coefficients of the girder due to moments
D	$\frac{E_s I_s}{1-\mu^2}$ = stiffness of an element of the slab
E_d	modulus of elasticity of the material in the diaphragm
E_g	modulus of elasticity of the material in the girder
E_s	modulus of elasticity of the material in the slab
F_B, F_D, F_G, F_S	flexibility matrices for bridge, diaphragm, girder, and slab, respectively
F_J	number of joint forces
F_x, F_y, F_z	internal forces of the modified girders in the directions x, y, and z, respectively
F_{cz}	vertical shear of girders with a composite slab
F_{rn}, F_{rf}, etc.	flexibility coefficients for a slab element
F_{11}, F_{12}, etc.	flexibility coefficients for a girder element
G	shear modulus of the material in the girder
H	$\frac{E_g I_g}{aD}$ = a dimensionless parameter which is a measure of the stiffness of the girder with a composite slab relative to that of the slab
I_d	moment of inertia of the cross section of the diaphragm
I_g	moment of inertia of the cross section of the girder with a composite slab

I_s — $\frac{h^3}{12}$ = moment of inertia per unit of width of the cross section of the slab

I_y, I_z, I_{yz} — moments of inertia and product of inertia of the modified girder cross section about y, z, and y-z axes

I_{my}, I_{mz}, I_{mo} — modified moments of inertia and product of inertia of the modified girder cross section about y, z, and y-z axes

J — torsional constant of the modified cross section of the girder

K_D — $2N_DN_G$ = order of matrices F_B, F_B', etc.

K_G — $2N_G$ = order of submatrices B^D, B_{11}, B_{12}', etc.

L_B, L_G, L_S — flexibility matrices of bridge, girder, and slab, respectively, due to external load

L_1, L_2, etc. — flexibility coefficients for girder due to external load

M, M_l, M_r — transverse bending moment per unit of length at the connection joints between slabs and girders, and at the left and right edge of slab and girder, respectively

M_m, M_{1m}, N_m, etc. — coefficients of $\sin \frac{m\pi x}{a}$ or of $\cos \frac{m\pi x}{a}$ in the expressions for M, M_1, N, etc., when M, M_1, N, etc., vary as the ordinates to a sine or cosine curve

M_d, M_{ig} — concentrated moment acting on the girder due to the diaphragms

M_x, M_y, M_{xy} — bending and twisting moments of an element of slab, positive directions shown in Fig. 1.4

M_x, M_y, M_z — twisting, bending, and lateral bending, moments of the modified girder as shown in Fig. 3.8

M_{cx}, M_{cy} — twisting and bending moments of the girder with a composite slab

N, N_l, N_r — in-plane forces per unit of length in the y-direction acting in a manner similar to M, M_l, and M_r

N_D, N_G, N_J, N_s — number of diaphragms, girders, joints, and slabs

N_E, N_U — force matrices

$\overline{N}$ — normal of the boundary force, positive as shown in Fig. 1.6

P — concentrated load applied vertically to the bridge

Q — $\frac{\pi^2 E_g C}{a^2 GJ}$ = a dimensionless parameter which is a measure of the warping stiffness to the torsional stiffness of the modified girder

R, R_l, R_r — vertical reactions per unit of length acting in a manner similar to M, M_l, and M_r

S, S_l, S_r — in-plane shearing forces per unit of length in the x-direction, acting in a manner similar to M, M_l, and M_r

T — $\frac{GJ}{E_g I_g}$ = a dimensionless parameter which is a measure of the torsional stiffness to the flexural stiffness of the modified girder

V_{ig}	reaction forces caused by diaphragms
W_B, W_D, W_G, W_S	displacement matrices of bridge, diaphragms, girder, and slab, respectively
$\overline{X}$	boundary force per unit area in the x-direction, positive as shown in Fig. 1.6
$\overline{Y}$	boundary force per unit area in the y-direction, positive as shown in Fig. 1.6
a	span length of bridge, center to center of supports
b	transverse spacing of girders; distance center to center of girders
b_t	width of the top flange of the girder
b_b	width of the bottom flange of the girder
c	clear spacing of girders; distances between the edges of the top flanges of girders
d	depth of the girder
d'	distance between mid-depths of the top and the bottom flanges of the cross section of the modified girder
h	thickness of the slab
h_o, h_s	distances from the mid-depth of the slab to the centroid and shear center of the modified girder, respectively
l	left edge of the typical slab and girder, and the direction cosine of the normal $\overline{N}$ with respect to x-axis

m	an integer designating the Fourier series term and the direction cosine of the normal $\overline{N}$ with respect to y-axis
m_t	distributed moment equivalent to the moment M_d
p	equivalent line load per unit of length
p_m, u_m, u_{1m}, etc.	coefficients of $\sin \frac{m\pi x}{a}$ or of $\cos \frac{m\pi x}{a}$ in the expressions for p, u, u_1, etc., when p, u, u_1, etc., vary as the ordinates to a sine or cosine curve
r	right edge of the typical slab and the top flange of the girder
t_b, t_t, t_w	thicknesses of the bottom flange, top flange, and web of the idealized corss section of the girder
u, u_1, u_r	in-plane displacements in the x-direction which correspond to forces S, S_1, and S_r, respectively
v, v_1, v_r	in-plane displacements in the y-direction which correspond to forces N, N_1, and N_r, respectively
w, w_1, w_r	deflections which correspond to reactions R, R_1, and R_r, respectively
x, y, z	coordinate axes. The origin is always at a simply supported edge of the slab and girder. The x-axis is always parallel to the span length, and the y-axis is parallel to the pair of simply supported edges. The positive direction of the z-axis is downward
x_d	coordinate along the x-axis of the diaphragm and also the moment caused by the diaphragm

x_p, y_p	coordinates x and y of the concentrated load, P
y_l, y_r	value of y for the left and right edges of the top flange of girder, respectively
y_s, z_s	values of y and z for the shear center of the cross section of the modified girder
$\Delta_{i,g}$, $\theta_{i,g}$	deflections and rotations at the points of intersection of diaphragms and girders, measured from line o-o shown in Fig. 4.3
$\Delta'_{i,g}$, $\theta'_{i,g}$	deflections and rotations at the points of intersection of diaphragms and girders, measured from line o'-o' shown in Fig. 4.3
θ, θ_l, θ_r	rotations which correspond to the transverse moments, M, M_l, and M_r, respectively
θ_m, θ_{lm}, etc	coefficients of $\sin \frac{m\pi x}{a}$ or of $\cos \frac{m\pi x}{a}$ in the expressions for θ, θ_l, etc., when θ, θ_l, etc., vary as the ordinates to a sine or cosine curve
β	angle of twist
Φ	Airy stress function
κ	$\frac{E_d I_d}{E_g I_g}$ = a dimensionless parameter which is a measure of the stiffness of the diaphragm relative to that of the girder
μ	Poisson's ratio of lateral contraction for the material in the slab and girder (for concrete μ is taken equal to 0.15)

$\frac{1}{\rho_y}, \frac{1}{\rho_z}$	curvatures in the y and z directions, respectively
$\sigma_x, \sigma_y, \tau_{xy}$	unit stresses in the x and y directions, and unit shearing stress of an element of slab, respectively, positive directions as shown in Fig. 1.5
$\varepsilon_x, \varepsilon_y, \gamma_{xy}$	unit strains and shearing strain which correspond to unit stresses σ_x, σ_y and shearing stress τ_{xy}, respectively
α_m	$\frac{m\pi}{a}$
β_m	$\frac{m\pi c}{a}$
γ_m	$\frac{m\pi y_p}{a}$
γ_m'	$\frac{m\pi(c-y_p)}{a}$

Chapter 2

STUDY OF THE PARAMETERS AND IDEALIZATION OF THE BRIDGE

2.1 Idealization of the Bridge and Its Components

In the analysis, the actual structures with their cross sections shown in Fig. 1.1 are replaced by an idealized section as shown in Fig. 1.2. The spacing of the girders and the span length are not changed.

The series of standard cross sections for prestressed concrete girders developed by the Bureau of Public Roads has been used for the analysis. This series is composed of eleven sections which are described in "Concrete Information," Portland Cement Association.[18] It would possibly satisfy a wide range of load conditions for spans varying from 30 ft to 150 ft. For obtaining the torsional constants of the girders of the composite prestressed concrete bridges, the actual cross section of the girders are idealized as shown in Fig. 2.7. The width of top and bottom flange, the thickness of web, the depth, the moment of inertia, and position of centroid of the idealized cross sections are identical to the actual cross sections.

2.2 Study of Parameters

The parameters to be considered in the analysis are listed in this section and typical ranges of their values are discussed in Sec. 2.3. These parameters, which describe the bridge structure, may be classified as dimensioned parameters and dimensionless parameters.

Dimensioned parameters are:

1. Material property, modulus of elasticity, E;
2. Thickness of the slab, h, and stiffness of the slab, D;
3. Spacing of girders, b;
4. Span length of the bridge, a.

Dimensionless parameters are:

1. Relative dimension of the bridge, ratio of the girder spacing to span length, b/a;
2. Relative flexural stiffness of the girder to that of the slab, H;
3. Relative torsional stiffness to flexural stiffness of the girder, T;
4. Relative warping stiffness to torsional stiffness of the girder, Q;
5. Relative flexural stiffness of the diaphragm to that of the girder, κ;
6. Number of diaphragms and their relative locations;
7. Poisson's ratio, μ.

2.3 Dimensioned Parameters

Each of the dimension parameters is studied and discussed as follows:

2.3.1 Material Property

In the slab and prestressed concrete girder bridges, the dimensioned material property used in the analysis is the modulus of elasticity

of concrete. The specified strength of the concrete in the slab given in many specifications is less than that of the girder. Consequently, the modulus of elasticity of the slab concrete, E_s, is taken from 0.6 to 0.8 of that of the girder concrete, E_g.

The test bridge at Tuscola, Illinois,[19] has been designed with the strength of the slab concrete of 3500 psi and strength of the girder concrete of 5000 psi. The modulus of elasticity of slab concrete, E_s, is taken as 0.8 E_g. But the actual values of the modulus of elasticity from test cylinders given in Table 2.1 show that the modulus of elasticity of slab concrete, E_s, is higher than that for girder concrete. Because of the uncertainty of the property of concrete and in order to simplify the problem, the modulus of elasticity of slab concrete is assumed to be equal to that of the girder and equal to 4,000,000 psi.

2.3.2 Thickness of the Slab, h, and Stiffness of the Slab, D

In the slab and girder bridge structure, the major factor in determining the distribution of the loads to the supporting girders is the flexural stiffness of the slab, D, which will be discussed in Sec. 2.4.2 and may be stated as follows:

$$D = \frac{E_s h^3}{12(1-\mu^2)} \qquad (2.1)$$

In order to obtain the stiffness, D, the thickness of the slab, h, has to be determined. From practical and economical considerations in designing the slab, the variations of the thickness of the slab from 5 in. to 8 in. have been used by most highway engineers. But some degree of uncertainty always exists regarding the reinforced concrete slab, such as cracks which

may reduce its actual thickness or the flexural stiffness while the reinforcement in the slab may increase its stiffness, depending upon the percentage of the reinforcement. However, Newmark and Siess[10] have carried out extensive tests of scale-model bridges. The results of the tests show that the gross section of the slab may be used for computing the stiffness of the slab. It provides simplicity and convenience in computing the stiffness, D.

2.3.3 Spacing of the Girders, b

The spacing of the girders affects the load distribution to the supporting girders. Also, from the economical and practical standpoints, the girder spacings in this type of bridge structure are varied from about 5 ft to 8 ft. However, in prestressed concrete girder bridges, the span lengths may be quite large and the corresponding widths of the top flanges of the girders may be as large as 3 ft to 4 ft. In this analysis, the spacing of girders is taken from 5 ft to 9 ft. It is also suited to the box section bridges.

2.3.4 Span Length of the Bridge, a

In any structures subjected to bending, the moment is a direct function of the span length. The girders in the bridge structure are subjected to not only the bending but also the combination of the torsion and warping as well. The influence of warping is a function of the span length, a. However, the results of the analysis which will be discussed in Chapter 5 show that the effect of warping for the standard prestressed concrete I-section is negligible. In the analysis within the practical range of b/a,

the span length may be varied from 25 ft to 180 ft which is the reasonable range for this type of bridge having prismatic girders.

2.4 Dimensionless Parameters

It has been mentioned previously that Newmark and Siess,[9] Wei,[11] and others at the University of Illinois have carried on extensive studies of the slab and girder bridges. The influence of the following dimensionless parameters on the load distribution have also been investigated, but their investigations are limited to the steel I-beam bridges and torsional restraint has been neglected. In this analysis, these parameters are considered and cover the range of prestressed concrete girders.

2.4.1 The Relative Dimension of the Bridge, b/a

The relative dimension of the bridge, b/a, is the ratio of the girder spacing to the span length of the bridge. From considerations of economy and stresses in the slab, the spacing of the girders ranges from 5 ft to 9 ft. Consequently, the smaller value of this parameter corresponds to the longer span of the bridge. The range of the ratio to be considered in the analysis is varied from 0.20 to 0.05, as shown in Table 2.2. The corresponding span of the bridge may vary from 25 ft to 180 ft which is adequate for the purpose of this type of bridge. However, the most common ratio being used in the interstate highway is equal to approximately 0.10. For example, two precast prestressed concrete girder bridges in the state of Illinois are under field investigations. The first bridge is in Jefferson County[20] which has the girder spacing 6.5 ft and span length 72 ft, and the ratio, b/a = 0.09. The second bridge is in Douglas County,[19] which

has the girder spacing 7.2 ft and the span length 72.5 ft, and the ratio, b/a = 0.10.

A detailed discussion of the effects of the b/a ratio will be presented in Chapter 5. However, a basic understanding of the effects of this parameter can be obtained from the following explanation. Assume a slab and girder bridge in which except for the spacing of the girders, all properties are kept constant. If a concentrated load is applied to this brdige, one would expect that a better load distribution would correspond to a smaller girder spacing or ratio , b/a, or reduction of the total width of the bridge. The extreme case is reached when the slab is diminished to zero width. In the case the whole bridge will act like a single beam.

2.4.2 The Relative Flexural Stiffness Parameter, H

The relative flexural stiffness parameter, H, is the ratio of the flexural stiffness of the girder to the flexural stiffness of the slab having a width equal to the span length of the bridge.

$$H = \frac{E_g I_g}{aD} \tag{2.2}$$

So, large value of H corresponds to a stiffer girder. On the other hand, a smaller value of H corresponds to a stiffer slab.

For simplicity in computing the flexural stiffness of the girder, a width of the slab equal to the spacing of the girders measured center to center of the girders is considered to be effective in composite action, and the composite section stiffness is used in computing H. The reasonable range of H values has been studied using the series of eleven sections of precast prestressed concrete I-section developed by the Bureau of Public

Roads. With the range of the parameter b/a varied from 0.20 to 0.05, the corresponding values of H may be varied from 5 to 40 as shown in Table 2.2. This range of H can cover the span length from 25 ft to about 150 ft. The smaller values of H correspond to the larger values of b/a or shorter spans. The reverse is true for the larger values of H which correspond to the longer spans or the smaller values of b/a.

The details of the discussion about the effects of this parameter will be given in Chapter 5. However, a brief explanation concerning the load distribution behavior is presented for the basic understanding. Suppose two five-girder bridges have the same properties, except that the slab of the first bridge is infinitely stiff, or H equal to 0, while the second bridge has rigid girders, or H equal to ∞. If a concentrated load, P, is applied at midspan of the center girder of these two bridges, the former will undergo uniform displacement across the section of the bridge, while the latter will not be subject to any displacement. Consequently, the load, P, is uniformly distributed among the supporting girders for the first bridge, but it is supported entirely by the center girder for the second bridge.

2.4.3 The Relative Torsional Stiffness Parameter, T

The relative torsional stiffness parameter, T, is the ratio of the torsional stiffness of the girder with the modified cross section to the flexural stiffness of the girder with a composite slab.

$$T = \frac{GJ}{E_g I_g} \tag{2.3}$$

In order to obtain the torsional stiffness of the girder of the composite

prestressed concrete I-section bridge, the actual cross section of the girder is idealized as shown in Figs. 2.1 and 2.3. The torsional constant, J, is computed from two rectangular flanges and a rectangular web, then summing up:

$$J = k_1 b_t (h + t_t)^3 + k_2 b_b t_b^3 + k_3 d' t_w^3 \qquad (2.4)$$

where k_1, k_2, and k_3 are St. Venant torsional coefficients.[21]

The various values of T in Table 2.2 are actual values which correspond to those bridges. The values of T in Table 2.3 were changed, while keeping other properties constant, in order to study the effects of torsional stoffness on the load distribution. It is observed that the values of the torsional stiffness, T, in Table 2.2 vary from 0.029, which corresponds to girder No. 1 of the standard I-sections developed by BPR,[18] to 0.008, which corresponds to girder No. 11.

Physically, it would be expected that the effect of introducing the torsional restraints to the girders is the same as the effect produced by increasing the flexural stiffness of the slab. If a concentrated load is applied on the bridge, the structure tends to rotate under the load. But girders possessing torsional stiffness will try to resist rotation which leads to increased load transfer to other girders. A large degree of torsional restraint will give a better load distribution.

2.4.4 The Relative Warping Stiffness Parameter, Q

The parameter, Q, defined by the ratio of the warping rigidity of the girder to the product of the square of the span of the bridge and the torsional rigidity of the girder:

$$Q = \frac{\pi^2 E_g C}{a^2 GJ} \tag{2.5}$$

where C is the warping constant of the girder and computed[22] as follows:

$$C = \frac{(d')^2 I_t I_b}{I_t + I_b} \tag{2.6}$$

where

d' = distance between mid-depths of top and bottom flanges (see Fig. 2.3)

I_t, I_b = moment of inertia of top flange and bottom flange, respectively, about axis z-z (see Fig. 2.3)

The warping stiffness parameters of the standard prestressed concrete I-section are given in Table 1.2. The variation is in the range of approximately 0.01 to 0.04. In order to study the effect of the warping stiffness of this type of girder on the load distribution, the series of warping stiffnesses shown in Table 2.3 has been studied.

2.4.5 The Relative Flexural Stiffness of Diaphragm, κ

A major objective of this study is to investigate the load distribution behavior of the slab and girder bridge with composite prestressed concrete I-section girder when diaphragms are added at different locations along the span. The degree of change in load distribution behavior also depends on the flexural stiffness of diaphragms and this should be taken into consideration.

The relative flexural stiffness of diaphragm, κ, is the ratio of flexural stiffness of diaphragm to that of the girder.

$$\kappa = \frac{E_d I_d}{E_g I_g} \tag{2.7}$$

In the analyses, the effects of adding the diaphragms to the seven structures shown in Table 2.4 are studied. These may be divided into two groups. The first group consists of four bridges having the same ratio of b/a but with the ratio H ranging from 5 to 40. The second group also consists of four bridges with constant ratio, H, while varying the parameter b/a from 0.05 to 0.20. Except for the bridge with b/a = 0.10 and H = 20, all bridges have been studied with four variations of the properties of diaphragms. Most of the highway bridges have been built with the parameters b/a close to 0.10 and the parameter H about 20. Thus, this particular bridge was analyzed with seven variations of the diaphragm properties.

2.4.6 Number of Diaphragms and Their Relative Locations

It has been mentioned in Sec. 2.4.5 that four diaphragm stiffness parameters have been studied for each bridge except the one with b/a = 0.10, H = 20, which included seven diaphragm stiffness parameters. The number of diaphragms and their locations may also affect the load distribution of the bridge structure. The relative location of diaphragm is the ratio of coordinate of diaphragms to the span length, x_d/a. So, for each property of diaphragm, there are five combinations of number and locations of diaphragms, as shown in Table 2.5. For example, the first case is one diaphragm at midspan, and the last is three diaphragms, two at quarter-points plus one at midspan.

2.4.7 Poisson's Ratio, μ

Poisson's ratio, $\mu = 0.15$ has been used for both girder concrete and slab concrete throughout the analysis.

Chapter 3

METHOD OF ANALYSIS

3.1 General

It has been mentioned in the previous studies that the second category of the plate theory treated the structures in a more realistic manner. In this category, the rectangular slab is assumed to be simply supported on two opposite edges and continuous over a number of flexible girders transverse to the simply supported edges. Several methods have been used to obtain solutions of this type of bridge structure, such as Fourier series, finite-element, finite-difference and energy methods. The Fourier series type method was first applied to this type of structure by Newmark[8] who developed the distribution procedure. Newmark and Siess,[9] Wei,[11] and others at the University of Illinois used the moment distribution procedure to analyze a large number of bridges so that the conventional design method for truck load distribution was developed. Goldberg and Leve[13] also used the Fourier series solution to introduce the in-plane forces, from plane stress theory of elasticity to the plate theory as used in prismatic folded plate structures. Recently, the idea of introducing the in-plane forces to the plate theory has been used in the spaced box girder bridges by VanHorn and Daryoush[14] so that the approximate modified girder stiffness, used in Newmark's method, does not have to be made. However, the effects due to warping and of adding the diaphragms were not taken into account in VanHorn's analysis.

The present method of analysis is derived from the existing Fourier

series methods developed by previous investigators. The effects of warping and of diaphragms have been added to the analysis method.

3.2 Basic Assumptions

The assumptions being made in this analysis are those for the ordinary theory of flexure and theory of elasticity for slabs plus:

1. The end diaphragms are rigid so that no displacements are permitted in their own planes, but the diaphragms are free to rotate in the direction normal to these planes;
2. Adequate shear connectors are provided to insure the full composite action between the slab and the girders;
3. The spacings of the girders are equal; and
4. Shear deformations of the girders and diaphragms are negligible.

3.3 Basis of Method of Analysis

The Fourier series solution is based on a resolution of the loading applied to the slab into components, each of which can be handled separately in the flexibility method of analysis. The effects of the total load are found by superposition of the effects of the component loadings, which are computed from the equations derived by means of the ordinary theory of flexure and theory of elasticity for slabs.

Consider the bridge structure shown in Fig. 3.1, with span "a" in the x-direction and with the two simply supported edges parallel to the y-axis. The direction of the z-axis is downward. The bridge structure consists of slab and girder elements which are connected along the joint lines.

When the bridge is loaded, joint forces are produced along the joint lines. Each joint force can be resolved into four components as shown in Fig. 3.2, namely, vertical reaction, R; transverse moment, M; force acting normal to the plane of the edge, N; and force acting along the plane of the edge of the elements, S.

Let

N_G = number of girder elements

N_S = number of slab elements

N_J = number of connection joints of the bridge

F_J = number of joint forces

So

$$N_S = N_G - 1$$

$$N_J = 2(N_G - 1) \tag{3.1}$$

$$F_J = 8(N_G - 1)$$

Since there are two free joints on the outer edges of the exterior girders, the number of connection joints is $2(N_G-1)$ instead of $2N_G$. Elements and joints are numbered as shown in Fig. 3.1

The analysis of the slab and girder elements is described in the next four sections. Sections 3.4, 3.5, and 3.6 describe the ordinary theory of flexure and plane stress theory of elasticity of slabs. The analysis of the girder is presented in Sec. 3.7. The analysis of the bridge, by connecting the slab and girder elements together so that the compatibility exists along the joint lines, is described in Sec. 3.8.

3.4 The Ordinary Theory of Flexure of the Slab

Two of the four components of the joint forces along the connected edges of the slabs, the vertical reaction, R, and the edge moment, M, and the transverse external load are treated in the ordinary theory of flexure of slab.

In the Fourier series method, the load is resolved into an infinite number of terms of the sine series. Each term of the series can be handled separately. The effect of the total load is found by superposition of the effects of the sine components of loading. The number of terms of the series evaluated is limited to a finite number, depending on the accuracy required for each particular case.

A typical slab element of the bridge shown in Fig. 3.3 has the span "a" in the x-direction and the two edges parallel to the y-axis are simply supported. The other two edges, which are connected to the girders, are supported or restrained in some manner depending on the properties of the slab and the girders. The deflection of this slab may be given by the equation:

$$w = Y_m \sin \frac{m\pi x}{a} \tag{3.2}$$

in which Y_m is a function of $\frac{m\pi y}{a}$, and consequently is a function of y only. With the notation $\alpha_m = \frac{m\pi}{a}$, Eq. 3.2 may be written as

$$w = Y_m \sin \alpha_m x \tag{3.3}$$

The moments, shears, reactions, and the loading found from the ordinary theory of flexure of the slab, which are in terms of the derivatives of the deflection, w, are stated in Sec. A.1 of Appendix A. By applying Eq. 3.3, these fundamental relationships may be stated in terms of Y_m and

the derivatives of Y_m, which are functions of $\alpha_m y$, multiplied by sin $\alpha_m x$ or cos $\alpha_m x$, and are presented in Sec. A.2 of Appendix A.

It is noted that the slope in the y-direction, θ_y, the bending moments per unit of length, M_x and M_y, the shears and reactions per unit of length acting on the edges perpendicular to the y-axis, V_y and R_y, and the load p, are all the same form as w and involve a function of y only, multiplied by a sine curve in the x-direction; and the twisting moment, M_{xy}, and the shears and reactions, V_x and R_x, involve a function of y only, multiplied by a cosine curve in the x-direction.

Thus, a transverse load on the slab may be replaced by the same form as Eq. 3.3

$$p = p_m \sin \alpha_m x \tag{3.4}$$

where p_m is a function of y only or a trigonometric function itself. The total load p may be expressed in the form of the trigonometric series

$$p = \sum_{m=1}^{\infty} p_m \sin \frac{m\pi x}{a} \tag{3.5}$$

For the truck load problem, each wheel load may be considered a concentrated load of magnitude P. The coordinates of P in the x-axis and y-axis are x_p and y_p, respectively. The value of p_m for the concentrated load is given by the equation

$$p_m = \frac{2P}{a} \sin \frac{m\pi x_p}{a} \tag{3.6}$$

When the transverse load is applied on the bridge, reactions and moments as well as deflections and rotations are developed along the two edges l and r, which are connected to the girders. As mentioned above, these reactions, moments, deflections and rotations can be given in the form

of a function of y only multiplied by a sine curve with a half wavelength in the x-direction as shown in Fig. 3.4.

$$R = \sum_{m=1}^{\infty} R_m \sin \alpha_m x \tag{3.7}$$

$$M = \sum_{m=1}^{\infty} M_m \sin \alpha_m x \tag{3.8}$$

3.4.1 Flexibility Constants for a Rectangular Slab

Consider the slab shown in Fig. 3.4(a) with two opposite edges simply supported, The other two edges, 1 and r, are subjected to the edge reactions, R, and edge moment, M. Their magnitudes are given by the relationships:

At edge r

$$R_r = R_{rm} \sin \alpha_m x$$

$$M_r = M_{rm} \sin \alpha_m x \tag{3.9}$$

At edge 1

$$R_1 = R_{1m} \sin \alpha_m x$$

$$M_1 = M_{1m} \sin \alpha_m x \tag{3.10}$$

The positive directions of the edge reactions, R, and the edge moments, M, are shown in Fig. 3.4(b). The positive directions of the edge deflections, w, and the edge rotations, θ, are shown in Fig. 3.4(c).

The edge deflections and the edge rotations caused by each component of the edge forces are determined separately as follows:

Let the edge r be subjected to a reaction whose magnitude is given by Eq. 3.9. The edge displacements of a cross section of the slab parallel to the simply supported edges are shown in Fig. 3.5(a). The deflections of the edges, r and l, are distributed as sine curves and may be written as:

$$w_r = F_{rn} R_r$$

$$w_l = F_{rf} R_r \tag{3.11}$$

where F_{rn} and F_{rf} are the shear flexibility coefficients for the slab at the near edge and the far edge, respectively. The slopes of the edges r and l are also distributed as sine curves and may be written as:

$$\theta_r = F_{cn} R_r$$

$$\theta_l = F_{cf} R_r \tag{3.12}$$

where F_{cn} and F_{cf} are flexure-shear flexibility coefficients for the slab at the near edge and the far edge, respectively. The shear and flexure-shear flexibility coefficients are given by Eq. A.25, Appendix A.

Now let the edge r be subjected to a moment whose magnitude is given by Eq. 3.9. The edge displacements of a cross section of the slab parallel to the simply supported edges are shown in Fig. 3.5(b). The rotations of the edges r and l are distributed as sine curves and may be written as:

$$\theta_r = -F_{mn} M_r$$

$$\theta_l = -F_{mf} M_r \tag{3.13}$$

where F_{mn} and F_{mf} are the flexure flexibility coefficients for the slab at the near edge and the far edge, respectively. The deflections of these two edges are also distributed as sine curves as stated below:

$$w_r = -F_{cn} M_r$$
$$w_1 = F_{cf} M_r \qquad (3.14)$$

where the terms F_{cn} and F_{cf} are the same as in Eq. 3.12, as should be evident from Maxwell's theorem of reciprocal deflection. The flexibility coefficients are given by Eq. A.31, Appendix A.

It is obvious that the flexibility coefficients for the edge displacements due to the reaction, R_1, acting at the edge 1 are the same quantities found from the reaction, R_r, acting at the edge r, taking into account the sign conventions. The displacements may be written as follows:

Deflections:

$$w_1 = -F_{rn} R_1$$
$$w_r = -F_{rf} R_1 \qquad (3.15)$$

Rotations:

$$\theta_1 = F_{cn} R_1$$
$$\theta_r = F_{cf} R_1 \qquad (3.16)$$

The terms F_{rn} and F_{rf} in Eq. 3.15 are the same as Eq. 3.11, and the terms F_{cn} and F_{cf} in Eq. 3.16 are the same as Eq. 3.12. The minus signs are from the sign conventions.

Similarly, the edge displacements due to the edge moment, M_1, acting on the edge 1 can be written as follows:

Deflections:

$$w_1 = -F_{cn} M_1$$

$$w_r = F_{cf} M_1 \tag{3.17}$$

Rotations:

$$\theta_1 = F_{mn} M_1$$

$$\theta_r = F_{mf} M_1 \tag{3.18}$$

3.4.2 Flexibility Constants for a Rectangular Slab Subjected to a Concentrated Load

The edge displacements of the slab, shown in Fig. 3.3, due to a wheel load which is considered as a concentrated load, can be obtained directly from the fundamental differential equation of the slab. A discussion is presented in Sec. A.2 of Appendix A. However, the indirect method of obtaining these displacements by using the reciprocal relations, or Betti's Law, is very simple.

Since the loadings, reactions, moments, deflections, and rotations are distributed as a series of sine curves, the deflection along the edge $y = c$, produced by a sine wave loading along the line $y = y_p$, is a sine wave, and the deflection along the line $y = y_p$, due to a sine wave reaction along the edge $y = c$, is also a sine wave.

For a sine wave loading given by Eq. 3.4 with the quantity p_m given in Eq. 3.6, the deflections at the edges are:

At y = c

$$w_r = F_{dr}\, p \tag{3.19}$$

At y = o

$$w_l = F_{dl}\, p$$

where F_{dr} and F_{dl} are flexibility coefficients which are presented in Eqs. A.35 and A.37 of Appendix A.

In a similar manner, the rotation at the edges may be stated as follows:

At y = c

$$\theta_r = -F_{rr}\, p \tag{3.20}$$

At y = o

$$\theta_l = F_{rl}\, p$$

when F_{rr} and F_{rl} are flexibility coefficients which are presented in Eqs. A.40 and A.42 of Appendix A.

3.5 Plane Stress Theory of Elasticity of the Slab

It has been pointed out in Sec. 3.3 that there are four components of the joint forces. Two of these four components, namely the reaction, R, and the moment, M, were treated by the ordinary theory of flexure of slabs in Sec. 3.4. The other two components are the in-plane normal force, N, and the in-plane shearing force, S, which are treated in this section by using the plane stress theory of elasticity.

Consider the slab shown in Fig. 3.6 in which the two edges parallel

to the y-axis are simply supported. The two edges parallel to the x-axis are subjected to forces N and S. The stress function which was introduced by G. B. Airy[21] may be given by the relation

$$\Phi = \Phi_m \sin \frac{m\pi x}{a} \tag{3.21}$$

when Φ is the Airy stress function and Φ_m is a function of y only. With the notation $\alpha_m = \frac{m\pi}{a}$, Eq. 3.21 may be written as

$$\Phi = \Phi_m \sin \alpha_m x \tag{3.22}$$

The relationships between stresses and strains, strains and displacements, the equations of equilibrium, the compatibility equation in terms of strains, and the boundary conditions, which are derived from plane stress theory of elasticity, are stated in Sec. B.1 of Appendix B. The stresses, strains, displacements, and compatibility equation, in the terms of the derivatives of the Airy stress function are also stated in Sec. B.1 of Appendix B. By introducing the stress function, Φ, Eq. 3.22, into these fundamental relationships, the stresses, strains, and displacements, may be stated in terms of Φ_m and its derivatives, multiplied by $\sin \alpha_m x$ or $\cos \alpha_m x$, as are presented in Sec. B.2 of Appendix B.

It is noted that the stresses, per unit of area, in the directions of x and y axes, σ_x and σ_y, the strains in the directions of x and y, ε_x and ε_y, and the displacement in the direction of y, v, are all the same form as Φ and involve a function of y only, multiplied by a sine curve in the x-direction; and the shearing stress, τ_{xy}, the shearing strain, γ_{xy}, and displacement in the x-direction, u, involve a function of y only, multiplied by a cosine curve in the x-direction.

The in-plane forces per unit of length are equal to the in-plane stresses multiplied by the thickness of the slab. Thus, the in-plane normal force per unit of length, N, and in-plane shearing force for a unit of length, S, can be written as follows:

$$N_x = h \cdot \sigma_x$$

$$N_y = h \cdot \sigma_y$$

$$S = h \cdot \tau_{xy}$$

where h is the thickness of the slab, which is assumed constant in this analysis.

The in-plane stresses, given in Sec. B.2 of Appendix B, can be written as:

$$\sigma_x = \sigma_{xm} \sin \alpha_m x$$

$$\sigma_y = \sigma_{ym} \sin \alpha_m x$$

$$\tau_{xy} = \tau_{om} \cos \alpha_m x$$

where σ_{xm}, σ_{ym}, and τ_{om}, are functions of y only.

Consequently, the in-plane forces may be stated as:

$$N_x = N_{xm} \sin \alpha_m x$$

$$N_y = N_{ym} \sin \alpha_m x \qquad (3.23)$$

$$S = S_m \cos \alpha_m x$$

where N_{xm}, N_{ym}, and S_m, are independent of x.

3.5.1 In-Plane Flexibility Constants for a Rectangular Slab

Consider the slab shown in Fig. 3.6(a) with two opposite edges simply supported. The other two edges, l anr r, are subjected to in-plane normal forces, N, and in-plane shearing forces, S. Their magnitudes may be stated by the following relations:

$$N_r = N_{rm} \sin \alpha_m x$$

$$S_r = S_{rm} \cos \alpha_m x \tag{3.24}$$

$$N_l = N_{lm} \sin \alpha_m x$$

$$S_l = S_{lm} \cos \alpha_m x \tag{3.25}$$

The positive directions of the in-plane edge forces are shown in Fig. 3.6(b). The positive directions of the in-plane displacements are shown in Fig. 3.6(c).

The in-plane displacements, u_l and v_l, at the edge l, and u_r and v_r at the edge r, produced by each component of edge forces, are determined separately as follows:

Let the edge, r, subjected to an in-plane normal force of magnitude given by Eq. 3.24. The edge displacements of the slab in the x-y plane are shown in Fig. 3.7(a). The displacements at the edges l and r in the y-direction, v_l and v_r are distributed as sine curves and may be written as

$$v_r = F_{nn} N_r$$

$$v_l = F_{nf} N_l \tag{3.26}$$

where the functions F_{nn} and F_{nf} are the axial flexibility coefficients for the slab at the near edge and the far edge, respectively and are presented in Eq. B.22 of Appendix B. The edge displacements in the x-direction, u_l and u_r, are distributed as cosine curves and may be written as:

$$u_r = -F_{kn} N_{rm} \cos \alpha_m x$$

$$u_l = F_{kf} N_{rm} \cos \alpha_m x \tag{3.27}$$

where F_{kn} and F_{kf} are the axial shear flexibility coefficients for the slab at the near edge and the far edge, respectively, and are presented in Eq. B.22 of Appendix B.

Now apply the in-plane shearing force of magnitude given by Eq. 3.24. The edge displacements of the slab in the x-y plane are shown in Fig. 3.7(b). The displacements in the x-direction of the edges l and r, u_l and u_r, are distributed as cosine curves and may be written as:

$$u_r = F_{sn} S_r$$

$$u_l = F_{sf} S_r \tag{3.28}$$

where the functions F_{sn} and F_{sf} are in-plane shear flexibility coefficients of the slab at the near edge and the far edge, respectively and are presented in Eq. B.28 of Appendix B. The edge displacements in the y-direction v_l and v_r are distributed as sine curves and may be written as:

$$v_r = -F_{kn} S_{rm} \sin \alpha_m x$$

$$v_l = -F_{kf} S_{rm} \sin \alpha_m x \tag{3.29}$$

The functions F_{kn} and F_{kf} are the same as in Eq. 3.27, as should be evident from the reciprocal theorem. The minus signs are used because of the sign conventions.

It is evident that the flexibility coefficients for the edge displacements with the edge 1 subject to the in-plane normal force, N_1, of magnitude given by Eq. 3.25, are the same quantities found by applying N_r at the edge r. By taking into account the sign conventions, the displacements may be written as follows:

Displacements in the y-direction

$$v_1 = -F_{nn} N_1$$

$$v_r = -F_{nf} N_1 \tag{3.30}$$

Displacements in the x-direction

$$u_1 = -F_{kn} N_{1m} \cos \alpha_m x$$

$$u_r = F_{kf} N_{1m} \cos \alpha_m x \tag{3.31}$$

where the functions F_{nn} and F_{nf} are the same as in Eq. 3.26, and the functions F_{kn} and F_{kf} are the same as in Eq. 3.27. The minus signs are taken into consideration for the sign conventions.

Similarly, the edge displacements due to the edge in-plane shearing force, S_1, of magnitude given in Eq. 3.25, acting on edge 1, can be written as follows:

Displacements in the x-direction

$$u_l = -F_{sn} S_l$$

$$u_r = -F_{sf} S_l \tag{3.32}$$

Displacements in the y-direction

$$v_l = -F_{kn} S_{lm} \sin \alpha_m x$$

$$v_r = -F_{kf} S_{lm} \sin \alpha_m x \tag{3.33}$$

where the functions F_{sn} and F_{sf} are the same as in Eq. 3.28, and the functions F_{kn} and F_{kf} are the same as in Eq. 3.27.

3.6 Formulation of Matrices for a Slab Element

A typical rectangular slab, with two opposite edges simply supported, has been analyzed in Secs. 3.4 and 3.5, and Appendixes A and B. The four components of displacement for the other two edges parallel to the axis of the span length, the left edge l and the right edge r, due to each cycle of each of the edge forces and the applied loading were determined in terms of the flexibility constants multiplied by those forces and loadings. The total displacement for each component is equal to the summation of the effects of all cases, namely, eight edge forces plus the applied load.

The total edge displacement functions are stated in a column matrix, W_S. The edge force functions are stated in a column matrix, N_E, and F_S is the flexibility matrix. Those matrices are presented in Eqs. B.31 and B.32 of Appendix B. The flexibility constants due to the transverse

load are stated in the matrix L_S and presented in Eq. B.34 of Appendix B, and p_m is the applied load. Thus, the total edge displacement functions may be stated in the form of matrices as follows:

$$W_S = F_S N_E + p_m L_S \tag{3.34}$$

3.7 Biaxial Bending, Axial Force, and Torsion in a Girder

It has been mentioned previously that the structure of a bridge consists of the slab elements and the girder elements connected along the joint lines as shown in Fig. 3.1. There are four components of the unknown joint forces acting along each joint line. These components of joint forces, as shown in Fig. 3.2, were treated as the edge forces acting at the edge $y = 0$ and $y = c$ of a panel of slab in Secs. 3.4 and 3.5. The girder element is also subjected to these forces along the edges of the top flange of the girder at the level of the mid-depth of the slab as shown in Fig. 3.2.

In this section, a girder subjected to the reaction R_1 and the moment M_1, with magnitudes given by Eq. 3.10, the in-plane normal force N_1 and the in-plane shearing force S_1, with magnitudes given by Eq. 3.25, acting on the left edge 1 of the cross section, the reaction R_r and the moment M_r, with magnitudes given by Eq. 3.9, the in-plane normal force N_r and the in-plane shearing force S_r, with magnitudes given by Eq. 3.24, acting on the right edge r, the transverse load p given by Eq. 3.6, and a torsional moment m_t is analyzed. The moment m_t is given by

$$m_t = M_{dm} \sin \alpha_m x \tag{3.35}$$

in which

$$M_{dm} = \frac{2M_d}{a} \sin \alpha_m x_d \tag{3.36}$$

where

M_d = concentrated moment about the axis passing through the shear center and parallel to the x-axis (only for the purpose of the analysis of the effects of diaphragms)

x_d = the x-coordinate of the moment M_d, or of the diaphragm.

In the prestressed concrete I-section bridge, the cross section of the interior girders is symmetrical about the z-axis. However, if the sidewalk is taken into account, the exterior girders are not symmetrical. For the general case, the unsymmetrical cross section is considered in this analysis.

Consider a small element of the girder as shown in Fig. 3.8. This element is in equilibrium under the external edge forces, the loadings, and internal forces. The internal forces are three forces, F_x, F_y, and F_z in the directions of the axes, and three moments, M_x, M_y, and M_z about the axes.

The x-axis passes through the centroid 0 of the cross section and is parallel to the span. The y-axis is parallel to the supports of the girder, and the z-axis is pointing downward. The right-hand rule is used in this analysis, for relating directions of moments and moment vectors.

In the girder analysis, each component of the edge force, and the loading, may be treated one at a time as in the case of the slab. But, it is more convenient to analyze all forces and the loading at the same time. the combination of biaxial bending, axial force, and the twisting moment is considered in the analysis. For the internal forces, the axial force, F_x,

and the bending moments, M_y and M_z, are considered to be acting at the centroid, O, of the cross section, and the shearing forces, F_y and F_z, the twisting moment, M_x, are considered to be acting at the shear center, S, of the cross section. The distances from the mid-depth of the slab to the centroid and shear center are h_o and h_s, respectively; y_s and z_s are the coordinates of the shear center, and y_l and y_r are the coordinates of the left edge and the right edge of the top flange of the girder.

3.7.1 Internal and External Force Relationships

Six fundamental differential equations were derived from consideration of the equilibrium of a small element of the girder as shown in Fig. 3.8, and are stated in Eqs. C.3 and C.4 of Appendix C. The three internal forces, F_x, F_y, and F_z, caused by the external forces and loadings were derived by the integration of Eq. C.3, and are presented by Eqs. C.15 and C.17. The three resisting moments, M_x, M_y, and M_z, caused by the external forces and loadings were derived by integration of Eq. C.4, and are presented in Eqs. C.16 and C.18.

For the girder with a composite slab, the resisting force and the resisting moments of the composite girder are as follows:

$$
\begin{aligned}
F_{cz} &= \frac{1}{\alpha_m}(-R_{lm} + R_{rm} + p_m)\cos\alpha_m x \\
M_{cy} &= \frac{1}{\alpha_m^2}(-R_{lm} + R_{rm} + p_m)\sin\alpha_m x \\
M_{cx} &= \frac{1}{\alpha_m}[-(y_l - y_s)R_{lm} + M_{lm} + (y_r - y_s)R_{rm} - M_{rm} \\
&\quad + (y_p - y_s)p_m + M_{dm}]\cos\alpha_m x
\end{aligned}
\tag{3.37}
$$

3.7.2 Flexibility Constants for a Girder

At any point in a corss section of the girder, there are four components of displacements, namely, w, θ, v and u, produced by the edge forces and the loadings. The general formulas for the displacements were derived and presented in Eqs. C.27, C.29 and C.30, of Appendix C. With these equations for the displacements and the functions M_T from Eq. C.6, F_{xm} for Eq. C.17, and M_{ym} and M_{zm} from Eq. C.18, the displacements at the edges l and r can be obtained by the appropriate substitutions of the coordinates y and z.

Consequently, the flexibility constants for each edge due to each of the edge forces and the loadings are obtained and stated in the matrix forms in Sec. C.4 of Appendix C.

3.7.3 Formulation of Matrices for a Girder Element

The discussion and analysis of a simply supported girder subjected to the combination of biaxial bending, axial force and torsion, were presented in Secs. 3.7, 3.71, 3.72, and Appendix C. The results were stated in terms of matrices. The column matrix, W_G, for the total displacement functions at edges l and r, and the column matrix, N_E, for the edge force functions are presented in Eq. C.33 of Appendix C. The flexibility matrix for the edge forces, F_G, and the flexibility matrices for the loadings, L_G and C_G, are presented in Eqs. C.34 and C.35 of Appendix C.

Thus, the total edge displacement functions of the girder may be stated in the form of matrices as follows:

$$W_G = F_G N_E + p_m L_G + M_{dm} C_G \tag{3.38}$$

3.8 Solution for Displacements and Internal Forces in a Bridge Structure

It was mentioned in Sec. 3.3 that a bridge structure consists of the slab elements and girder elements connected along the joint lines as shown in Fig. 3.1. When the bridge is subjected to transverse loads, each joint line will undergo deformations and be subjected to internal forces. The deformation along each joint line may be resolved into four components: the displacement, w, in the direction of z-axis; the rotation, θ, about the x-axis; the displacement, v, in the direction y; and the displacement, u, in the direction x. The accompanying forces along each joint line may be resolved into four components corresponding to the displacements: the reaction, R, in the direction of z-axis; the moment, M, about the x-axis; the in-plane force, N, in the direction y; and the in-plane force, S, in the direction x. The displacements are distributed in a series of sine curves and cosine curves as follows:

$$w = \sum_{m=1}^{\infty} w_m \sin \alpha_m x$$

$$\theta = \sum_{m=1}^{\infty} \theta_m \sin \alpha_m x$$

$$v = \sum_{m=1}^{\infty} v_m \sin \alpha_m x$$

$$u = \sum_{m=1}^{\infty} u_m \cos \alpha_m x$$

The forces are also distributed in a series of sine curves and cosine curves as follows:

$$R = \sum_{m=1}^{\infty} R_m \sin \alpha_m x$$

$$M = \sum_{m=1}^{\infty} M_m \sin \alpha_m x$$

$$N = \sum_{m=1}^{\infty} N_m \sin \alpha_m x$$

$$S = \sum_{m=1}^{\infty} S_m \cos \alpha_m x$$

The solution of the bridge problem requires solution for either the four displacement functions, w_m, θ_m, v_m, and u_m, at each joint for each cycle of the loading by the stiffness method, or for the four force functions, R_m, M_m, N_m, and S_m, at each joint for each cycle of the loading by the flexibility method. The flexibility method has been chosen for this analysis.

In the flexibility method, the adjacent slab and girder elements have to be connected so that the deformations along the joint lines are compatible. The force functions at each joint can be obtained by equating the displacement functions of the slab and girder elements at the connected joints to form a number of simultaneous equations in terms of, and equal to, the unknown force functions.

Consider a bridge structure (Fig. 3.1) consisting of a series of girders and slabs alternately connected so that the left edges, l, of the slabs connect to the right edges, r, of the girders, and the right edges of the slabs connect to the left edges of the girders. By equating Eq. 3.34 to Eq. 3.38, a series of simultaneous equations of number equal to $8(N_G-1)$ will be formed. The unknown force functions at the joints, of number also equal to $8(N_G-1)$, can be obtained by solving the simultaneous equations.

The vertical shear, F_{cz}, the bending moment, M_{cy}, and the twisting moment, M_{cx}, along the span of each girder taking into account the composite action of the slab can be obtained by substituting the computed edge forces (unknown joint forces) into Eq. 3.37, multiplied by sin $\alpha_m x$ for M_{cy}, and cos $\alpha_m x$ for F_{cz} and M_{cx}.

The displacements along the edges of the top flanges of girders can be obtained by substituting the computed edge forces into Eq. 3.38, multiplied by sin $\alpha_m x$ for w, θ, and v, and by cos $\alpha_m x$ for u.

Chapter 4

METHOD OF ANALYSIS OF DIAPHRAGMS

4.1 General

The slab in the slab and girder bridge serves two major functions, first as the roadway, and second as the transverse framing device. As has been discussed in Sec. 2.4.2 of Chapter 2, a major factor in the transverse load distribution in this type of structure is the stiffness of the slab, which is spread uniformly throughout the length of the bridge. When the load is applied over a girder, the slab tends to spread the load to the adjacent girders, thus reducing the burden of the loaded girder. The better load distribution is accompanied by a stiffer, or thicker, slab. However, a relatively thick slab causes a heavier dead load on the structure and, furthermore, involves excessive cost of concrete.

The diaphragms, discussed in Sec. 2.4.5 of Chapter 2, are transverse framing devices introduced into the structure to assist in the distribution of load. To understand the action of the diaphragms, one may consider a structure consisting of the girders and the diaphragms, without the slab. The diaphragms unite with the girders to form a space structure, enabling the structure to act more efficiently as an integral unit under load, particularly when the capacity is approached.

The major difference between these two devices as a means of distributing the load lies in the nature of the loading transferred to the girders. For the slab, the loads transferred take the form approximately of a sine curve of distributed load. On the other hand, the loads from diaphragms are transferred in the form of concentrated loads and moments applied

at the points where the diaphragms intersect the girders. These concentrated loads and moments, instead of the approximate sine curve of distributed loads from the slab, reduce the burden on the loaded girder.

The torsional stiffness parameter, discussed in Sec. 2.4.3 of Chapter 2, is not a framing device, but its function also tends to reduce the burden of the loaded girder. For a prismatic girder, the torsional stiffness is uniformly distributed throughout the span. The load transferred thus also takes the form approximately of a sine curve of distributed load similar to the slab.

In this study, all the bridges treated have both a roadway slab and girders with torsional stiffness. The addition of diaphragms to these structures will cause a combination of the action of the approximate sine curves of distributed loads and the concentrated loads and moments. Whether the diaphragms actually help (reduce maximum moments in loaded beams) or not when they are added to a bridge with adequate slab thickness and substantial torsional stiffnesses of the girders for each particular structure and loading. For example, it would be conceivable that if all other conditions remain the same, the diaphragms will prove to be more effective in a structure with a high H and low T, having a relatively flexible slab and small torsional restraints from the girders, than in one with a low H and high T, having a relatively stiff slab and large torsional restraints from the girders.

4.2 Idealization of Diaphragm

The diaphragms in most prestressed and reinforced concrete bridges are cast monolithically with the slab as shown in Fig. 4.1(a). However, to

simplify the problem, the diaphragm is assumed to be separated from the slab as shown in Fig. 4.1(b). Thus, the stiffness of the diaphragm has to be modified to include the composite action of the slab as a T-beam. The width of the slab taken for the T-beam action may be taken from the AASHO Bridge Specifications or the ACI Building Code. If the diaphragm is not cast monolithically to the slab, its actual stiffness should be used.

4.3 General Description of Principle of Analysis

The basic principle of the solution of the problem is developed from the concept that the nature of the loading transferred to the girders by means of the diaphragms is in the form of concentrated loads and moments at the points where the diaphragms intersect the girders. Thus, the diaphragms in the structure as shown in Fig. 4.2(a) may be replaced by a set of equivalent forces and concentrated moments, with positive directions as shown in Fig. 4.2(b), acting at the points of intersection of the diaphragms and the girders. The forces act through the shear center, S, and the moments about it. The problem of finding the effects of adding diaphragms is then reduced to one of finding moments in the girders of a bridge without diaphragms, but subjected to additional forces and concentrated moments.

The displacements of a cross section of the bridge, subjected to the combination of loads and forces shown in Fig. 4.2(b), are shown in Fig. 4.3. Downward deflections and clockwise rotations are positive.

Consider a bridge consisting of a slab supported by N_G identical girders. The diaphragms may be framed transversely to the girders at various locations along the span of the bridge as given in Table 2.5. It is assumed that the connections between the individual diaphragms and the girders are

fully effective so that all separate pieces of diaphragm can be replaced by one continuous cross beam, as shown in Fig. 4.4, with transverse forces and concentrated moments applied on it.

The solution of the problem is tremendously simplified by considering the diaphragm as a single continuous beam, and may be summarized as follows:

1. Remove the diaphragms and replace them by unknown reactions and concentrated moments at the points of intersection of the diaphragms and the girders as shown in Fig. 4.2(b).
2. Compute the total deflections and rotations at the points of intersection of the diaphragms and the girders due to the unknown reactions, concentrated moments, and the external load on the bridge, by the method developed in Chapter 3 and Appendixes A, B and C. For the symmetrical cross sections, the deflection at each point of intersection of the diaphragm and the girder is the average of the deflections at both edges of the top flange of the girder. Find the net deflection at the interior points and the net rotation at all points; the net deflection and the net rotation are measured from a line passing through the points of intersection of the diaphragms and the deflected edge girders.
3. Consider the diaphragm as a simply supported cross beam subjected to the reaction forces at the points of intersection of the diaphragms and the girders as shown in Fig. 4.4(a), and the couples at the same points as shown in Fig. 4.4(b). Compute the total deflection at the interior points and the

rotation at all points, due to the reaction forces and the couples, relative to the ends of the diaphragms.

4. There should be no separation between the girders and the diaphragm. The summation of deflections and rotations computed in 2 and 3 at each point of intersection of the diaphragm and the girders must be zero. In a bridge having N_G girders, the $2N_G$ unknowns have to be found for each diaphragm. But, the number of equations formed by equating the displacements in Step 3 is equal to $2(N_G-1)$. Thus, for each diaphragm, two more equations are needed to solve the problem. These two equations can be obtained from statics as follows:
   a. The summation of all forces acting on the diaphragm is equal to zero;
   b. The summation of moments caused by forces and couples about either support is equal to zero.

   Thus, each of the diaphragms of the bridge will cause $2N_G$ unknowns, reactions and couples, that have to be solved from $2N_G$ simultaneous equations. If the bridge has N_D diaphragms (cross beams), the number of unknowns and simultaneous equations have to be multiplied by N_D.
5. The reactions and couples found in Step 4 represent the equivalent forces and concentrated moments applied to the structure by the diaphragms. Moments in the girders of the bridge with diaphragms can be obtained by summing up the moments caused by the diaphragm reactions and couples, and the external loads.

The arrangement of the diaphragms in the bridges may be classified into three cases as follows:

Case 1. Bridge with one diaphragm at midspan only, as shown in Fig. 4.5(a);

Case 2. Bridge with two diaphragms at symmetrical positions with respect to midspan, as shown in Fig. 4.5(b); and

Case 3. Bridge with three diaphragms, one at midspan and two at symmetrical positions with respect to midspan, as shown in Fig. 4.5(c).

4.4 Matrix Formulations and Solution of Bridge Problem with Diaphragms

The general formulas for computing deflections and slopes of a simply supported diaphragm due to reaction forces and couples were derived from the conjugate beam method, and presented in Sec. D.1 of Appendix D. The static equilibrium equations of the diaphragm are also presented in Sec. D.1.

The general formulas for computing deflections and rotations of the girders of the bridge at the points of intersection with the diaphragms, relative to the line o-o of Fig. 4.3, are developed and presented in Sec. D.2 of Appendix D. These deflections and rotations are produced by the unknown forces due to the diaphragms and the loadings.

The displacements of diaphragms and girders of the bridge are given in the forms of matrices W_D and W_B, respectively, and stated in Eq. D.20 of Appendix D. The force-displacement relationships are derived and presented in Eq. D.22 of Appendix D and may be stated as follows:

$$W_D = F_D N_U \tag{4.1}$$

$$W_B = F_B N_U + P L_B \tag{4.2}$$

where N_u is the column matrix of the unknown forces and is stated in Eq. D.10 of Appendix D. F_D and F_B are flexibility matrices of diaphragms and girders of the bridge, respectively, and are stated in Eqs. D.23 and D.24 of Appendix D. The column matrix, L_B, is the flexibility matrix due to external load, and is presented in Eq. D.25 of Appendix D. P is the concentrated load on the bridge.

The solution of the problem of the bridge with diaphragms lies on the determination of the unknown reaction forces and moments at the points of intersection of diaphragms and girders. These unknown forces can be obtained by equating the displacements of diaphragms W_D in Eq. 4.1 to the displacements of the girders of the bridge W_B in Eq. 4.2 to form a group of simultaneous equations, in number equal to the number of unknowns, K_D. The internal forces and the displacements of the girders can be determined from the summation of all effects, reaction forces, moments, and loadings.

However, for three cases of diaphragm arrangements mentioned in Sec. 4.3, the matrix F_B is simplified because of symmetry and is presented in Eqs. D.29, D.30, and D.31 of Appendix D.

Chapter 5

DISCUSSION OF RESULTS

5.1 General Discussion

The method of analysis for the slab and girder bridge structure without intermediate diaphragms was described in Chapter 3. The analysis of the effects of adding diaphragms to the structure was described in Chapter 4. The results of the analyses were summarized in the forms of matrices, and a computer program for an IBM 360/75 was written to develop and solve the matrices. The program can be used for structures with and without diaphragms.

For the bridge without diaphragms, the program consists of one main program and fifteen subroutines. By adding seven more subroutines to it, the program can be used to solve problems of structures with various properties, number and locations of diaphragms.

With the aid of the computer program mentioned above, a large number of bridges, with different properties of the various parameters described in Chapter 2 and presented in Tables 2.2, 2.3, 2.4 and 2.5, were analyzed. All bridges studied have five girders. Tha particular bridge with b/a = 0.10 and H = 20 has also been studied for the case of a six-girder structure, and the results compared to those for a five-girder bridge with the same properties. The output from the computer program gave the internal forces and displacements of the girders of the bridges. The results will be presented and discussed in Secs. 5.2 to 5.7.

It was mentioned previously that the purpose of this study was to obtain a better understanding of the behavior of this type of structure

so that a more rational design procedure could be developed. In order to develop this design procedure, the influence coefficients for moments in girders due to loads at various locations have to be determined. Thus, each bridge has to be solved for the effects of a unit concentrated load placed at different locations transversely and longitudinally in the span. In this study, the influence coefficients were obtained for a concentrated load, P, located at each of the points of intersection of the girders with seven transverse lines at different locations along the span, as shown in Fig. 1.3, and at the center of each slab. However, the number of loading locations can be greatly reduced by taking into account the symmetry of the structure about its midspan and about girder C. Consequently, the number of load locations to be considered for each bridge is fourteen. Twelve locations of the load are at the points of intersection of the girders A, B and C, with the lines 3a/12, 4a/12, 5a/12, and 6a/12, or midspan. Two locations are at the centers of slabs AB and BC. For the bridges in which the diaphragms are to be added, the effects of a concentrated or a unit moment acting at each of the twelve locations on the girders also have to be determined.

The internal forces and the displacements of each girder at the supports and the other sevel locations along the span, as shown in Fig. 1.3, were computed. The results were obtained from the summation of twenty-one terms of the series. All computations were made using double-precision arithmetic, although only eight significant figures were printed out.

5.1.1 Standard Truck Loadings

The standard truck loadings for computing the maximum moments in

the girder are those specified in the AASHO Standard Specification for Highway Bridges.[17] The Specification provides two systems of loadings, namely, the H loadings and HS loadings. The H loadings represent a two-axle truck as shown in Fig. 5.1(a). The HS loadings represent a two-axle tractor plus a single-axle semitrailer as shown in Fig. 5.1(b).

The total weight of the truck in tons is designated by a numeral following H, as H20-44. The designation HS20-44 indicates a 20 ton truck with a 16 ton trailer, with the distance to the trailer axle adjusted to produce the maximum forces in the structure. The relative wheel loads are as shown in Fig. 5.1, where the wheel load P is equal to 0.4W, where W is the weight of the truck portion of the design vehicle.

Each truck is considered to occupy the central part of a 10-ft traffic lane; thus, the distance between the center of a wheel and the face of a curb is taken at 2 ft, and the minimum distance between the centers of wheels of trucks in adjacent lanes is taken as 4 ft.

The transverse position of the loads is of considerable importance, and two limiting cases are considered, as shown in Fig. 5.2. In some structures, the outer wheels can be directly over the outer girder as shown in Fig. 5.2(a), and in other structures the curb is constructed directly over the girder and the load cannot be closer than 2 ft from the axis of the outer girder, as shown in Fig. 5.2(b).

5.2 Load Distribution Behavior for a Concentrated Load on Bridges Without Diaphragms

The load distribution behavior of steel I-beam bridges without intermediate diaphragms was studied by Newmark and Siess.[9] In their study,

the parameters b/a and H were limited to the ranges encountered in steel I-beam bridges, and the torsional parameters, T and Q, were not taken into account. For the present study, the parameters b/a and H are extended to cover the range possible with prestressed concrete I-section girders, and the torsional stiffness, T, and the warping stiffness, Q, of the girders are also taken into consideration. The in-plane forces are considered in this study so that assumptions about the modified bending stiffnesses of the girders to take into account the T-beam behavior do not have to be made. Influence coefficients for moments along the span of the girders due to various locations of a concentrated load were obtained and plotted. The comparison of the results with the previous study and the discussion of the effects of each parameter will be made below.

5.2.1 Comparison with Previous Study

The results of the present analysis of the load distribution in five-girder bridges are compared with the previous study carried out by Newmark and Siess.[9] The influence coefficients for moments in the girders of the bridge found by both methods are in good agreement. Since the distribution procedure developed by Newmark[8] and the present method of analysis are derived from the same principle in which the equivalent Fourier series distribution of loads, forces and displacements have been used, the good agreement would be expected. Typical influence curves for moments at midspan of girders A, B, and C due to a concentrated load, P, moving transversely across the midspan of the bridge are shown in Fig. 5.3. The bridges, for which the influence curves are shown in Fig. 5.3, have the parameters b/a = 0.10 and H = 20, and b/a = 0.20 and H = 5.

In the present analysis, the bridge with b/a = 0.10 and H = 20 was analyzed for T ≃ 0 (T = 0.00001) and T = 0.011, which is the actual value of the torsional stiffness of the prestressed concrete I-section. The bridge with b/a = 0.20 and H = 5 was analyzed only for T = 0.028, which is its actual value. The influence curves for moment at midspan of the girders are represented by the solid lines for T equal to the actual values, the broken lines for T ≃ 0, and the dotted lines for T = 0, from the analysis by Newmark and Siess. It is evident, from the influence curves for T = 0 in Fig. 5.3, that the present method of analysis and the distribution method developed by Newmark are in good agreement, since the ordinates of the curves are nearly identical. The effect of the torsional restraint, as represented by the solid lines, is to cause appreciable reductions of the moments in the loaded girders.

5.2.2 Effects of Varying the Parameter, b/a

It was mentioned in Sec. 2.4.1 that the dimensionless parameter concerning the geometry of the bridge, b/a, is one of the essential parameters controlling the load distribution and was studied by Newmark and Siess. Small values of the parameter b/a correspond to the long-span bridges. On the other hand, large values of the parameter b/a correspond to short-span bridges.

A basic understanding of the effects of this parameter on the load distribution has also been described. A long-span bridge, accompanied by the small value of b/a, will behave more like a single beam than like a slab. Consequently, one would expect a better load distribution for the bridge with the small value of the ratio b/a than the one with the large

value of b/a. This phenomenon may be shown by the influence lines for moment at midspan of the girders, as are presented in Figs. 5.4 and 5.5. The curves shown in Fig. 5.4 are the influence lines for moment at midspan of girders A, B, and C due to a concentrated load, P, moving transversely across the bridge at midspan and at the quarter-point, for the ratios b/a = 0.05 and H = 10, 20 and 40. The curves shown in Fig. 5.5 are the influence lines for moment at midspan of the girders of the bridges, the ratios b/a = 0.20 and H = 5, 10 and 20, and are similar to the curves shown in Fig. 5.4. By comparing the curves in Fig. 5.4 to those in Fig. 5.5, it is evident that the bridges with b/a = 0.05 have better load transfer from the loaded girder to other girders than the ones with b/a = 0.20. For example, the influence lines for moment at midspan of girder C in Fig. 5.4, show that the moments at midspan of all girders due to the load, P, applied at the quarter-point of girder C are only slightly different. But the similar curves given in Fig. 5.5 show that the moment at midspan of girder C is much larger than the moments in the other girders.

The relationships between the moment at midspan of the loaded girders A, B, and C, and the relative bridge geometry b/a, for the various values of H, are given in Fig. 5.6. For each value of H as shown in the figures, the moments in the loaded girders increase as the ratio b/a increases.

5.2.3 Effects of Varying the Parameter H

The relative girder stiffness, H, which is the ratio of the stiffness of the girder to that of the slab, is another essential parameter controlling the load distribution, and was also studied by Newmark and Siess.[9]

As mentioned in Sec. 2.4.2, a large value of the ratio H corresponds to a bridge with stiff girders. On the other hand, the bridge having a small value of the ratio H will have a stiffer slab. It was also shown that the load distribution in the bridge with a stiffer slab is more uniform than in one with stiffer girders. This behavior may be shown by the influence lines for moment in the girders shown in Figs. 5.4 and 5.5. For a certain value of the ratio b/a, a more uniform load distribution among the girders of the bridge always corresponds to the smaller value of the ratio H.

Consider the bridges, with b/a ratios of 0.05 and 0.20, for which the influence lines are shown in Figs. 5.4 and 5.5, respectively. It can be seen that the effect of the parameter H on the load distribution in the bridges with the large value of b/a is considerably greater than in the bridge with the smaller value of b/a. The load distributions are much more uniform for all values of H in the bridges with b/a = 0.05 than in ones with b/a = 0.20, and one result is that the effects of the parameter H are much smaller in long-span than in short-span bridges.

The relationships between the moments at midspan in girders A, B, and C and the relative girder stiffness, H, for various values of the ratio b/a, are given in Fig. 5.7. For any value of the ratio b/a, the moment increases as the value of H increases.

5.2.4 Effects of Varying Parameters T and Q

The relative torsional stiffness parameter, T, and the relative warping stiffness, Q, were not studied by Newmark and Siess. Since the prestressed concrete I-section girder possesses appreciable torsional and

warping stiffnesses, these two parameters are introduced in this study. A brief discussion of the ranges and the effects of these two parameters is given in Secs. 2.4.3 and 2.4.4.

First, the effect due to the warping stiffness is discussed. As presented in Table 2.2, the values of the warping stiffness parameter, Q, of the standard prestressed concrete I-sections vary from 0.008 to 0.037. A series of four variations of the warping stiffnesses for each of four values of T, as shown in Table 2.3, were studied. The bridge studied has the parameters b/a = 0.10 and H = 20 and has been adopted as the "Standard Bridge" in this report. The results of the study show that the effects of varying the warping stiffness of the currently used standard prestressed concrete I-section girders are negligible. Typical curves showing the relationships between moments at midspan of the loaded girders and the relative warping stiffness, Q, for T = 0.010 and 0.040, are presented in Fig. 5.8. The curves show that the moments in the loaded girders are almost constant as the parameter Q varies from 0 to 0.040.

The relative torsional stiffness, T, is a very important parameter to be considered in this study. Since the torsional stiffness of the prestressed concrete I-section girder is considerably larger than that of a steel I-beam, use of concrete girders may improve the load distribution among the girders of the bridge. In order to study the effect due to this parameter, the standard bridge with the ratios b/a = 0.10 and H = 20 has been studied. The torsional parameter, T, was varied from 0.0001 to 1.00, as shown in Table 2.3. In general, the relative torsional stiffness, T, of the steel I-beam bridge is negligible; the prestressed concrete I-section girder varies from 0.009 to 0.030, and the prestressed concrete box section girder varies from about 0.50 to 1.00. Thus, the range of the torsional

parameter given in Table 2.3 should cover these three types of girders of bridges.

The results of the study are presented in the curves shown in Fig. 5.9. The curves show the relationships between the moments at midspan of the girders and the relative torsional stiffness, T, for cases of loads on the girders and slabs.

It is noted from the curves shown in Fig. 5.9 that the moments of the loaded girder and girders adjacent to the loaded slab decrease as the torsional stiffness increases. The rate of decrease in this moment is large when the parameter T is in the range between 0 to about 0.20. It may be concluded that the better load distribution in this type of bridge corresponds to the larger torsional stiffness of the girders.

The reduction of the moment in the loaded girder of the bridge with prestressed concrete I-sections, taking into account the torsional stiffness, is considerable. However, this reduction is not as large as some investigators may have expected. Since the I-section is an open section, the torsional stiffness is small in comparison to that of a box section, which is a closed section. In order to compare the load distribution of the steel I-beam, prestressed concrete I-section, and prestressed concrete box section bridges, the standard bridge with parameters b/a = 0.10 and H = 20 has been analyzed for T = 0.0001, 0.011 and 1.0, which correspond to three types of bridges mentioned above. Other properties are kept the same. The influence lines for moments at midspan of Girders A, B, and C of these bridges are plotted as shown in Fig. 5.10.

The curves presented in Fig. 10 are the influence lines for moment at midspan of the girders due to a concentrated load, P, moving transversely

across the bridge at midspan and at the quarter-point. It is obvious that the load distribution of the prestressed concrete I-section is slightly better than in the steel I-beam bridge. On the other hand, the load distribution of the box section is greatly improved. Especially, the curves show that the load distribution at the midspan of the prestressed concrete box section bridge, due to a load P moving transversely across the bridge at a distance a/4 from the support, is almost uniform.

5.2.5 Comparison of Five-Girder and Six-Girder Bridges

Since many bridges have more than five girders, an important question is that of whether the load distribution is changed if the number of girders is increased. In order to obtain a better understanding in the problem, the standard bridge, b/a = 0.10, H = 20, and T = 0.011, also has been solved for six girders. The influence lines for moment at midspan of Girders A, B, and C, for both five-girder and six-girder bridges, due to a load, P, moving transversely across the bridges at various locations along the span are shown in Fig. 5.11. From the curves of the influence lines of Girder A shown, the load transfer of Girder A is very slightly better for the five-girder than for the six-girder bridge. The curves show that the load transfer for Girders B and C is slightly better for the six-girder than for the five-girder bridge. However, the differences in the load distribution between these two bridges are very small and can be neglected.

5.2.6 Behavior of Bridge Due to a Concentrated Load, P, Moving Along the Bridge

A bridge structure is a complicated structure, since it is three-dimensional and is highly indeterminate. To obtain a better understanding

about this type of problem, the behavior of the bridge under a concentrated load, P, moving in both directions, along and transverse to the span, has to be determined. Influence lines for moments in the girders due to a load, P, moving in both directions (or an influence surface), and moment envelopes for the girders have to be obtained.

The curves shown in Fig. 5.12 are the influence lines for moment at midspan and moment envelopes of the girders of two bridges, b/a = 0.10 and H = 5 and 20, due to a load, P, moving along the span of the bridge over Girder A, along the centerline of Slab AB, and so on. Since both the influence lines for moment at midspan and moment envelopes are symmetrical about the midspan, all curves presented in Fig. 5.12 are half-curves from the midspan. All the curves on the left-hand side of the center of the figure are influence lines for moment at midspan of the girders. Those curves on the right-hand side are moment envelopes for the same girders.

It is noted that the curves of the influence lines for moment at midspan of loaded girders and interior girders adjacent to loaded slabs are concave upward. On the other hand, the curves of the unloaded girders are always convex.

The curves in Fig. 5.13 are the influence line for moment at midspan and the moment envelope for a simply supported bridge or a simple isolated beam. The influence line for moment at midspan of the bridge is a straight line with the maximum ordinate at the midspan equal to 0.25 Pa. If there is no error due to the evaluation of a limited number of terms of the series and if no moment is taken by the slab, the curve which represents the summation of the coefficients for moment at midspan of all girders is identical to the influence line for moment at midspan of the bridge shown

in Fig. 5.13, and the curve which represents the summation of the coefficients for the moment envelopes of all girders is identical to the moment envelope of the bridge on the right-hand side of Fig. 5.13.

It is also noted in Fig. 5.12 that the influence lines for moment at midspan of the loaded interior girders are more concave than those for the exterior girders.

5.3 Load Distribution Behavior for a Concentrated Load on Bridge with Diaphragms

Seven bridges with various values of the dimensionless parameters b/a and H as shown in Table 2.4 were studied to determine the effects of diaphragms on load distribution. The stiffnesses of diaphragms to be studied are also given in the same table. Five combinations of locations of diaphragms are considered and given in Table 2.5. The diaphragms and their locations in the bridges were discussed in Secs. 2.4.5 and 2.4.6. The internal forces, deflections, and rotations of the girders at various locations along the span for each combination of stiffness and location of diaphragms were obtained. The influence lines for moments in the girders due to a concentrated load, P, moving transversely across the bridge at different locations of the span were plotted. The results are compared with the previous study and will be discussed in the following sections.

5.3.1 Comparison with Previous Study

The effects of diaphragms on load distribution were studied extensively by Wei.[11] The torsional restraint of the girders was neglected in his analysis. To compare the results with Wei's study, the standard bridge,

b/a = 0.10 and H = 20, has been analyzed for T = 0.0001, which is approximately equivalent to the bridge without torsional restraint of the girders. The results are in good agreement with Wei's analysis. Typical influence lines for moment at midspan of the girders of two bridges, one with a diaphragm at midspan and another with two diaphragms at the third-points, due to a load, P, moving transversely across midspan are shown in Fig. 5.14. The relative diaphragm stiffness is 0.40. The curves for the bridge taking into account the actual torsional stiffnesses of the prestressed concrete I-section girders are also presented.

It is noted that the bridge taking into account the torsional stiffness of the girders has a slightly better load distribution than the one without considering the torsional restraint.

5.3.2 Relative Stiffness, Number and Locations of Diaphragms

Seven bridges with various stiffnesses and locations of diaphragms as given in Sec. 5.3 have been analyzed. In order to study the effects of varying the stiffness, number and locations of diaphragms, influence lines for moment in girders at various locations along the span due to a concentrated load moving transversely across the bridge were plotted. The curves, shown in Figs. 5.15 to 5.18, are the influence lines for moment in Girders A, B, and C of three bridges with the following properties:

1. b/a = 0.05, H = 20, T = 0.010
2. b/a = 0.10, H = 5, T = 0.012
3. b/a = 0.10, H = 20, T = 0.011

The relationship between the moment at midspan of the loaded girder and the relative girder stiffness for the bridges which the ratio b/a = 0.10

and one diaphragm at midspan are shown in Fig. 5.19. The relationship between the moment at midspan of the loaded girder and the relative bridge geometry for the bridges with the ratio H = 20 and one diaphragm at midspan are given in Fig. 5.20.

In general, the influence lines for moment in the girders, given in Figs. 5.15 to 5.18, show that the moment in the loaded girder decreases as the relative diaphragm stiffness increases. Consequently, it may be stated that, under a concentrated load on the bridge, a better load distribution is always produced by a stiffer diaphragm. Thus, the diaphragms do improve the load distribution in the case of a single load.

Consider the influence lines for moment at midspan of the girders of the first bridge, b/a = 0.05, H = 20 and T = 0.010, due to P moving transversely across the midspan of the bridge, as shown in Fig. 5.15. It is obvious that the largest reduction of moment of the loaded girder, or the best load distribution, occurs when the diaphragm is at midspan. This moment reduction decreases as the diaphragm is moved away from midspan. The curves shown in Fig. 5.15, which represent the influence lines for moment in Girders A, B, and C for κ = 0, on the bridge without diaphragms, and the curves for moments in the same girders in bridges with two diaphragms at the quarter-point, are almost identical. Similarly, the influence lines for the bridge with one diaphragm at midspan, as shown in Fig. 5.15, and the corresponding curves for the bridge with three diaphragms, one at each quarter-point and one at midspan, are almost identical. Thus, the effects of the diaphragms located at the quarter points of the bridge on the moment at midspan of the girders is insignificant for this bridge and loading condition.

The curves given in Fig. 5.16, for the bridge with b/a = 0.10, H = 5 and T = 0.012, also show that the diaphragms at the quarter-points do not improve the moment distributions at midspan of the girders.

It was pointed out in Secs. 5.2.2 and 5.2.3 that the bridges corresponding to a small ratio of b/a and H, i.e., bridges with relatively long spans and stiff slabs, will have a favorable transfer of load from the loaded girder to the others even though the bridges do not have the diaphragms. Thus, the effect of diaphragms is small, unless the diaphragms are located close to the section where the moment is to be determined.

On the other hand, the curves for the bridge with intermediate span and slab stiffness, b/a = 0.10, H = 20 and T = 0.011, which are presented in Fig. 5.17, show that diaphragms at each quarter-point do improve the load distribution somewhat. However, the curves given in the same figure show that the diaphragms at the quarter-points, for the bridge having three diaphragms, do not significantly improve the load distribution from that in bridges having only one diaphragm at midspan.

The curves shown in Fig. 5.18 are the influence lines for moment at midspan of the girders of the same bridge due to P moving transversely across the bridge at a/3 from the support. This set of curves also shows that the most effective location of the diaphragm, for moment at midspan of the girders, is the midspan. The reason lies in the nature of the loading transferred to the girders, since the loads from diaphragms are transferred in the form of concentrated loads and moments applied at the point of intersection of the diaphragms and the girders.

For the particular bridges having b/a = 0.10, the relationships between the moment at midspan of the loaded girders, A, B, and C, and the

relative girder stiffness are given in Fig. 5.19. There is a curve corresponding to $\kappa = 0$ for each girder. These curves represent the loaded girders for the bridges without diaphragms, and will reach the peak ordinate of 0.25 when H reaches infinity. It represents the case of a rigid girder, in which the load P is entirely taken by the loaded girder without distribution to other girders. In the curves for Girder C, the straight line with constant ordinates equal to 0.05, represents the bridges having a rigid diaphragm, $\kappa = \infty$ In this case, the load P is equally taken by all five girders.

It is noted that if the relative diaphragm stiffness increases to 0.10 or larger, the curves for Girders B and C are almost horizontal lines; i.e., the moments in Girders B and C will remain the same, when H increases from 5 to 40, if $\kappa \geq 0.10$. For the exterior girder, the moment will increase as H increases. It should also be noted that for a constant value of κ, the actual diaphragm stiffness will increase as H increases. For example, if two bridges have the same girder spacing and b/a ratio, the actual diaphragm stiffness of the bridge with H = 40 is eight times as large as the bridge with H = 5.

Since the bridges have the same b/a, the better load distribution will correspond to the small value of H. The relative differential deflections among the girders are small for bridges with small values of H. On the other hand, bridges with large values of H will have larger relative differential deflections among the girders. Thus, the stiffness of the diaphragm required to improve the load distribution has to be increased as the relative girder stiffness increases. As H reaches zero, the diaphragms do not have any effect on the load distribution.

The relationships between the moment at midspan of the loaded girder and the relative bridge geometry, for various relative diaphragm stiffness, are shown in Fig. 5.20. All bridges have the same relative girder stiffness, H = 20. As has been discussed previously, the bridge corresponding to the small value of b/a has a more favorable load distribution than in a bridge with a large value of b/a, if H remains the same. The reason for this is that the relative differential deflections between the girders are larger for the bridge having a large value of b/a than the one having a small value of b/a. Consequently, the stiffness of diaphragm to improve the load has to be increased as b/a increases. Since

$$H = \frac{E_g I_g}{aD}$$

where a is the span length, the actual girder stiffness of a bridge with a small value of b/a is larger than in one with a large value of b/a, provided that both bridges have the same H and girder spacing. Thus, for a constant relative diaphragm stiffness, the actual stiffness of the diaphragm is larger in a bridge with a small b/a ratio than in one with a large value of b/a. This is the reason that the moment in the loaded girder, shown in Fig. 5.20, is much larger for the bridge with a large value of b/a than in one with a small b/a ratio, even though κ is the same. For example, the curves for Girder C, as given in Fig. 5.20, show that the moment in the girder in a bridge with b/a = 0.05 and κ = 0.40 is very close to the moment corresponding to $\kappa = \infty$. On the other hand, the moment in the same girder for a bridge with b/a = 0.20 and κ = 0.40 is much higher than the moment corresponding to the line $\kappa = \infty$.

5.4 Load Distribution Behavior for 4-Wheel Loads Moving on Bridge without Diaphragms

The behavior of the structures discussed so far have been concerned with only a single load on the bridge, which is not realistic loading condition. The actual loads which are of interest to bridge engineers are truck loadings. The standard truck loadings to be considered for computing the maximum moments in the girders are specified by AASHO Standard Specification for Highway Bridges[17] as shown in Figs. 5.1 and 5.2. Each truck consists of two or three axle loads, spaced as shown, and the front axle is loaded to one-quarter of the load on the other axles. Most arterial highways are currently being designed for either H20 or HS20 loadings, in which the heavy axles are loaded to 32 kips.

The effects of entire three-axle trucks are discussed in Sec. 5.7. In this section, the effects of four isolated wheel loads, each designated as P and spaced as shown in Fig. 5.2, are discussed. This loading is representative of the effects of two heavy axles located side by side at the same position in the span of a bridge. Influence lines and moment envelopes due to this loading condition have been developed and are presented below. Each of the front wheels carries one-fourth of the rear wheel weight. Thus, the moments due to the front wheels may be determined from the results of the rear wheels by simply substituting P/4 for P.

Since the wheel spacings are specified as a certain number of feet, the girder spacing must also be specific rather than a general dimension as was the case in the previous sections of this chapter. The spacings of the girders to be considered in this study are 5, 6, 7, 8 and 9 ft, and the bridges are considered as having two traffic lanes.

Influence lines and moment envelopes for the maximum moments in

each girder were determined as described below. In each case, the lateral position of loads to give the maximum midspan moment was determined by trial and error, and all other moments in the same girder were determined with the wheel loads the same distance from the curb.

The maximum value of moment in each girder was obtained by placing the 4-wheel loads at the highest ordinates of the respective influence lines for moment due to a single load, P, moving transversely across the bridge. The loads are placed at various locations along the span, namely, midspan, 5a/12, 4a/12, and 3a/12 from the support. At each location of the loads, the maximum moments at midspan and at the locations of the loads are obtained. Thus, the influence lines for moment at midspan and moment envelopes for the girder, due to the 4-wheel loading moving along the span of the bridge, can be plotted. In the prestressed concrete girder bridge, the prestressing strands may be curved, and the maximum moment at various locations along the span due to the truck loads moving on the bridge are of special importance.

To serve as practical purposes for designing slab and prestressed concrete grider bridges, the influence lines for maximum moment at midspan and moment envelopes of the fourteen bridges listed in Table 2.2 were obtained and are presented in Figs. 5.21 to 5.26. Since these curves are symmetrical about the midspan of the bridge, only half of the curves are plotted. The curves plotted on the left-hand side of the midspan are the influence lines for moments at midspan of the girders. The curves plotted on the right side of the midspan are the moment envelopes of the same girder. The girder spacings vary from 5 to 9 ft.

The curves, shown in Figs. 5.21 to 5.24, were obtained for the loading condition where the outer wheel is located at least 2 ft from the edge girder. The curves, shown in Figs. 5.25 to 5.26, were obtained for

the condition where the outer wheel can be over the edge girder. The first condition is applied to bridges in which the cross sections are as shown in Fig. 5.2(b). The second condition is applied to the bridge in which the curbs are located two ft away from the edge girders, as shown in Fig. 5.2(a), and the moments are larger than those obtained from the first case.

Five-girder bridges with the girder spacings equal to 8 or 9 ft may be considered as three-lane bridges. Thus, the maximum moments due to 6-wheel loads were determined for several cases. In all cases, the moments due to the 6-wheel loading are larger than caused by the 4-wheel loading. However, the AASHO Standard Specification for Highway Bridges[17] states that the following percentages of the resultant live-load stresses shall be used, in view of improbable coincident maximum loadings:

Numer of Lanes	Percent
1 or 2	100
3	90
4 or more	75

Multiplying the moments caused by 6-wheel loading by the factor 0.9 always results in moments which are less than those caused by 4-wheel loadings. Then, it is reasonable to obtain the maximum moments for two-lane loadings for the type of structure considered in this study.

It should be pointed out that the tangents of the curves corresponding to the moment envelopes have to be horizontal at midspan. As mentioned previously, the influence lines for moments in the girders due to a load, P, moving across the bridge at various locations, except the midspan,

do not have the points on the slabs. Thus, these curves are not quite as accurate as the ones due to the load applied at the midspan. Because of the accumulation of small systematic plotting errors, the moment envelopes for the interior girders due to the 4-wheel loading obtained from those curves are usually slightly too low for points away from midspan. Consequently, the tangents at midspan of the moment envelopes are not quite horizontal. However, these errors are small and may be neglected. This problem does not exist for the influence lines.

With this set of curves, the maximum moments in the girders due to the truck loads can be obtained by simply summing up the coefficients for moment at midspan due to a 4-wheel loading at each location corresponding to the axles of the trucks.

5.4.1 Outer Wheel at Least 2 Ft from Edge Girder

This loading condition may happen in the case of either of the bridge cross sections shown in Fig. 5.2. The curves shown in Figs. 5.21 to 5.24 are the influence lines for moment at midspan and moment envelopes of the girder carrying the maximum load, for values of b/a = 0.20, 0.15, 0.10, and 0.05, respectively. The outer wheel is at least 2 ft from the edge girder.

For any combination of b/a and H, the maximum moment coefficients increase as the girder spacing increases. Thus, the lowest curves in each figure are the influence line for moment at midspan and the moment envelope for b = 5 ft. On the other hand, the highest curves in each figure are the influence line for moment at midspan and the moment envelope for b = 9 ft.

The curves representing the moment envelopes for any girder are always convex. The curves representing the influence lines for moment at

midspan of the interior girders are either nearly straight or slightly concave, while the influence lines for moment at midspan of the exterior girders are always convex curves. This phenomenon is evident in the set of curves of the influence lines for moment at midspan and moment envelopes of the girders due to a single load, P, moving along the span of the bridge as shown in Fig. 5.12, and as discussed in Sec. 5.2.6.

Which girder is subjected to the maximum moment in a particular bridge depends on the values of H, b/a, b, and the position of the load relative to the edge of the structure. Table 5.1 contains a tabulation listing the controlling girder in each of the bridges studied. Fourteen combinations of H and b/a, with five beam spacings and two load positions for each combination, are included in the table, for a total of 140 bridges.

For any value of H between 5 and 40, and with b/a = 0.20 and 0.15, Girder C, or the center girder, always carries the maximum load. For the bridges with b/a = 0.10 and H = 5 and 10, either Girder B or C may carry the maximum load, depending on the girder spacings. Girder B controlling always corresponds to the larger spacings, and Girder C to the smaller spacings. However, for H = 20 and 40, Girder C always carries the maximum load. For the bridges with b/a = 0.05 and H = 10 and 20, the maximum moment may occur in any girder.

It may be concluded that in short-span bridges, b/a = 0.20 and 0.15, and in medium span bridges with stiff girders, b/a = 0.10 and H = 20 and 40, the controlling girder for maximum moment is always the center girder, C, since the load distributions of these bridges are not as uniform as the ones with b/a = 0.05 or 0.10 and H = 5 and 10, as shown in Figs. 5.4 and 5.5. It is evident from Fig. 5.5 that placing the 4-wheel loading

symmetrically about Girder C, the position that gives the maximum moment in Girder C, all four wheels have a large effect on the moment in that girder, and especially the two loads close to the girder. On the other hand, placing this set of loads on the influence lines for Girder A, shows that only two loads close to the girder have a strong effect on the moment in that girder. The other two loads that are farther away from Girder A have much smaller contributions to the moment in that girder. For Girder B, the moments due to 4-wheel loading are between the values for Girders A and C, but closer to that latter.

Consider the influence lines for moment in the girders for bridges with b/a = 0.05, as shown in Fig. 5.4. One may recognize that the moment in each girder due to 4-wheel loading should not be greatly different. Thus, it is possible that either Girders B or C may have the maximum moment; and, for small values of H, the edge girder may have the maximum moment.

It should be noted that for the 4-wheel loading located at midspan, the moments at midspan of the interior girders are always greater than the edge girder. If the loads are located away from the midspan, the moment in the edge girder may be greater than the interior girders. It may be seen from the influence lines for moments at midspan of Girder A, as shown in Fig. 5.24, that the curves are convex, while the curves of the interior girders are concave. Thus, when 4-wheel loads are considered, the maximum moment is always in the interior Girders B or C; but, when three-axle truck loads are considered, the maximum moment may be in the edge girder.

5.4.2 Outer Wheel on Edge Girder

This condition of loadings may happen in the bridges in which the

cross section is shown in Fig. 5.2(a). The curbs of the bridges are located at least 2 ft from the edge girder, so that the outer wheel of the truck may come over the girder. From the influence lines for moment in the girders shown in Figs. 5.4 and 5.5, it is obvious that the outer wheel is the most effective load producing moment in the edge girder. Since the ordinates of the moment coefficients for Girder A are very high when the load is placed directly on it, the maximum moments in the edge girders due to 4-wheel loadings have to be obtained by placing one wheel load directly on the edge girder and keeping the spacing between adjacent pairs of loads as small as possible.

The case in which the outer wheel can move outside of the edge girder has not been considered.

The set of curves of the influence lines for moment at midspan and moment envelopes, shown in Figs. 5.25 and 5.26, are similar to the first set as presented in Figs. 5.21 to 5.24. However, the curves in the second set were obtained by placing the outer load, P, on the edge girder. When this loading controls, Girder A always carries the maximum moment. The results for the bridges with b/a = 0.20 and 0.15, and b/a = 0.10 and H = 40 have not been presented, since the moments in the edge girders for these cases are still less than the moments in the interior girders of the first case. But the moments in the edge girders of the bridges with b/a = 0.10 and H = 5, 10 and 20, and b/a = 0.05 and H = 10, 20 and 40, are always greater than the moments in the interior girders of the first loading condition, and have to be used for design of the girders for bridges having the cross sections as shown in Fig. 5.2(a).

It is noted that, since the maximum moments of the second loading condition are in the edge girder, the influence lines for moment at midspan are convex curves and are almost identical to the moment envelopes.

5.4.3 Relationships Between Maximum Moment Due to 4-Wheel Loading and Relative Girder Stiffness

The relationships between the maximum moments in the girders due to 4-wheel loadings and the relative girder stiffness, for various values of b/a, are given in Fig. 5.27. The girder spacings are 5, 6, 7, 8, and 9 ft. Since the influence lines for moment at midspan and moment envelopes, given in Figs. 5.21 to 5.26 and discussed in Secs. 5.4.1 and 5.4.2, correspond specifically to values of H = 5, 10, 20, and 40, the moments for other values of H cannot obtain directly from those curves. However, they can be obtained from the curves shown in Fig. 5.27. The solid lines represent the moments corresponding to the first loading condition, or the outer load, P, at least 2 ft from the edge girder. The dotted lines represent the moments corresponding to the second loading condition, or the outer load, P, on the edge girder.

It may be concluded, in general, that the maximum moment in the girders of bridges with b/a = 0.20 and 0.15 will correspond to the first loading condition. For the bridges with b/a = 0.10 and b $\leq$ 6 ft, the maximum moment will be produced by the first loading condition if H $\geq$ 10, and by the second loading condition, if H $\leq$ 10. If b $>$ 6 ft, the limit of H will change from 10 to 15. For the bridges with b/a = 0.05, the maximum moment is in the edge girder and produced by the loads corresponding to the second loading condition for any values of H between 10 to 40, and b between 5 to 9 ft.

It should be remembered that the curves represented by the dotted lines, or the second loading condition, apply to bridges with the cross sections shown in Fig. 5.2(a), where the outer wheel can be directly over the outer girder.

5.4.4 Relationship between Maximum Moment Due to 4-Wheel Loading and Relative Bridge Dimension

The relationships between the maximum moment of the girder due to 4-wheel loading and the relative bridge dimension, for various values of H and b, are presented in Fig. 5.28. From this set of curves, the maximum moments in girders for bridges with values of b/a other than those given in Figs. 5.21 to 5.26 may be obtained. The solid lines represent the moments corresponding to the 4-wheel loading with the outer wheel located at least 2 ft from the edge girder. The broken lines represent the moments corresponding to the 4-wheel loading with the outer wheel located on the edge girder.

It may be observed that the transition points of the maximum moments from the second loading condition to the first loading condition are as follows:

1. For H = 5, the transition point is between b/a = 0.14 and 0.16,
2. For H = 10, the transition point is between b/a = 0.10 and 0.14,
3. For H = 20, the transition point is between b/a = 0.07 and 0.09, and
4. For H = 40, the transition point is b/a = 0.06.

The ranges in the ratio b/a depend on the spacings of the girders.

As noted previously, the second loading condition applies to bridges with the cross section shown in Fig. 5.2(a).

5.5 Box Section Girder Bridge Subjected to 4-Wheel Loading

It was noted in Sec. 5.2.4 that the single load distribution of the standard bridge, with the torsional stiffnesses of the girders increased to the range of the box section, is greatly improved. In this section, the load distribution of this bridge subjected to 4-wheel loading is studied.

The influence lines for moment at midspan and moment envelopes of Girders A, B, and C due to 4-wheel loading were obtained and are presented in Fig. 5.29. The curves for both Girders A and B were obtained from the loading condition where the outer wheel is on the edge girder. The maximum moments for this loading condition are in Girder B instead of Girder A for the I-section girder bridges. It is evident from the influence lines for moments in the girders, as shown in Fig. 5.10, that the effect of the outer wheel on the moment in Girder A of the box section is less than in the I-section girders. The summation of the effects of 4-wheel loads for Girder B is greater than for Girder A. If the outer wheel is at least 2 ft from the edge girder, the maximum moments are in Girder C. However, the maximum moments in both cases, Girders B and C, are only very slightly different, and either case may be used for design.

Consider the curves shown in Fig. 5.29 and the corresponding curves for a bridge with the same values of H and b/a, as shown in Figs. 5.23 and 5.25. It is obvious that the load distribution for the standard bridge with box section girders is much better than for the I-sections. The effects of increasing moment in any girder due to increasing the girder spacings in the

box-section are less than the I-section. For example, increasing the girder spacings from 5 to 9 ft increases the moment in Girder A of the box section girder bridge from 0.212 Pa to 0.257 Pa, and Girder C increases from 0.227 Pa to 0.267 Pa. But the moment in Girder A of the I-section bridge increases from 0.233 Pa to 0.347 Pa, and Girder C increases from 0.257 Pa to 0.362 Pa.

5.6 Effects of Diaphragms on Load Distribution Behavior of Bridge Due to 4-Wheel Loadings

It was shown in Sec. 5.3.2 that the diaphragms do reduce the moments in the loaded girders of bridges subjected to single loads. The reductions of moments in the loaded girders are related to the relative diaphragm stiffness. The loaded girders may be either edge or interior girders.

Adding diaphragms to bridges that carry 4-wheel loadings does not always reduce the moments in the girders. It depends on which girder is the significant girder, or which girder controls the moment. For instance, adding a diaphragm to a bridge increases the moment in the edge girder, but decreases those in the interior girders. If the edge girder is the girder which controls the moment, the addition of diaphragms would increase the maximum moment and thus be harmful. On the other hand, if the interior girder is the significant girder, the addition of diaphragms would reduce the maximum moment and thus cause desirable effects.

In order to obtain a better understanding of the effects of diaphragms on the load distribution in the bridges, the series of bridges listed in Table 2.4 have been studied. Several kinds of curves are obtained for this study. The first set consists of the influence lines for moment at midspan and moment envelopes for the standard bridge with five locations of

diaphragms, as shown in Figs. 5.30 to 5.34. For each location of diaphragms, the curves are plotted for the girder spacings equal to 5, 7 and 9 ft, and the outer wheel may come over the edge girder or be at least 2 ft from it.

The second set of curves consists of the relationships between the maximum moments in each girder due to 4-wheel loading and the relative diaphragm stiffness for various bridges, as shown in Figs. 5.35 to 5.37. These curves are also plotted for the case where the outer wheel can come directly over the edge girder and where the outer wheel is at least 2 ft from it.

The third set of curves are the relationships between the maximum moment in the controlling girder and the relative diaphragm stiffness, and are presented in Fig. 5.38 and 5.39. The curves for bridges which have the ratios b/a = 0.10 and H = 5, 10, 20, and 40 are shown in Fig. 5.38. The curves for bridges which have values of H = 20 and b/a = 0.05, 0.10, 0.15, and 0.20 are shown in Fig. 5.39. The curves for both the second and third sets are plotted for b = 5, 7, and 9 ft.

5.6.1 Effects of Varying Relative Diaphragm Stiffness

The effects of varying the relative diaphragm stiffness on the load distribution of the bridges may be studied from these three sets of curves. The curves in the first set show the influence lines for moment at midspan and moment envelopes for the values of κ = 0, 0.05, 0.20 and 1000. The curves corresponding to κ = 0 and 1000 represent the bridges without diaphragms and with rigid diaphragms. For each girder spacing, there are two curves corresponding to κ = 0. One represents the case where the outer wheel may come over the edge girder. The other curve represents the case where the outer wheel is located at least 2 ft from the edge girder. When 4-wheel loadings are

concerned, the significant girder of this particular bridge without diaphragms is always Girder C.

When adding diaphragms with various stiffnesses to the bridge, the moment in Girder A always increases as the relative diaphragm stiffness increases, whereas the moments in Girders B and C decrease. These variations may be seen from the curves shown in Figs. 5.35 to 5.37. The curves shown in Fig. 5.35 are the relationships between maximum moments in the girders and the relative diaphragm stiffness for the standard bridge with various locations of diaphragms.

If the outer wheel can come over the edge girder, the curves, for this particular bridge, show that except when there are two diaphragms at the quarter-points, Girder A always become the controlling girder for any location of diaphragms for κ less than 0.05, and for any girder spacing between 5 and 9 ft. For two diaphragms at the quarter-points, Girder A becomes the significant girder at the values of $\kappa = 0.05$ to 0.08. However, if three-axle truck loadings are considered, the addition of the diaphragms to this particular bridge will cause harmful effects if the outer wheel can come over the edge girder. A discussion of the load distribution in structures subjected to three-axle truck loadings is presented in Sec. 5.7.

If the outer wheel is located at least 2 ft from the edge girder, the curves reveal that as the girder spacing and the relative diaphragm stiffness vary, different girders become significant. For the small girder spacing, b = 5 ft, the curves show that Girder C is always the controlling girder. For the larger girder spacings, b = 7 and 9 ft, the girder that controls the maximum moment can be any girder, A, B, or C, depending on the relative diaphragm stiffness, and the location of diaphragms. The curves

for the bridge with one diaphragm at midspan show that the maximum moment is resisted by Girder C for the bridge without diaphragm or with a very flexible diaphragm, κ less than 0.04, and Girder B for the bridge with a flexible or medium stiff diaphragm, κ = 0.04 to 0.15. If the relative diaphragm stiffness is greater than 0.15, Girder A becomes most significant.

However, these transition points of the various significant girders may be varied by changing the location of diaphragms. The curves in the same figure, but for the bridge with two diaphragms at the quarter-points, show that if b = 7 ft, the maximum moment is in Girder C, B, and A for κ from 0 to 0.05, 0.05 to 0.21 and greater than 0.21, respectively. If b = 9 ft, the moment is taken by Girder B for any value of κ between 0.01 to 0.40. The effects of the different locations of diaphragms will be discussed in Sec. 5.6.2.

It should be noted that, in general, either Girder A or B may be the controlling girder in the standard bridge, depending on the relative stiffness and location of fiaphragms, and the girder spacing. It may be observed, from the curves for this bridge and those shown in Figs. 5.36 and 5.37 for the bridges with b/a = 0.10 and H = 5 and 40, and H = 20 and b/a = 0.05 and 0.20, respectively, that for a certain girder spacing, the transition points of transferring the maximum moment from Girder B to Girder A move away from the vertical axis if the diaphragms are moved from the midspan to the supports. On the other hand, the transition points move closer to the axis if the girder spacing is increased with the diaphragms held in the same locations. It means that, for a certain girder spacing, the value of κ at which Girder A becomes significant is small if the diaphragms are located

at the midspan or close to it, and increases as they move from the midspan. If the bridges have the same location of diaphragms, the value of κ at which Girder A becomes significant, is smaller for a bridge with a large girder spacing than for one with small girder spacing.

The effects of varying the relative diaphragm stiffness in bridges having the same relative geometry but different relative girder stiffness may be seen in the curves shown in Fig. 5.36. The bridges have the same b/a = 0.10, but H = 5 for one bridge and 40 for the other. The bridge with H = 5 has a relatively stiff slab, whereas the one with H = 40 has relatively stiff girders. The curves show that the variations of moments in the girders due to the diaphragms are small for the former, but large for the latter, since the bridge with a stiff slab has a better load distribution, even without diaphragms, than the one with stiff girders.

If the outer wheel can come over the edge girder, the curves show that the diaphragms should not be added to the bridge with H = 5, since the maximum moment is controlled by the edge girders regardless of the location of diaphragms and girder spacing. However, the maximum moment in the girders for the bridge with H = 40 may be reduced considerably by adding relatively flexible diaphragms at the most effective location.

If the outer wheel is located at least 2 ft from the edge girder, the maximum moment in the girders of both bridges is in Girder C for b = 5 ft. If b = 7 or 9 ft, either Girder A or B for the bridge with H = 5, or any girder for the bridge with H = 40, may be the significant girder, depending on the relative stiffness and location of diaphragms and the girder spacing. The girder moments are very insensitive to changes in relative diaphragm stiffness if H = 5. However, the maximum moments in the

girders of the bridge with H = 40, are greatly reduced by adding the diaphragms having the same relative stiffness as in the bridge with H = 5. For example, adding the diaphragms with κ = 0.15, at 5/12 points of the spans of these two bridges with b = 9 ft, reduces the maximum moment in the stiff slab bridge from 0.317 Pa to 0.300 Pa, whereas that in the stiff girder bridge is reduced from 0.395 Pa to 0.313 Pa. The reduction of moment for the former is 5.4 percent, whereas the latter is 20.4 percent. If the diaphragms with κ = 0.40 are added at the third-points of the bridges with b = 7 ft, the maximum moment in the stiff slab bridge is reduced from 0.276 Pa to 0.266 Pa, whereas that in the stiff girder bridge is reduced from 0.344 Pa to 0.275 Pa. In this case, the reduction of moment for the former is 3.6 percent, whereas the latter is 20.1 percent.

Thus, it may be concluded that the addition of diaphragms to a bridge with b/a = 0.10 and H = 5, may not improve the load distribution, and may cause harmful effects. The diaphragms do improve the load distribution in a bridge with b/a = 0.10 and H = 40, whether the outer wheel can come over the edge girder or remain at least 2 ft from it.

The effects of varying the relative diaphragm stiffness in bridges having the same relative girder stiffness, but differing in relative bridge geometry, may be studied from the curves shown in Fig. 5.37. The one with b/a = 0.05 is a relatively long span bridge, but the other with b/a = 0.20 is a relatively short span bridge. The curves show that the variations of moments in the girders of the bridge with b/a = 0.05 due to the effects of diaphragms are small and similar to those for the bridge with b/a = 0.10 and H = 5, since both bridges have good load distributions. But the curves for the bridge with b/a = 0.20 show that the moments in the girders are

greatly changed if the diaphragms are added. The variations of moments of this bridge are similar to the one with b/a = 0.10 and H = 40.

As was the case for the bridge with b/a = 0.10 and H = 5, if the outer wheel may come over the edge girder, diaphragms should not be added to the bridge with b/a = 0.05. But, adding the relatively flexible to medium stiff diaphragms to the bridge with b/a = 0.20, reduces the maximum moment in the girders substantially. For b = 9 ft, the maximum moment can be reduced from 0.431 Pa to 0.350 Pa by adding diaphragms, with κ = 0.11 at the 5/12 points, or κ = 0.19 at the third-points. For b = 7 ft, the maximum moment can be reduced from 0.362 Pa to 0.300 Pa by adding the diaphragms with κ = 0.17 at the 5/12 points, or κ = 0.29 at the third-points. The reductions of moments are 18.8 percent and 17.3 percent for b = 9 and 7 ft, respectively.

If the outer wheel is located at least 2 ft from the edge girder, the maximum moment in the girders of the bridge with b/a = 0.05 may be reduced slightly by adding relatively flexible diaphragms at the most effective location, midspan or close to it. But the curves of the bridge with b/a = 0.20 show that the maximum moments in the girders are greatly reduced by adding the diaphragms. For b = 5 and 7 ft, Girder C is significant. Either Girder B or C becomes significant for b = 9 ft. With κ ranges from 0 to 0.40, the curves of the edge girders and interior girders never intersect. Thus, the maximum moments are controlled by the interior girders for any girder spacing between 5 to 9 ft, and κ = 0 to 0.40.

5.6.2 Effects of Varying Locations of Diaphragms

The diaphragms, as discussed in Sec. 5.3.2 for a single load on

the bridge, have the most effect on the moments in the girders at the points of intersection of diaphragms and girders, and are less effective for other points. It is also true for the 4-wheel loadings. The effects of varying the location of diaphragms may be studied from the three sets of curves mentioned below.

Consider the influence lines for moment at midspan and moment envelopes for the bridges with one diaphragm at midspan and two diaphragms at the quarter-points, as shown in Figs. 5.30 and 5.33, respectively. It may be observed that the variations of the moments, with changes in diaphragm stiffness, at midspan in both the edge and interior girders for the bridge with one diaphragm at midspan are greater than those for the bridge with two diaphragms of the same stiffness at quarter-points. On the other hand, the curves in the same figures show that the variations of the moments at quarter-points in both the edge and interior girders for the bridge with two diaphragms at quarter-points are greater than in the bridge with one diaphragm at midspan. Another example is in the bridges with one diaphragm and three diaphragms, as shown in Figs. 5.30 and 5.34, respectively. The influence lines for moment at midspan of the edge and interior girders of both bridges show that the differences of the variations of moments at midspan due to 4-wheel loading moving along the span of the bridge with one diaphragm and the corresponding values of the bridge with three diaphragms are small. But, the moment envelopes of the girders in both bridges show that the variations of the moments at other locations along the span for the bridge with three diaphragms are greater than in the bridge with one diaphragm.

It may be concluded that the contribution of the diaphragms located at the quarter-points to the moments of the midspan is small, and the effect of the diaphragm located at midspan upon the moments at the quarter-points is also small. However, the combined effects of the diaphragms located both at midspan and quarter-points are greater than either one diaphragm at midspan or two diaphragms at quarter-points. Consequently, if several diaphragms are closely spaced along the span of the bridge as the load transferring device, one may expect that the load distribution of this bridge is similar to the bridge without diaphragms, but with increased slab stiffness or torsional stiffness of the girders.

The effects of varying the locations of diaphragms on the maximum moment in the girder of the bridge can be studied from the second set of curves, as shown in Figs. 5.35 to 5.37. For example, adding diaphragms with $\kappa = 0.20$ at the 5/12 points, third-points and quarter-points of the bridge shown in Fig. 5.35, the maximum moment in Girder A, for b = 9 ft, changes from 0.345 Pa to 0.375 Pa, 0.365 Pa and 0.355 Pa, respectively; that in Girder B changes from 0.354 Pa to 0.310 Pa, 0.329 Pa and 0.345 Pa; and that of Girder C from 0.361 Pa to 0.259 Pa, 0.287 Pa and 0.302 Pa, respectively. For a constant relative diaphragm stiffness, the increase of the maximum moment in Girder A, and the decreases of the maximum moments in Girders B and C, are largest when the diaphragms are located near the midspan, and become smaller as the diaphragms move away from the midspan. This is also true for other girder spacings.

Consider a bridge with a diaphragm at midspan and one with two diaphragms at the 5/12 points with all diaphragms having the same stiffness. The curves show that the variations of moments in the girders, both interior

and edge girders, are slightly different. This means that the effects of adding one diaphragm at midspan or two diaphragms at the 5/12 points to the bridge are almost the same.

For the bridges with b/a = 0.10 with H = 5 and 40, and H = 20 with b/a = 0.05 and 0.20, the curves show that the effects of varying the locations of diaphragms are similar to those in the standard bridge. That is, for constant stiffnesses of diaphragms, the changes in the maximum moments in the girders are larger for the diaphragms located at the 5/12 points than for those located at the third-points.

With the relative diaphragm stiffness in the practical range, κ = 0 to 0.40, the effects of varying the locations of diaphragms may be summarized as follows:

1. The diaphragms are effective in reducing the moments in the girders at the points of intersection of girders and diaphragms;
2. For a certain value of κ, the variations of the maximum moments at midspan are large if the diaphragms are located at midspan or close to it, and become small if the diaphragms move from midspan toward the supports. One may say that for a certain increase of the moment at midspan of the edge girder, or a certain reduction of the moment at midspan of the interior girder, which is produced by relatively flexible diaphragms if they are located at or close to midspan, but by stiffer diaphragms if they are located away from the midspan;

3. With a certain value of κ, the variations of the maximum moments in both the edge and interior girders are almost the same for bridges with a diaphragm at midspan, two diaphragms at the 5/12 points, and three diaphragms at the quarter-points and midspan; and
4. For a certain b, the transition points at which the maximum moments change from the interior girders to the edge girder correspond to more flexible diaphragms if they are located at or close to midspan, and to stiffer diaphragms if they are located close to the supports.

5.6.3 Effective Stiffness and Location of Diaphragms for Various Bridges

In the slab and girder bridge structures, the maximum moments in the girders due to wheel loads are always at the midspan. The purpose of this study is to find the reductions in the maximum moments caused by adding the most effective diaphragms to each particular bridge. A series of bridges has been studied with various stiffnesses and locations of diaphragms. The effects of varying the relative diaphragm stiffness and their locations were studied in Sec. 5.6.1 and 5.6.2.

The studies of the effects of varying the stiffness and location of diaphragms show that load distribution are not always improved by adding the diaphragms. Diaphragms do reduce the maximum moments in some girders of some bridges, but they may increase the maximum moments in others. One should keep in mind that the diaphragms always reduce the moments in the interior girders, but increase the moments in the edge girders.

It may be stated, in general, that diaphragms should not be added to those bridges in which the load distribution without diaphragms is quite uniform, or fairly uniform when the outer wheel can be located on the edge girder. Diaphragms may be added to those bridges in which the load distribution is nonuniform and needs to be improved, since in the bridges with nonuniform load distribution, the maximum moment is always controlled by the interior girder, C.

One should recall the discussion in Sec. 5.4 concerning the load distribution in the fourteen bridges due to 4-wheel loadings. The influence lines for moment at midspan and moment envelopes of those bridges are given in Figs. 5.21 to 5.26. It has been mentioned that the bridges with small values of b/a and H have better load distributions than the other bridges. The classifications of the load distribution of the fourteen bridges may be summarized as follows:

1. The bridges with uniform load distribution include those with b/a = 0.05 and H = 10, 20 and 40, and b/a = 0.10 and H = 5 and 10;
2. The bridges with fairly uniform load distribution include those with b/a = 0.10 and H = 20, b/a = 0.15 and H = 5, and b/a = 0.20 and H = 5; and
3. The bridges with nonuniform load distribution include those with b/a = 0.10 and H = 40, b/a = 0.15 and H = 10, 20 and 40, with b/a = 0.20 and H = 10 and 20.

The studies of the relative stiffness and location of diaphragms show that for a constant value of κ, the load distribution of the bridge with a diaphragm at the midspan, two diaphragms at the 5/12 points, and

diaphragms at the quarter-points and midspan are almost the same. If the economic cost and time savings in construction are concerned, only a diaphragm at midspan need be considered. Thus, the five locations of diaphragms are reduced to three, namely, a diaphragm at midspan, two diaphragms at the third-points, and two diaphragms at the quarter-points.

The most effective combination of stiffness and location of diaphragms for the various bridges may be studied from the curves given in Figs. 5.38 and 5.39. The curves in Fig. 5.38 are the relationships between the maximum moment in the significant girder and the relative diaphragm stiffness for the bridges with b/a = 0.10 and H = 5, 10, 20, and 40. Similar curves, for the bridges with H = 20 and b/a = 0.05, 0.10, 0.15, and 0.20, are given in Fig. 5.39. Two locations of diaphragms are presented, namely, a diaphragm at the midspan and two diaphragms at the third-points. The curves in Fig. 5.38 represent the bridges with medium length span. The bridges with H = 5 and 10 are classified as having uniform load distribution. The bridges with H = 20 and 40 are classified as having fairly uniform or nonuniform load distribution.

If the outer wheel may come over the edge girder, the curves for the bridges with b/a = 0.10 and with H = 5, 10, and 20 show that the diaphragms should not be added for any girder spacing between 5 to 9 ft, since they increase the maximum moment in the girder. It should be noted that the moment in the bridge with H = 20 and b = 7 ft can be reduced slightly by adding a flexible diaphragm, κ = 0.05, at the midspan. However, it may be harmful for the truck loads. The curves for the bridge with H = 40 and b = 5 ft show that by adding a diaphragm with κ = 0.05 at midspan, or two diaphragms each having κ = 0.05 at the third-points, the maximum moment can

be reduced from 0.265 Pa to 0.242 Pa. For b = 7 ft, the maximum moment can be reduced from 0.344 Pa to 0.302 Pa by adding a diaphragm with κ = 0.06 at midspan, or to 0.309 Pa with diaphragms with κ = 0.06 at the third-points. If b = 9 ft, the maximum moment can be reduced from 0.396 Pa to 0.353 Pa or 0.358 Pa, by adding a diaphragm with κ = 0.02 at the midspan, or two diaphragms with κ = 0.05 at the third-points, respectively.

It may be concluded that if the outer wheel may come over the edge girder, bridges with H = 5, 10 and 20 should not have the diaphragms. With a flexible diaphragm, κ = 0.02 to 0.06 depending on the girder spacing at midspan of the bridge with H = 40, the maximum moment can be reduced significantly. A diaphragm at the midspan is most effective.

If the outer wheel is located at least 2 ft from the edge girder, the maximum moment in all bridges can be reduced by adding the diaphragms. The reductions of moments are greater for the bridges with a diaphragm at the midspan than those with two diaphragms at the third-points. For b = 5 ft, the maximum moments in all bridges are controlled by the interior girders for κ = 0 to 0.40, since the moments decrease as the values of κ increase. However, the rates of decreasing become small if κ is greater than 0.20. With a medium stiff diaphragm, κ = 0.20, at the midspan, the maximum moment for the bridge with H = 5 is reduced from 0.225 Pa to 0.210 Pa, and the one with H = 40 is reduced from 0.266 Pa to 0.224 Pa. The reduction of moment is 6.5 percent for the former and 15.8 percent for the latter. For b = 7 ft, the maximum moments for all bridges are controlled by the interior girders if a diaphragm for which κ is not greater than 0.20 to 0.25, depending on the value of H, is located at midspan. With a stiffer diaphragm, Girder A becomes significant. With this value of κ, the maximum

moment of the bridge with H = 5 is reduced from 0.275 Pa to 0.258 Pa, and the one with H = 40 is reduced from 0.344 Pa to 0.268 Pa, the reductions of moments are 6.2 percent for the former and 22.1 percent for the latter.

It is noted that the maximum moments of the bridges with a diaphragm, κ = 0.10, at the midspan and two diaphragms, each having κ = 0.40, are almost identical. A flexible diaphragm at the midspan is as effective as two stiff diaphragms at the third-points.

For b = 9 ft, the values of κ where the transition points occur, are 0.06, 0.08, 0.13 and 0.17 for the bridges with H = 5, 10, 20 and 40, respectively. With these values of κ, the moment is reduced from 0.317 Pa to 0.300 Pa for the bridge with H = 5, and from 0.396 Pa to 0.320 Pa for the bridge with H = 40. The percentages of the reductions of moments are 5.4 percent for the former, and 19.2 percent for the latter.

It may be concluded that, if the outer wheel is located at least 2 ft from the edge girder, the diaphragms need not be added to the bridges with H = 5 and 10, since the reductions of moments are small. With a fairly flexible or medium stiff diaphragm, κ = 0.05 to 0.25, at the midspan of the bridges with H = 20 to 40, the maximum moments can be reduced substantially. A diaphragm at the midspan is the most effective.

If the outer wheel can come over the edge girder of the bridges with H = 20 and b/a = 0.05, 0.10, 0.15 and 0.20, the curves in Fig. 5.39 show that the diaphragms should not be added to the bridges with b/a = 0.05 and 0.10, since Girder A controls, and the maximum moments, consequently, are increased for all values of b. But the curves for the bridges with b/a = 0.15 and 0.20 show that the maximum moments are reduced by adding the diaphragms with various stiffnesses at the midspan or the third-points. It was

mentioned earlier that the bridges with b/a = 0.05 and 0.10 are classified as having the uniform, and fairly uniform load distributions, respectively. But the bridges with b/a = 0.15 and 0.20 have nonuniform load distributions.

For b = 5 ft, the maximum moment of the bridge with b/a = 0.15 can be reduced from 0.275 Pa to 0.250 Pa by adding a diaphragm with κ = 0.05 at the midspan, or two diaphragms, κ = 0.10 for each, at the third-points. The reduction of moment is 9.1 percent. For the same girder spacing, the maximum moment for the bridge with b/a = 0.20 is controlled by the interior girder for κ ranging from 0 to 0.40, even though the outer wheel may come over the edge girder. By adding the diaphragm with κ = 0.20 at the midspan, or the third-points, the moment is reduced from 0.280 Pa to 0.250 Pa, or by 10.7 percent. However, the rate of decreasing of the moment with increases of the diaphragm stiffness is small for both bridges.

For b = 7 ft, the curves for the bridge with b/a = 0.15 show that with a medium stiff diaphragm, κ = 0.15 at the midspan, or two diaphragms, κ = 0.20 or greater, at the third-points, the moment can be reduced from 0.351 Pa to 0.308 Pa, or by 12.3 percent. An increase in the stiffness of the midspan diaphragm causes Girder A to become significant, thus increasing the moment. The maximum moment of the bridge with b/a = 0.20 is still controlled by the interior girder for κ = 0 to 0.40. With a midspan diaphragm, or third-points diaphragms, the maximum moment may be reduced from 0.361 Pa to 0.312 Pa and 0.307 Pa for κ = 0.20 and 0.40, respectively. The reductions of moments are 13.6 percent for the former and 15 percent for the latter. It is noted that the maximum moments with a diaphragm at the midspan, or with two diaphragms having the same stiffnesses as the midspan diaphragm, are almost identical.

For b = 9 ft, the most effective relative diaphragm stiffnesses, for the bridge with b/a = 0.15, are 0.05 if there is one diaphragm at midspan, or 0.10 if there are two located at the third-points. With these values of κ, the maximum moment is reduced from 0.41 Pa to 0.355 Pa for both locations of diaphragms, a reduction of 13.6 percent. For the stiffer diaphragms, Girder A becomes significant, thus the moment will increase. The most effective values of κ for the bridge with b/a = 0.20 are 0.16 for a diaphragm at the midspan, or 0.25 for two diaphragms at the third-points. The maximum moments for both cases are reduced from 0.430 Pa to 0.357 Pa, which is a 17 percent reduction.

If the outer wheel is located at least 2 ft from the edge girder, the interior girder controls the maximum moment for all bridges with b = 5 ft. A diaphragm at the midspan is the most effective. With the values of κ between 0 to 0.40, the moments decrease as κ increases. However, the rate of decrease is slow, especially if κ is greater than 0.20. The reduction of moment is small for the bridge with b/a = 0.05.

For b = 7 ft, the diaphragms do not improve the moment of the bridge with b/a = 0.05. A diaphragm at the midspan is more effective than two diaphragms at the third-points for the bridge with b/a = 0.10. The most effective diaphragm stiffness for this bridge is κ = 0.20, with which the maximum moment can be reduced from 0.320 Pa to 0.278 Pa, a reduction of 13.1 percent. If κ is greater than 0.20, Girder A control. For bridges with b/a = 0.15 and 0.20, the effects of a diaphragm located at the midspan is slightly better than two diaphragms located at the third-points. The interior girders control the maximum moments for these two bridges. The curves for the bridge with b/a = 0.15 show that if κ is greater than 0.35,

the reduction of moment is small. With this value of κ, the moment can be reduced from 0.350 Pa to 0.275 Pa which is 21.4 percent reduction. But the curve of the bridge with b/a = 0.20, show that the reduction of moment may still be considerable if κ is greater than 0.40. However, with κ = 0.40, the moment is reduced from 0.360 Pa to 0.290 Pa. The reduction is 19.5 percent, and may reach 25 percent for the stiffer diaphragm.

For b = 9 ft, diaphragms should not be added to bridges with b/a = 0.05. A diaphragm with κ = 0.13 at the midspan of the bridge with b/a = 0.10 is very effective, but a stiffer diaphragm is harmful. For b/a = 0.15 and 0.20, a diaphragm at the midspan is slightly better than two diaphragms at the third-points. If κ is greater than 0.40, the rate of decrease of moment becomes small. With κ = 0.13 and 0.40, the moments are reduced from 0.360 Pa to 0.312 Pa, 0.411 Pa to 0.325 Pa, and 0.430 Pa to 0.341 Pa, for the bridges with b/a = 0.10, 0.15 and 0.20, respectively. The corresponding percentages of reduction are 13.3 percent, 20.9 percent and 20.7 percent.

It is noted that, for b = 7 ft, there are two curves for the bridge with b/a = 0.10, and where the outer wheel is located at least 2 ft from the edge girder. The solid line represents the bridge with T = 0.011, which is the actual value of the prestressed concrete I-section. The broken line represents the bridge with T = 0. As discussed in Sec. 5.2.4 for a single load moving across the bridge, the load distribution of the bridge with T = 0.011 is slightly better than the one with T = 0. For the 4-wheel loadings, the former also has a slightly better load distribution than the latter. However, the percentages of reduction of moments due to adding diaphragms is slightly greater for the bridge with T = 0 than the one with T = 0.011.

It is also noted that the curves for moments in bridges with large values of H, for example, H = 40, in Fig. 5.38, descend very fast with increasing values of κ between 0 to 0.10. But the curves for the large values of b/a, for example, b/a = 0.15 and 0.20 in Fig. 5.39, descend much more slowly for that range of κ, in comparison to those for large values of H. All of these bridges are classified as having nonuniform load distributions. The reasons for the differences in behavior lie in the fact that even for the same value of κ, the actual diaphragms in the bridges vary with b, b/a, and H. For example, the diaphragm in the bridge with b/a = 0.10 and H = 40 is four times as stiff as the one in the bridge with b/a = 0.20 and H = 20, provided that κ and b remain the same.

From the study of the variations of moments for various stiffness and locations of diaphragms of several bridges, it may be concluded, in general, that:

1. The most effective and economical location of the diaphragm is at the midspan;
2. The diaphragms should not be added to those bridges which are classified as having uniform load distribution, for any loading conditions;
3. For those bridges classified as having fairly uniform load distributions, diaphragms should not be added if the outer wheel can come over the edge girder. If the outer wheel is located at least 2 ft from the edge girder, the maximum moment may be reduced by 10 percent to 15 percent by adding a diaphragm ranging from fairly flexible to medium stiff, κ = 0.10 to 0.20, at midspan. The stiffer diaphragms

correspond to smaller girder spacing. The maximum reduction of moment for the bridge with b/a = 0.10 and H = 20 is 13 percent;

4. For those bridges classified as having nonuniform load distribution, the diaphragms do reduce the maximum moments. If the outer wheel can come over the edge girder, the moment may be reduced by 8 percent to 12 percent for the bridges with b/a = 0.10 and 0.15, and 12 percent to 17 percent for the bridges with b/a = 0.20. The most effective κ is from 0 to 0.05 for the bridges with b/a = 0.10, 0.05 to 0.10 for those with b/a = 0.15,and 0.15 to 0.40 for the bridges with b/a = 0.20. The larger percentages of reduction of moments correspond to the larger girder spacings.

   If the outer wheel is located at least 2 ft from the edge girder, the maximum moment can be reduced by 19 percent to 22 percent by adding a diaphragm ranging from medium to very stiff, κ = 0.15 to 0.40, at midspan. The most effective values of κ are from 0.15 to 0.20 for the bridge with b/a = 0.10, and 0.20 to 0.40 for those with b/a = 0.15 and 0.20.

5.7 Bridges Subjected to Truck Loads

The discussions presented in Secs. 5.4, 5.5 and 5.6, are concerned with the 4-wheel loadings moving on the bridges. This type of loading represents two rear axles of two adjacent trucks. The maximum moments in the girders of most bridges occur at the midspan due to 4-wheel loadings located

at the midspan, except that in bridges with a stiff diaphragm at the midspan the maximum moments occur at a section between the midspan and the third-points. However, most of the diaphragms used in practice have relative stiffnesses less than 0.40, and the differences between the maximum moment and the moment at the midspan are small.

In the following discussion, in order to simplify the problem, the moment at the midspan is taken as the maximum moment. Thus, the curves representing the influence lines for moment at midspan and the moment envelopes, given in Figs. 5.21 to 5.26 and 5.29 to 5.34, can be used to obtain the maximum moments in the girders at midspan due to multi-axle truck loadings on various bridges. Since the maximum moments in the girders are considered to be midspan, the trucks have to be arranged so that the center axle of each three-axle truck is located at midspan. This loading condition is possible when one truck passes another in the adjacent lane, as shown in Fig. 5.1.

It has been mentioned previously that the influence lines for moment at midspan of the edge girder are convex curves, but those for the interior girders are slightly concave. Thus, the moment at midspan in an edge girder due to the truck loads may be greater than that in the interior girder even though the moment due to 4-wheel loading at midspan was less.

With the influence lines for moment at midspan, the maximum moments in the significant girder of the standard bridge subjected to two trucks were obtained for various girder spacings. Two trucks with HS20 loadings as shown in Fig. 5.1(b) were considered. The relationships between the maximum moment in the significant girder and the girder spacing for the bridges without diaphragms, with various locations of diaphragms, and with

the torsional stiffnesses of the girders equivalent to the box section, are given in Fig. 5.40. Loading condition with the outer line of wheels over the edge girder or 2 ft from the girder were considered. The relative diaphragm stiffnesses were 0.05, 0.20, and 1000.

The curves show that the maximum moments in the girders are greatly reduced for the bridge with box section girders, for both loading conditions. But the curves of the bridges with diaphragms show that the maximum moments may either increase or decrease depending on the loading condition, the stiffness of diaphragm, and the girder spacing.

If the outer wheel can come over the edge girder, the maximum moments in the girder of the bridges with I-section are 0.390 Pa and 0.665 Pa for b = 5 and 9 ft, respectively. But, the maximum moments for the corresponding b of the bridges with box sections, are 0.330 Pa and 0.490 Pa, which are 84.7 percent and 73.7 percent of moment in the I-section bridges. It is noted that the coefficients for the box section girders and for the I-section for small girder spacings are taken from the curves in which the outer wheel is located at least 2 ft from the edge girder, since this gives the maximum values.

In adding the diaphragms at various locations, the curves show that the maximum moments are increased for any girder spacing and relative diaphragm stiffness, except that the moment for b = 5 ft and κ = 0.05, is slightly reduced. The increase of moment corresponds to the increase of the diaphragm stiffness. Thus, diaphragms should not be added to this standard bridge if the outer wheel may come over the edge girder.

It is noted that, for κ = 0.05 and 0.20, the curves for a diaphragm at midspan, two diaphragms at 5/12 points, and three diaphragms, are almost identical.

If the outer wheel is located at least 2 ft from the edge girder, the maximum moments in the girder of the bridges with I-section girders are 0.390 Pa and 0.660 Pa and b = 5 and 9 ft, respectively. For the same girder spacings, the maximum moments in the girder of the bridges with box section girders, are 0.330 Pa and 0.461 Pa, which are 84.7 percent and 70 percent of the I-section bridges.

The maximum moments are also reduced by adding diaphragms at various locations, except a stiff diaphragm should not be placed at or close to midspan for the larger values of b. For these three values of κ, the curves show that the most effective diaphragm stiffness are 0.05 for b = 7, 8, and 9 ft, and 0.20 for b = 5 and 6 ft. The three most effective locations of diaphragms are midspan, 5/12 points, and midspan and quarter-points. However, the differences of moments among these three locations of diaphragms are small. Thus, a diaphragm at midspan is preferable, since it is more economical.

For κ = 0.05, the maximum moments are controlled by the interior girder for any girder spacing and location of diaphragms. If κ = 0.20 or greater, the edge girder becomes significant for the three effective locations of diaphragms and b = 7, 8 and 9 ft, thus the maximum moments are increased. However, for b = 5 and 6 ft, the maximum moments are still controlled by the interior girder, so the values are smaller than those with κ = 0.05. If κ = 1000, the maximum moments are controlled by the edge girder, except the bridge with two diaphragms at quarter-points, and b = 5 ft for other locations of diaphragms.

It has been discussed in Sec. 5.6.3 that the transition points where the maximum moments change from the interior girder to the edge girder

of this standard bridge subjected to 4-wheel loadings are at the values of κ = 0.15 and 0.20 for b = 9 and 7 ft, respectively. However, since the influence lines for moment at midspan of the edge girders are convex curves and for the interior girders are concave curves, the moment in the edge girder due to the truck loads is greater than that in the interior girder, with the same diaphragm stiffnesses.

Thus, the most effective values of κ determined from the 4-wheel loadings as discussed in Sec. 5.6.3 have to be reduced for turck loadings. The values of κ for this standard bridge should be less than 0.20 for a diaphragm located at midspan if b is equal to or greater than 7 ft. It has been found that the maximum moment due to the truck loads is still taken by the edge girder for κ = 0.10 and b = 9 ft, while an interior girder controls if κ = 0.

It may be concluded that a diaphragm, with κ varying from 0.05 to 0.20 depending on the value of b, located at midspan is effective for this standard bridge, if the outer wheel is located at least 2 ft from the edge girder. The value of κ = 0.05 corresponds to b = 9 ft, and κ = 0.20 corresponds to b = 5 ft. For b = 5 ft, the maximum moment can be reduced from 0.390 Pa to 0.330 Pa by adding a diaphragm with κ = 0.20 at the midspan of the bridge. The latter moment is 85 percent of the former. For b = 9 ft, the maximum moment can be reduced from 0.660 Pa to 0.570 Pa by adding a diaphragm with κ = 0.05 at the midspan. The percentage for this case is 86 percent.

If the outer wheel can come over the edge girder, the diaphragms should not be added to the bridge.

Chapter 6

RECOMMENDATION FOR DESIGN

The slab and girder bridge is a very complicated structure. A very large amount of computation is needed to obtain, accurately, the forces in the girders, and this is usually not possible in practice. Consequently, in present design practice, assumptions have been made which neglect the effects of some important parameters controlling the load distribution in this type of structure.

In the present analysis of the slab and girder bridges with prestressed concrete I-section girders, the most important parameters affecting the load distribution, as discussed in Chapter 2 , have been taken into account. With the aid of an electronic computer, a large number of bridges have been analyzed, taking into account the ranges of the various parameters.

The results obtained from this study and discussed in Chapter 5 have provided information for the bridge engineers to design this complicated structure with a more realistic and accurate method. A set of curves of the influence lines for moment at midspan and moment envelopes due to 4-wheel loadings moving along the span of the bridges with prestressed concrete I-section girders is presented in Figs. 5.21 to 5.26.

This set of curves can be used to determine design moments for any bridges with the ratio of the relative bridge geometry, b/a = 0.20 to 0.05, the ratio of the relative girder stiffness, H = 5 to 40, and the girder spacing, b = 5 to 9 ft. With this range of b/a and the present standard prestressed concrete I-section girders, the curves may be used for the bridges with spans varying from 30 to 150 ft. The curves presented in Figs. 5.27 and

5.28 give a general method of obtaining the moment coefficients if the values of b/a and H are not exactly the same as those given in Figs. 5.21 to 5.26.

The curves are provided for two loading conditions, namely, when the outer load, P, can come over the edge girder, and when it is located at least 2 ft from the edge girder. However, in the bridges with any values of H from 5 to 40 and for b/a = 0.15 and 0.20, and for H = 40 and b/a = 0.10, the maximum moments are always in Girder C, and the controlling loading is always with the outer P located at least 2 ft from the edge girder.

For the bridges with b/a = 0.05 and H = 10 and 20 and with the outer load, P, located at least 2 ft from the edge girder, the moment at midspan of the interior girder is greater than the edge girder if the 4-wheel loads are located at midspan, but it may be less than that of the edge girder if the loads are located away from the midspan. Thus, the curves of both the interior and edge girders are given, since the moments due to the truck loads may be greater for the edge girder.

The maximum moment in the girders due to the truck loads can be obtained by placing the trucks as shown in Fig. 5.1. The axles of these two adjacent trucks form a number of 4-wheel loadings, and the design moment coefficients are obtained by adding the appropriate ordinates of the influence lines for moment at midspan, using the curves for the proper values of b/a, H, and b. If these values do not correspond exactly to those of the bridge being designed, interpolations should be made. The total moment is determined by summing up the moment coefficients and multiplying by the load, P, and span, a.

The study of the effects of diaphragms on the load distribution of this type of structure shows that the addition of diaphragms in the

prestressed concrete I-section girder bridge does not always reduce the maximum moments. In certain cases, they increase the maximum moments and thus cause harmful effects. It was found that a flexible diaphragm properly located may have more advantageous effects than two stiffer diaphragms at some other locations. At the same location in the bridge, a flexible diaphragm may reduce the maximum moment, but a stiffer diaphragm may increase it. Thus, a stiff diaphragm is not necessarily better than a flexible one in accomplishing its purpose of lowering the controlling moment in a certain girder.

From the extensive study of the effects of diaphragms on various bridges, it was found that the addition of diaphragms to a bridge already having a uniform load distribution may either reduce or increase the maximum moment, depending on the loading conditions and girder spacing. For bridges having a less uniform load distribution, the addition of diaphragms may reduce the maximum moments significantly.

For the purpose of helping determine whether a diaphragm may be effective for particular cases, the bridges, with the restriction that the value of H should not be less than 5, may be classified into three groups as follows:

1. Bridges with uniform load distribution: Values of b/a not greater than 0.10, with the upper limits of H = 40 for b/a = 0.05 and 10 for b/a = 0.10. For b/a between 0.05 to 0.10, the upper limit of H may be obtained from the interpolation between H = 10 and 40.
2. Bridges with fairly uniform load distribution: Values of b/a not greater than 0.15 with the lower limits of H = 40 for b/a = 0.05 and 10 for b/a = 0.10, and the upper limits

of H = 60 for b/a = 0.05 and 10 for b/a = 0.15. For b/a between 0.05 and 0.15, the upper limit of H may be obtained by interpolation between H = 10 and 60.

3. Bridges with nonuniform load distribution: Values of b/a not less than 0.05, and the lower limits of H are 60 and 10 for b/a = 0.05 and 0.15, respectively. For b/a between 0.05 and 0.15, the lower limit of H may be obtained from the interpolation between 10 and 60.

These relationships are shown graphically in Fig. 6.1.

Since the purpose of a good design is to utilize the material to its best advantage, it is important in the design of the diaphragms for this type of bridge to choose the appropriate stiffness of diaphragm to be placed at the most effective location for a certain bridge. A study of the results of the analysis, however, leads to certain conclusions of the behavior of bridges with diaphragms. These conclusions may serve as useful rules in actual practice in obtaining the most benefit from diaphragms in the slab and girder bridges with prestressed concrete I-section girders. The rules that follow are derived entirely from this analytical study and apply directly to simple-span right bridges consisting of a continuous slab supported by at least five identical girders with the girder spacing between the limits of 5 to 9 ft:

1. For bridges classified as having uniform load distribution, diaphragms should not be added if the outer P may come over the edge girder. If the outer P is located at least 2 ft from the edge girder, unless b/a is less than 0.10 and b = 9 ft, a flexible or fairly flexible diaphragm, κ = 0.05 for

b = 7 to 9 ft and κ = 0.10 for b = 5 and 6 ft, may be added to the bridge at the midspan. The maximum moment in the bridge may be taken as 95 percent of that in the same bridge without the diaphragm.

2. For bridges classified as having fairly uniform load distribution, diaphragms should not be added if the outer P may come over the edge girder. If the outer P is located at least 2 ft from the edge girder, a fairly flexible or medium stiff diaphragm, κ = 0.10 for b = 7 to 9 ft and 0.20 for b = 5 and 6 ft, may be added to the bridge at the midspan. The maximum moment in the bridge may be taken as 85 to 90 percent of the moment in the same bridge without the diaphragm.
3. For bridges classified as having nonuniform load distribution, a midspan diaphragm may be added to certain bridges as follows: If the outer P may come over the edge girder:
   a. κ = 0.05, for bridge with b/a $\leq$ 0.10 and b = 5 to 7 ft, and b/a = 0.10 to 0.15 with b = 8 or 9 ft;
   b. κ = 0.05 to 0.10 for bridge with b/a = 0.10 to 0.15 and b = 5 to 7 ft, the larger κ corresponding to the larger b/a;
   c. κ = 0.10 to 0.15 for bridge with b/a = 0.15 to 0.20 and b = 8 or 9 ft, the larger κ corresponding to the larger b/a;
   d. κ = 0.15 to 0.40 for bridge with b/a = 0.15 to 0.20 and b = 5 to 7 ft, the larger κ corresponding to the larger b/a.

The maximum moment in the bridge may be taken as 90 percent of the moment in the same bridge without diaphragms for cases a, b, and d, and 85 percent for case c.

If the outer P is at least 2 ft from the edge girder:

a. $\kappa = 0.15$ for a bridge with b/a not greater than 0.10;

b. $\kappa = 0.15$ to 0.40 for a bridge with b/a = 0.10 to 0.15;

c. $\kappa = 0.40$ for a bridge with b/a = 0.15 to 0.20.

The maximum moment in the bridge may be taken as 85 percent of that in the same bridge without diaphragms, for b = 5 and 6 ft, and 80 percent for b = 7 to 9 ft.

In the study of the standard bridge with the torsional stiffnesses of the girders equivalent to those of the prestressed concrete box section, the results show that the maximum moment of the bridge is reduced substantially. For example, the maximum moment in the bridge with box section girders is 85 percent of that of the I-section girders if b = 5 ft, and 70 percent if b = 9 ft.

The results of this study lead to a suggestion that a thorough study of bridges with prestressed concrete box section girders should be made. The influence lines for moment at midspan and moment envelopes should be obtained for practical use. The study of bridges with prestressed concrete box section girders may show that it is possible to use limit design concepts for this type of bridge.

Chapter 7

SUMMARY

The method of analysis for solving the problems of slab and girder bridges is presented in Chapter 3 and in Appendixes A, B, and C. The flexibility method using Fourier series type solution was used. The in-plane forces and the torsional and warping stiffnesses of the girders are taken into consideration. The method of analysis of the effects of diaphragms is also developed, and is presented in Chapter 4 and Appendix D. A computer program has been written for the IBM-360/75.

With the aid of the electronic computer, a large number of bridges has been analyzed. The structures considered in the analyses are simple-span right bridges, consisting of a continuous slab supported by five uniformly spaced parallel girders of equal stiffness, with the girders running in the direction of traffic.

A bridge with six girders was analyzed, and the results compared with those for five girder bridges. In order to study the effects of the torsional and warping stiffnesses of the girders, a standard bridge has also been analyzed, varying these parameters. The torsional stiffness is increased up to that of the box section girder.

The diaphragms, which are usually cast monolithically with the slab, were modified for purposes of analysis as discussed in Chapter 4. In this study, a number of these structures with different proportions with diaphragms of various stiffnesses and at different locations in the bridge are considered.

Several variable parameters were studied, including:

1. Relative dimensions of the bridge,
2. Relative stiffness of girders to that of the slab,
3. Relative torsional to flexural stiffness of girder,
4. Relative warping to torsional stiffness of girder,
5. Relative stiffness of diaphragm to that of girder,
6. Number and location of diaphragms in the structure,
7. Type and location of loadings.

Studies of the practical ranges of these parameters are presented in Chapter 2.

The results of the analyses were discussed in Chapter 5. Several kinds of curves are presented in Figs. 5.3 to 5.40. The influence lines for maximum moment in the girder at midspan and moment envelopes due to 4-wheel loadings moving along the span for a series of bridges suitable for spans ranging from 25 to 150 ft and with relative girder stiffnesses corresponding to standard prestressed concrete I-sections are presented in Figs. 5.21 to 5.26. The purpose of providing these curves is to enable the designer to obtain the maximum moments due to the truck loadings, and to aid in location of the profile of the prestressing strands.

In the study of the effects of diaphragms on this type of structure, comparisons were made to obtain the most effective stiffnesses and locations of diaphragms for various bridges. The criterion of comparison is, in general, the maximum moment in the girders produced by a concentrated load, the 4-wheel loading, and the truck loading. These studies are presented in Cahpter 5 and certain rules that should lead to favorable use of diaphragms in slab and girder bridges with prestressed concrete I-sections are formulated in Chapter 6

The output from the computer has also provided information, for future study, on the forces in the diaphragms, and the shearing forces between the slab and the top flange of the girders of the bridges. This information is necessary if the diaphragms and shear connectors are to be properly designed.

A number of important conclusions concerning the effects of diaphragms on the distribution of moments within the bridge structure may be drawn, as was shown in Chapter 6.

First, the addition of diaphragms to a structure may not reduce the maximum moments and may in some cases cause moderate increases. The addition of diaphragms to a bridge with a span in excess of 60 or 70 ft produces either no reduction or an increase in maximum girder moments. Properly designed diaphragms may be capable of reducing the maximum moments in some structures, usually in the cases of short span structures with relatively wide beam spacings. In no case can diaphragms result in major reductions in controlling moments.

Second, only diaphragms at or very near the section of maximum moment can cause measurable changes in the controlling girder moments. A single diaphragm at midspan or two diaphragms located one sixth of the span each side of midspan were found to have the same effects, though not the same costs. Diaphragms located at the third or quarter points of the span were not effective in reducing the maximum moments in the girders.

Third, the diaphragm must be of the correct flexural stiffness to be effective. Increasing the stiffness of a diaphragm beyond some particular value may lead to maximum moment values in excess of those existing before the diaphragm was added, even if the structure being considered is one which diaphragms can help.

LIST OF REFERENCES

1. Pippard, A. J. S. and J. P. A. Dewaele, "The Loading of Interconnected Bridge Girders," Journal, Institution of Civil Engineers, Vol. 10, No. 1, November, 1938, pp. 97-114.

2. Leonhardt, F. and W. Andra, "Die veremfachte Trägerrost-berechnung (The Calculation of Grillage Beams)," Julius Hoffman Press, Stuttgart, 1950.

3. Hendry, A. W. and L. G. Jaeger, The Analysis of Grid Frameworks and Related Structures, Chatto and Windus, London, 1958.

4. Timoshenko, S. and S. Woinowsky-Krieger, Theory of Plate and Shells, McGraw-Hill Book Company, 1959.

5. Guyon, Y., "Calcul des Ponts Larges á Poutres Multiples Solidarises par des Entretoises," Annales des Ponts et Chausees, Paris, 1946, September-October, pp. 553-612.

6. Massonnet, C., "Method de Calcul des Ponts á Poutres Multiples tenant Compte de Leur Resistance a la Torsion," Publications International Association for Bridge and Structural Engineering, Zurich, 1950, Vol. 10, pp. 147-182.

7. Morice, P. B. and G. Little, "Load Distribution in Prestressed Concrete Bridge Systems," The Structural Engineer, Vol. 32, No. 3, March, 1954, pp. 83-111.

8. Newmark, N. M., "A Distribution Procedure for the Analysis of Slabs Continuous over Flexible Beams," University of Illinois Engineering Experiment Station, Bulletin 336, 1942.

9. Newmark, N. M. and C. P. Siess, "Moments in I-Beam Bridges," University of Illinois, Engineering Experiment Station, Bulletin 336, 1942.

10. Newmark, N. M., C. P. Siess and R. R. Penman, "Studies of Slab and Beam Highway Bridges: Part I, Test of Simple-Span Right I-Beam Bridges," University of Illinois, Engineering Experiment Station, Bulletin 363, 1946.

11. Wei, B. C. F., "Effects of Diaphragms in I-Beam Bridges," Ph.D. Thesis, University of Illinois, Urbana, Illinois, 1951.

12. Siess, C. P. and A. S. Veletsos, "Distribution of Loads to Girders in Slab-and-Girder Bridges: Theoretical Analyses and Their Relation to Field Tests," Civil Engineering Studies, Structural Research Series No. S-13, Department of Civil Engineering, University of Illinois, Urbana, 1953.

13. Goldberg, J. E. and H. L. Leve, "Theory of Prismatic Folded Plate Structures," Memoirs, International Association for Bridge and Structural Engineering, Vol. 17, 1957, p. 59.

14. VanHorn, D. A. and D. Motarjemi, "Theoretical Analysis of Load Distribution in Prestressed Concrete Box-Beam Bridges," Lehigh University, Fritz Engineering Laboratory, Report No. 315-9, 1969.

15. Gustafson, W. C., "Analysis of Eccentrically Stiffened Skewed Plate Structures," Ph.D. Thesis, University of Illinois, Urbana, Illinois, 1966.

16. Badaruddin, S., "Analyses of Slab-and-Girder Highway Bridge," Ph.D. Thesis, University of Illinois, Urbana, Illinois, 1965.

17. "Standard Specifications for Highway Bridges," American Association of State Highway Officials, 1969.

18. "Design of Highway Bridges in Prestressed Concrete," Portland Cement Association, Structural and Railways Bureau, Concrete Information, 1969.

19. Gamble, W. L., D. M. Houdeshell and T. C. Anderson, "Field Investigation of a Prestressed Concrete Highway Bridge Located in Douglas County, Illinois," Civil Engineering Studies, Structural Research Series No. 375, Dept. of Civil Engineering, University of Illinois, Urbana, May 1971.

20. Gamble, W. L., "Field Investigation of a Continuous Composite Prestressed I-Beam Highway Bridge Located in Jefferson County, Illinois," Civil Engineering Studies, Structural Research Series No. 360, Department of Civil Engineering, University of Illinois, Urbana, June 1970.

21. Timoshenko, S. and J. N. Goodier, Theory of Elasticity, McGraw-Hill Book Company, 1957, p. 26 and p. 277.

22. Bleich, F., Buckling Strength of Metal Structures, McGraw-Hill Book Company, 1952, p. 122.

23. Timoshenko, S. and J. M. Gere, Theory of Elastic Stability, McGraw-Hill Book Company, 1961, p. 224.

Table 2.1

Strength of Concrete*

Type of Concrete	Stored in the Lab			Stored in the Field		
	Age days	f'_c psi	E^{**} in 10^6 psi	Age days	f'_c psi	E^{**} in 10^6 psi
Girder	16	5512	3.37	16	4930	3.45
	28	6128	3.63	28	5142	3.37
	90	7053	3.62	90	5906	3.24
	219	6840	4.19	219	7856	4.73
	420	5630	3.87	420	6920	4.57
Slab	29	6200	4.83	29	6560	5.50
	202	5400	4.55	202	5820	4.66
	367	6310	4.53	364	7050	4.90

* Values based on the average of three cylinders.

** Values measured from stress-strain curves.

Table 2.2

Parameters for Studies of Bridges Without Diaphragms

Dimensionless Parameters				Dimension Parameters			Beam	Depth	Range of Span
b/a	H	T	Q	Bridge span, a, ft	Girder spacing, b, ft	Slab thickness, h, in.	No.	in.	ft
0.20	5	0.028	0.014	42.50	8.50	8.00	1	28	
	10	0.026	0.015	42.50	8.50	6.00	1	28	25 - 45
	20	0.018	0.037	35.00	7.00	6.00	3	36	
0.15	5	0.029	0.012	46.75	7.00	7.50	1	28	
	10	0.013	0.020	56.50	8.50	8.00	5	44	35 - 60
	20	0.012	0.023	56.50	8.50	7.00	7	48	
	40	0.010	0.037	55.00	8.25	6.00	8	54	
0.10	5	0.028	0.008	55.00	5.50	7.75	2	32	
	10	0.012	0.012	80.00	8.00	8.00	7	48	50 - 90
	20	0.011	0.015	80.00	8.00	6.75	8	54	
	40	0.009	0.028	80.00	8.00	6.50	10	68	
0.05	10	0.012	0.008	120.00	6.00	8.00	9	60	
	20	0.010	0.012	120.00	6.00	7.00	10	68	90 -180
	40	0.009	0.014	130.00	6.50	6.00	11	78	

Table 2.3

Parameters for Studies of the
Effects of Torsion and Warping

Dimensionless Parameters			
b/a	H	T	Q
0.10	20	0.0001	0, 0.01, 0.02, 0.04
		0.01	0, 0.01, 0.02, 0.04
		0.02	0, 0.01, 0.02, 0.04
		0.04	0, 0.01, 0.02, 0.04
		0.06	0
		0.10	0
		0.20	0
		0.40	0
		0.60	0
		1.00	0

Table 2.4

Parameters for Studies of Effects of Diaphragm

Dimensionless Parameters					Dimension Parameters		
b/a	H	T	Q	κ	Bridge Span, a, ft	Girder Spacing, b, ft	Slab Thickness, h, in.
0.20	20	0.012	0.055	0.05, 0.10, 0.20, 0.40	35.00	7.00	6.00
0.15	20	0.012	0.023	0.05, 0.10, 0.20, 0.40	56.50	8.50	7.00
0.10	5	0.012	0.018	0.05, 0.10, 0.20, 0.40	55.00	5.50	7.75
	10	0.012	0.012	0.05, 0.10, 0.20, 0.40	80.00	8.00	8.00
	20	0.011	0.015	0.05, 0.10, 0.20, 0.40	80.00	8.00	6.75
				0.60, 1.00, 1000			
	40	0.009	0.028	0.05, 0.10, 0.20, 0.40	80.00	8.00	6.50
0.05	20	0.010	0.012	0.05, 0.10, 0.20, 0.40	120.00	6.00	7.00

Table 2.5

Locations of Diaphragms

No.	Number of Diaphragms	Ratio of Diaphragm Coordinate to Span Length		
		x_{d1}/a	x_{d2}/a	x_{d3}/a
1	1	6/12		
2	2	5/12	7/12	
3	2	4/12	8/12	
4	2	3/12	9/12	
5	3	6/12	3/12	9/12

Table 5.1

Listing of Girders Subjected to the Maximum Moment in Bridges

Ratio, b/a	H	Girder Spacing, b ft	Outer P on Girder A Girder	Outer P at least 2 ft from Girder A Girder
0.20	5	5	C	C
		6	C	C
		7	C	C
		8	C	C
		9	A&C	C
	10	5	C	C
		6	C	C
		7	C	C
		8	C	C
		9	C	C
	20	5	C	C
		6	C	C
		7	C	C
		8	C	C
		9	C	C
0.15	5	5	C	C
		6	B	C
		7	A	C
		8	A	B
		9	A	B
	10	5	C	C
		6	C	C
		7	C	C
		8	C	C
		9	C	C
	20	5	C	C
		6	C	C
		7	C	C
		8	C	C
		9	C	C
	40	5	C	C
		6	C	C
		7	C	C
		8	C	C
		9	C	C

Table 5.1 (Cont.)

Ratio, b/a	H	Girder Spacing, b ft	Outer P on Girder A Girder	Outer P at least 2 ft from Girder A Girder
0.10	5	5	A	C
		6	A	B
		7	A	B
		8	A	B
		9	A	B
	10	5	A	C
		6	A	C
		7	A	B
		8	A	B
		9	A	B
	20	5	C	C
		6	C	C
		7	C	C
		8	A&C	C
		9	A&C	C
	40	5	C	C
		6	C	C
		7	C	C
		8	C	C
		9	C	C
0.05	10	5	A	B&C
		6	A	A&B
		7	A	A&B
		8	A	A&B
		9	A	A&B
	20	5	A	C
		6	A	A&B
		7	A	A&B
		8	A	A&B
		9	A	A&B
	40	5	A	C
		6	A	B
		7	A	B
		8	A	A&B
		9	A	A&B

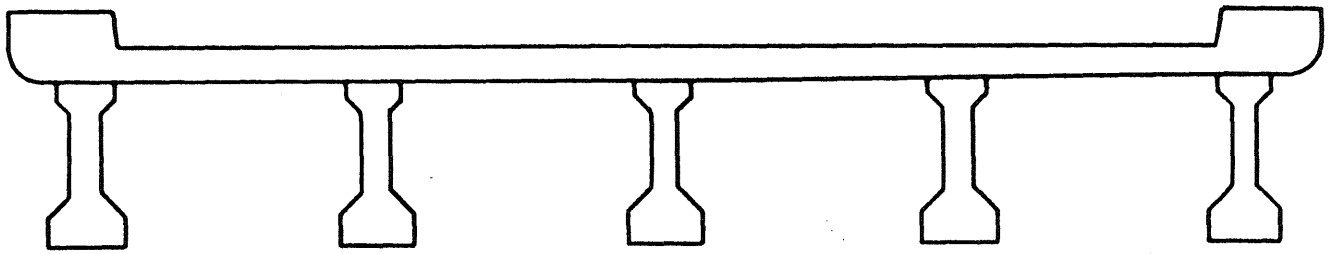

(a) Five-Girder Bridge

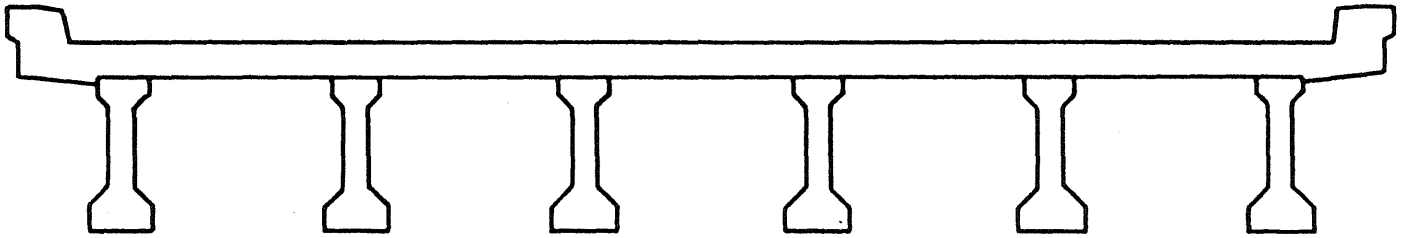

(b) Six-Girder Bridge

FIG. 1.1 CROSS SECTION OF BRIDGES

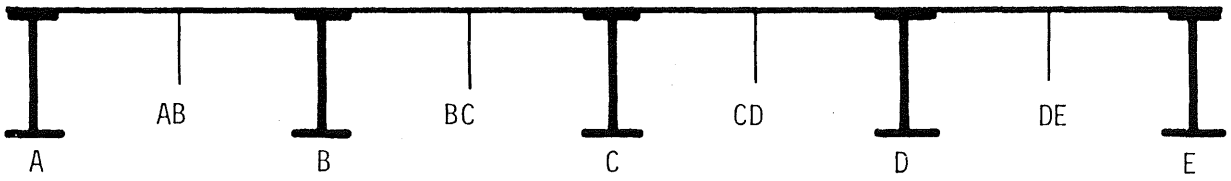

(a) Five-Girder Bridge

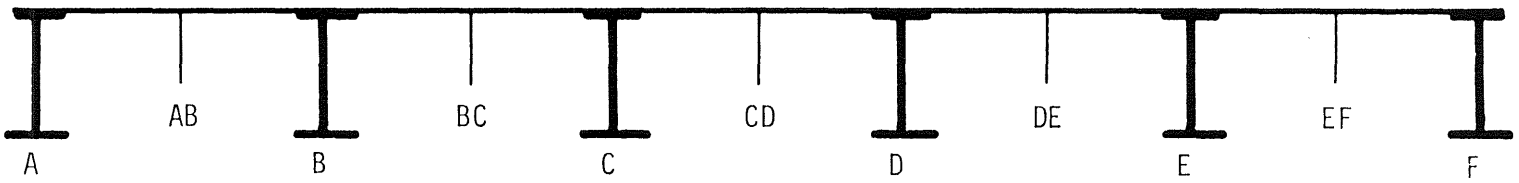

(b) Six-Girder Bridge

FIG. 1.2 TRANSVERSE SECTION OF BRIDGES SHOWING NOTATION USED

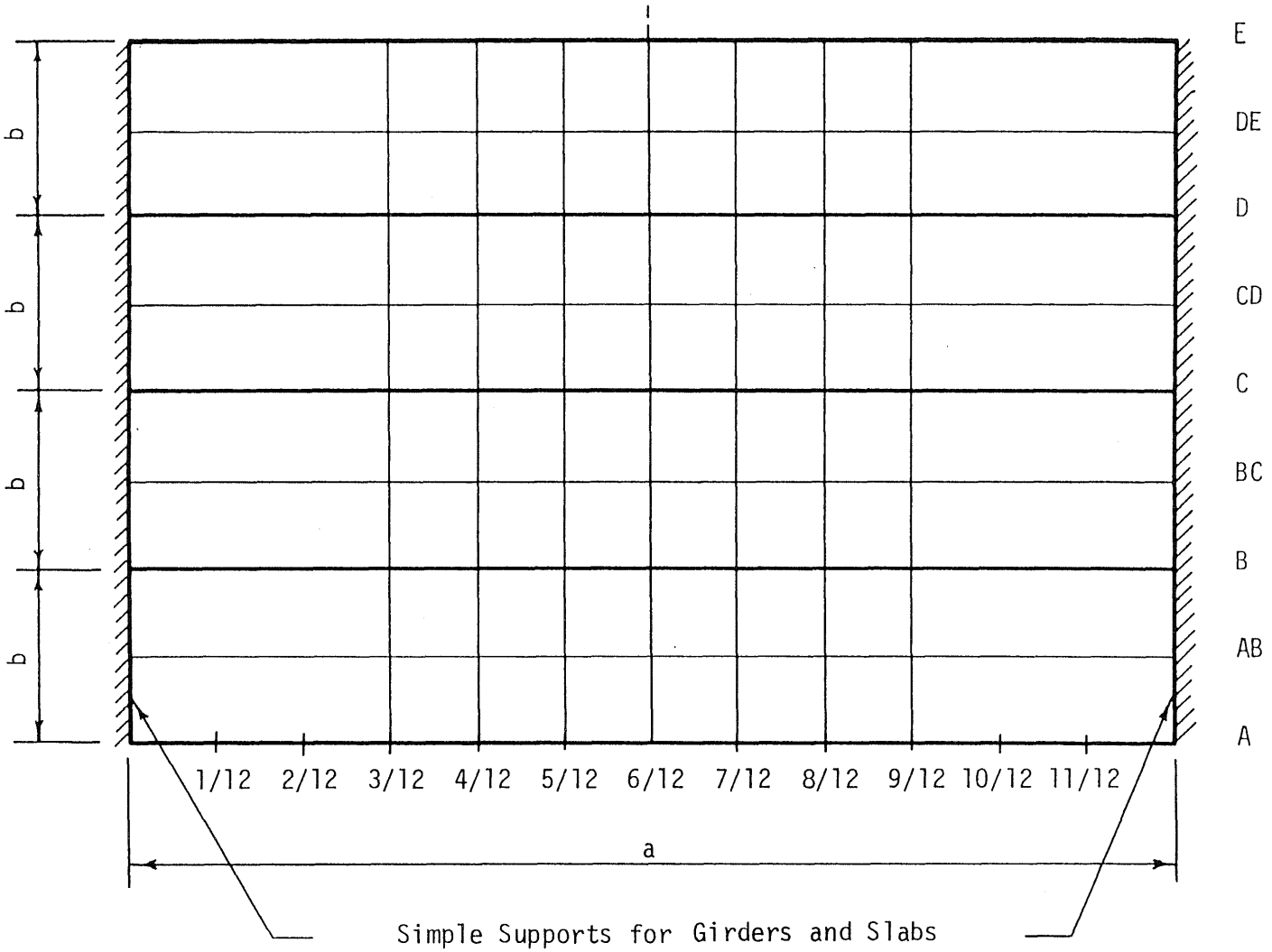

FIG. 1.3 DIAGRAM SHOWING NOTATION FOR SLAB-AND-GIRDER BRIDGES

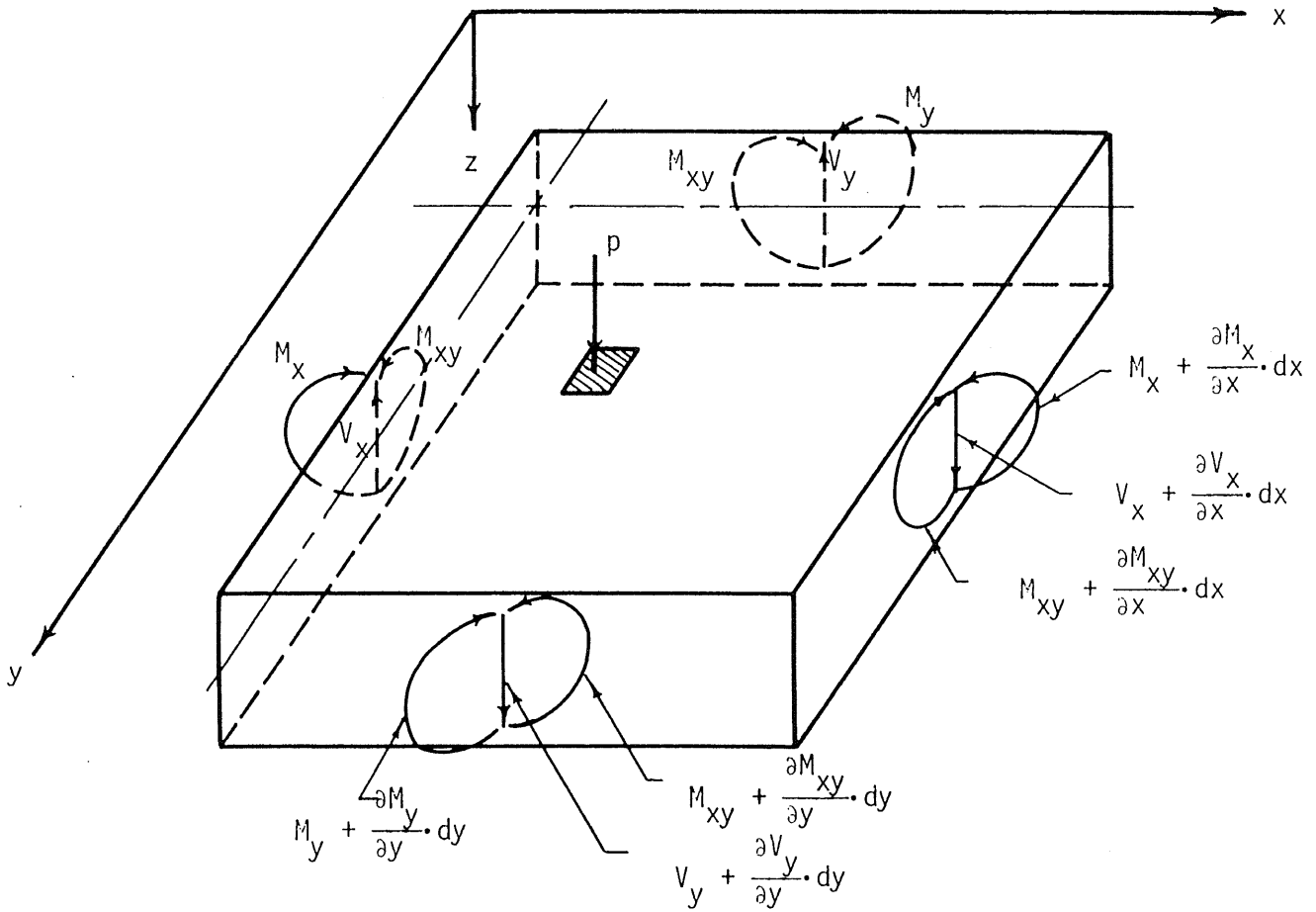

FIG. 1.4 DIAGRAM SHOWING POSITIVE DIRECTIONS OF FORCES ACTING ON A SLAB ELEMENT

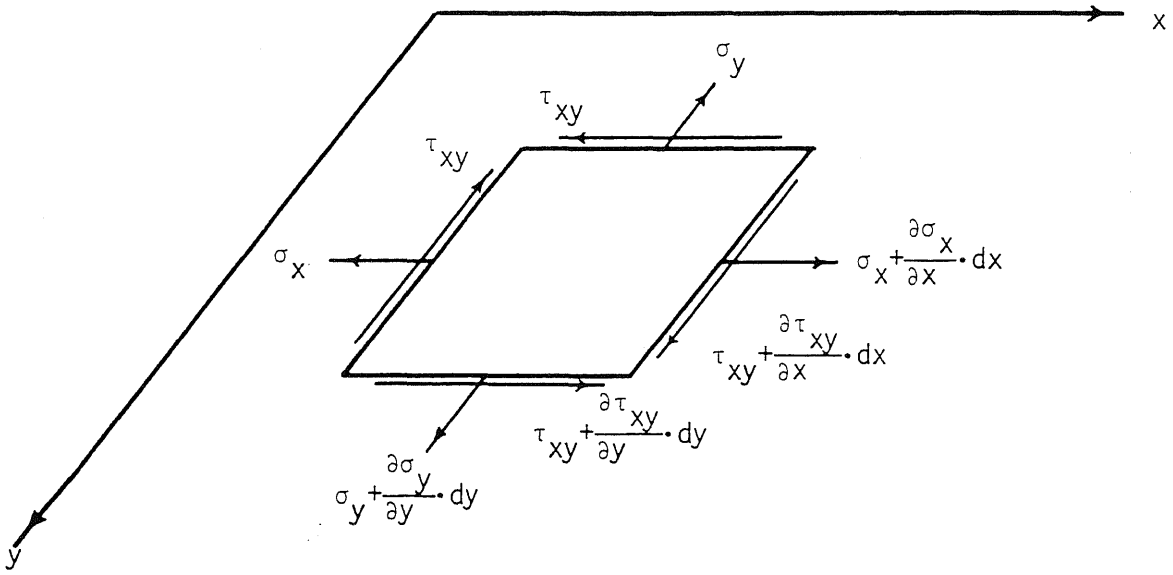

FIG. 1.5 DIAGRAM SHOWING POSITIVE DIRECTIONS OF THE IN-PLANE STRESSES ACTING ON SLAB ELEMENT

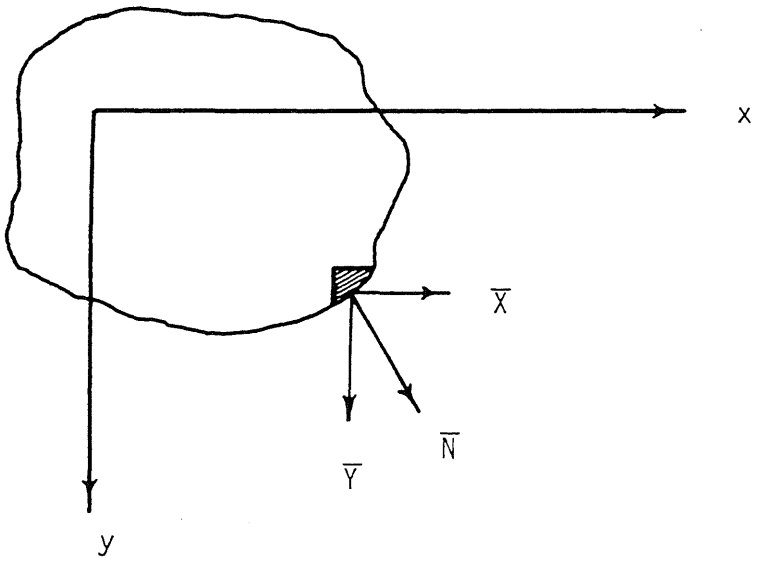

FIG. 1.6 NORMAL AND ITS COMPONENTS IN x AND y DIRECTIONS ACTING ON BOUNDARIES OF A BODY

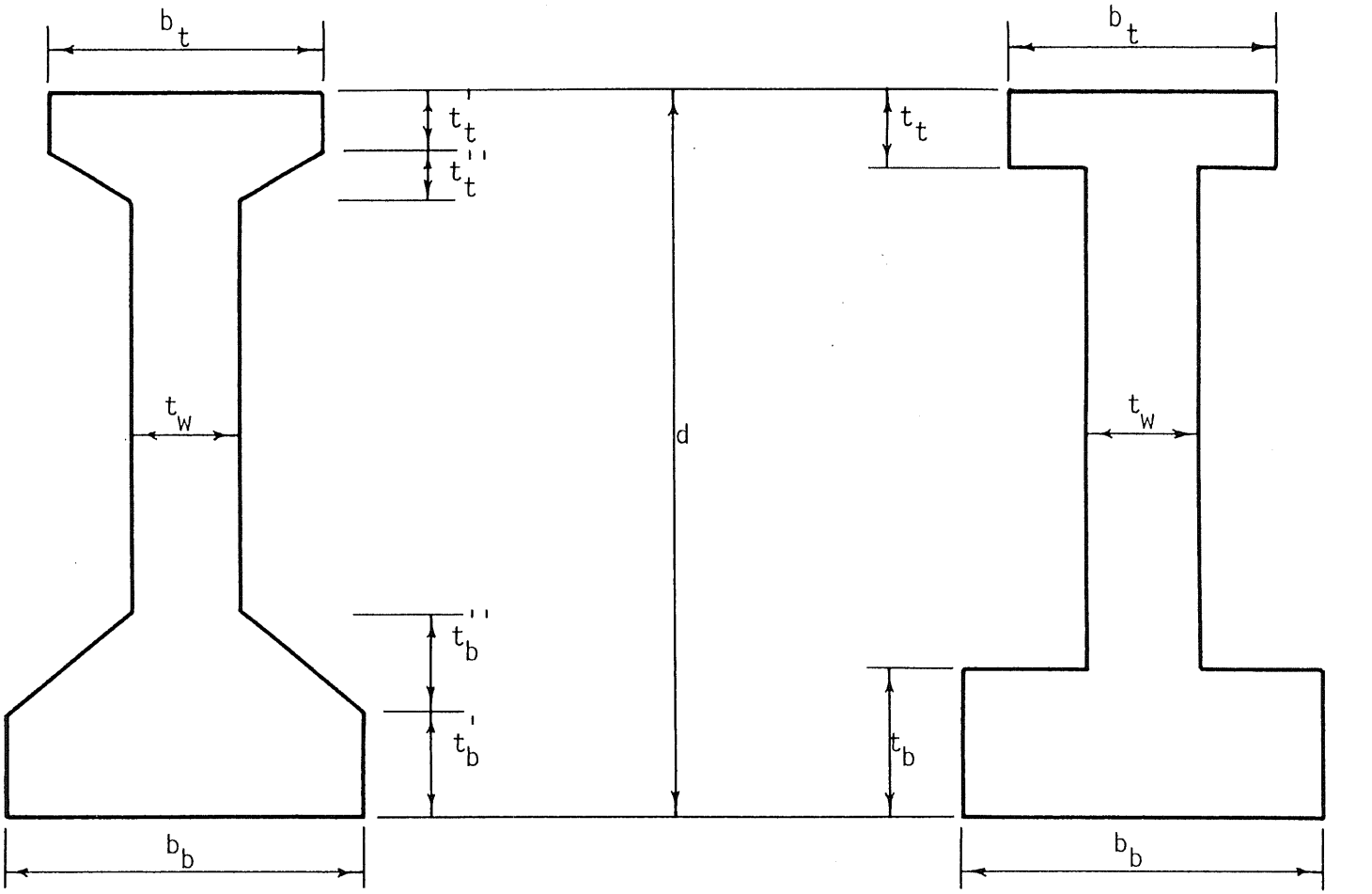

(a) Actual Cross-Section (b) Idealized Cross-Section

FIG. 2.1 IDEALIZATION OF CROSS SECTION OF PRESTRESSED CONCRETE GIRDERS

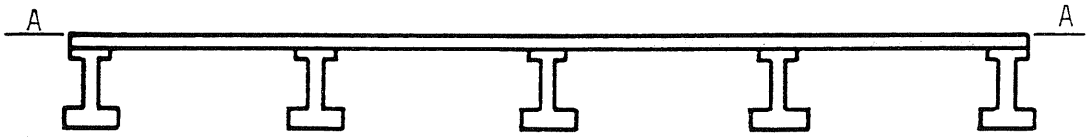

(a) Unloaded Bridges, H = 0 and H = ∞

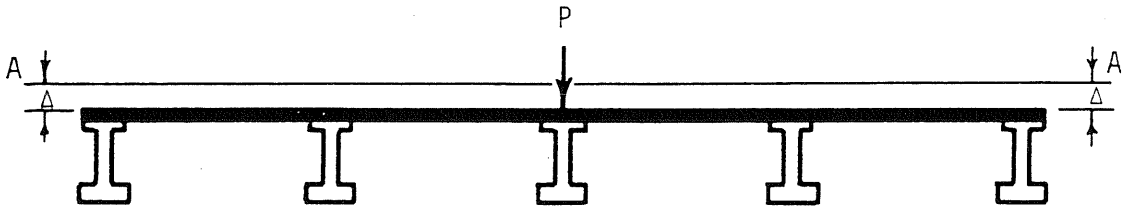

(b) Displacement of the Loaded Bridge, H = 0

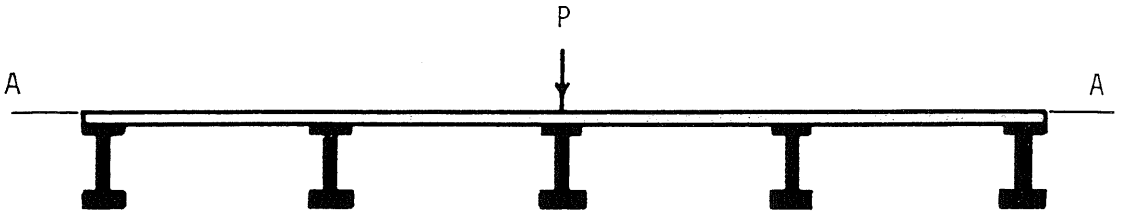

(c) Displacement of the Loaded Bridge, H = ∞

FIG. 2.2 BRIDGE DISPLACEMENT FOR H = 0 AND H = ∞

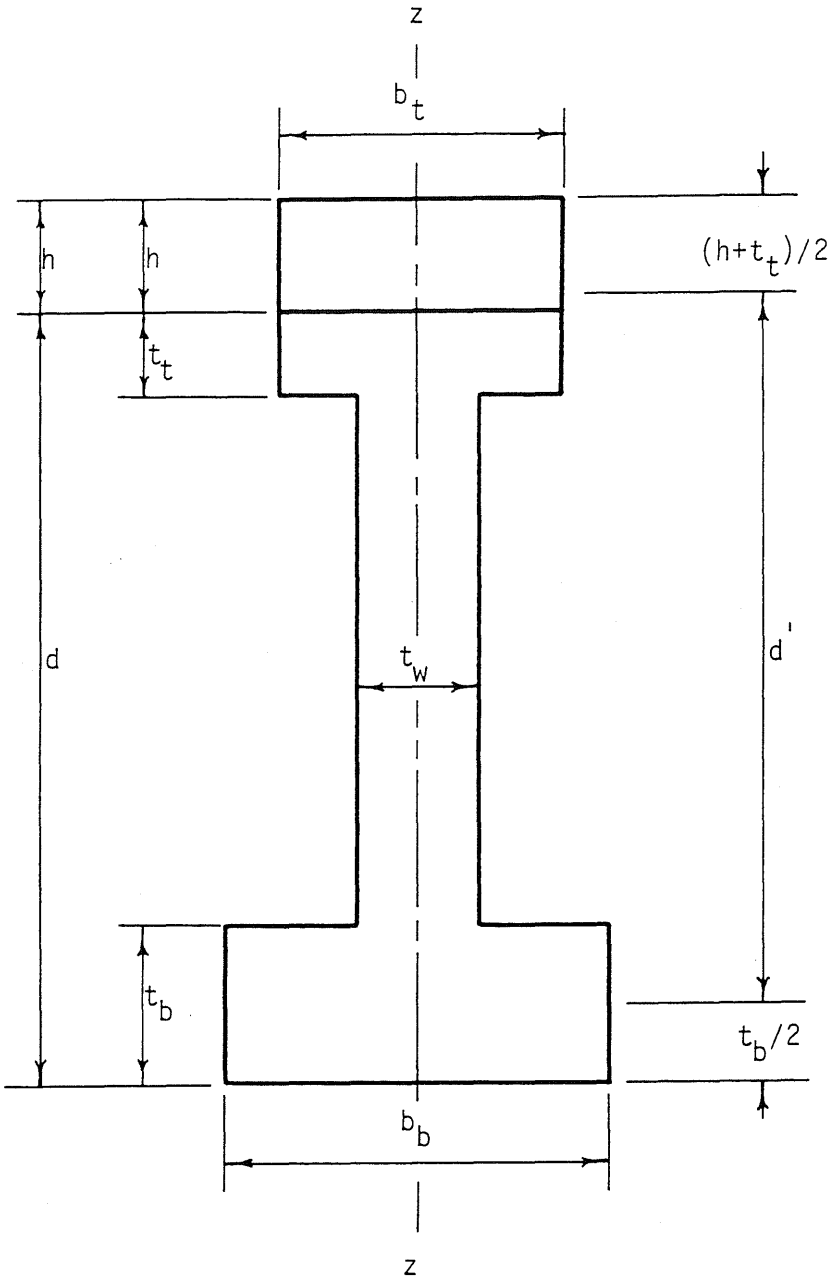

FIG. 2.3 CROSS SECTION FOR TORSIONAL CONSTANT COMPUTATION

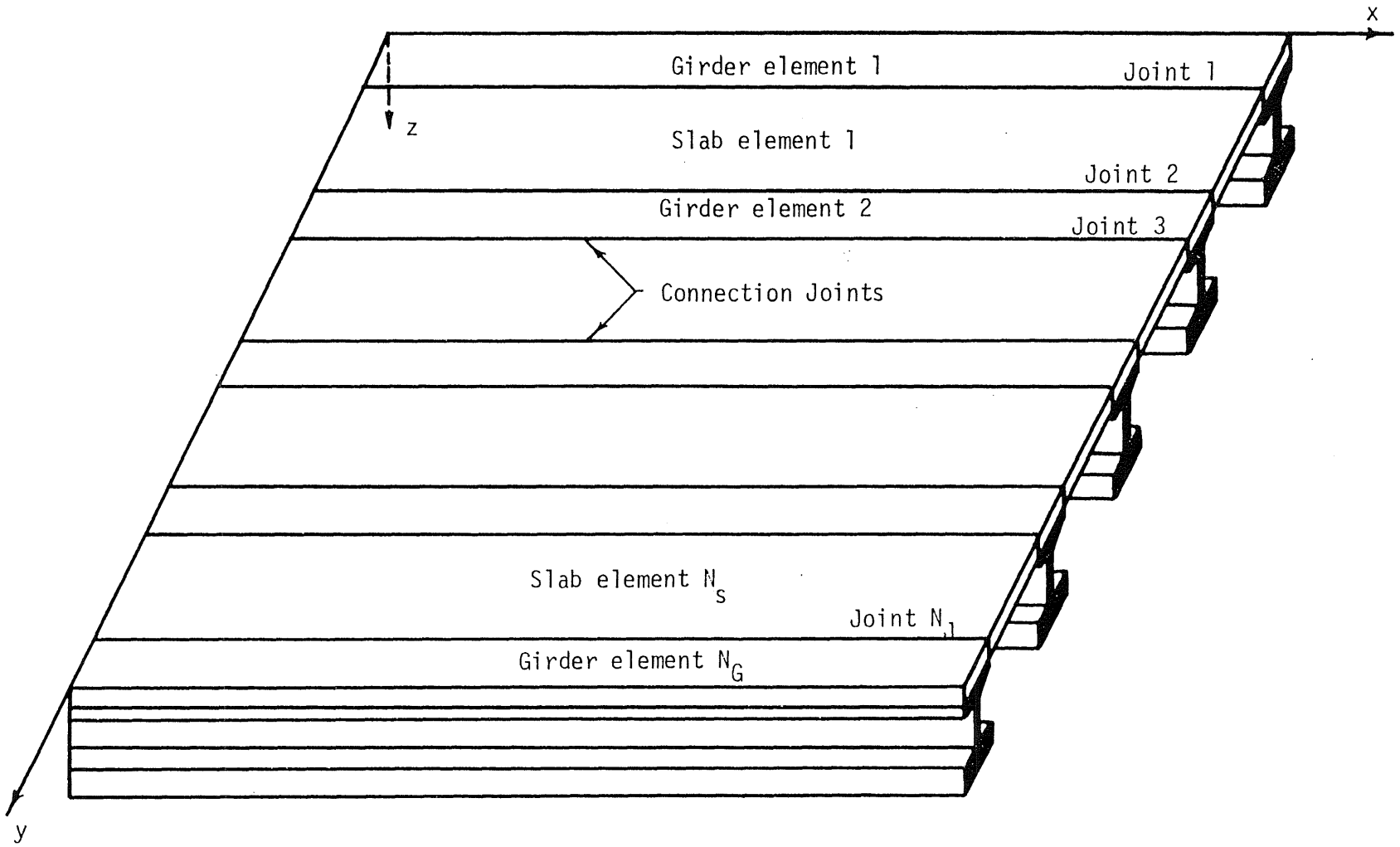

FIG. 3.1 GIRDER AND SLAB ELEMENTS AND THEIR CONNECTION JOINTS

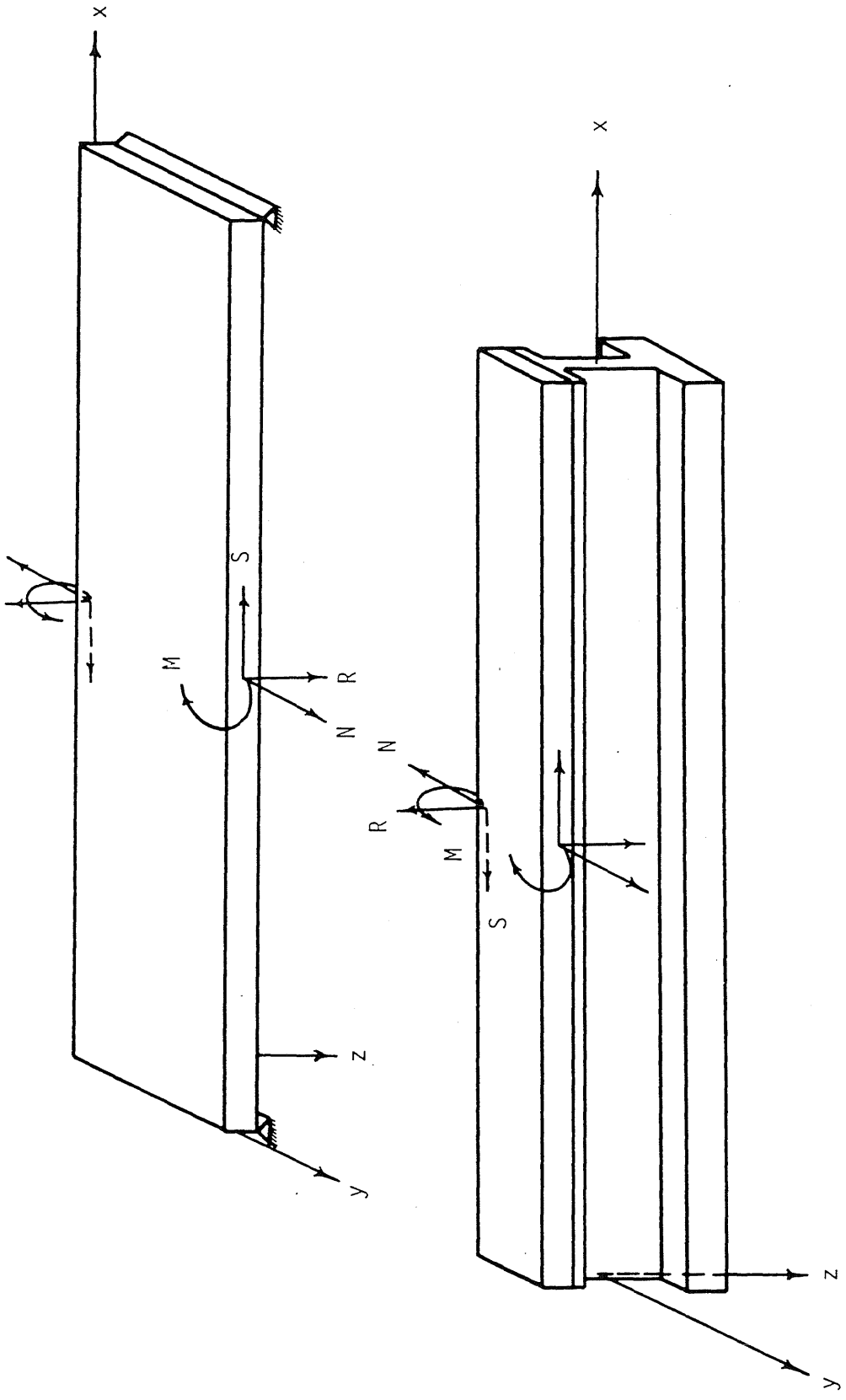

FIG. 3.2 FORCES ALONG THE CONNECTION JOINTS

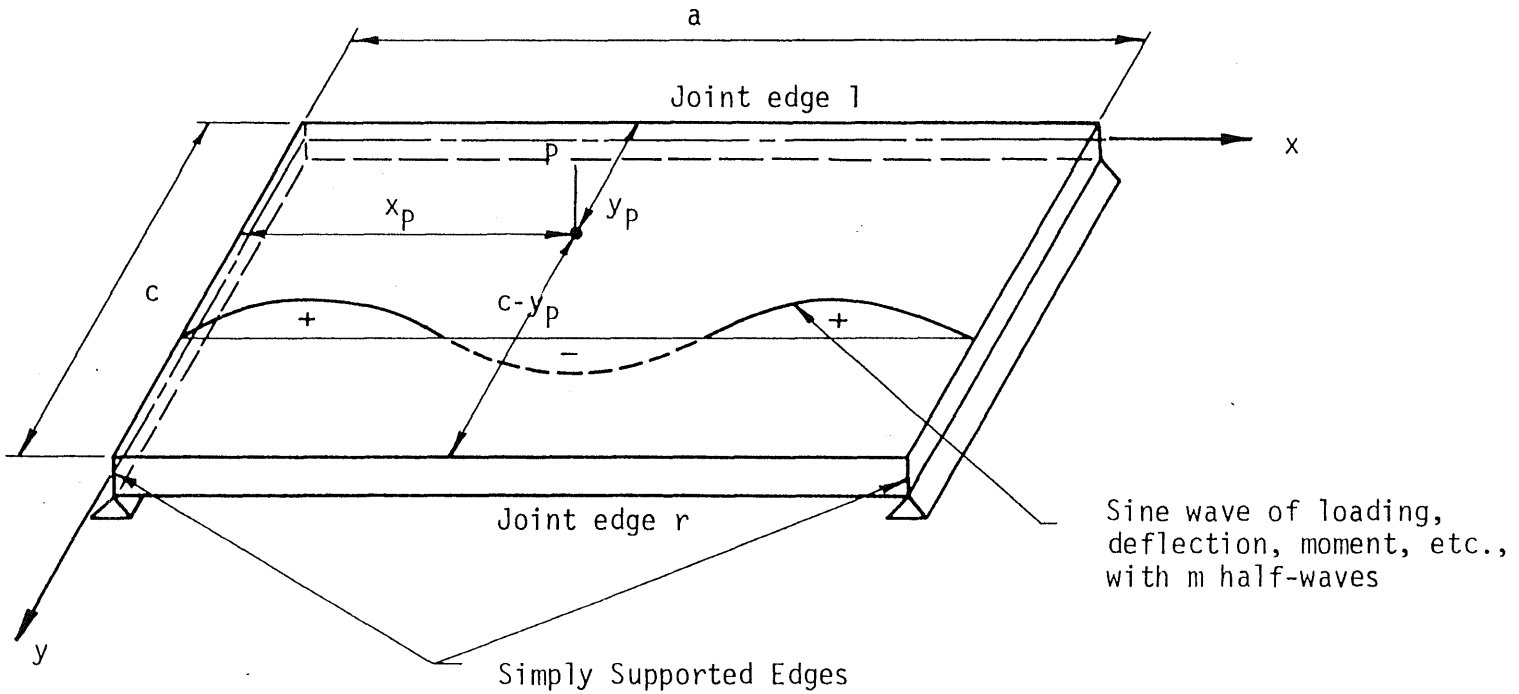

FIG. 3.3 RECTANGULAR PANEL OF SLAB CONSIDERED IN THE ANALYSIS

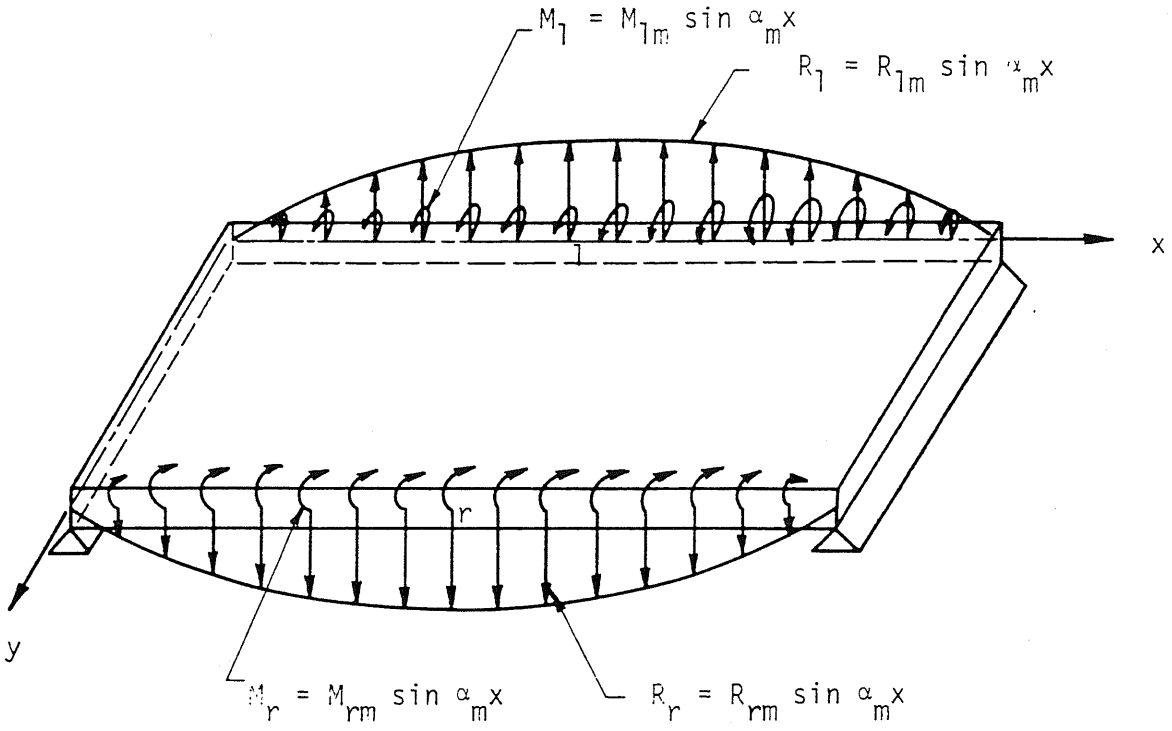

(a)

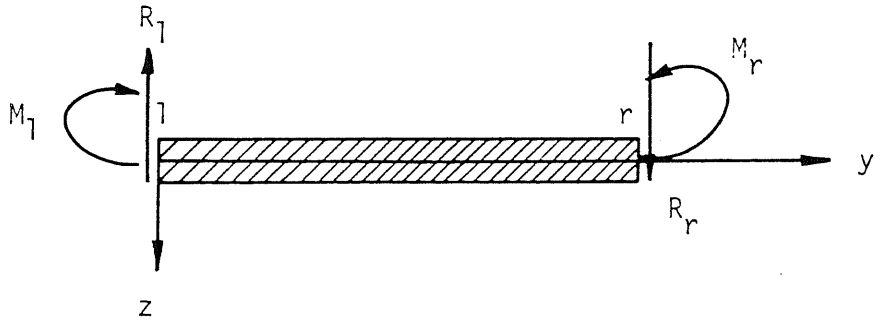

(b)

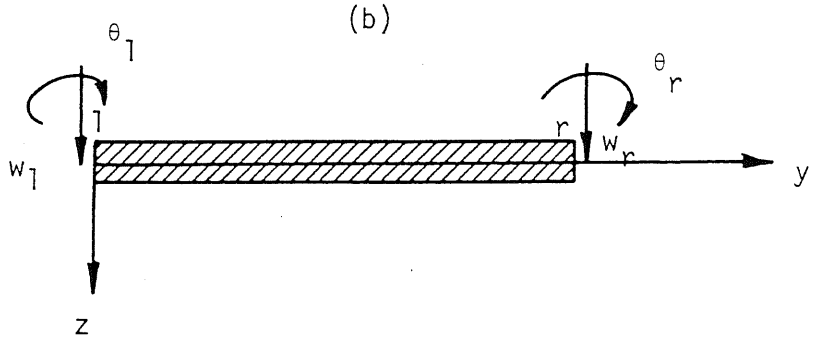

(c)

FIG. 3.4 SLAB WITH TWO OPPOSITE EDGES SIMPLY SUPPORTED, SHOWING POSITIVE DIRECTIONS OF FORCES AND DISPLACEMENTS OF THE FREE EDGES

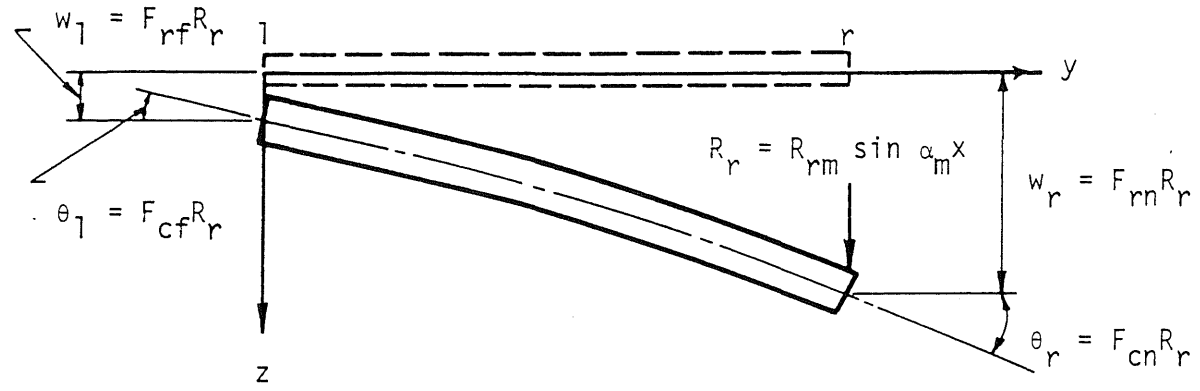

(a)

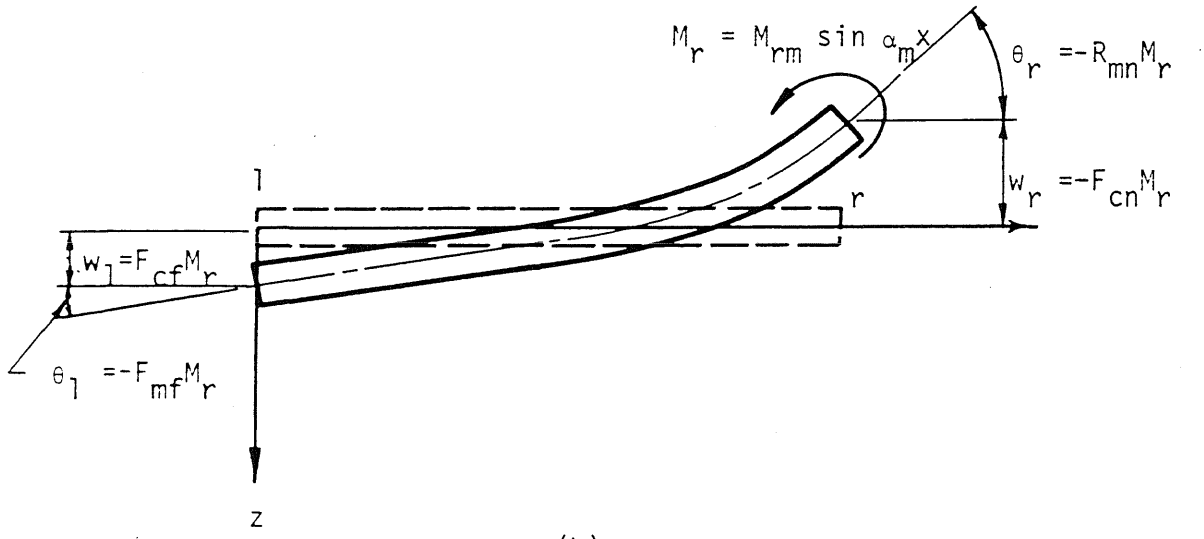

(b)

FIG. 3.5 DISPLACEMENTS OF SECTIONS ON LINES PARALLEL TO y-AXIS OF SLAB DUE TO EDGE REACTION AND MOMENT

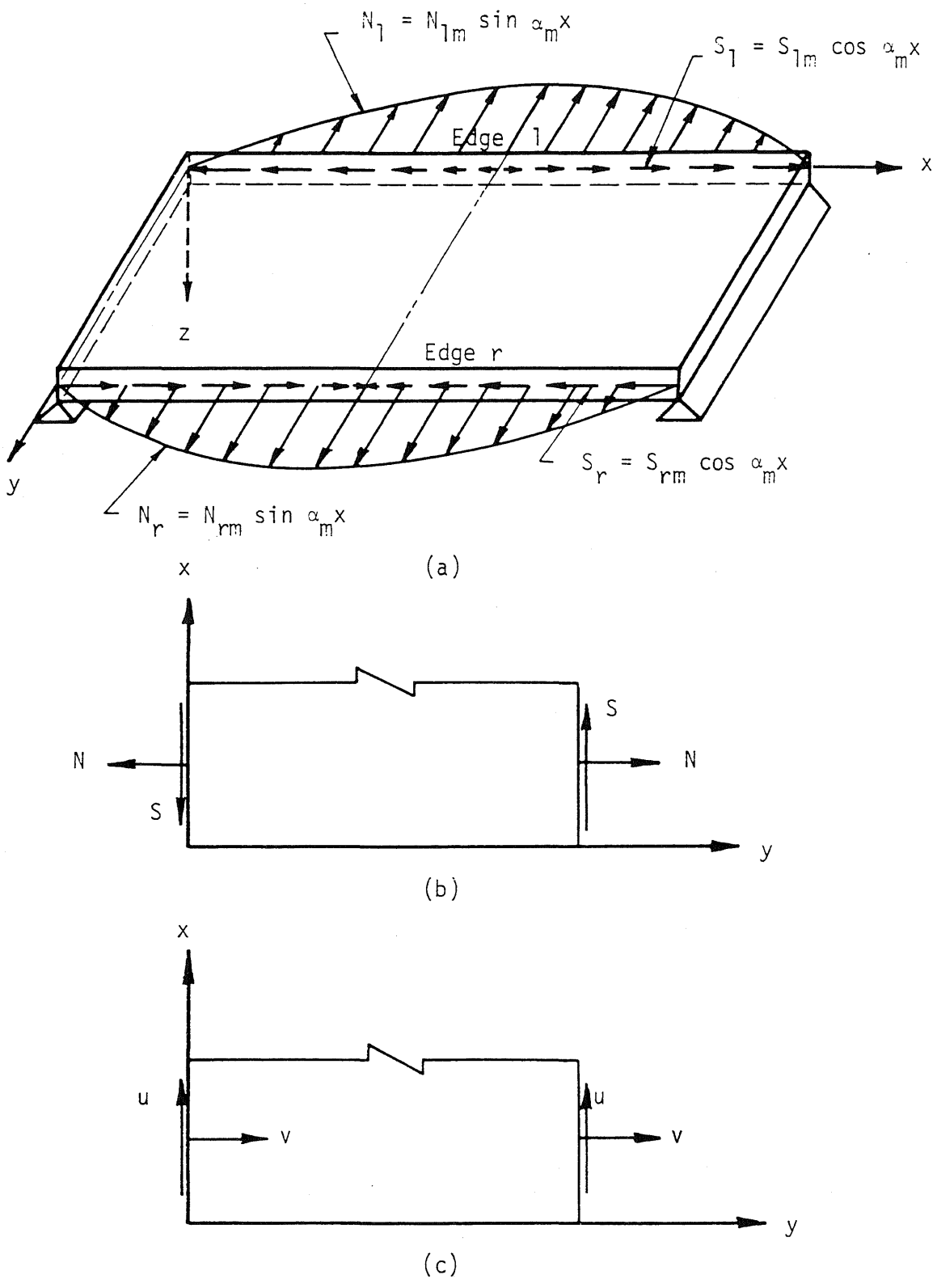

FIG. 3.6 SLAB WITH TWO OPPOSITE EDGES SIMPLY SUPPORTED, SHOWING POSITIVE DIRECTIONS OF IN-PLANE FORCES AND DISPLACEMENTS OF THE FREE EDGES

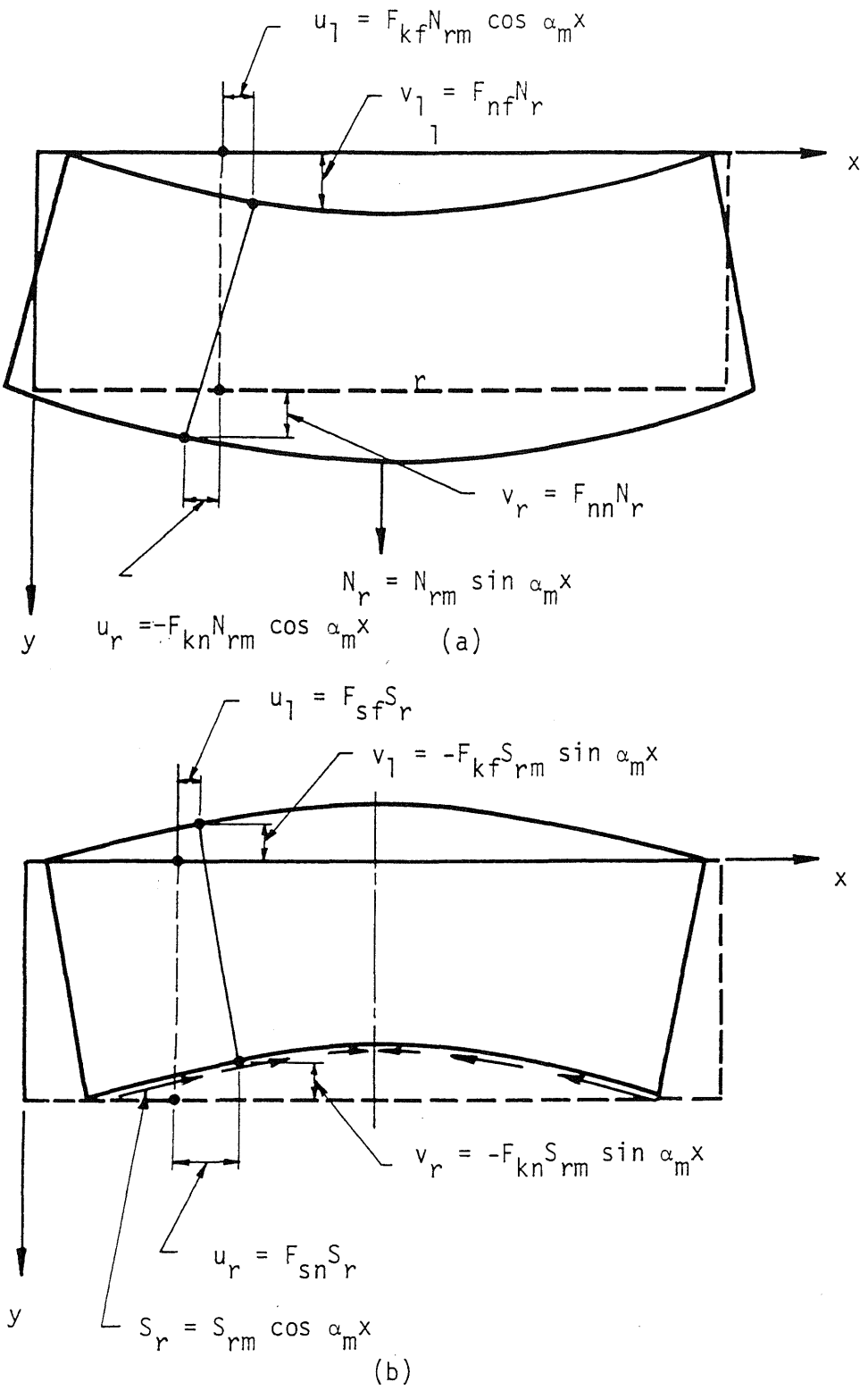

FIG. 3.7 DISPLACEMENTS OF A PANEL OF SLAB DUE TO IN-PLANE EDGE NORMAL AND SHEARING FORCES

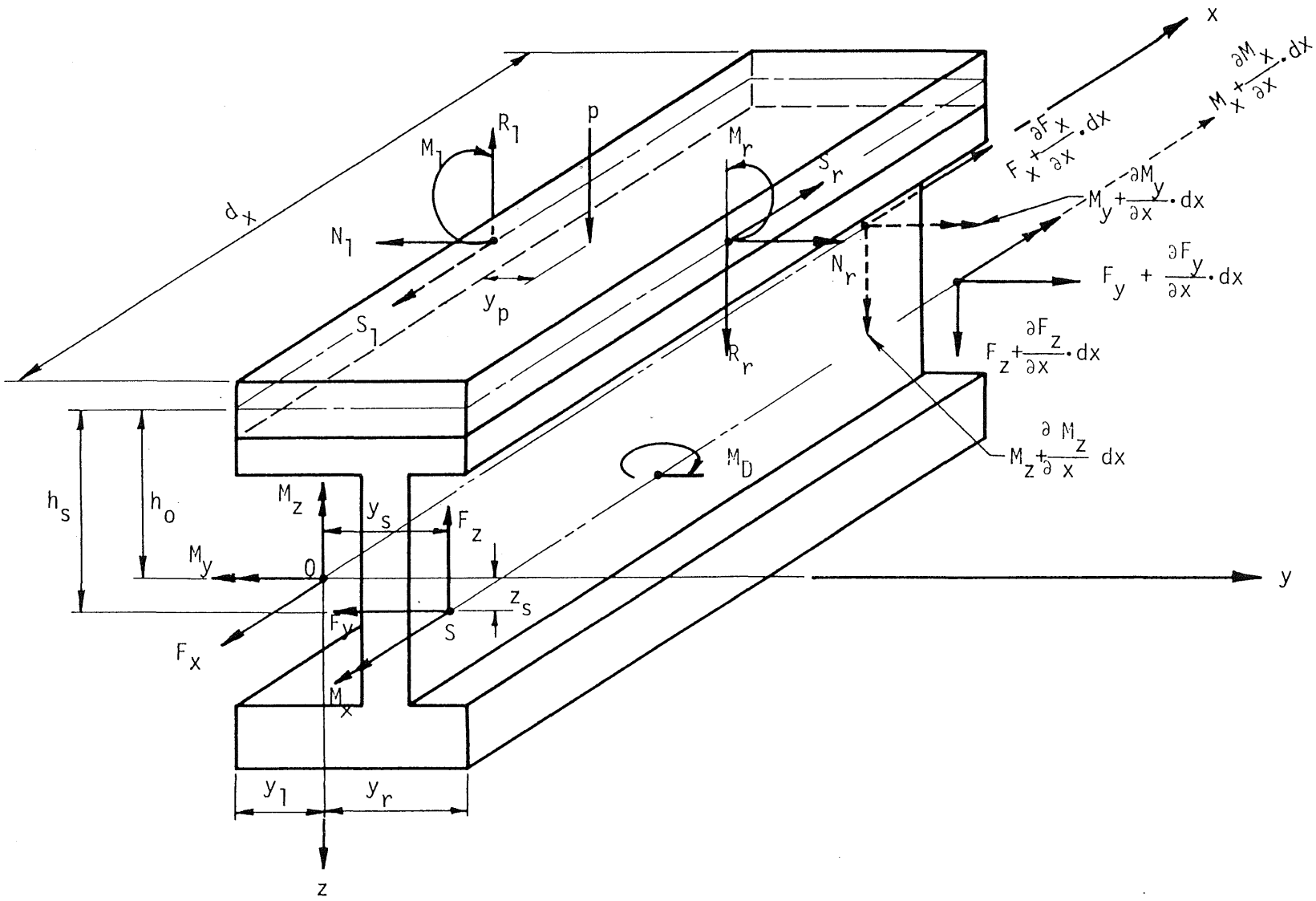

FIG. 3.8 EQUILIBRIUM OF A SMALL ELEMENT OF GIRDER

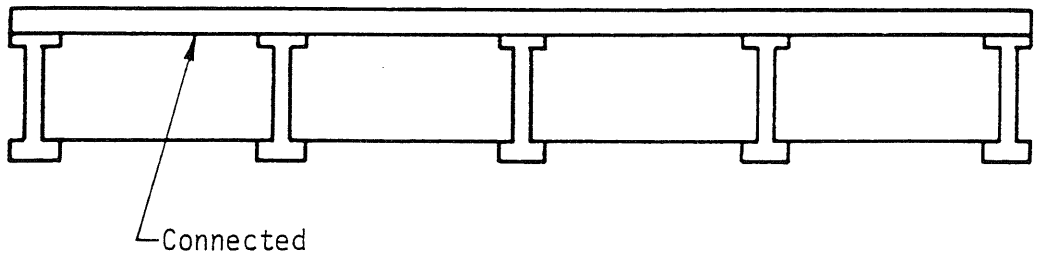

(a) Actual Diaphragm

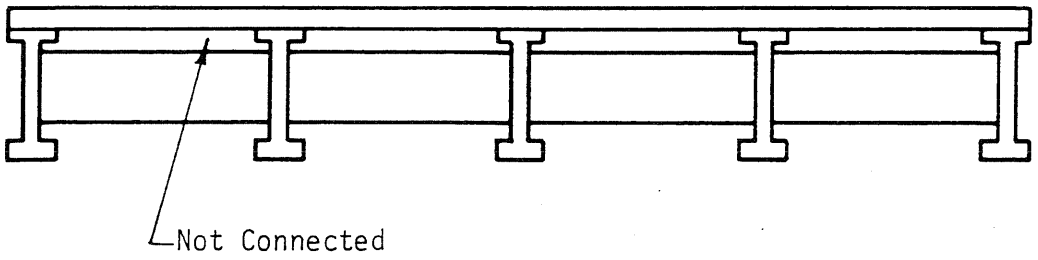

(b) Idealized Diaphragm

FIG. 4.1 ACTUAL AND IDEALIZED DIAPHRAGMS

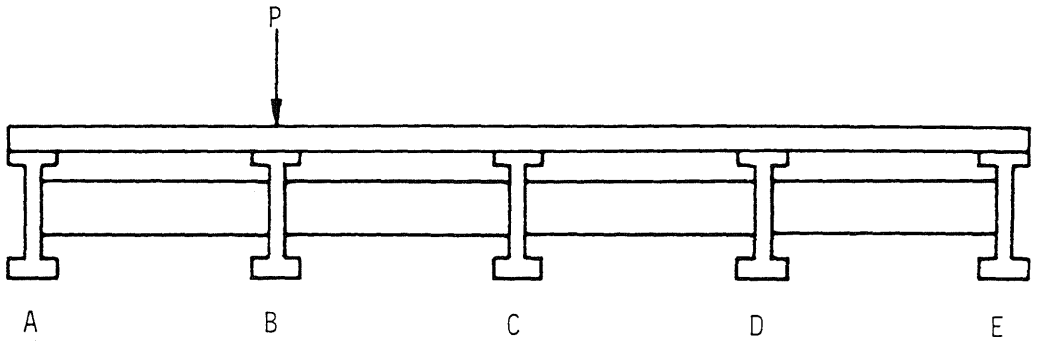

(a) Cross Section of Bridge with Diaphragm

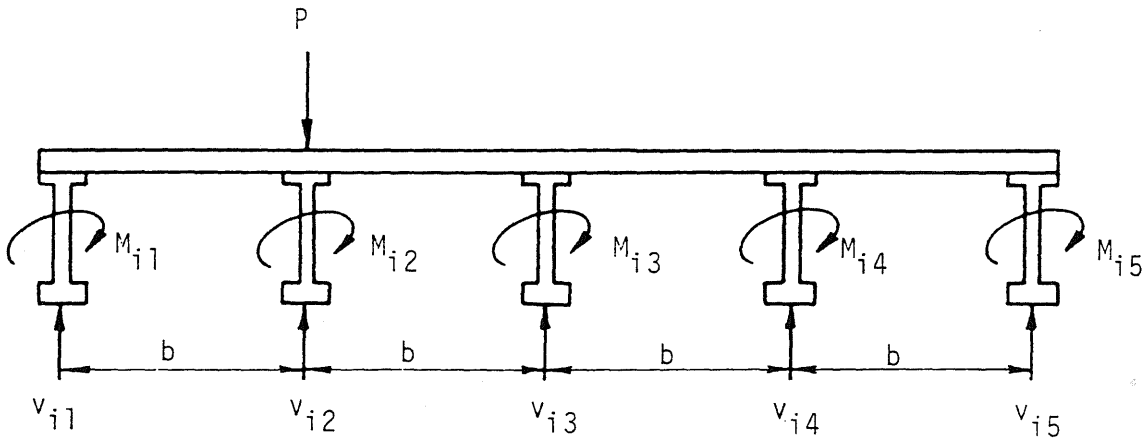

(b) Forces and Moments Replacing Diaphragm

FIG. 4.2 REPLACEMENT OF DIAPHRAGMS BY EQUIVALENT FORCES

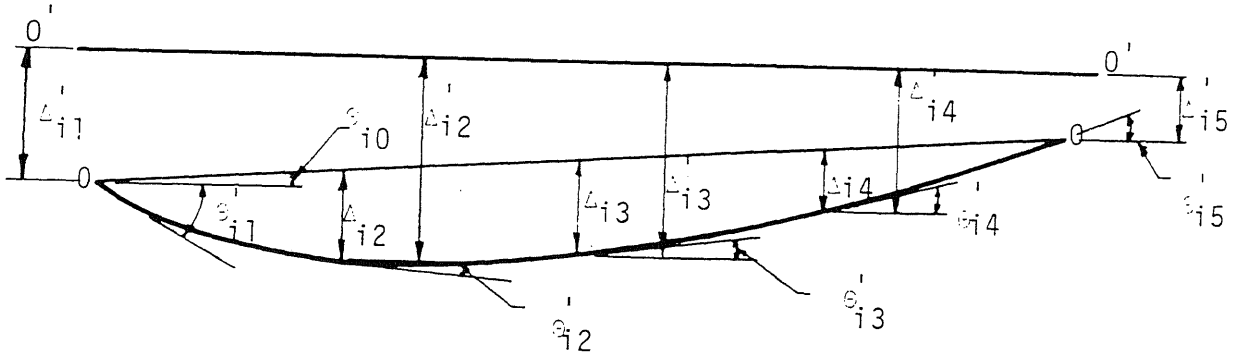

FIG. 4.3 DISPLACEMENTS OF CROSS SECTION OF BRIDGE

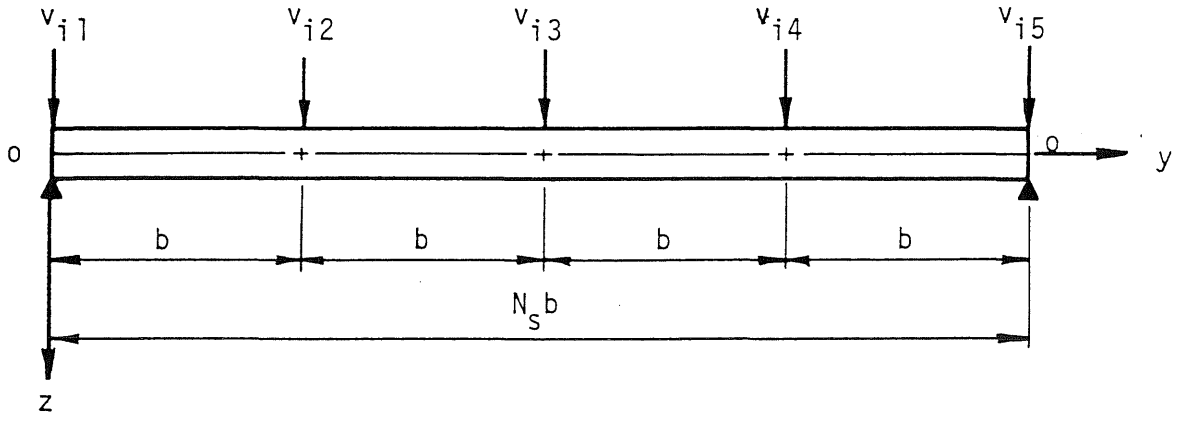

(a) Vertical Forces Acting on Diaphragm

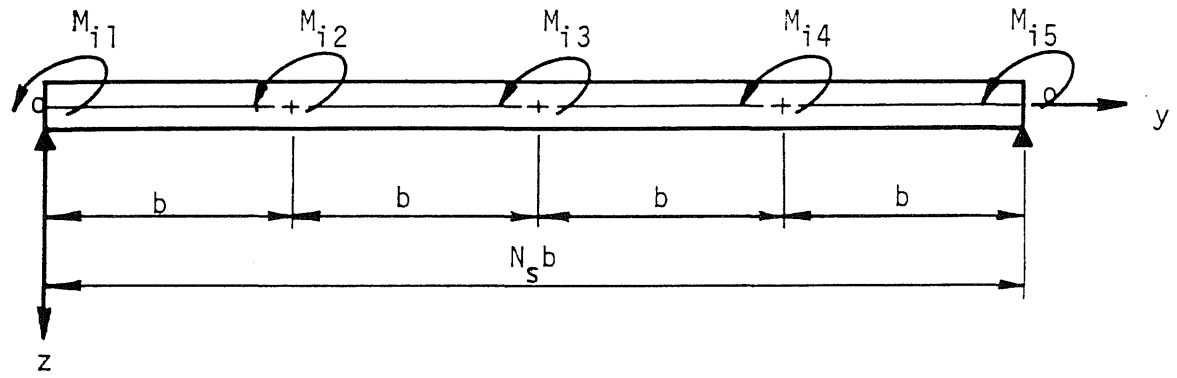

(b) Moments Acting on Diaphragm

FIG. 4.4 LOADS AND MOMENTS ON DIAPHRAGM

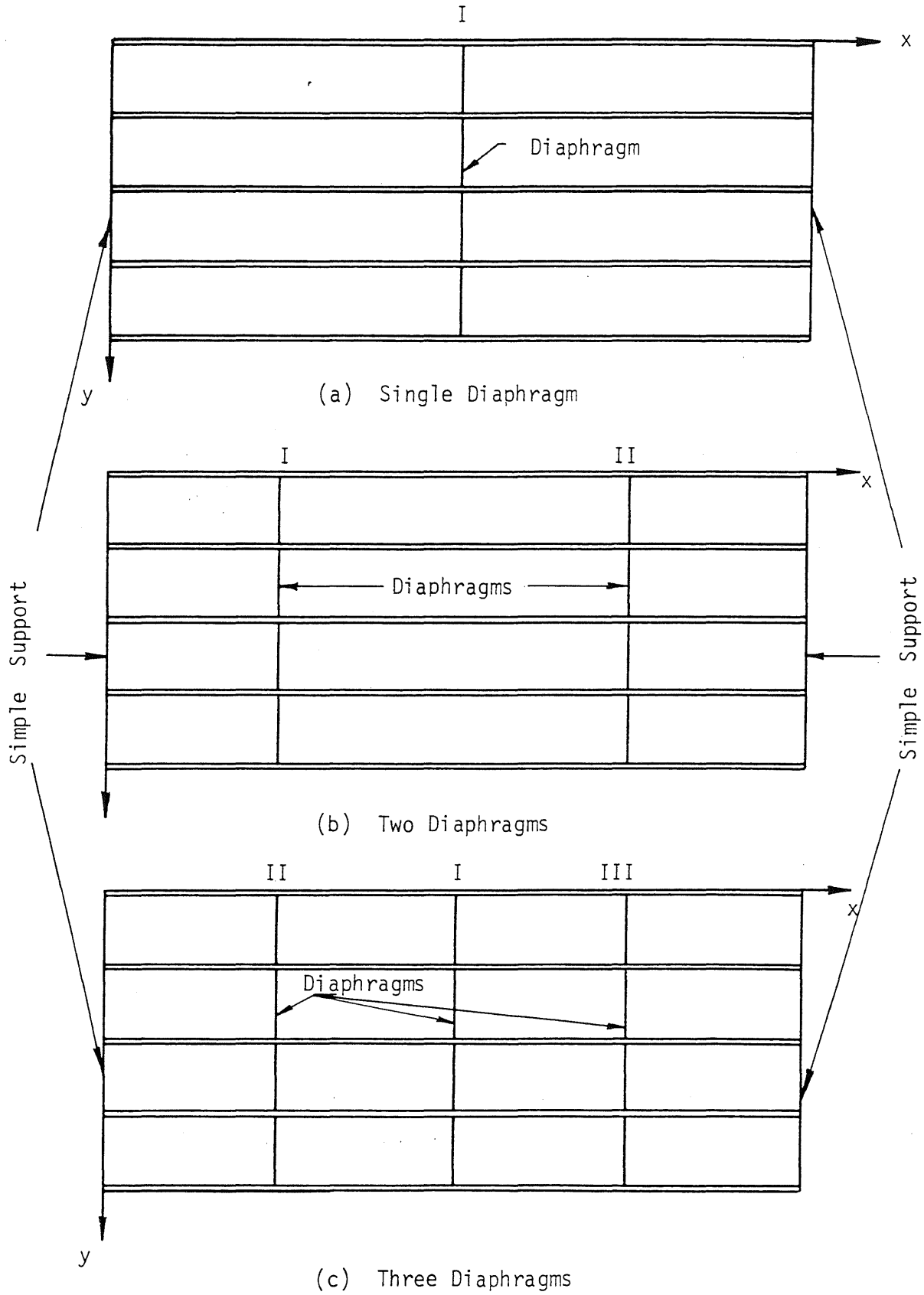

FIG. 4.5 ARRANGEMENTS OF DIAPHRAGMS

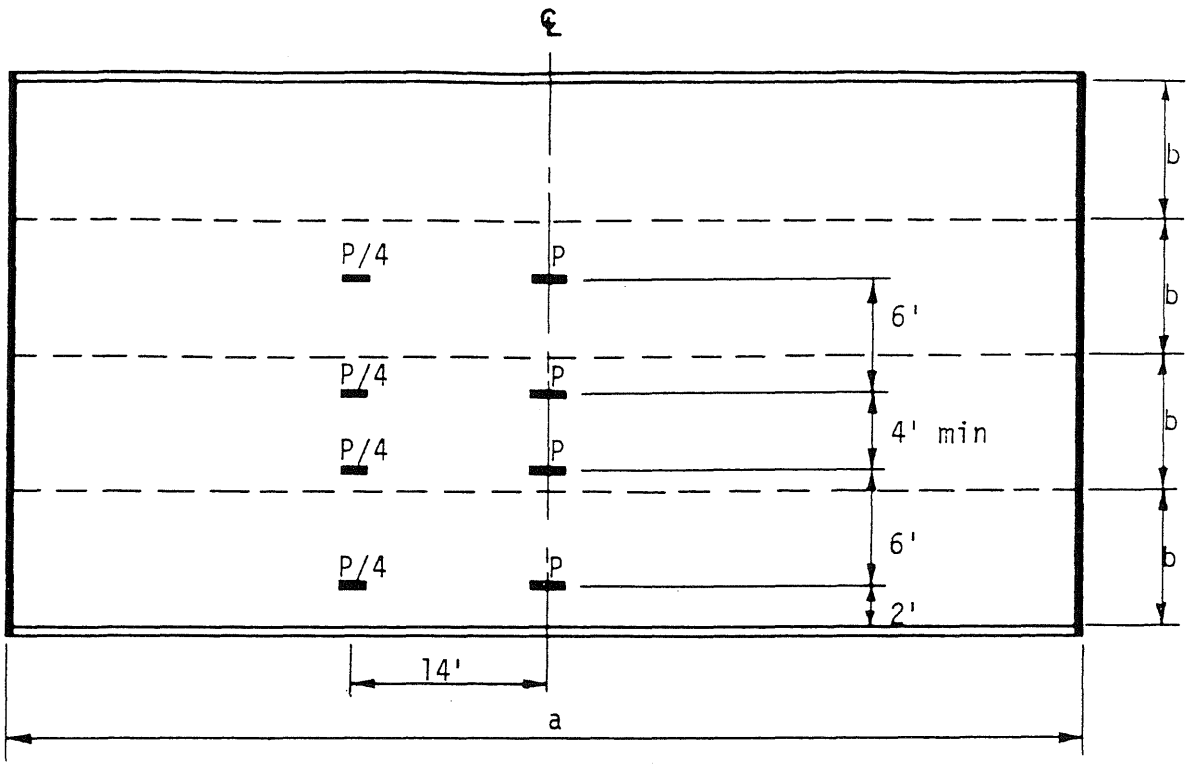

(a) H Loadings

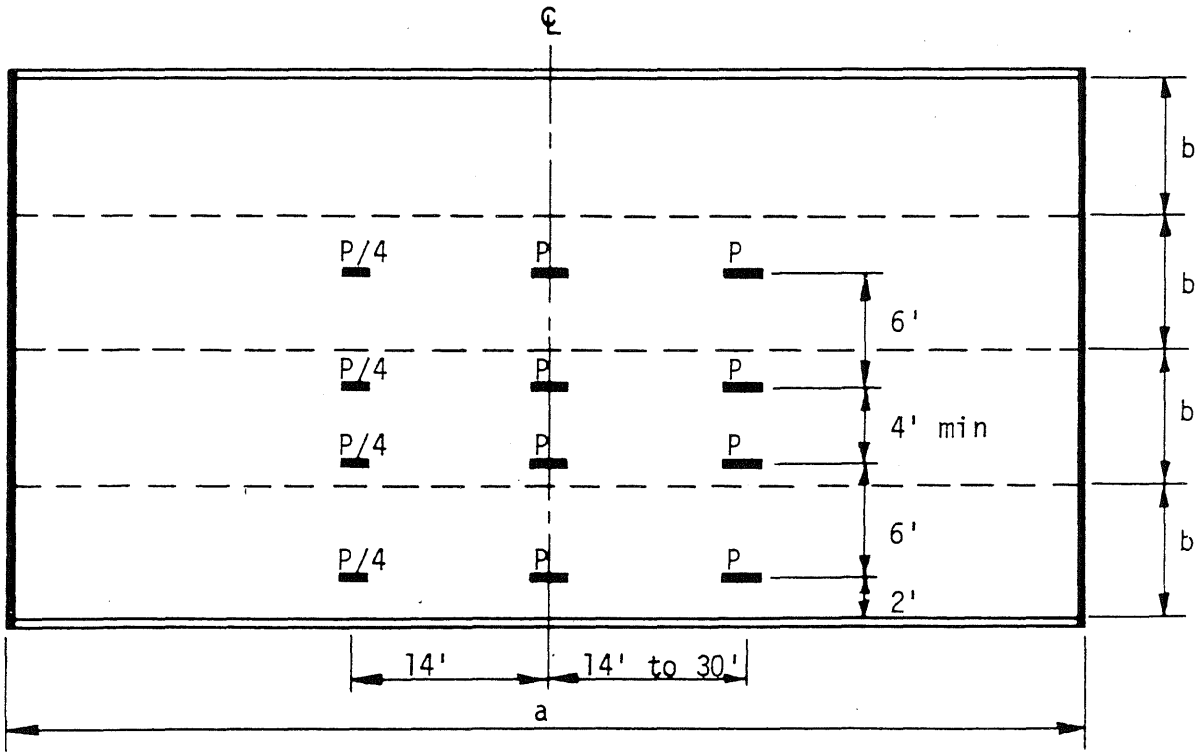

(b) H-S Loadings

FIG. 5.1 AASHO SPECIFICATION FOR STANDARD TRUCK LOADINGS

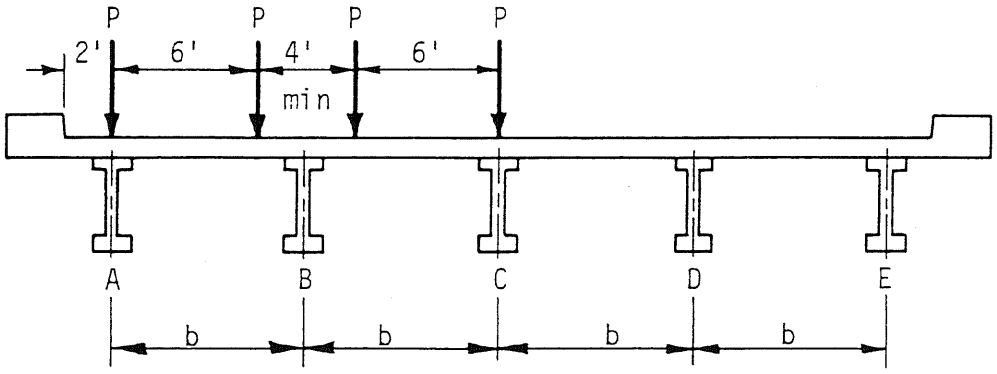

(a) Outer P on Girder A

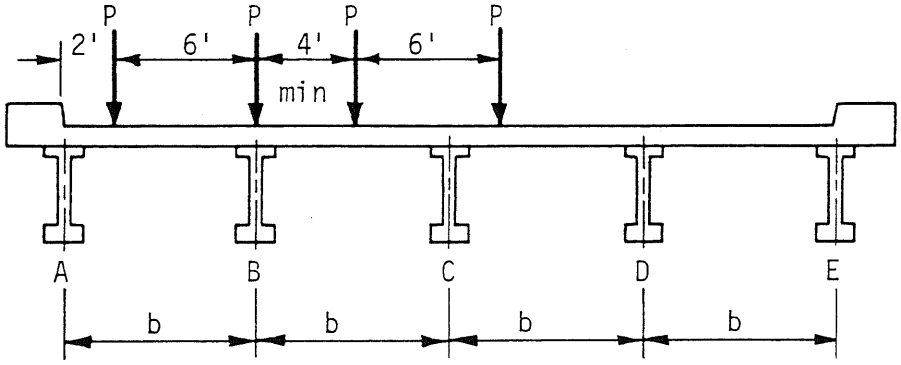

(b) Outer P at least 2 ft from Girder A

FIG. 5.2 CROSS SECTIONS OF BRIDGE SHOWING 4-WHEEL LOADINGS

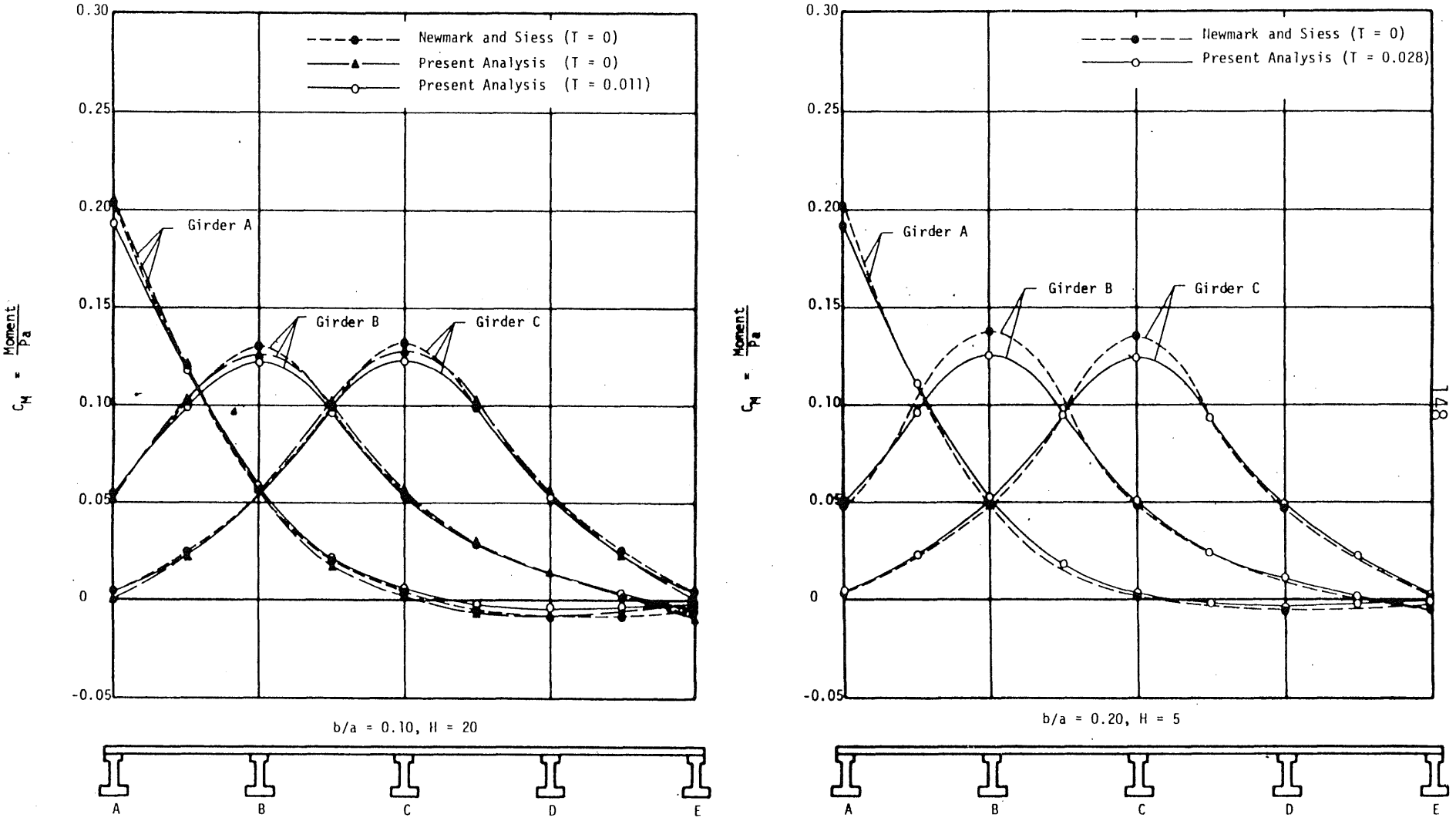

FIG. 5.3 COMPARISON OF INFLUENCE LINES FOR MOMENT AT MIDSPAN OF GIRDERS, LOAD P MOVING TRANSVERSELY ACROSS MIDSPAN WITHOUT DIAPHRAGMS

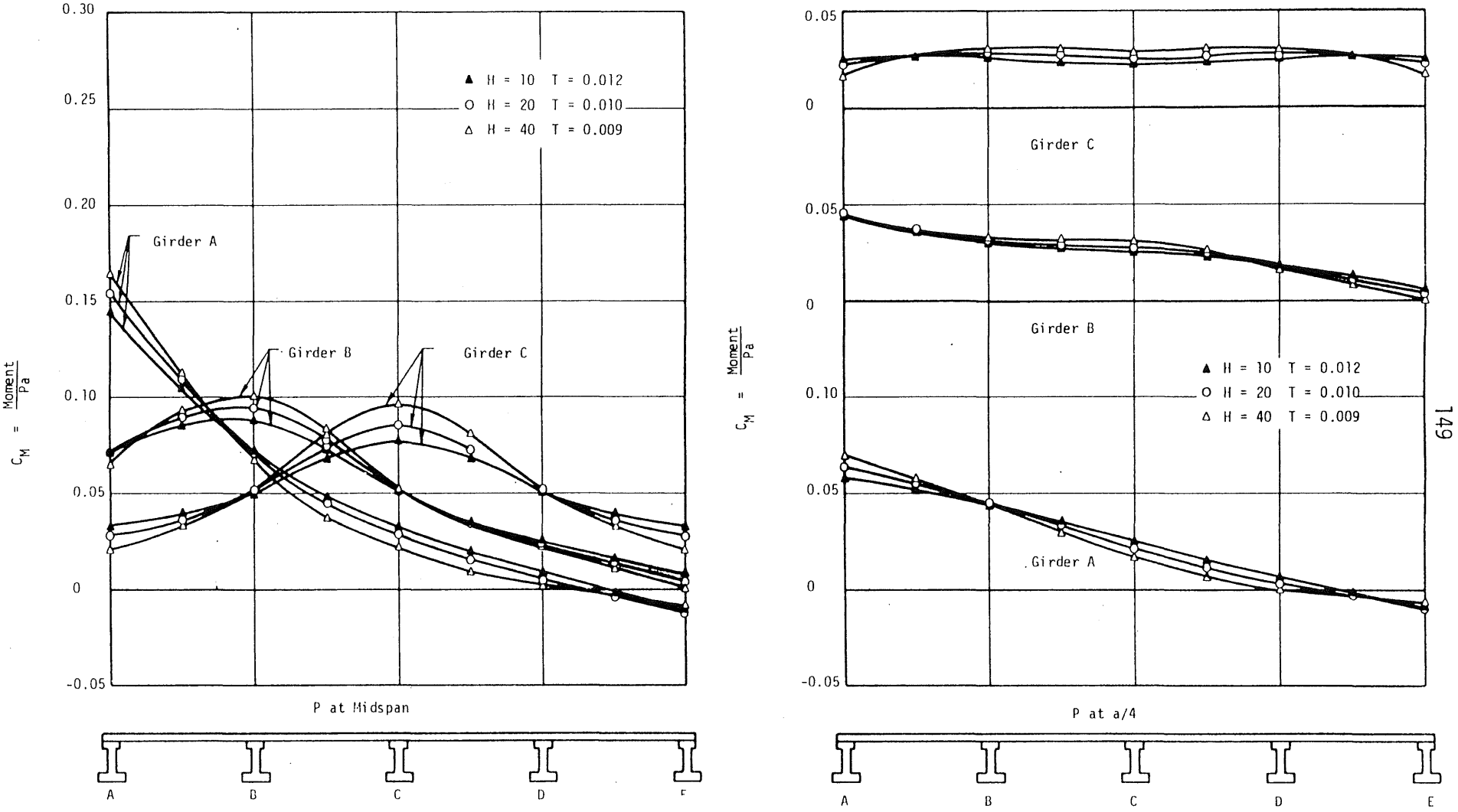

FIG. 5.4 INFLUENCE LINES FOR MOMENT AT MIDSPAN OF GIRDERS DUE TO LOAD P MOVING TRANSVERSELY ACROSS BRIDGE: b/a = 0.05, WITHOUT DIAPHRAGMS

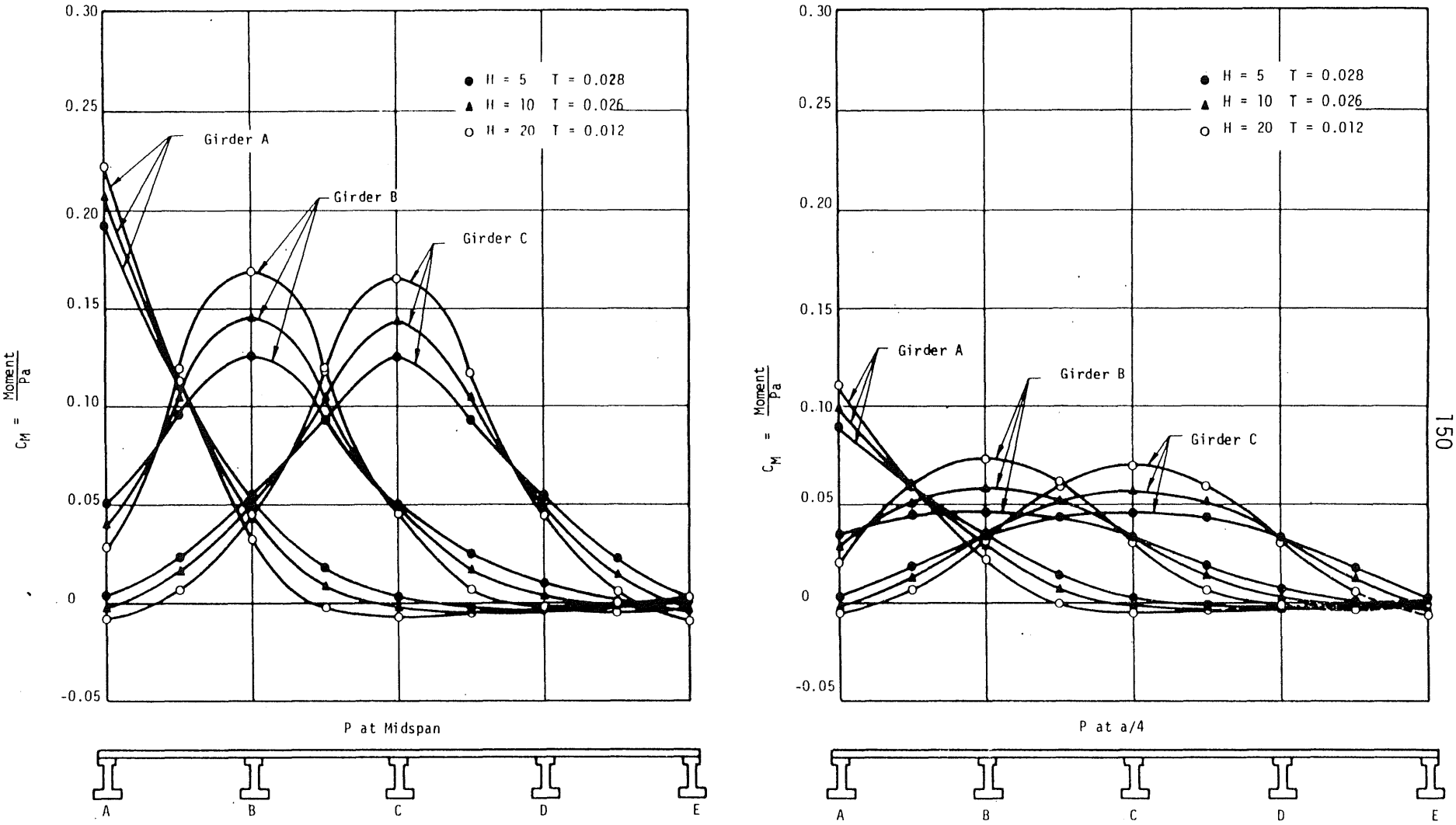

FIG. 5.5 INFLUENCE LINES FOR MOMENT AT MIDSPAN OF GIRDERS DUE TO P MOVING TRANSVERSELY ACROSS BRIDGE: b/a = 0.20, WITHOUT DIAPHRAGMS

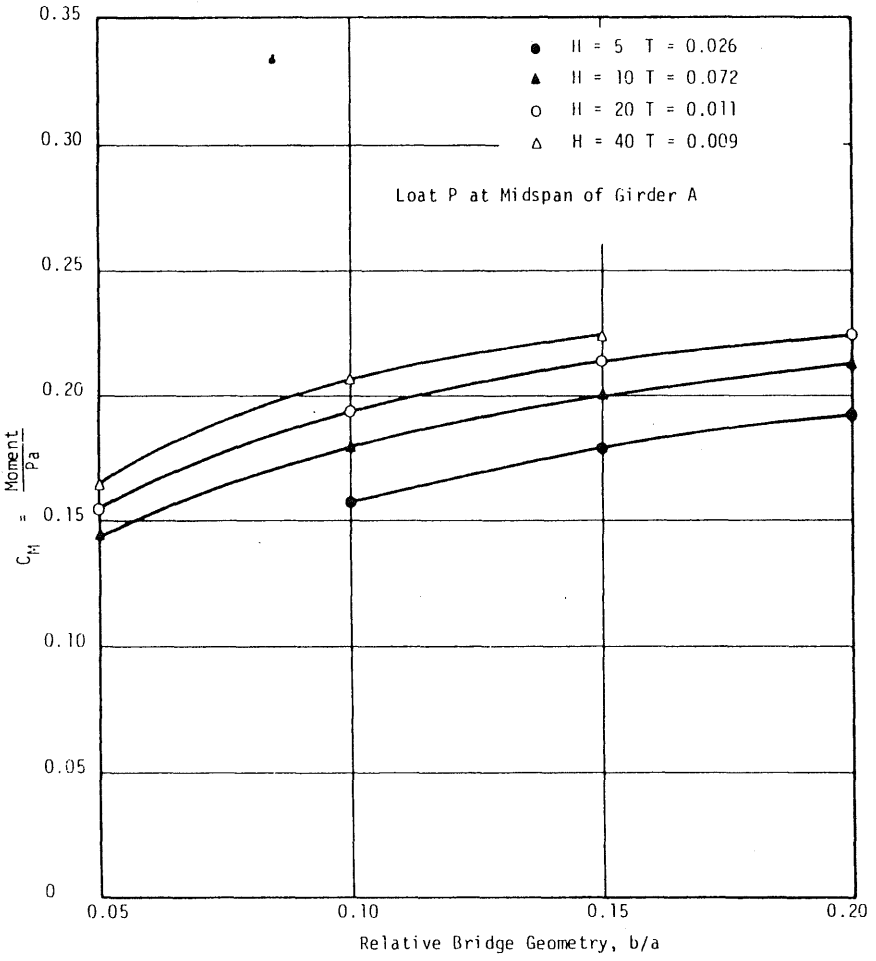

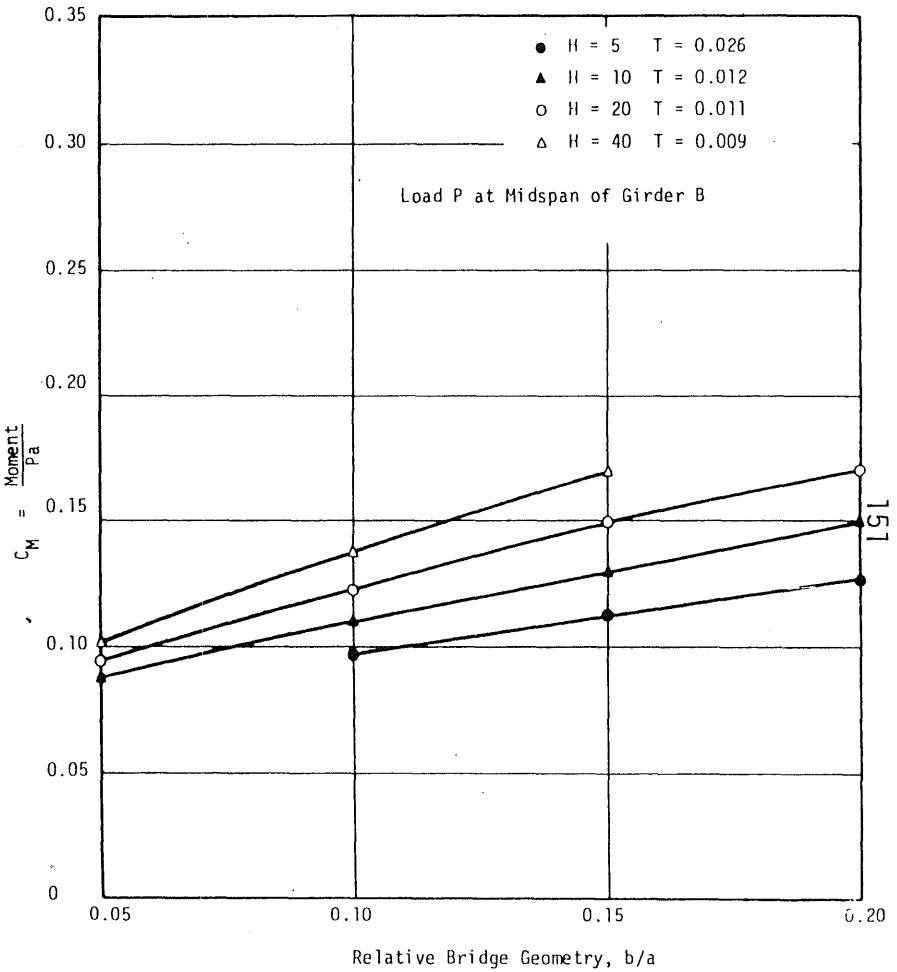

FIG. 5.6 RELATIONSHIP BETWEEN MOMENT AT MIDSPAN OF LOADED GIRDER AND RELATIVE BRIDGE GEOMETRY, b/a, WITHOUT DIAPHRAGMS

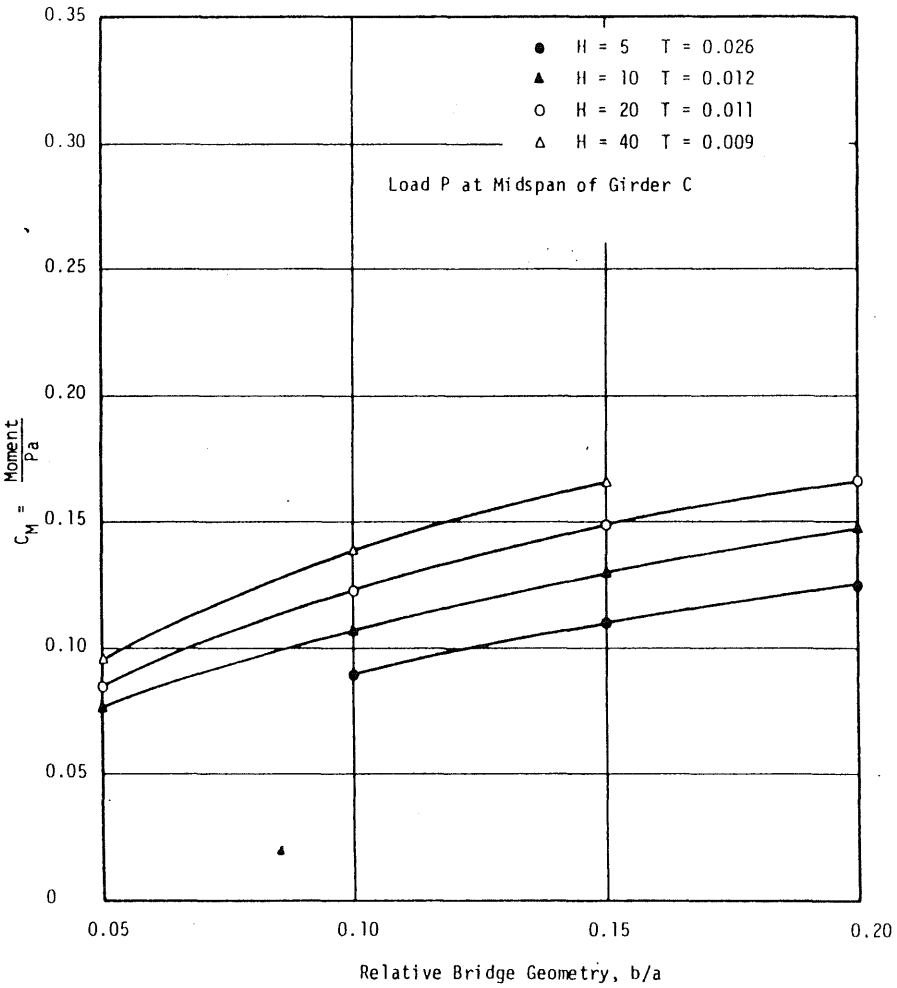
0.35
0.30
0.25
0.20
0.15
0.10
0.05
0
$C_M = \frac{Moment}{Pa}$
H = 5 T = 0.026
H = 10 T = 0.012
H = 20 T = 0.011
H = 40 T = 0.009
Load P at Midspan of Girder C
0.05
0.10
0.15
0.20
Relative Bridge Geometry, b/a

FIG. 5.6 (Cont.)

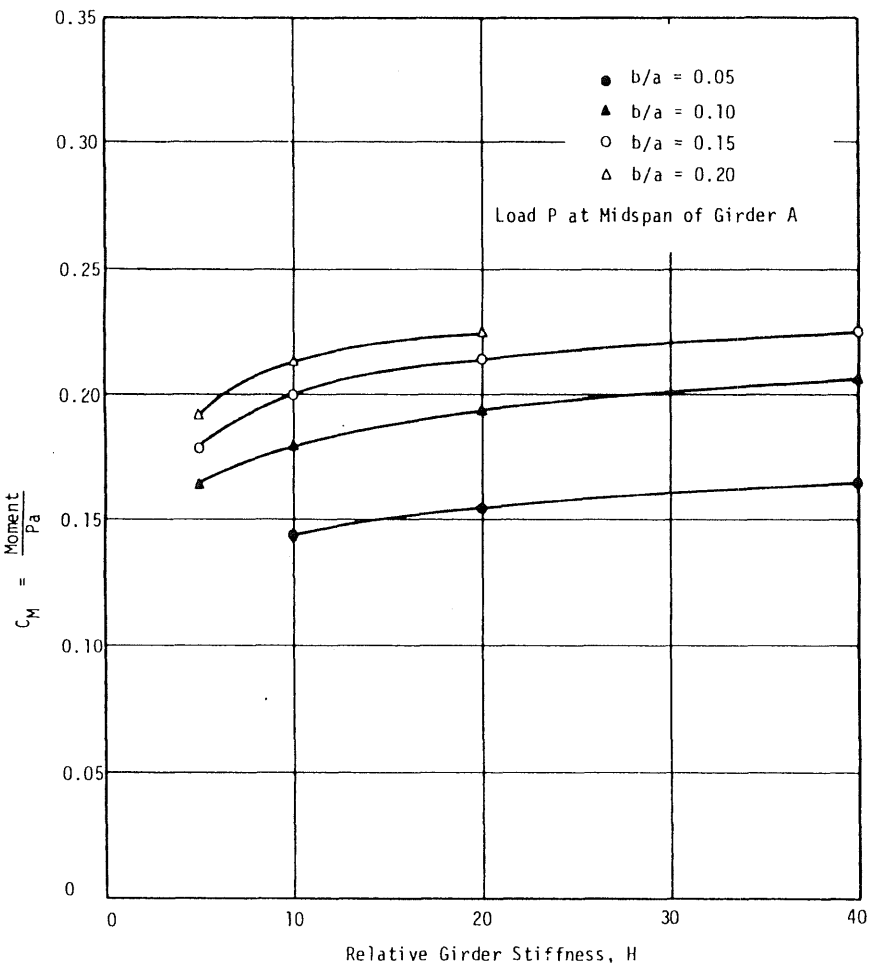

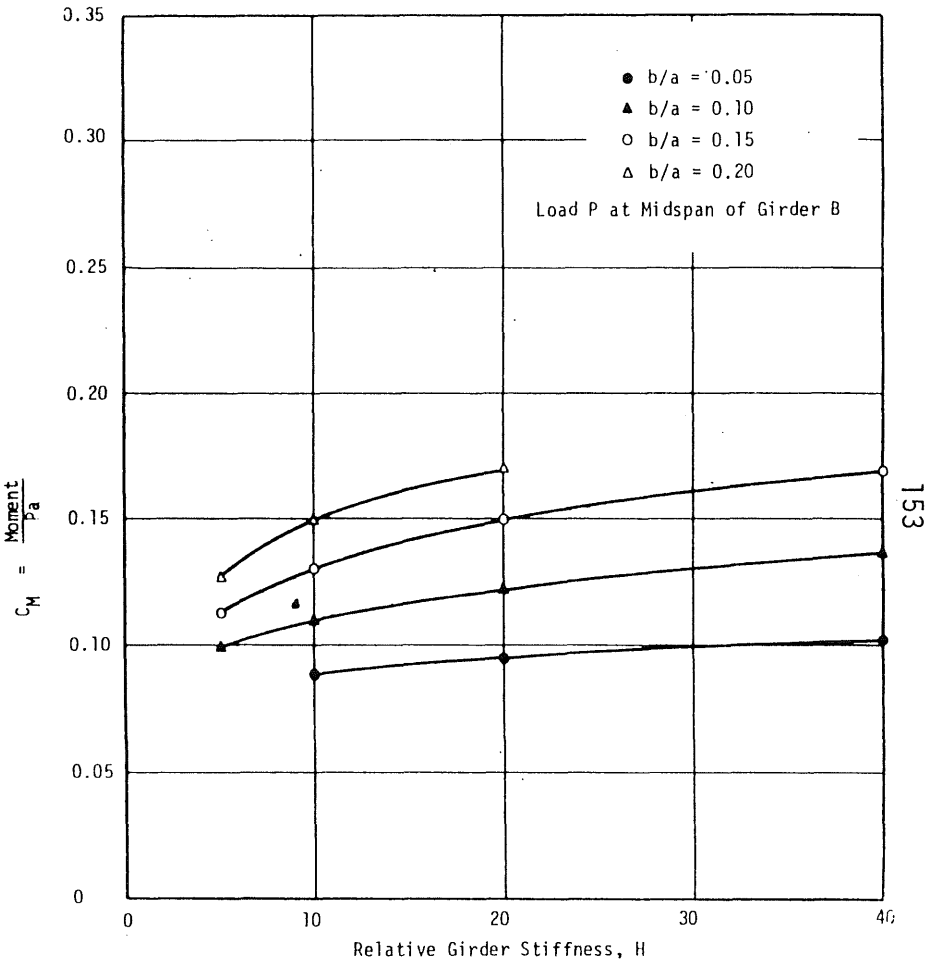

FIG. 5.7 RELATIONSHIP BETWEEN MOMENT AT MIDSPAN OF LOADED GIRDER AND RELATIVE GIRDER STIFFNESS, H, WITHOUT DIAPHRAGMS

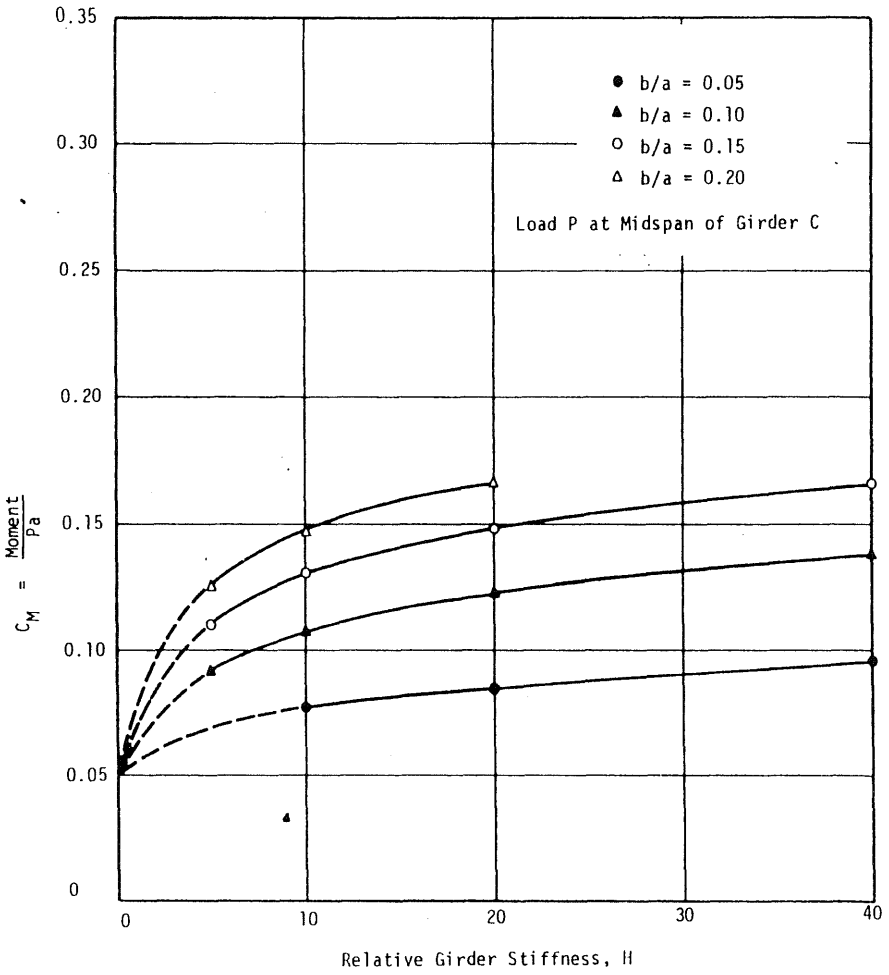
0.35
0.30
0.25
0.20
0.15
0.10
0.05
0
$C_M = \frac{\text{Moment}}{Pa}$
b/a = 0.05
b/a = 0.10
b/a = 0.15
b/a = 0.20
Load P at Midspan of Girder C
0
10
20
30
40
Relative Girder Stiffness, H

FIG. 5.7 (Cont.)

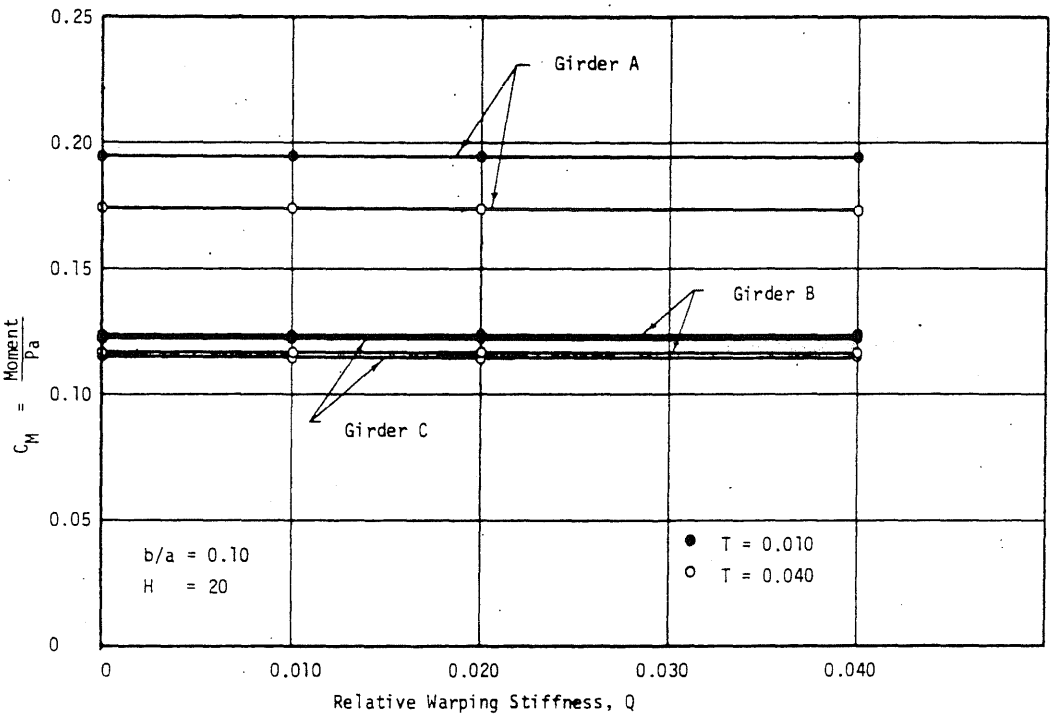

FIG. 5.8 RELATIONSHIP BETWEEN MOMENT AT MIDSPAN OF THE LOADED GIRDER AND RELATIVE WARPING STIFFNESS, Q

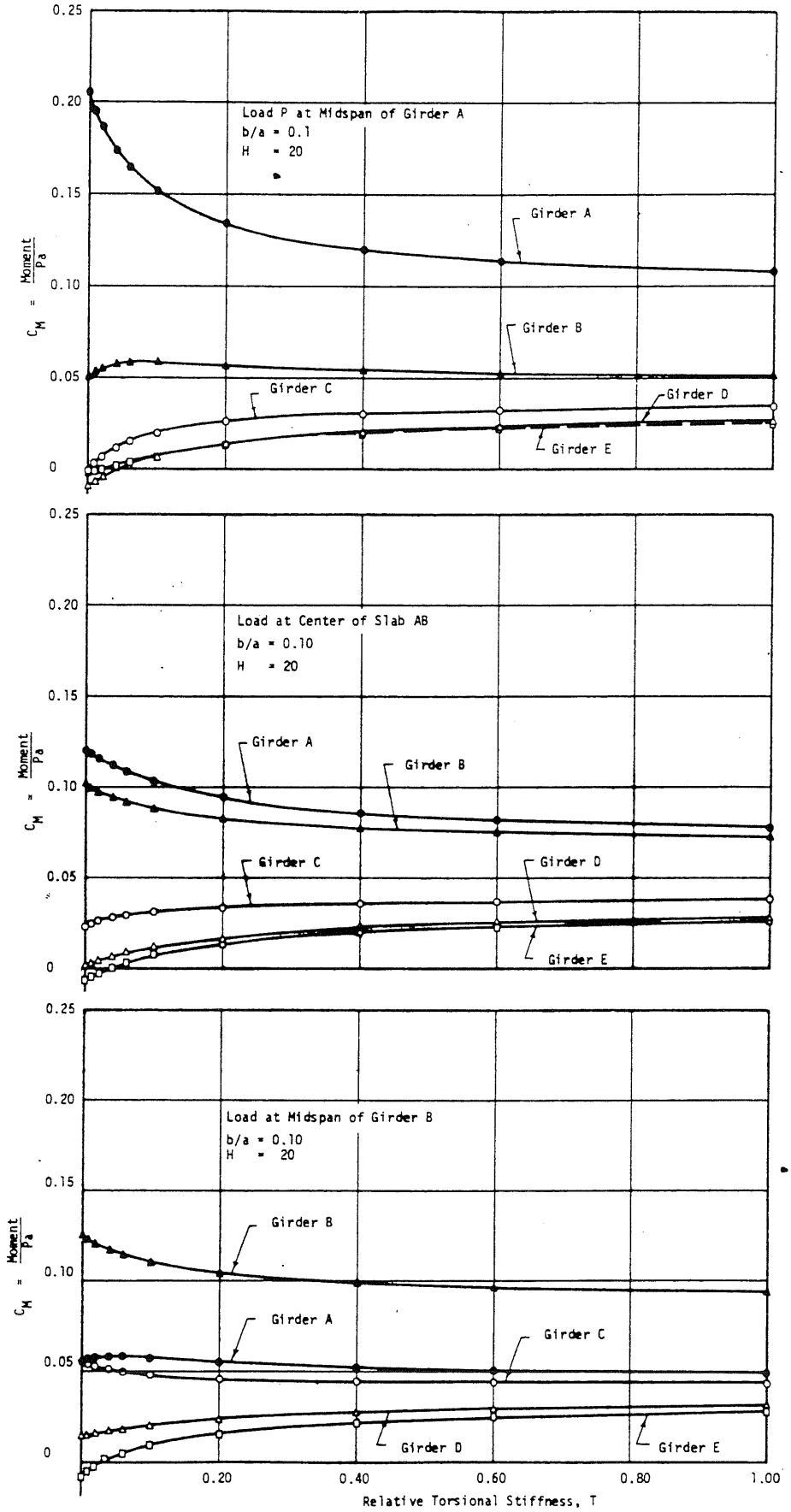

FIG. 5.9 RELATIONSHIP BETWEEN MOMENT AT MIDSPAN OF GIRDERS DUE TO LOAD P AND RELATIVE TORSIONAL STIFFNESS, T

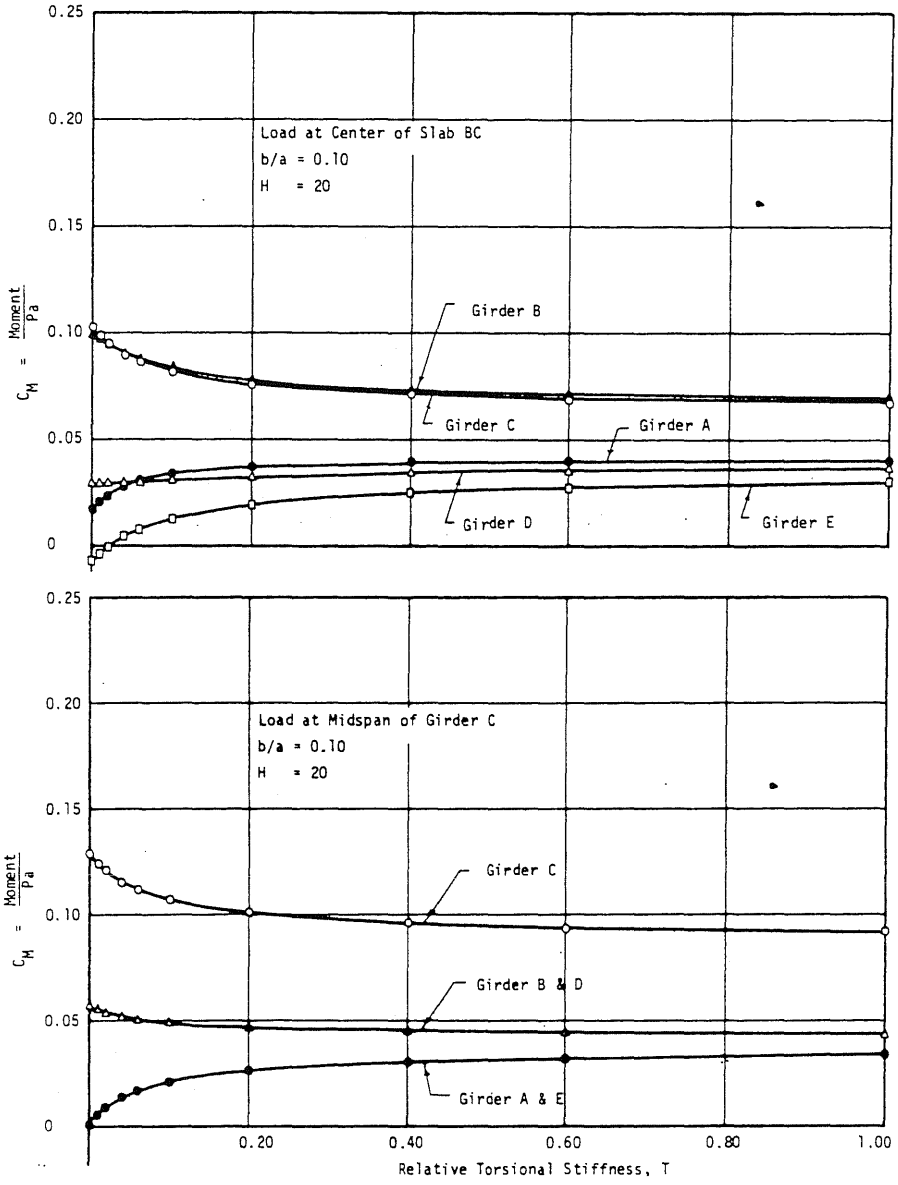
Load at Center of Slab BC
b/a = 0.10
H = 20
Girder B
Girder C
Girder A
Girder D
Girder E
Load at Midspan of Girder C
b/a = 0.10
H = 20
Girder C
Girder B & D
Girder A & E
$C_M = \frac{\text{Moment}}{Pa}$
0.25
0.20
0.15
0.10
0.05
0
0.20
0.40
0.60
0.80
1.00
Relative Torsional Stiffness, T

FIG. 5.9 (Cont.)

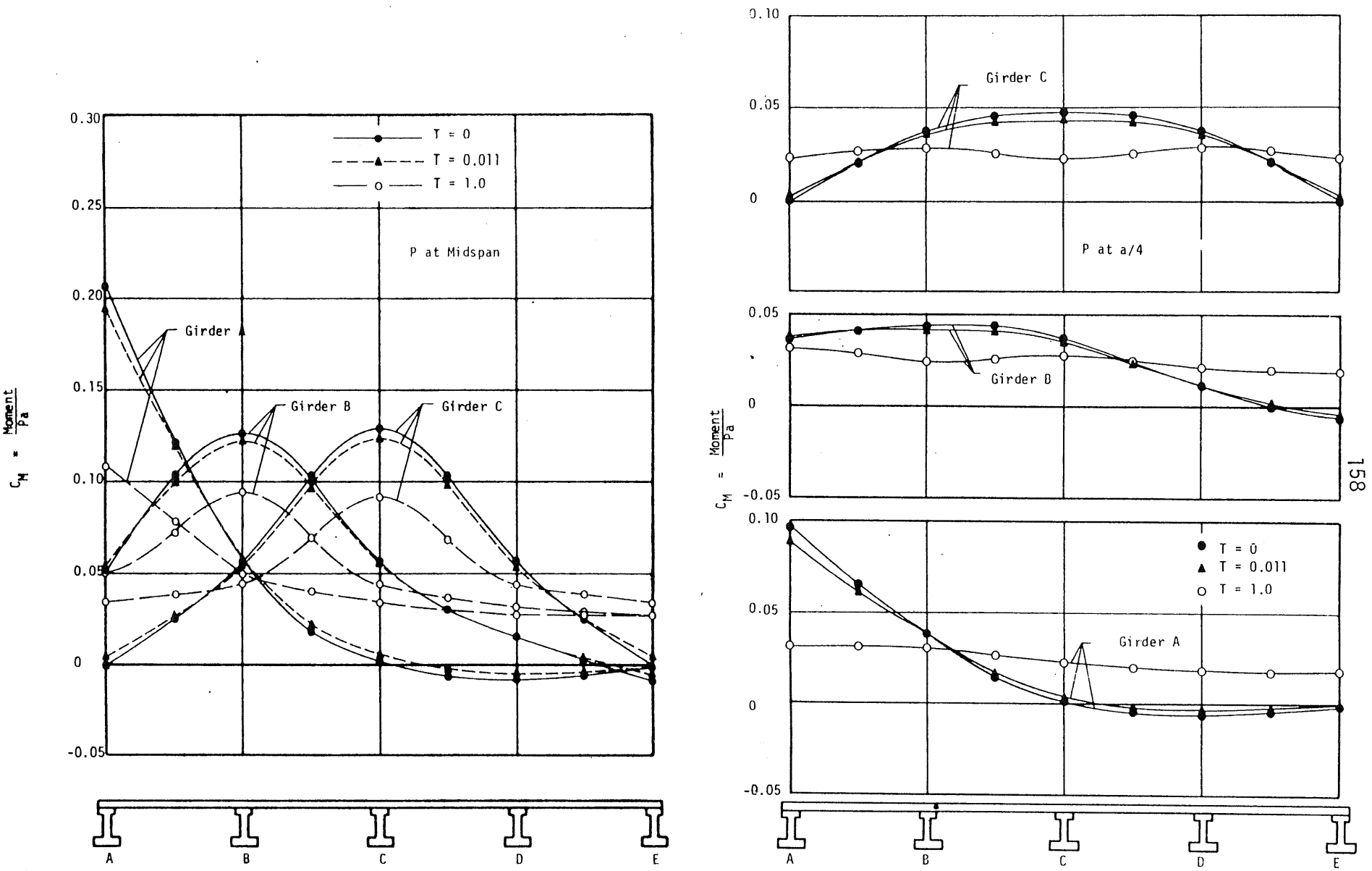

FIG. 5.10 INFLUENCE LINES FOR MOMENT AT MIDSPAN FOR DIFFERENT VALUES OF T DUE TO LOAD P MOVING ACROSS BRIDGE; b/a = 0.10, H = 20, WITHOUT DIAPHRAGMS

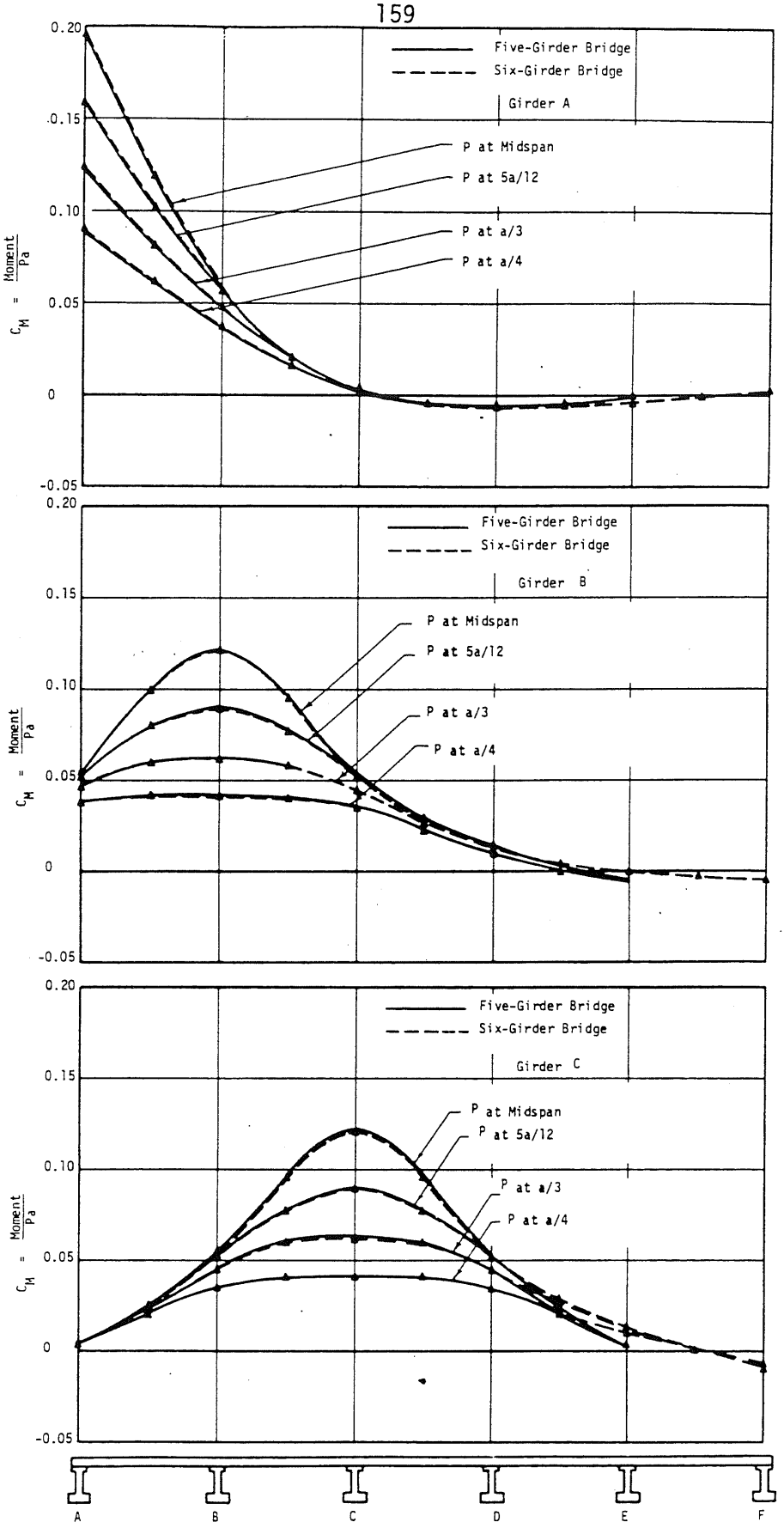

FIG. 5.11 INFLUENCE LINES FOR MOMENT AT MIDSPAN OF FIVE-GIRDER AND SIX-GIRDER BRIDGES DUE TO LOAD P MOVING TRANSVERSELY ACROSS BRIDGE: b/a = 0.10, H = 20, T = 0.011

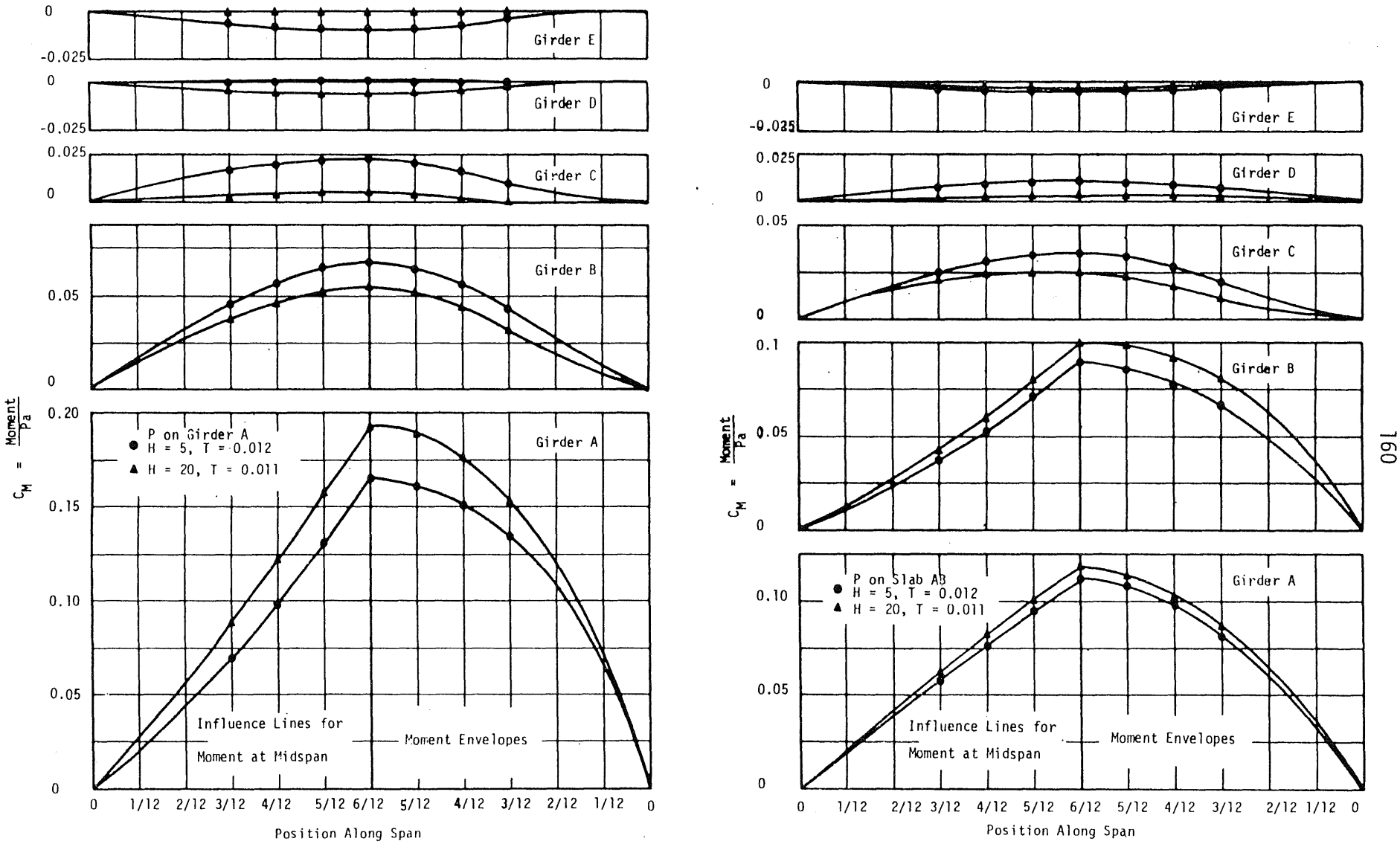

FIG. 5.12 INFLUENCE LINES FOR MOMENT AT MIDSPAN AND MOMENT ENVELOPES OF GIRDERS DUE TO LOAD P MOVING ALONG BRIDGE: b/a = 0.10

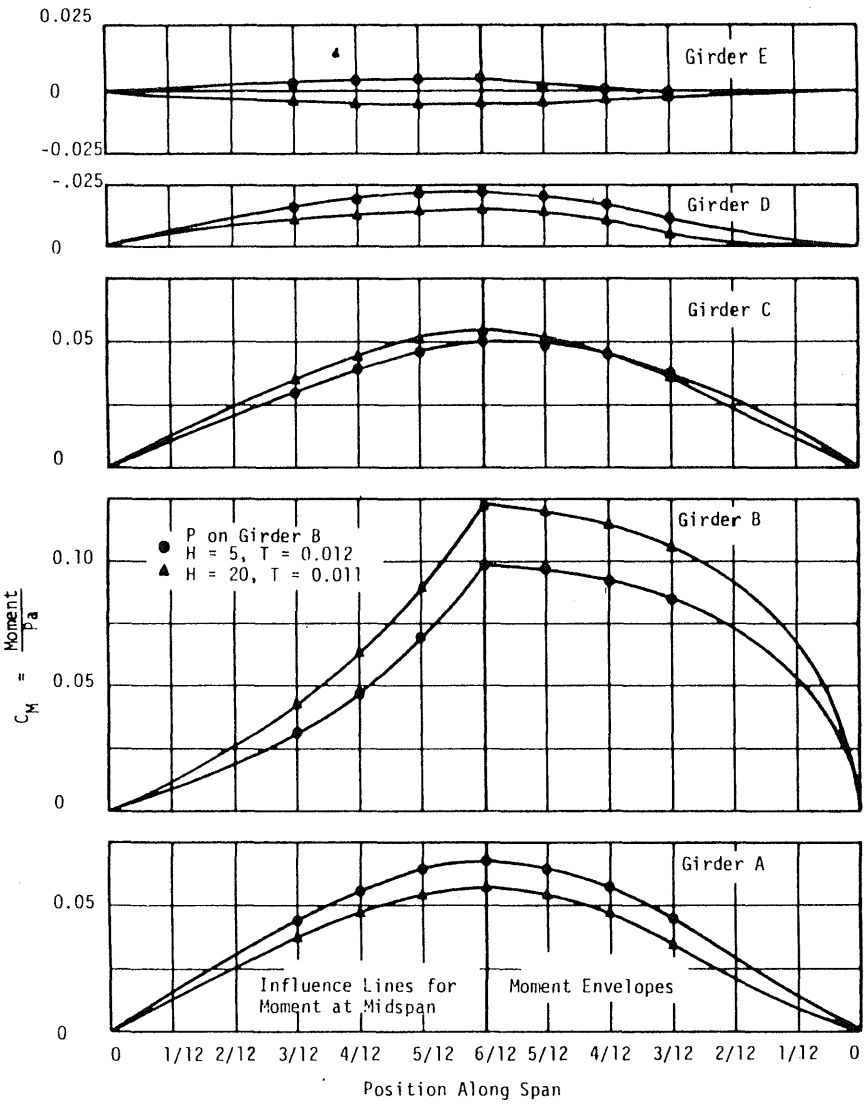
Girder E
Girder D
Girder C
Girder B
Girder A
P on Girder B
H = 5, T = 0.012
H = 20, T = 0.011
Influence Lines for Moment at Midspan
Moment Envelopes
$C_M = \frac{\text{Moment}}{Pa}$
Position Along Span

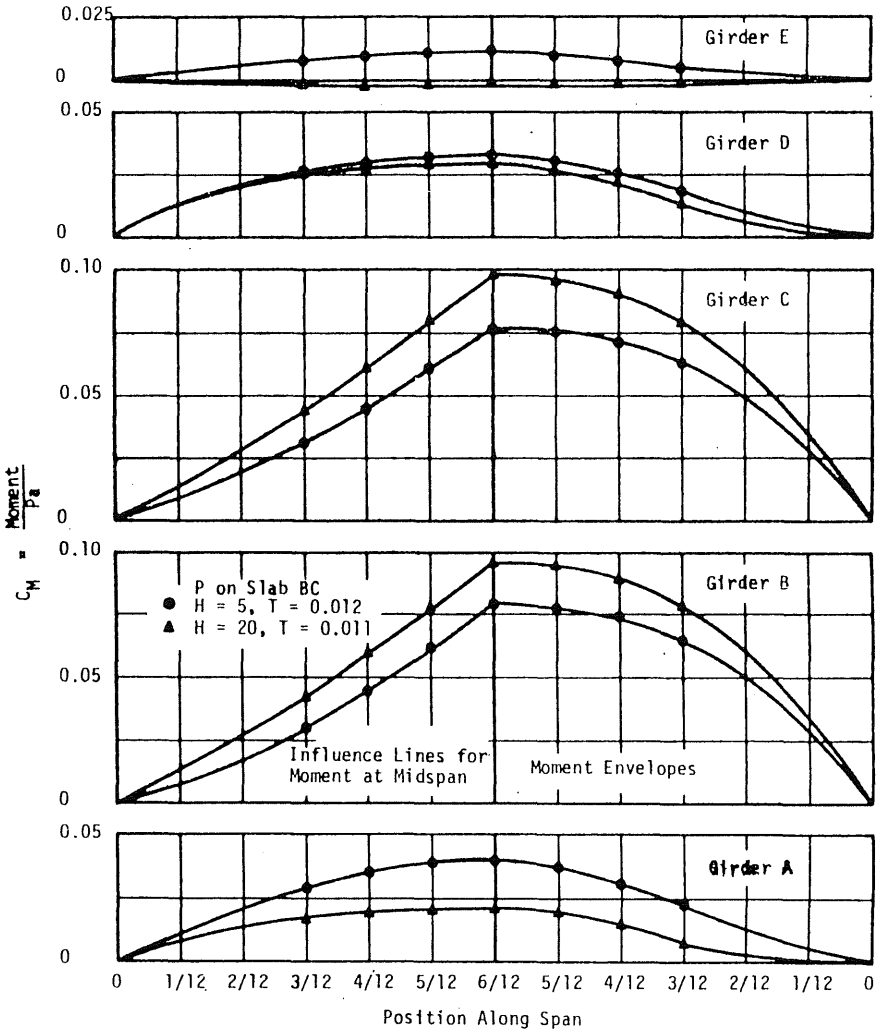
Girder E
Girder D
Girder C
Girder B
Girder A
P on Slab BC
H = 5, T = 0.012
H = 20, T = 0.011
Influence Lines for Moment at Midspan
Moment Envelopes
$C_M = \frac{\text{Moment}}{Pa}$
Position Along Span

FIG. 5.12 (Cont.)

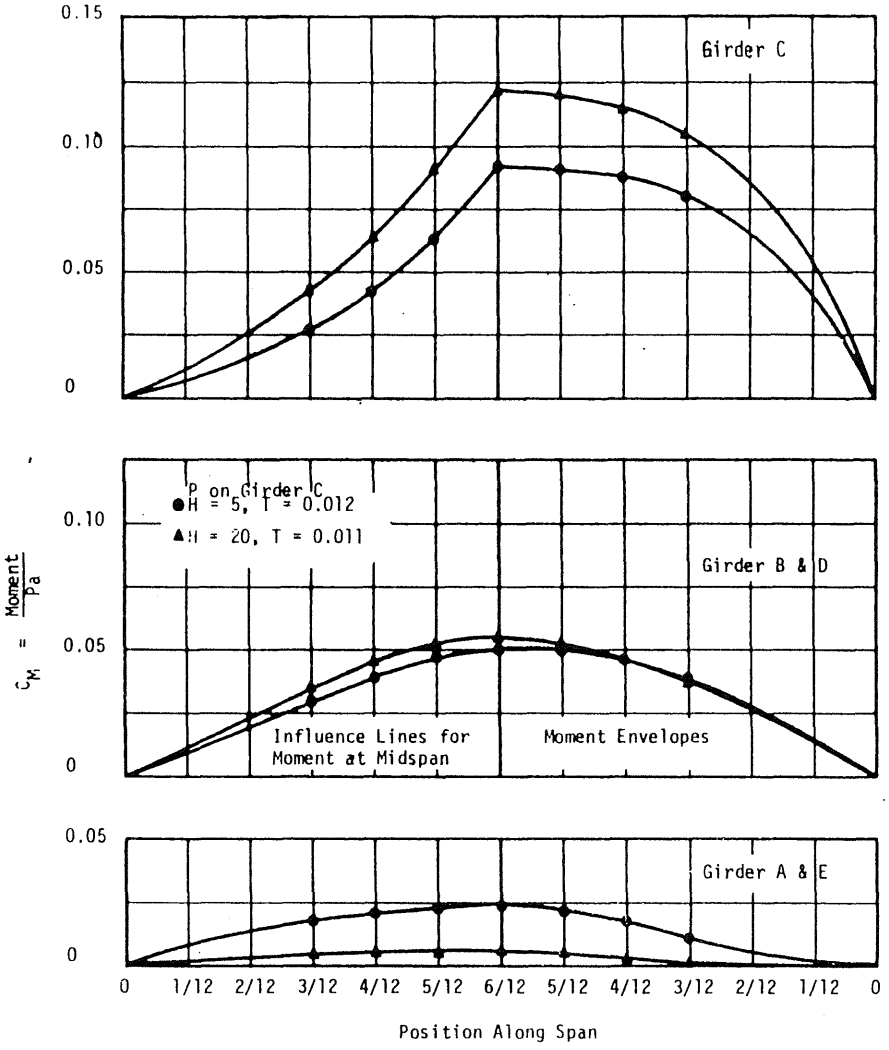
0.15
0.10
0.05
0
Girder C
P on Girder C
●H = 5, T = 0.012
▲H = 20, T = 0.011
Girder B & D
Influence Lines for Moment at Midspan
Moment Envelopes
$C_M = \frac{\text{Moment}}{Pa}$
0.05
0
Girder A & E
0 1/12 2/12 3/12 4/12 5/12 6/12 5/12 4/12 3/12 2/12 1/12 0
Position Along Span

FIG. 5.12 (Cont.)

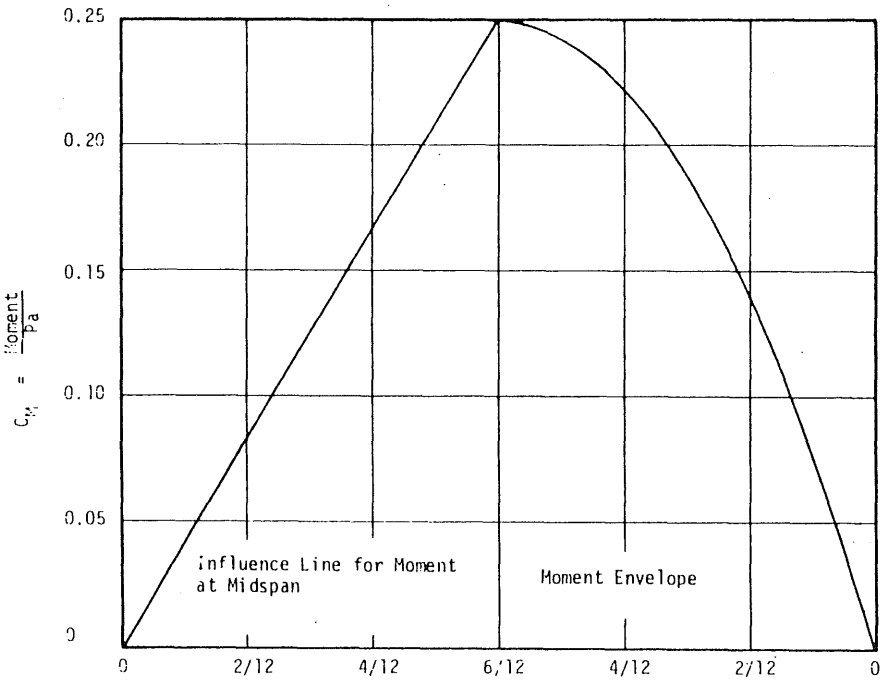

FIG. 5.13 INFLUENCE LINE FOR MOMENT AT MIDSPAN AND MOMENT ENVELOPE OF BRIDGE DUE TO LOAD P MOVING ALONG THE BRIDGE

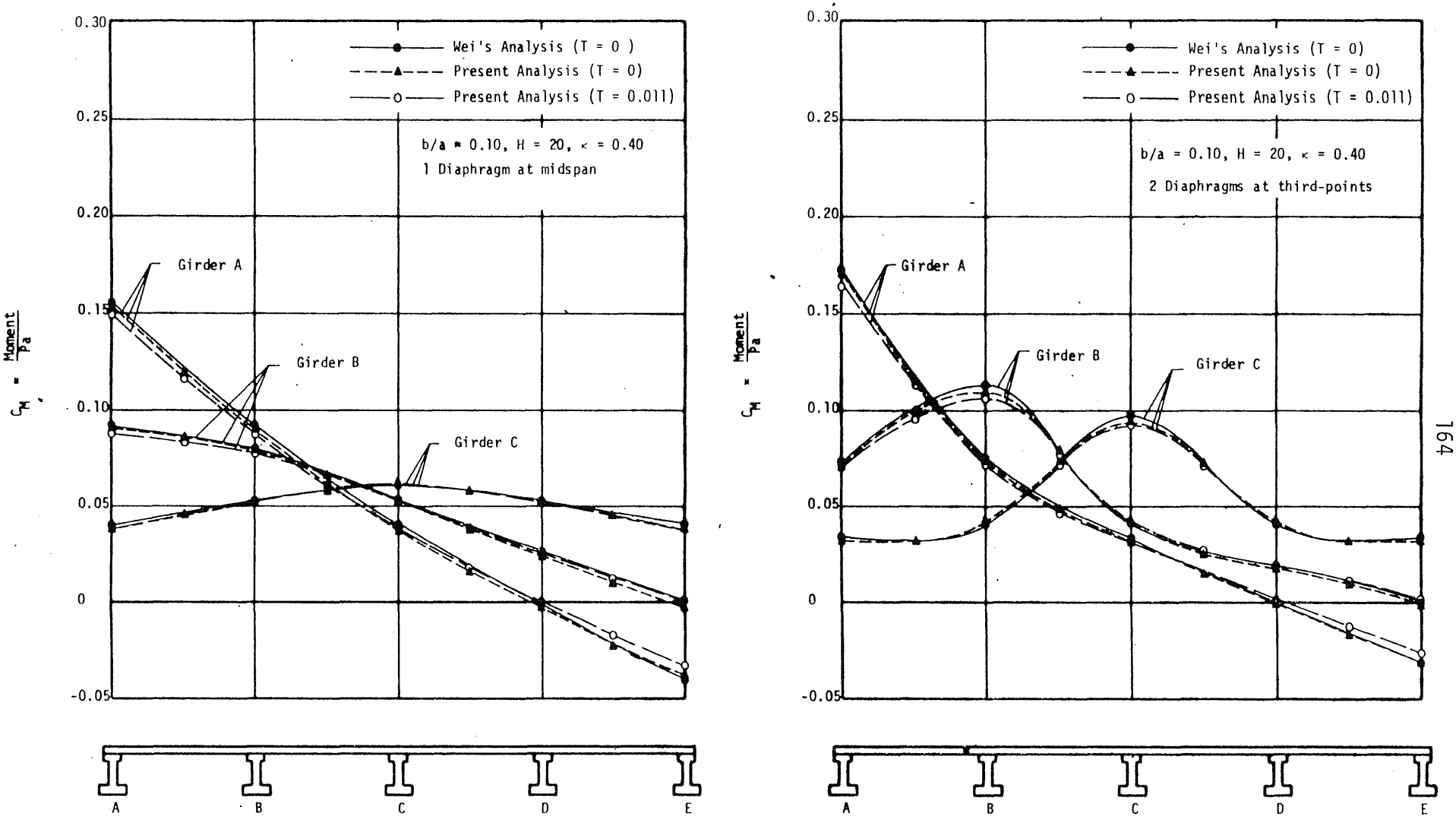

FIG. 5.14 COMPARISON OF EFFECTS OF DIAPHRAGMS ON INFLUENCE LINES FOR MOMENT AT MIDSPAN OF GIRDERS; LOAD P MOVING TRANSVERSELY ACROSS MIDSPAN

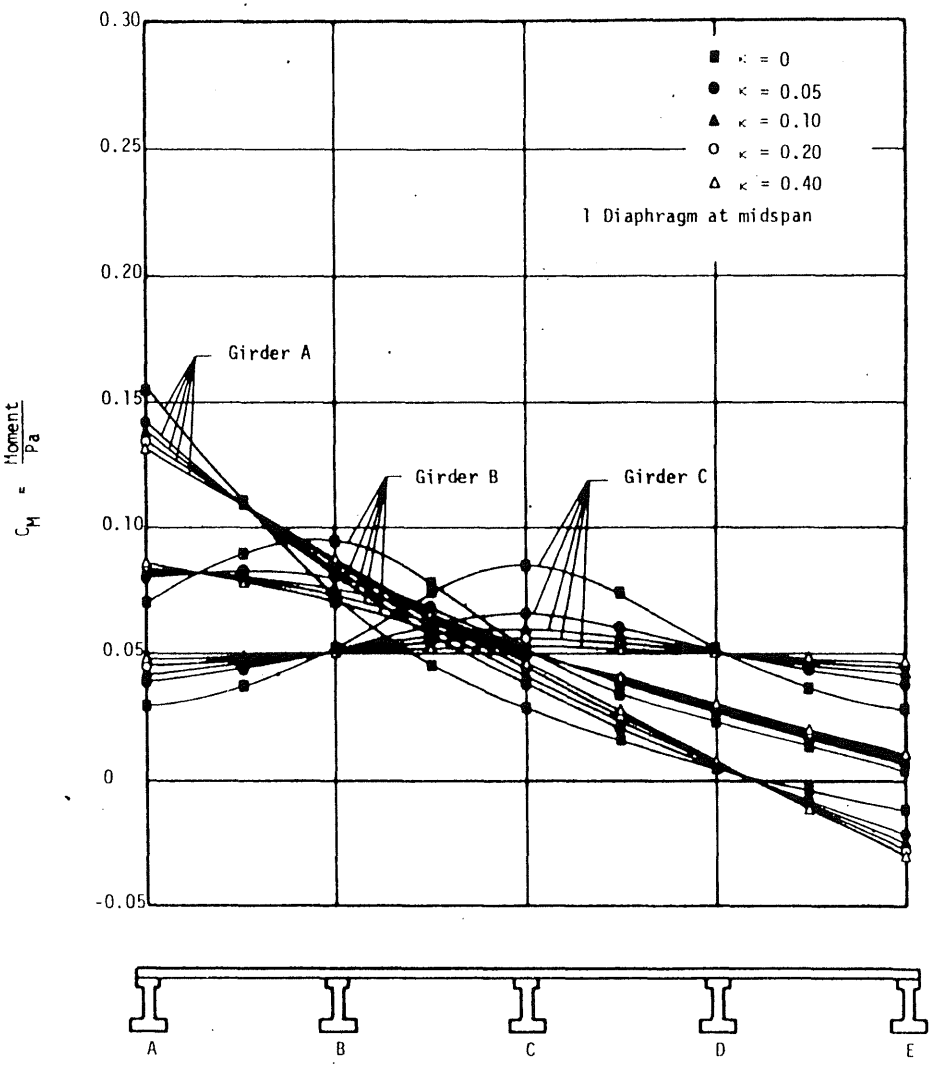

FIG. 5.15 EFFECTS OF DIAPHRAGMS ON INFLUENCE LINES FOR MOMENT AT MIDSPAN OF GIRDERS DUE TO LOAD P MOVING TRANSVERSELY ACROSS MIDSPAN; b/a = 0.05, H = 20, T = 0.010

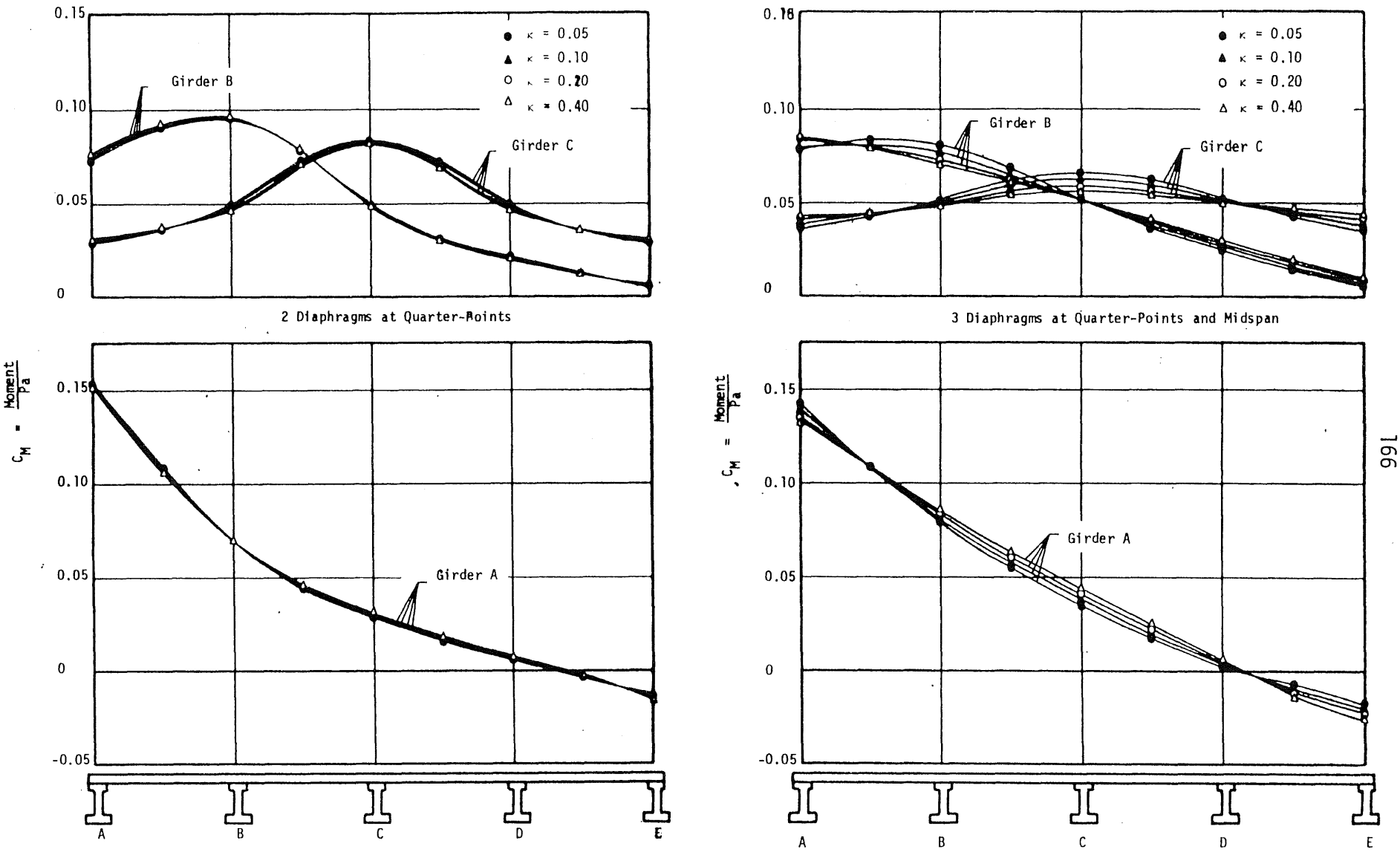
0.15
0.10
0.05
0
κ = 0.05
κ = 0.10
κ = 0.20
κ = 0.40
Girder B
Girder C
2 Diaphragms at Quarter-Points
3 Diaphragms at Quarter-Points and Midspan
$C_M = \frac{\text{Moment}}{Pa}$
Girder A
-0.05
A
B
C
D
E

FIG. 5.15 (Cont.)

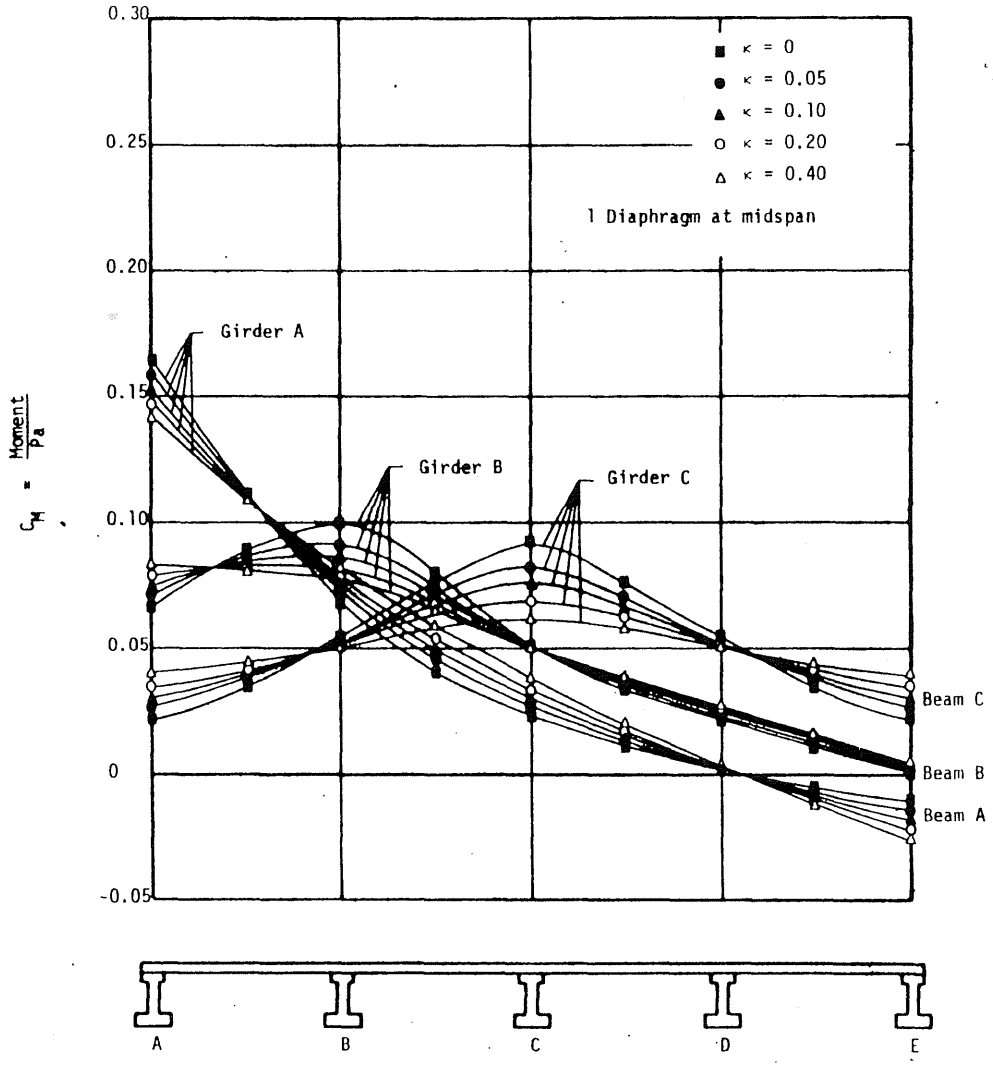

FIG. 5.16 EFFECTS OF DIAPHRAGMS ON INFLUENCE LINES FOR MOMENT AT MIDSPAN OF GIRDERS DUE TO LOAD P MOVING TRANSVERSELY ACROSS MIDSPAN; b/a = 0.10, H = 5, T = 0.012

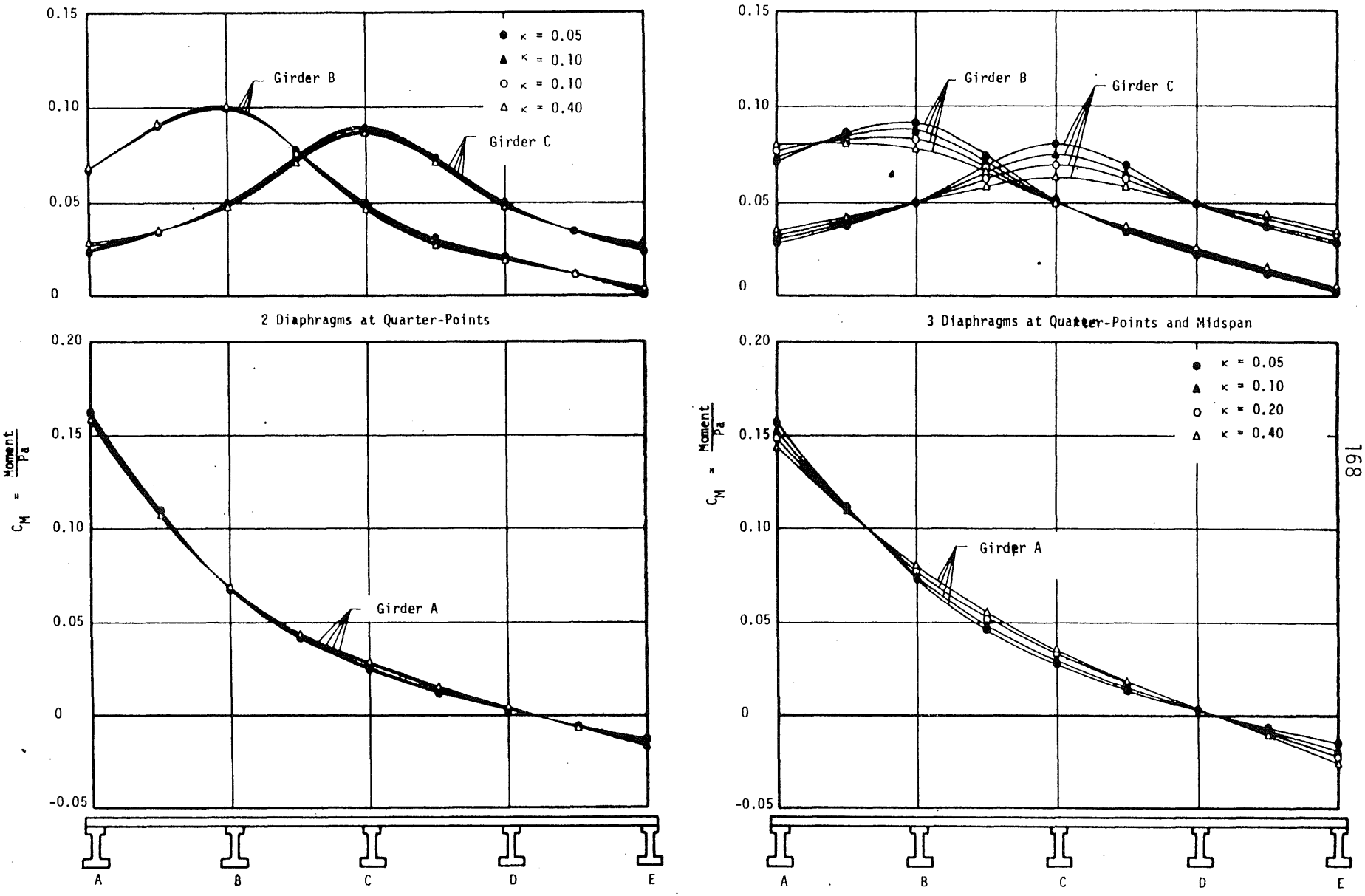
0.15
0.10
0.05
0
κ = 0.05
κ = 0.10
κ = 0.10
κ = 0.40
Girder B
Girder C
2 Diaphragms at Quarter-Points
3 Diaphragms at Quarter-Points and Midspan
$C_M = \frac{\text{Moment}}{Pa}$
0.20
0.15
0.10
0.05
0
-0.05
Girder A
κ = 0.05
κ = 0.10
κ = 0.20
κ = 0.40
A
B
C
D
E

FIG. 5.16 (Cont.)

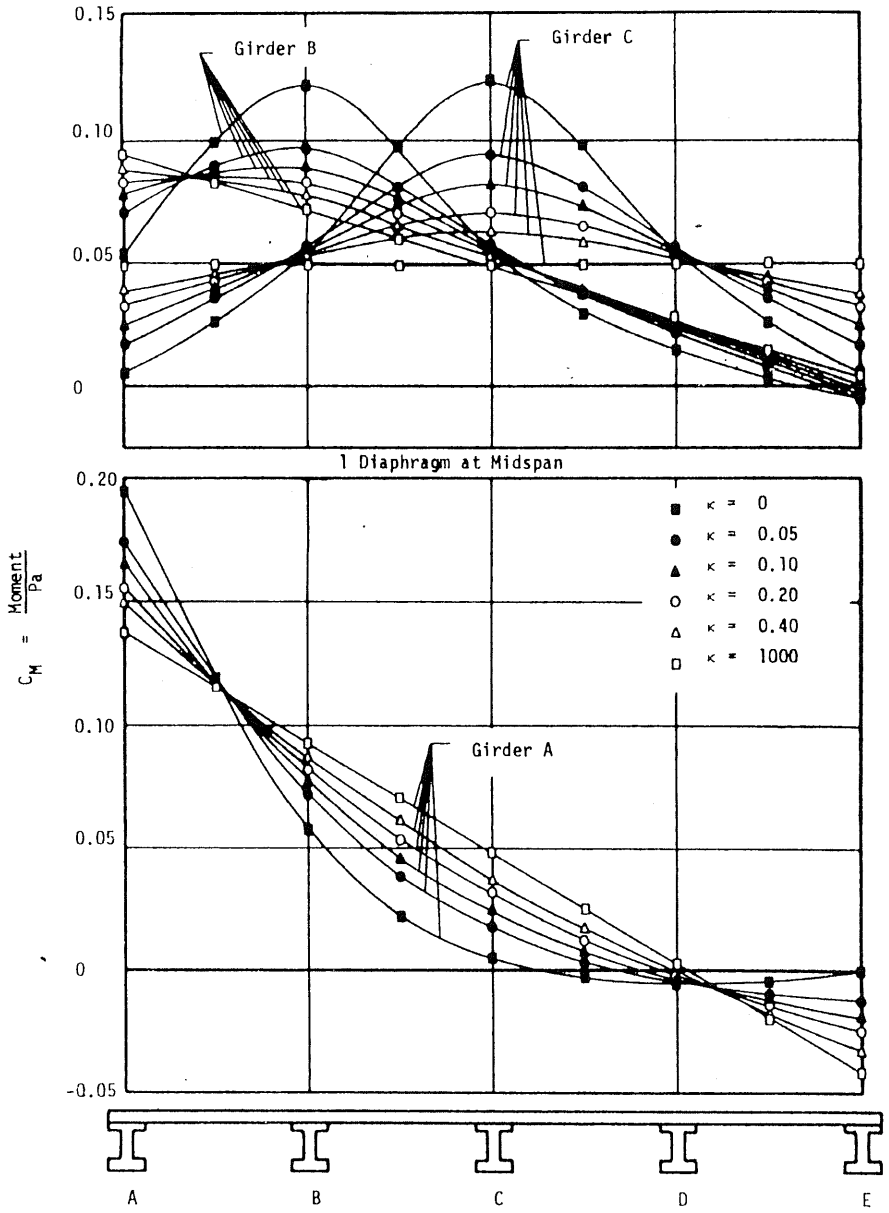

FIG. 5.17 EFFECTS OF DIAPHRAGMS ON INFLUENCE LINES FOR MOMENT AT MIDSPAN OF GIRDERS DUE TO LOAD P MOVING TRANSVERSELY ACROSS MIDSPAN; b/a = 0.10, H = 20, T = 0.011

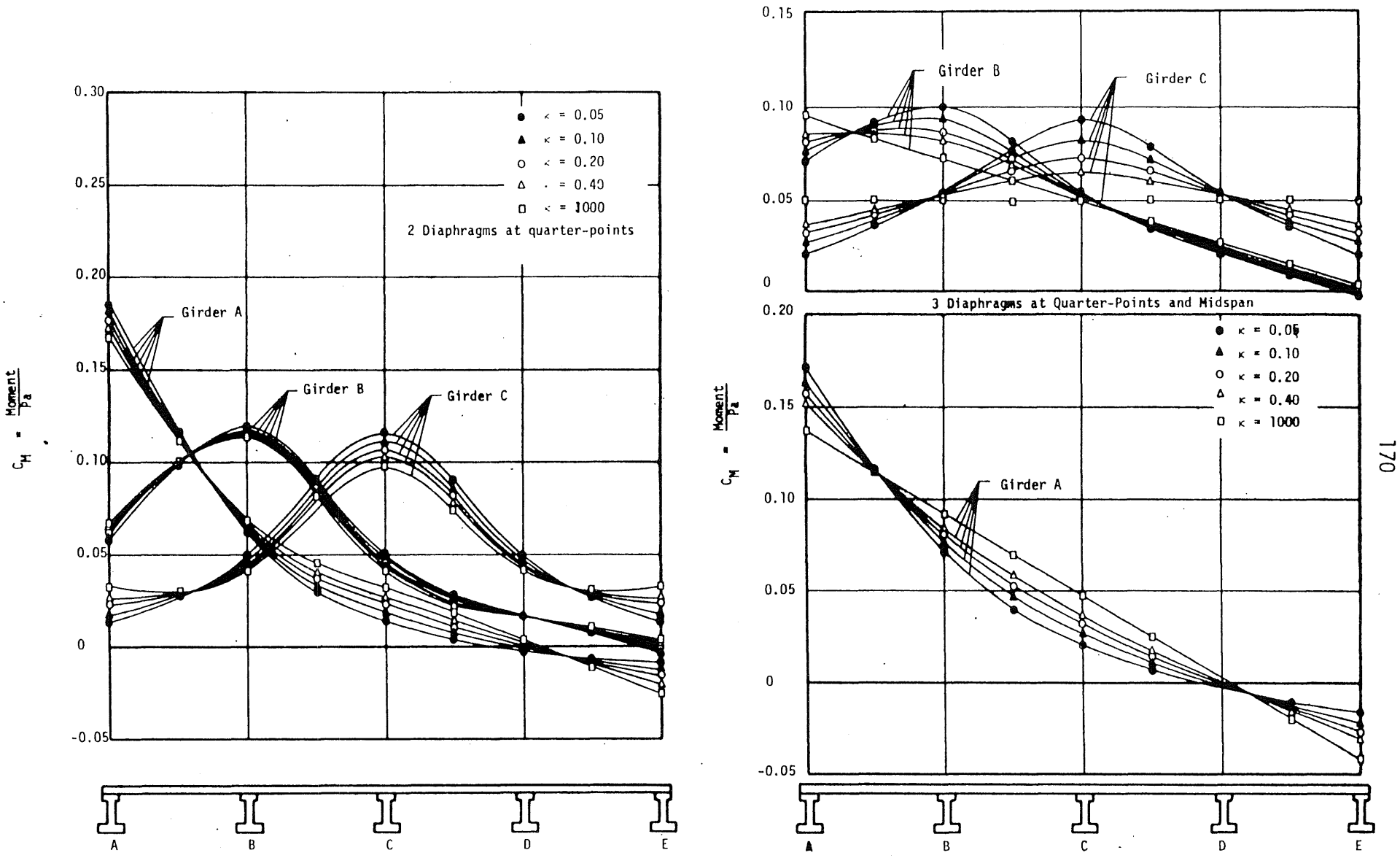
0.30
0.25
0.20
0.15
0.10
0.05
0
-0.05
$C_M = \frac{\text{Moment}}{Pa}$
κ = 0.05
κ = 0.10
κ = 0.20
κ = 0.40
κ = 1000
2 Diaphragms at quarter-points
Girder A
Girder B
Girder C
A
B
C
D
E
0.15
0.10
0.05
0
Girder B
Girder C
3 Diaphragms at Quarter-Points and Midspan
0.20
0.15
0.10
0.05
0
-0.05
κ = 0.05
κ = 0.10
κ = 0.20
κ = 0.40
κ = 1000
Girder A
A
B
C
D
E

FIG. 5.17 (Cont.)

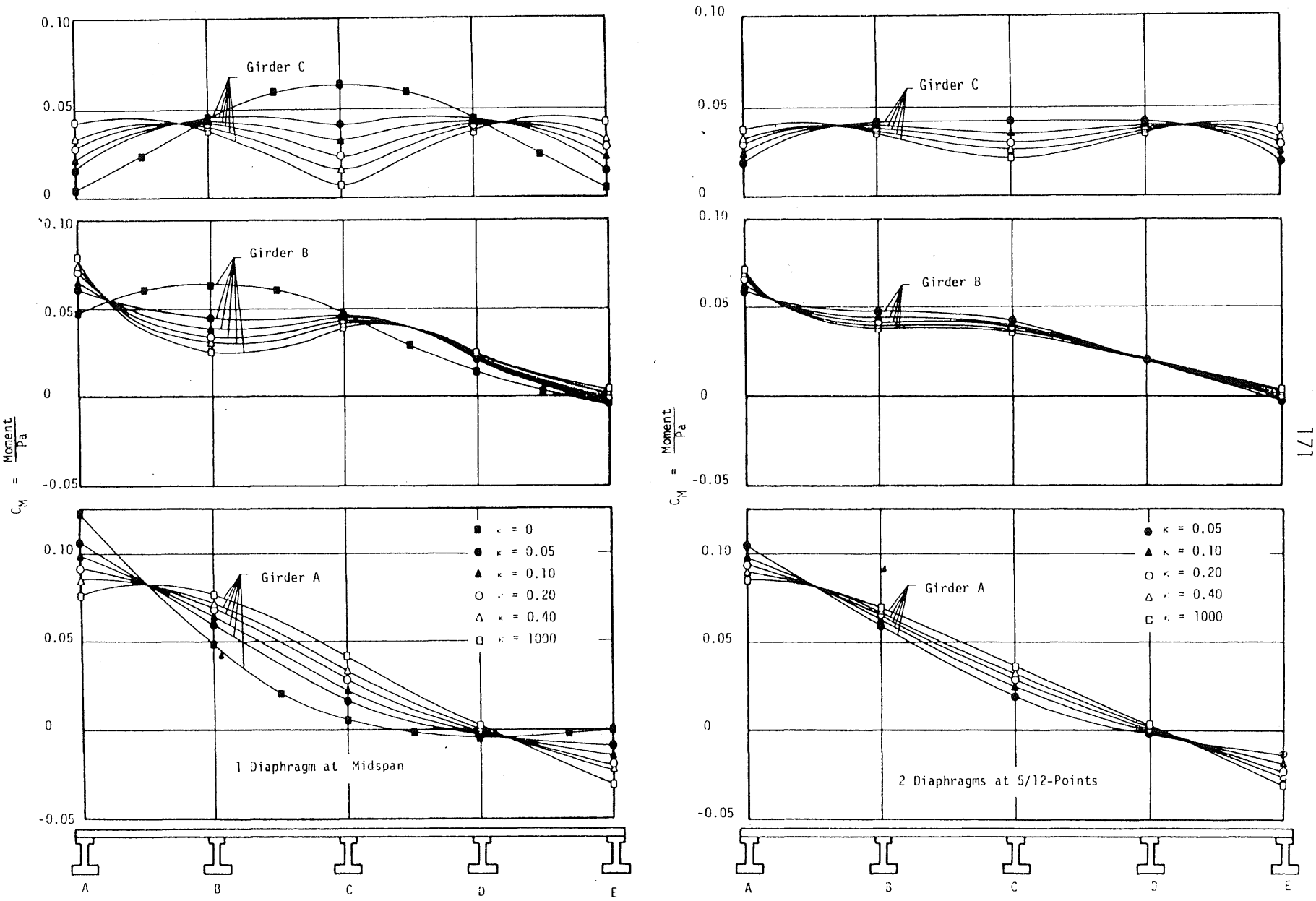

FIG. 5.18 EFFECTS OF DIAPHRAGMS ON INFLUENCE LINES FOR MOMENT AT MIDSPAN OF GIRDERS DUE TO LOAD P MOVING TRANSVERSELY ACROSS a/3; b/a = 0.10, H = 20, T = 0.011

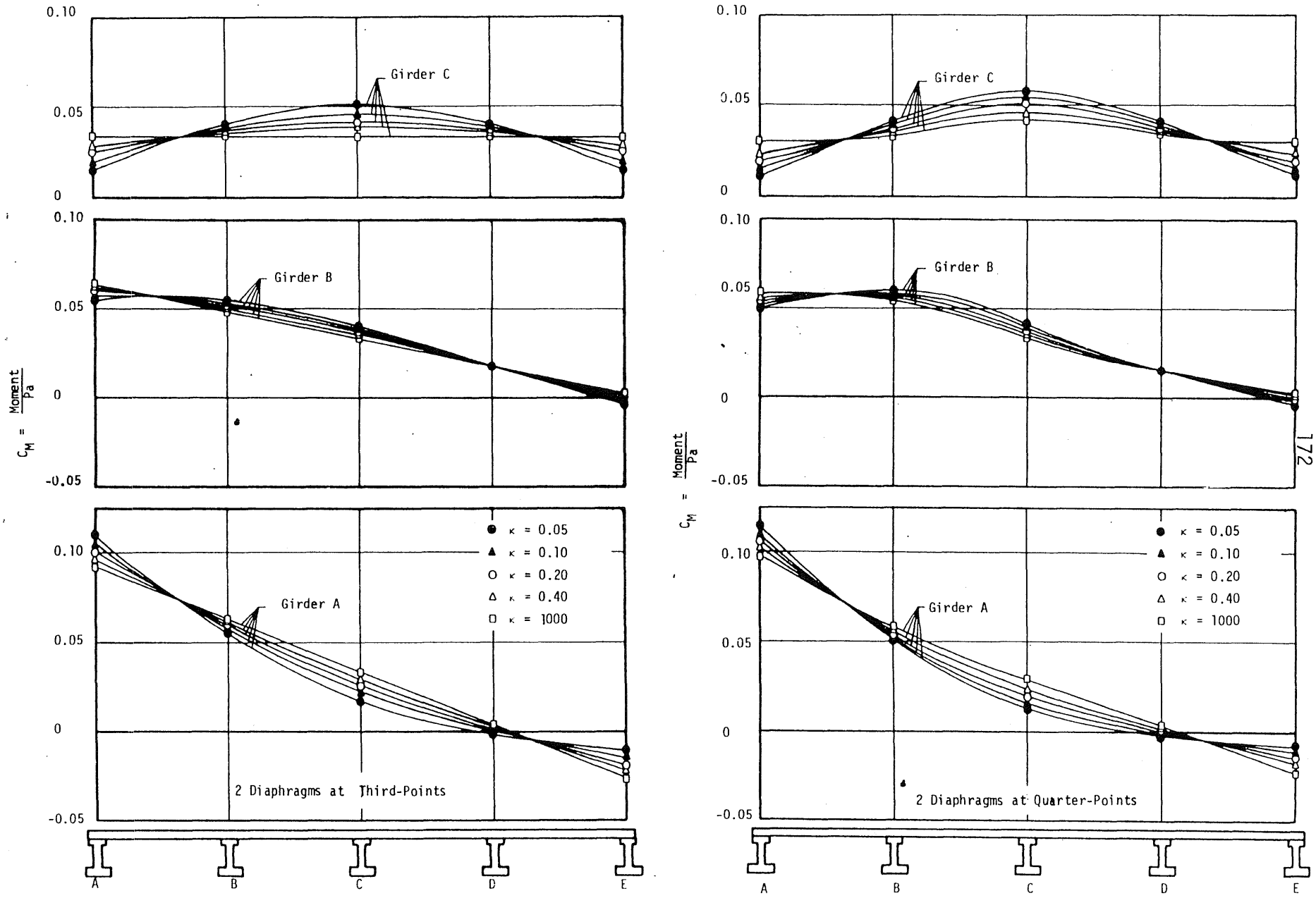
0.10
0.05
0
-0.05
Girder C
Girder B
Girder A
$C_M = \frac{\text{Moment}}{Pa}$
κ = 0.05
κ = 0.10
κ = 0.20
κ = 0.40
κ = 1000
2 Diaphragms at Third-Points
2 Diaphragms at Quarter-Points
A
B
C
D
E

FIG. 5.18 (Cont.)

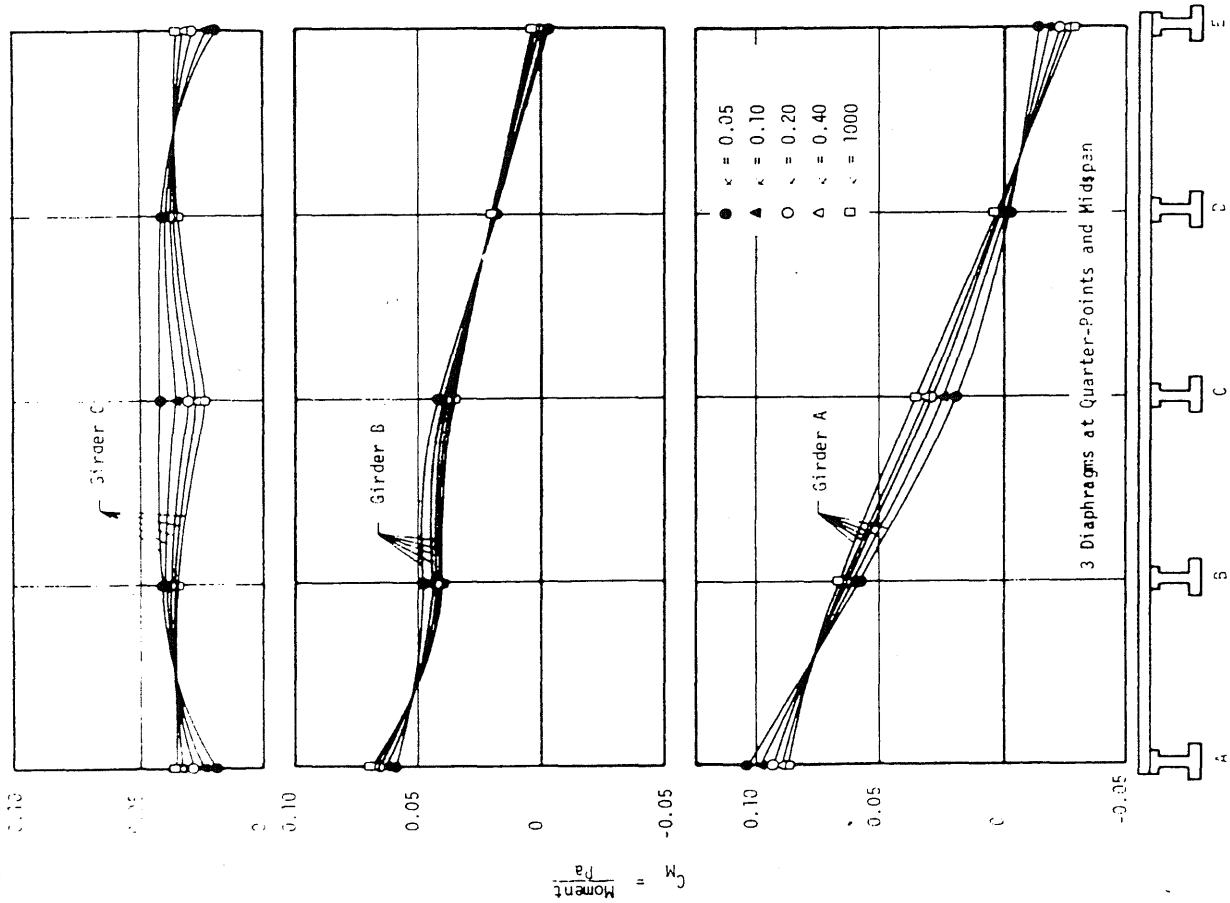
Girder C
Girder B
Girder A
0.10
0.05
0
-0.05
$C_M = \frac{\text{Moment}}{Pa}$
κ = 0.05
κ = 0.10
κ = 0.20
κ = 0.40
κ = 1000
3 Diaphragms at Quarter-Points and Midspan
A
B
C
D
E

FIG. 5.18 (Cont.)

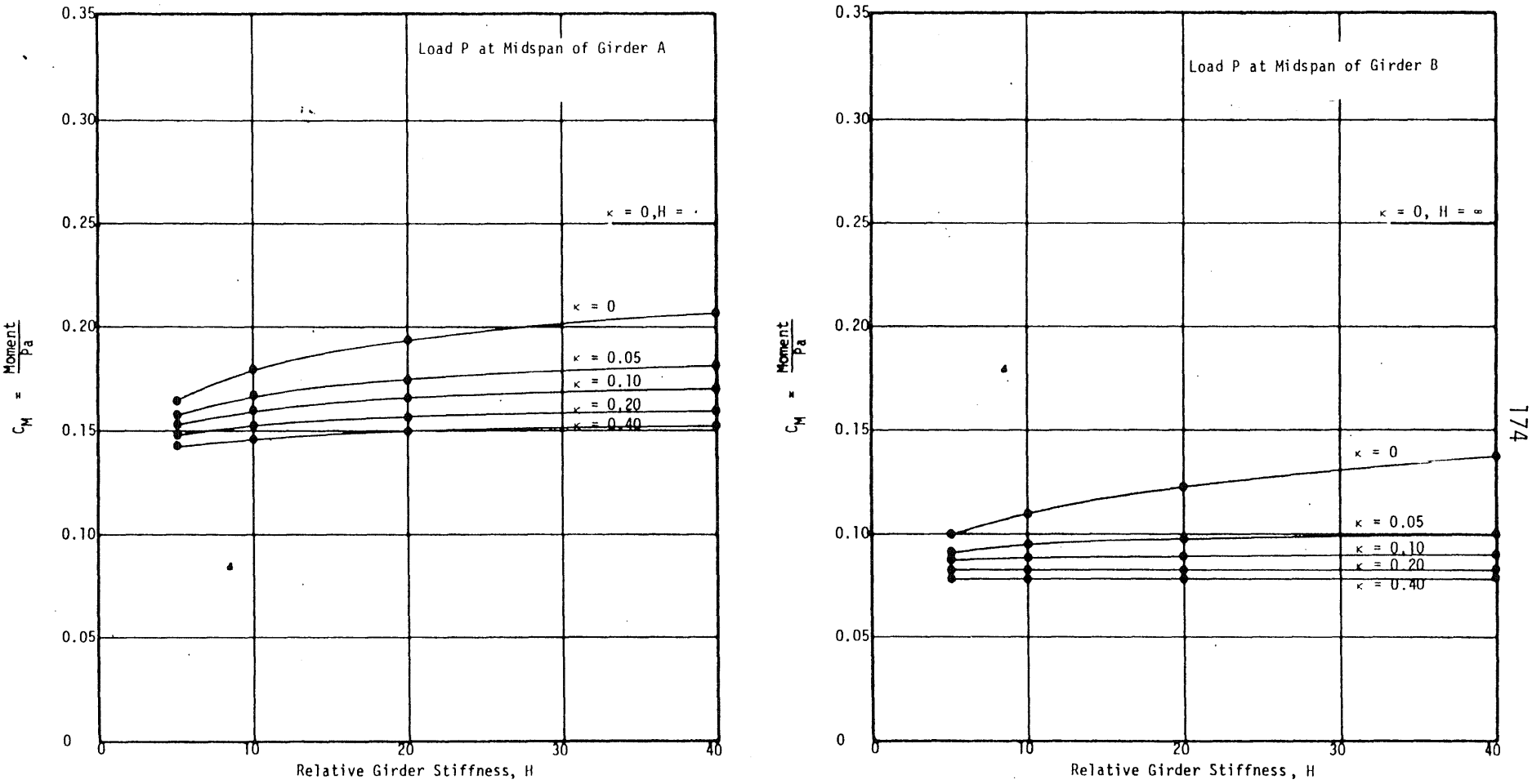

FIG. 5.19 RELATIONSHIP BETWEEN MOMENT AT MIDSPAN OF LOADED GIRDER AND RELATIVE GIRDER STIFFNESS, H; b/a = 0.10, 1 DIAPHRAGM AT MIDSPAN

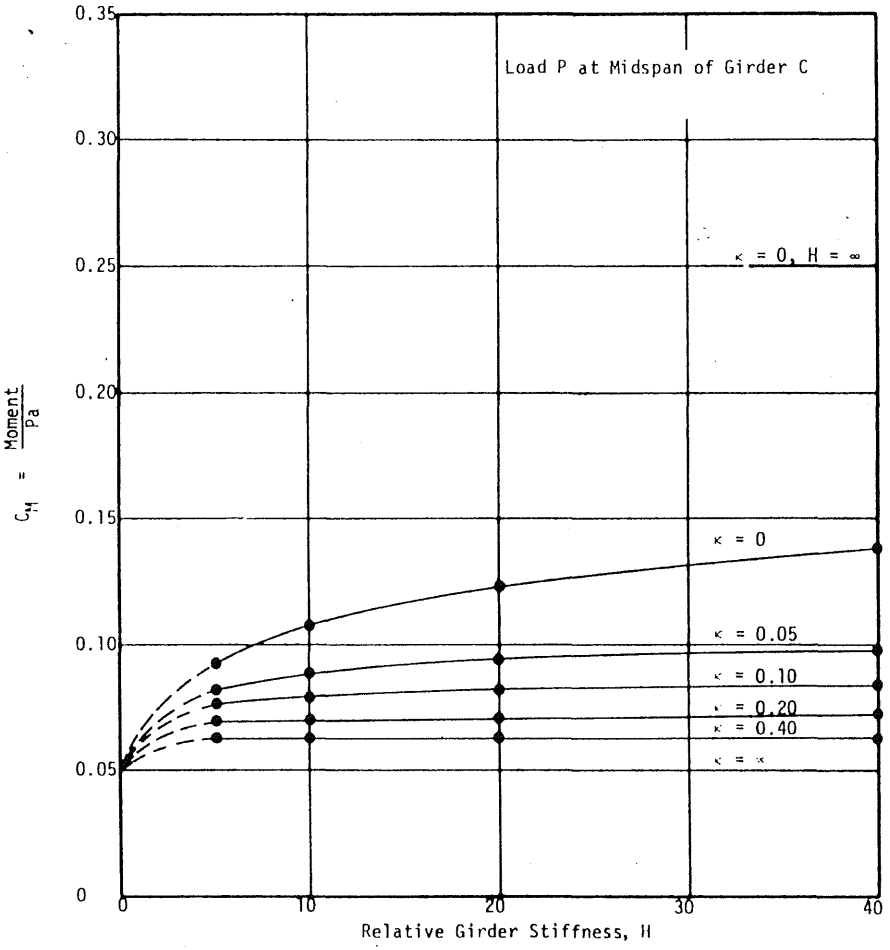
Load P at Midspan of Girder C
κ = 0, H = ∞
κ = 0
κ = 0.05
κ = 0.10
κ = 0.20
κ = 0.40
κ = ∞
$C_{MH} = \frac{\text{Moment}}{Pa}$
0.35
0.30
0.25
0.20
0.15
0.10
0.05
0
0
10
20
30
40
Relative Girder Stiffness, H

FIG. 5.19 (Cont.)

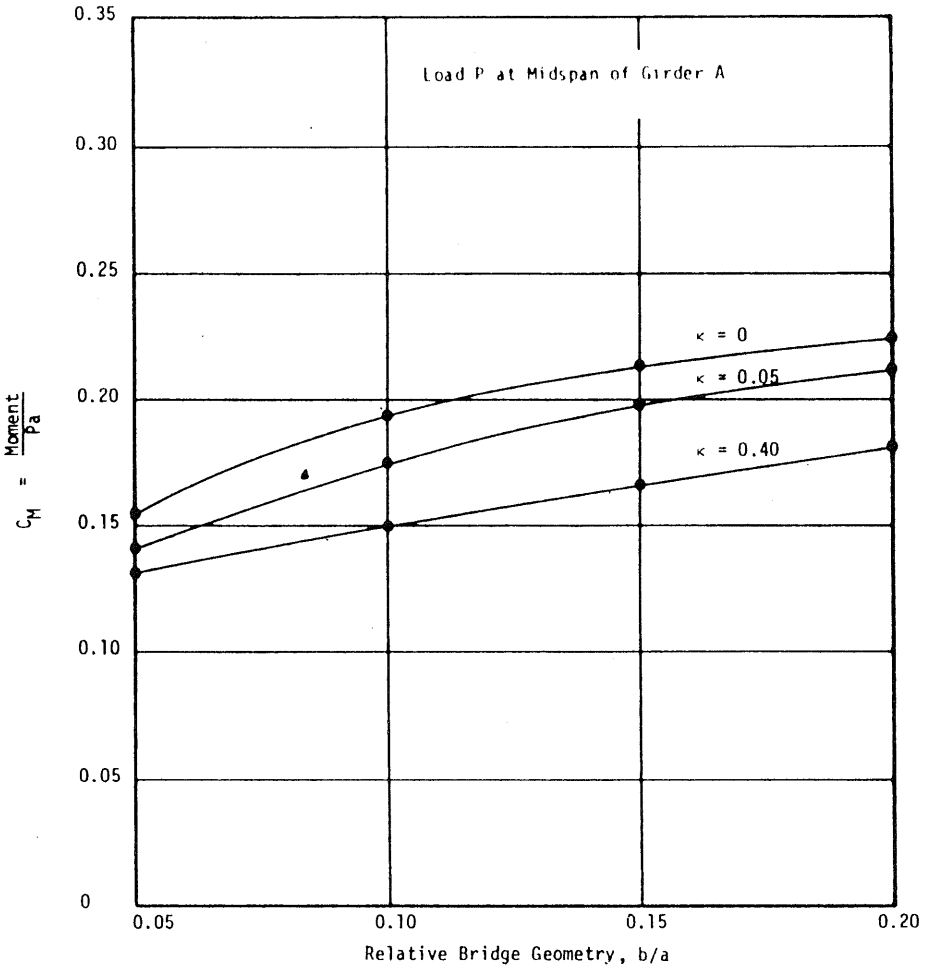

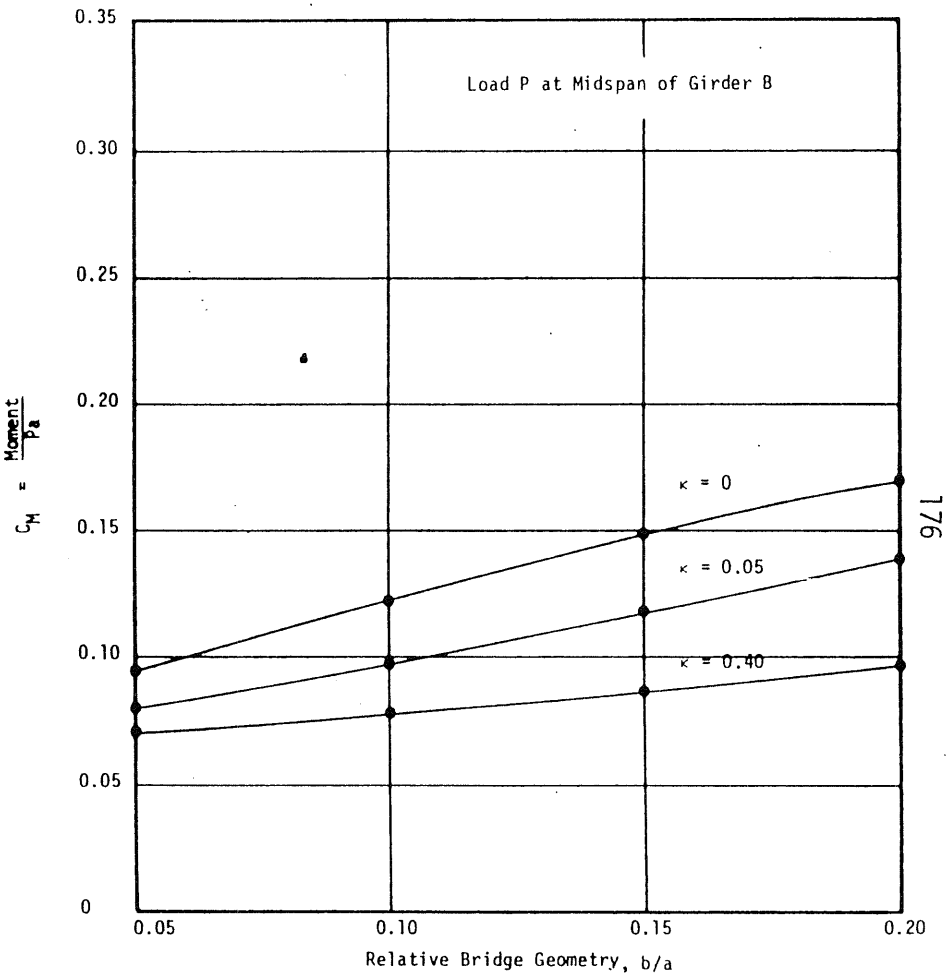

FIG. 5.20 RELATIONSHIP BETWEEN MOMENT AT MIDSPAN OF LOADED GIRDER AND RELATIVE BRIDGE GEOMETRY b/a; H = 20, 1 DIAPHRAGM AT MIDSPAN

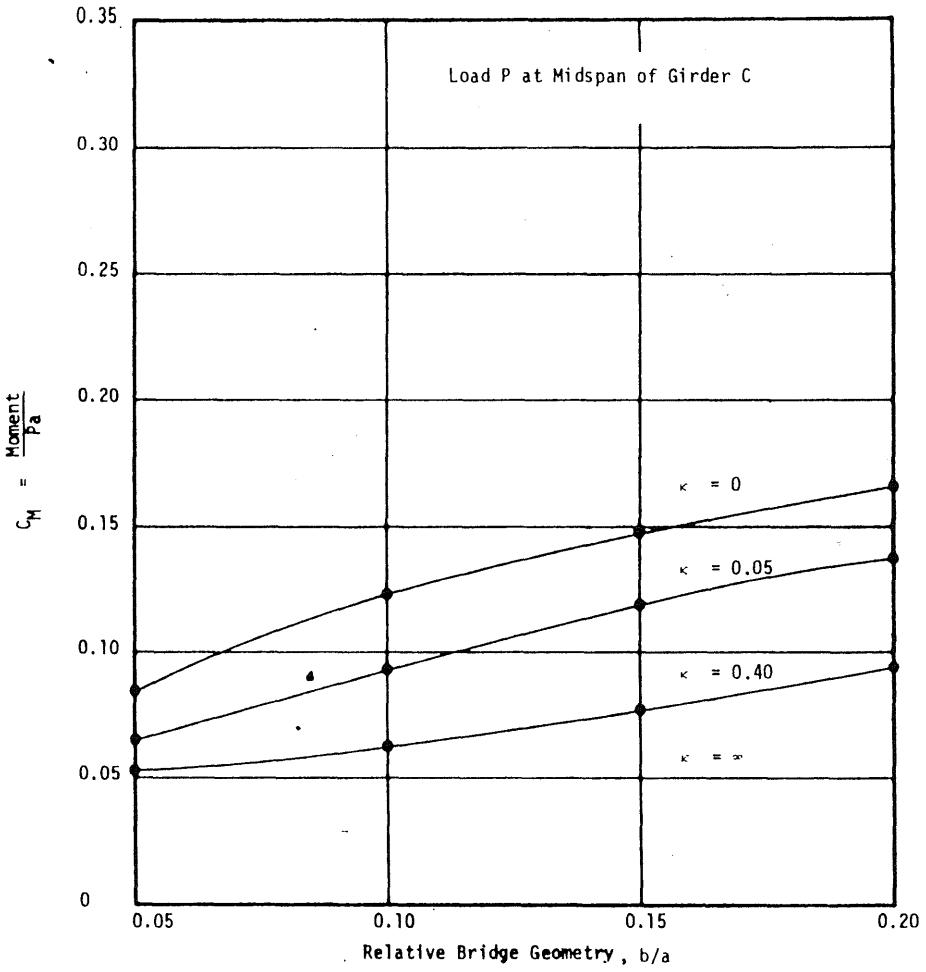
Load P at Midspan of Girder C
0.35
0.30
0.25
0.20
0.15
0.10
0.05
0
$C_M = \frac{\text{Moment}}{Pa}$
κ = 0
κ = 0.05
κ = 0.40
κ = ∞
0.05
0.10
0.15
0.20
Relative Bridge Geometry, b/a

FIG. 5.20 (Cont.)

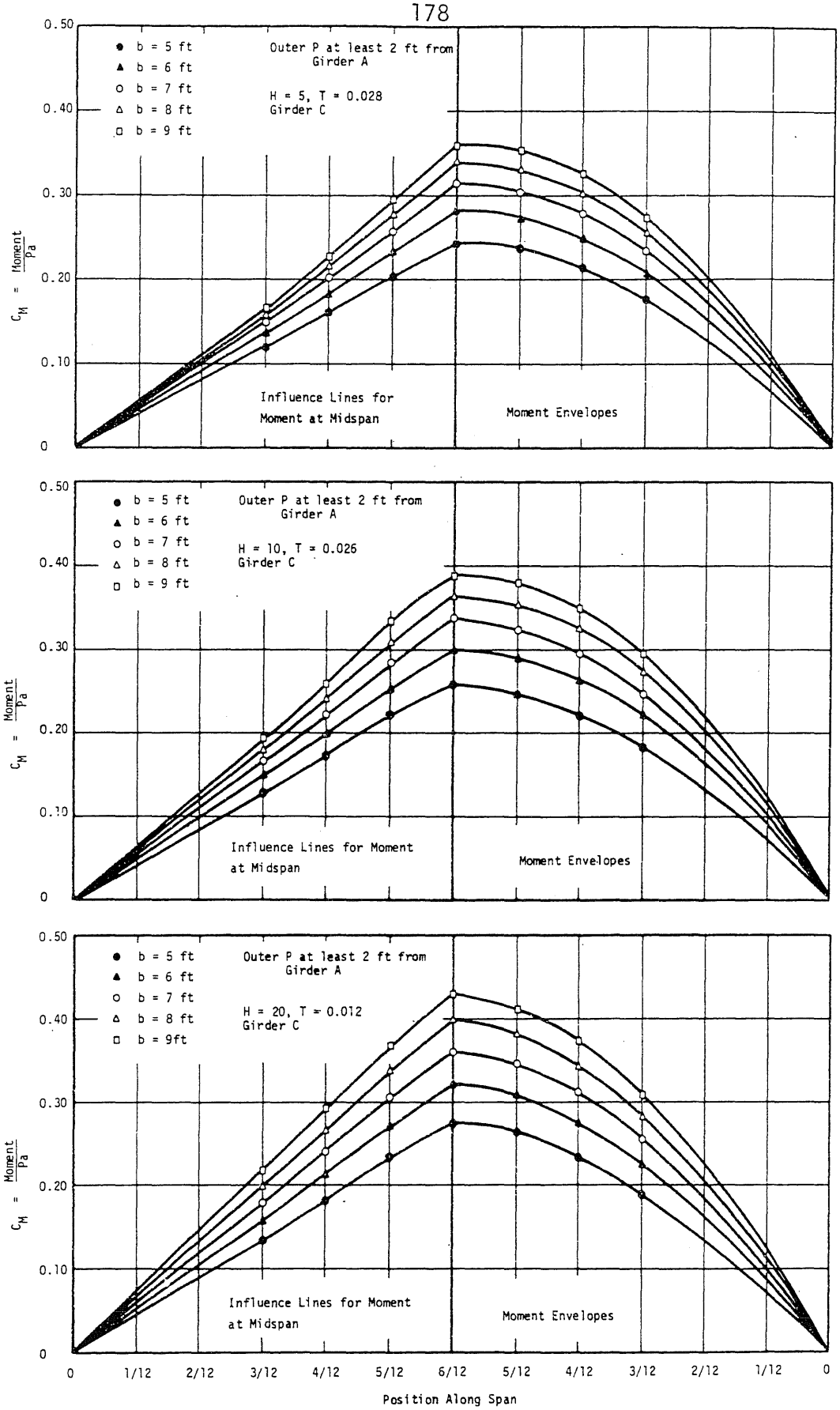

FIG. 5.21 INFLUENCE LINES FOR MAXIMUM MOMENT AT MIDSPAN AND MOMENT ENVELOPES OF GIRDER DUE TO 4-WHEEL LOADING MOVING ALONG SPAN OF BRIDGE; b/a = 0.20, WITHOUT DIAPHRAGMS

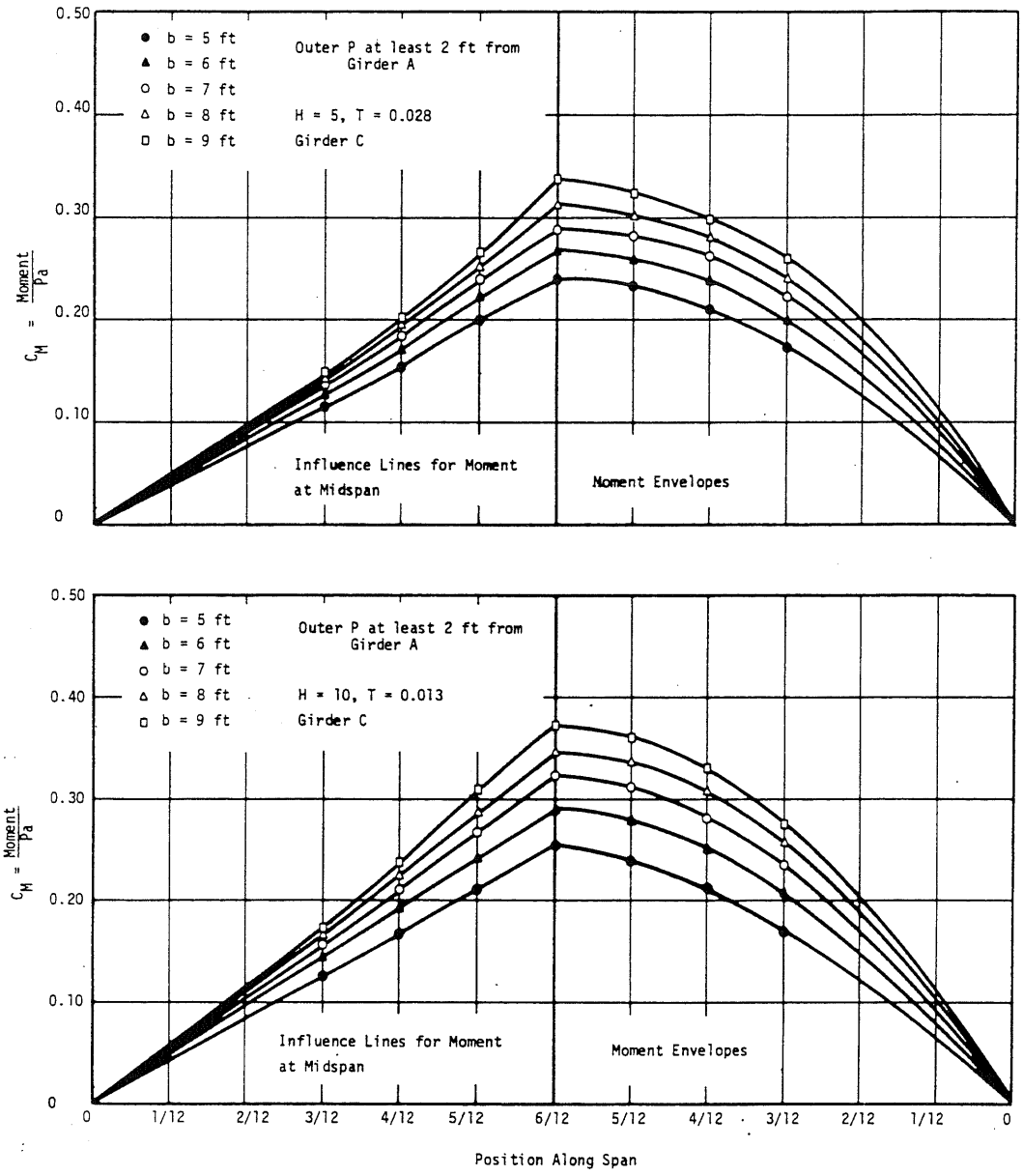

FIG. 5.22 INFLUENCE LINES FOR MAXIMUM MOMENT AT MIDSPAN AND MOMENT ENVELOPES OF GIRDERS DUE TO 4- WHEEL LOADING MOVING ALONG SPAN OF BRIDGE; b/a = 0.15, WITHOUT DIAPHRAGMS

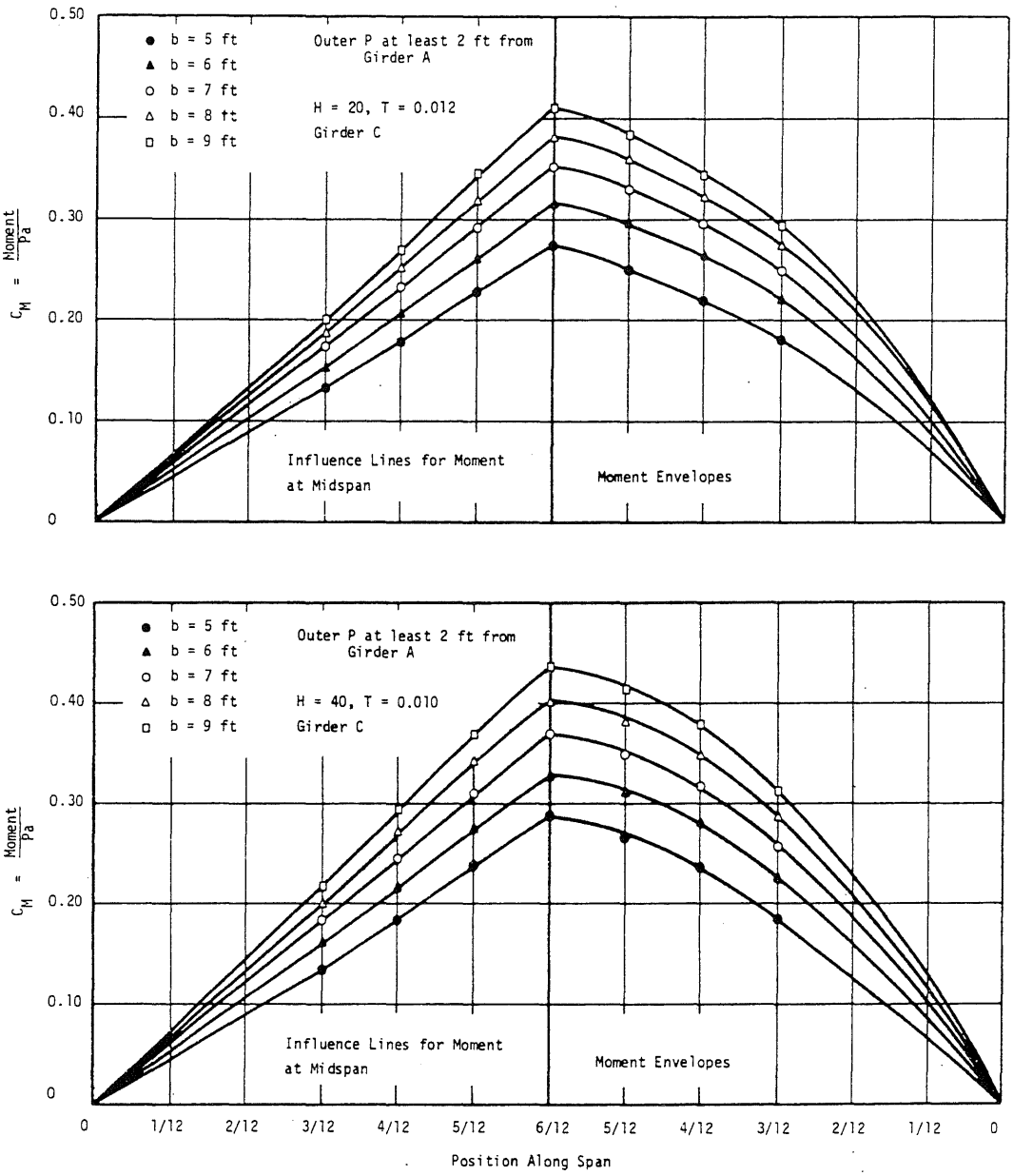
0.50
0.40
0.30
0.20
0.10
0
$C_M = \frac{\text{Moment}}{Pa}$
● b = 5 ft
▲ b = 6 ft
○ b = 7 ft
△ b = 8 ft
□ b = 9 ft
Outer P at least 2 ft from Girder A
H = 20, T = 0.012
Girder C
Influence Lines for Moment at Midspan
Moment Envelopes
0.50
0.40
0.30
0.20
0.10
0
$C_M = \frac{\text{Moment}}{Pa}$
● b = 5 ft
▲ b = 6 ft
○ b = 7 ft
△ b = 8 ft
□ b = 9 ft
Outer P at least 2 ft from Girder A
H = 40, T = 0.010
Girder C
Influence Lines for Moment at Midspan
Moment Envelopes
0
1/12
2/12
3/12
4/12
5/12
6/12
5/12
4/12
3/12
2/12
1/12
0
Position Along Span

FIG. 5.22 (Cont.)

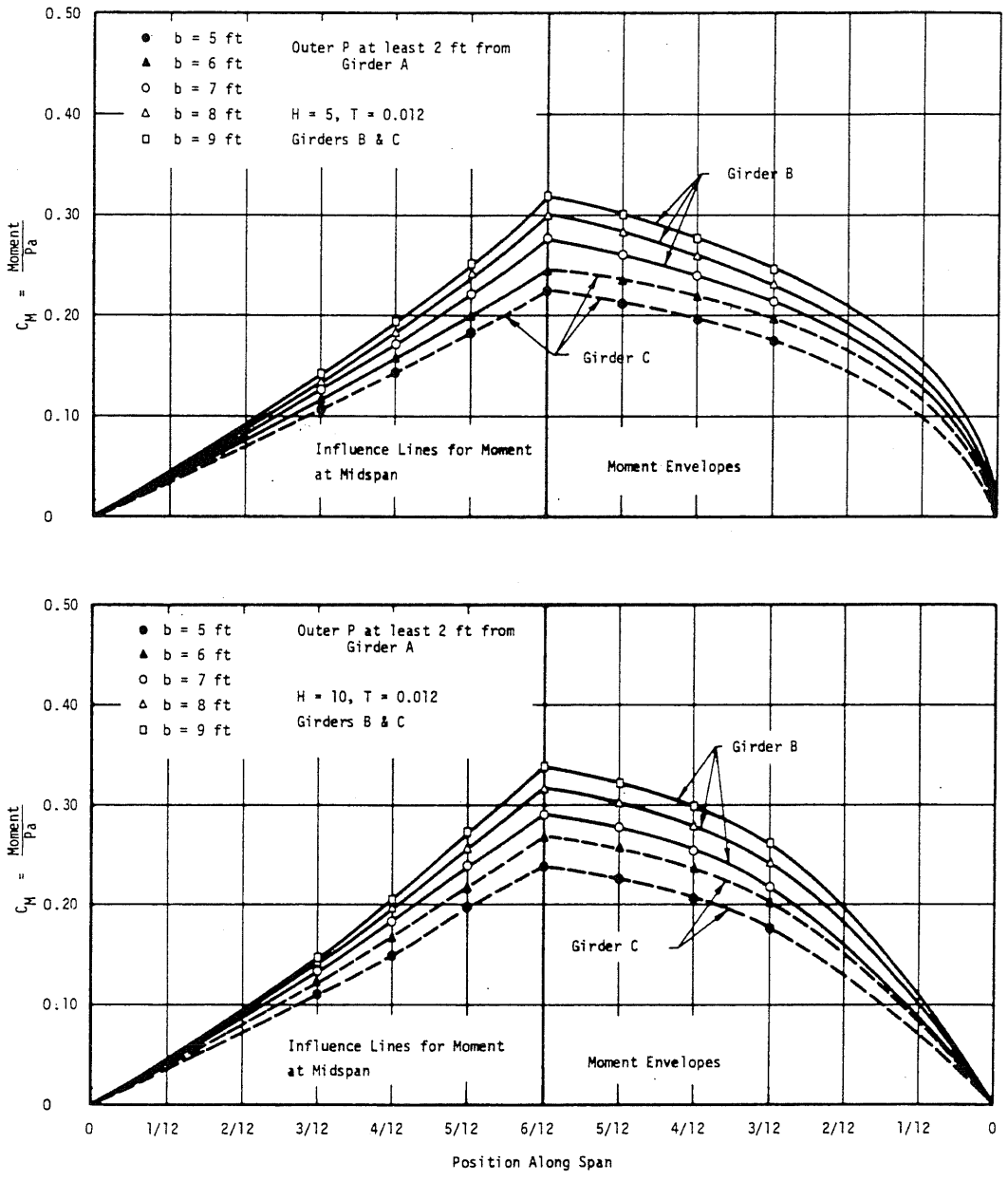

FIG. 5.23 INFLUENCE LINES FOR MAXIMUM MOMENT AT MIDSPAN AND MOMENT ENVELOPES OF GIRDERS DUE TO 4-WHEEL LOADING MOVING ALONG SPAN OF BRIDGE; b/a = 0.10, WITHOUT DIAPHRAGMS

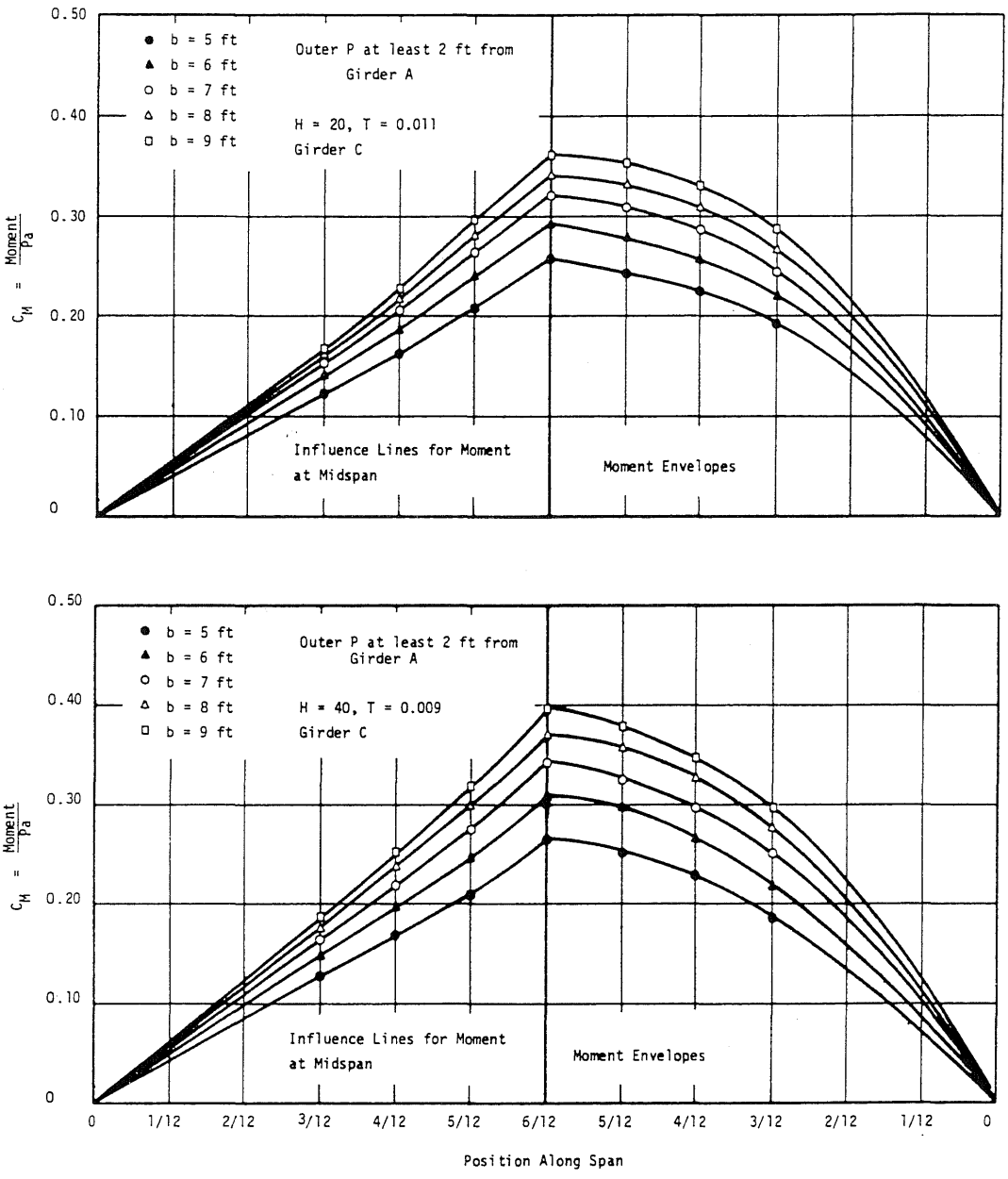
0.50
0.40
0.30
0.20
0.10
0
$C_M = \frac{\text{Moment}}{Pa}$
b = 5 ft
b = 6 ft
b = 7 ft
b = 8 ft
b = 9 ft
Outer P at least 2 ft from Girder A
H = 20, T = 0.011
Girder C
Influence Lines for Moment at Midspan
Moment Envelopes
0.50
0.40
0.30
0.20
0.10
0
$C_M = \frac{\text{Moment}}{Pa}$
b = 5 ft
b = 6 ft
b = 7 ft
b = 8 ft
b = 9 ft
Outer P at least 2 ft from Girder A
H = 40, T = 0.009
Girder C
Influence Lines for Moment at Midspan
Moment Envelopes
0
1/12
2/12
3/12
4/12
5/12
6/12
5/12
4/12
3/12
2/12
1/12
0
Position Along Span

FIG. 5.23 (Cont.)

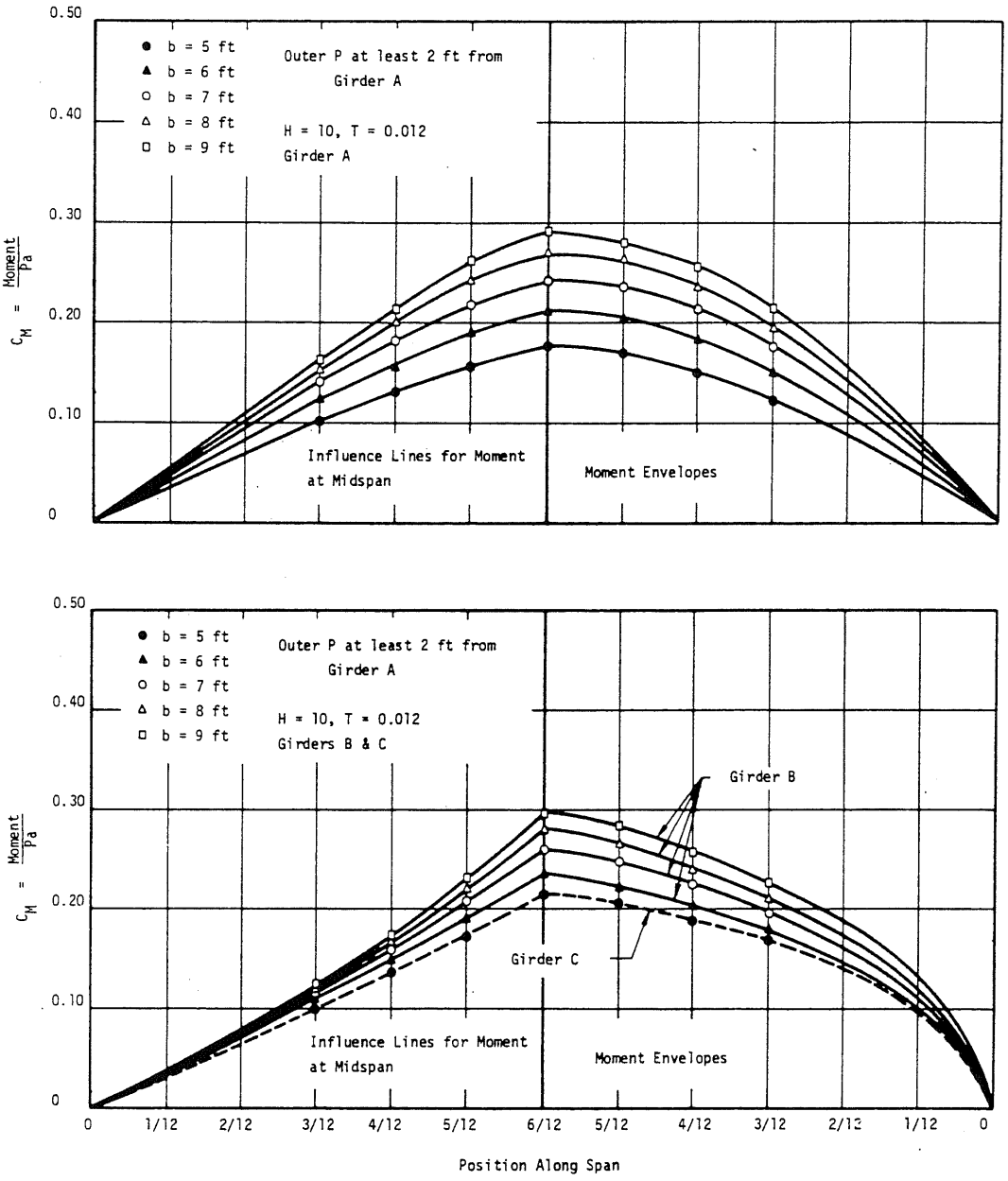

FIG. 5.24 INFLUENCE LINES FOR MAXIMUM MOMENT AT MIDSPAN AND MOMENT ENVELOPES OF GIRDERS DUE TO 4-WHEEL LOADING MOVING ALONG SPAN OF BRIDGE; b/a = 0.05, WITHOUT DIAPHRAGMS

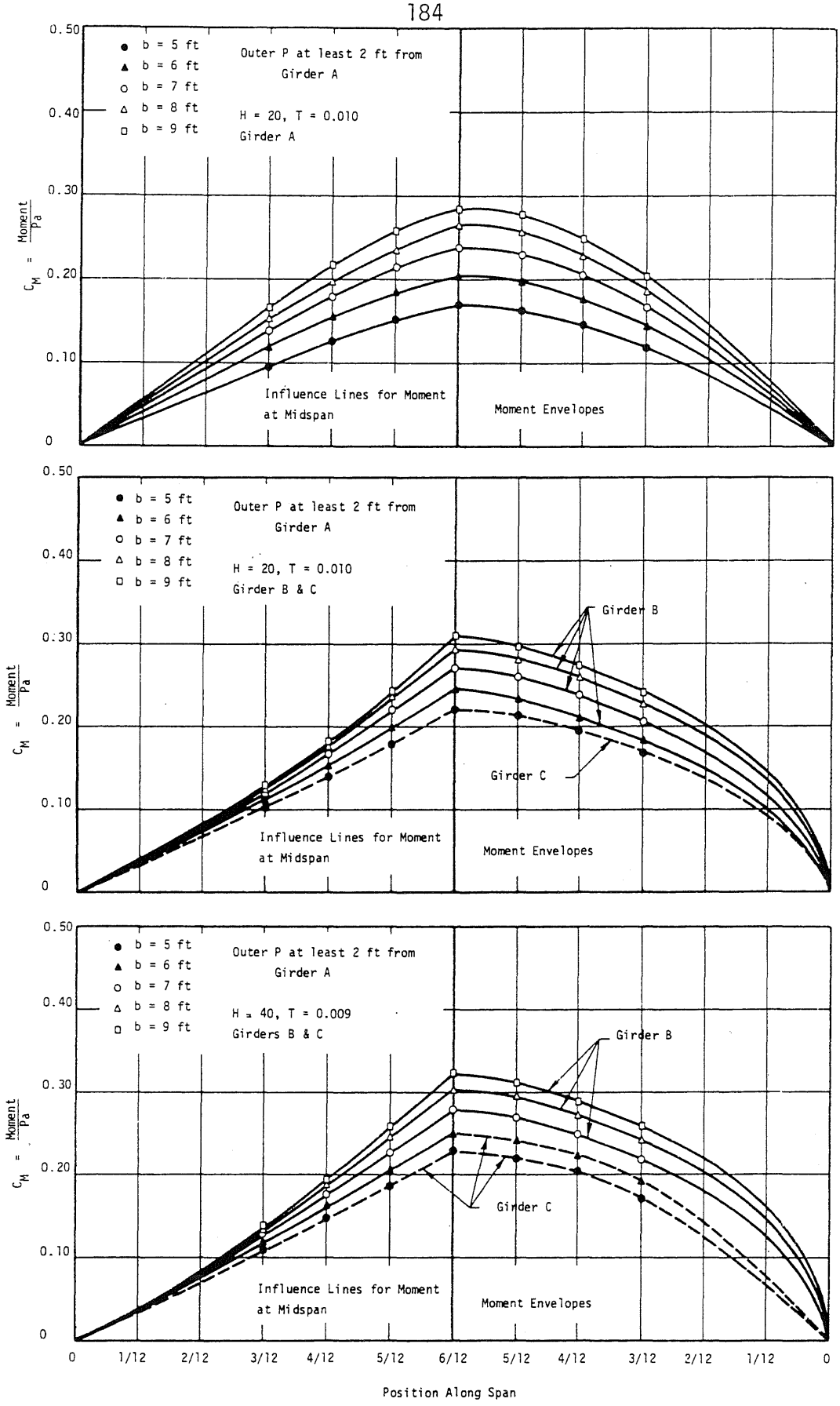
b = 5 ft
b = 6 ft
b = 7 ft
b = 8 ft
b = 9 ft
Outer P at least 2 ft from Girder A
H = 20, T = 0.010
Girder A
Influence Lines for Moment at Midspan
Moment Envelopes
Girder B & C
Girder B
Girder C
H = 40, T = 0.009
Girders B & C
$C_M = \frac{\text{Moment}}{Pa}$
0.50
0.40
0.30
0.20
0.10
0
0 1/12 2/12 3/12 4/12 5/12 6/12 5/12 4/12 3/12 2/12 1/12 0
Position Along Span

FIG. 5.24 (Cont.)

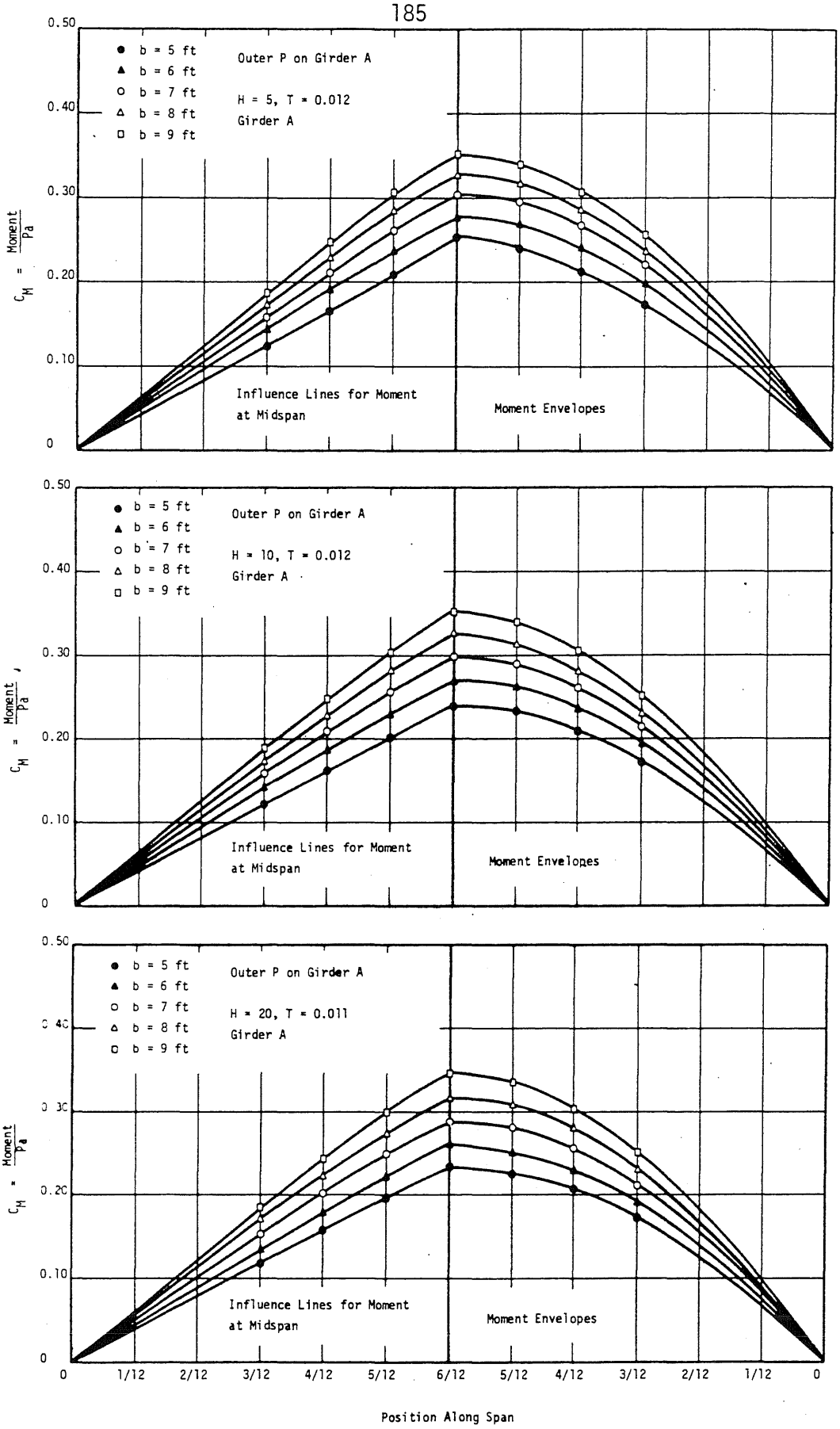

FIG. 5.25 INFLUENCE LINES FOR MAXIMUM MOMENT AT MIDSPAN AND MOMENT ENVELOPES OF GIRDER DUE TO 4-WHEEL LOADING MOVING ALONG SPAN OF BRIDGE; b/a = 0.10, WITHOUT DIAPHRAGMS

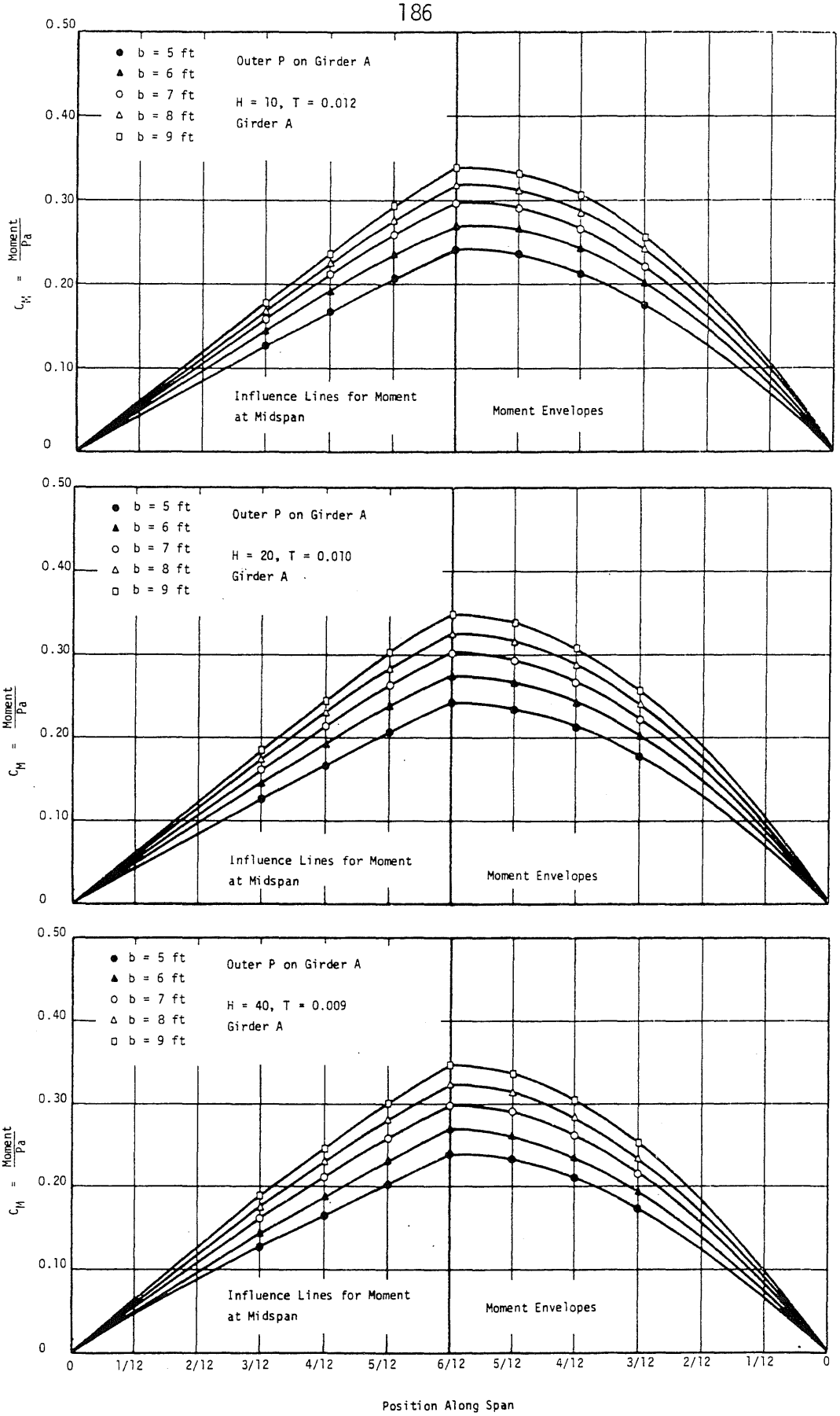

FIG. 5.26 INFLUENCE LINES FOR MAXIMUM MOMENT AT MIDSPAN AND MOMENT ENVELOPES OF GIRDERS DUE TO 4-WHEEL LOADING MOVING ALONG SPAN OF BRIDGE; b/a = 0.05, WITHOUT DIAPHRAGMS

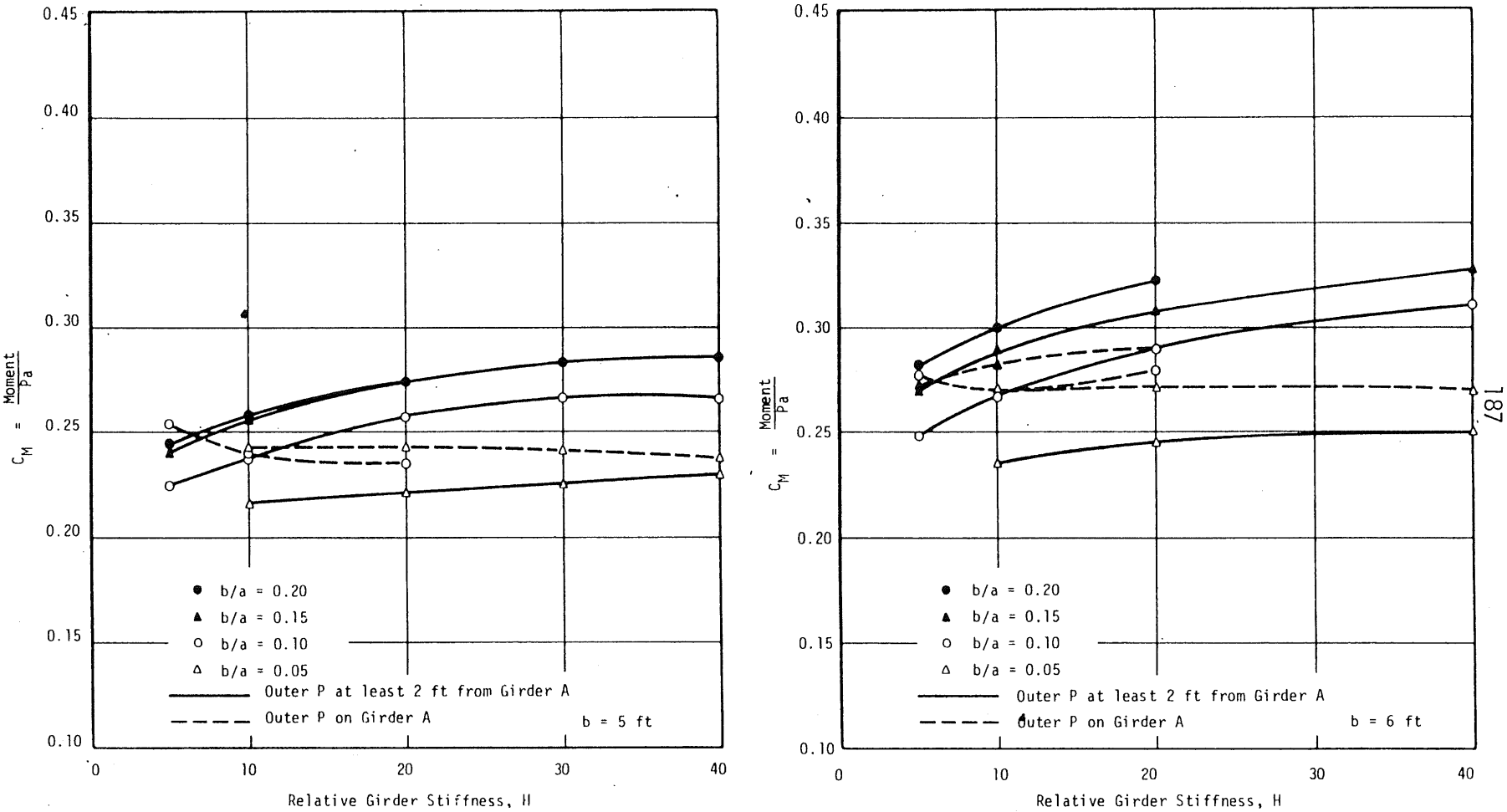

FIG. 5.27 RELATIONSHIP BETWEEN MAXIMUM MOMENT AT MIDSPAN DUE TO 4-WHEEL LOADING AT MIDSPAN AND RELATIVE GIRDER STIFFNESS, H

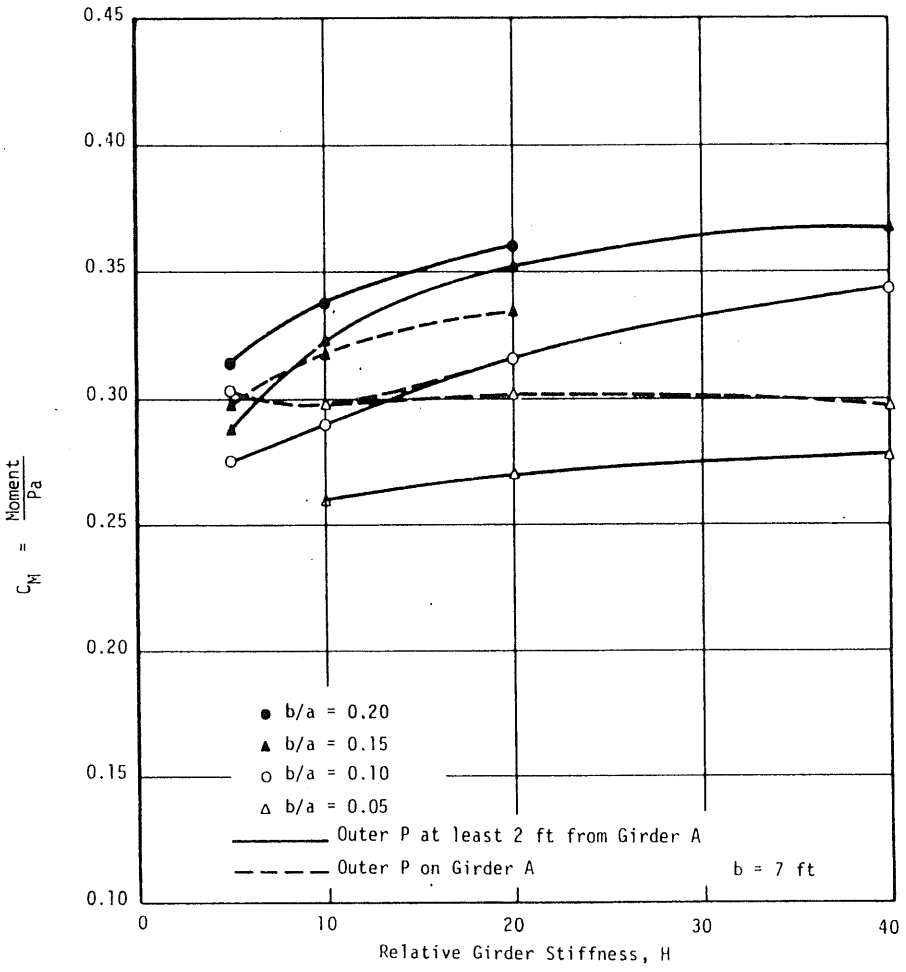
0.45
0.40
0.35
0.30
0.25
0.20
0.15
0.10
$C_M = \frac{\text{Moment}}{Pa}$
0
10
20
30
40
Relative Girder Stiffness, H
b/a = 0.20
b/a = 0.15
b/a = 0.10
b/a = 0.05
Outer P at least 2 ft from Girder A
Outer P on Girder A
b = 7 ft

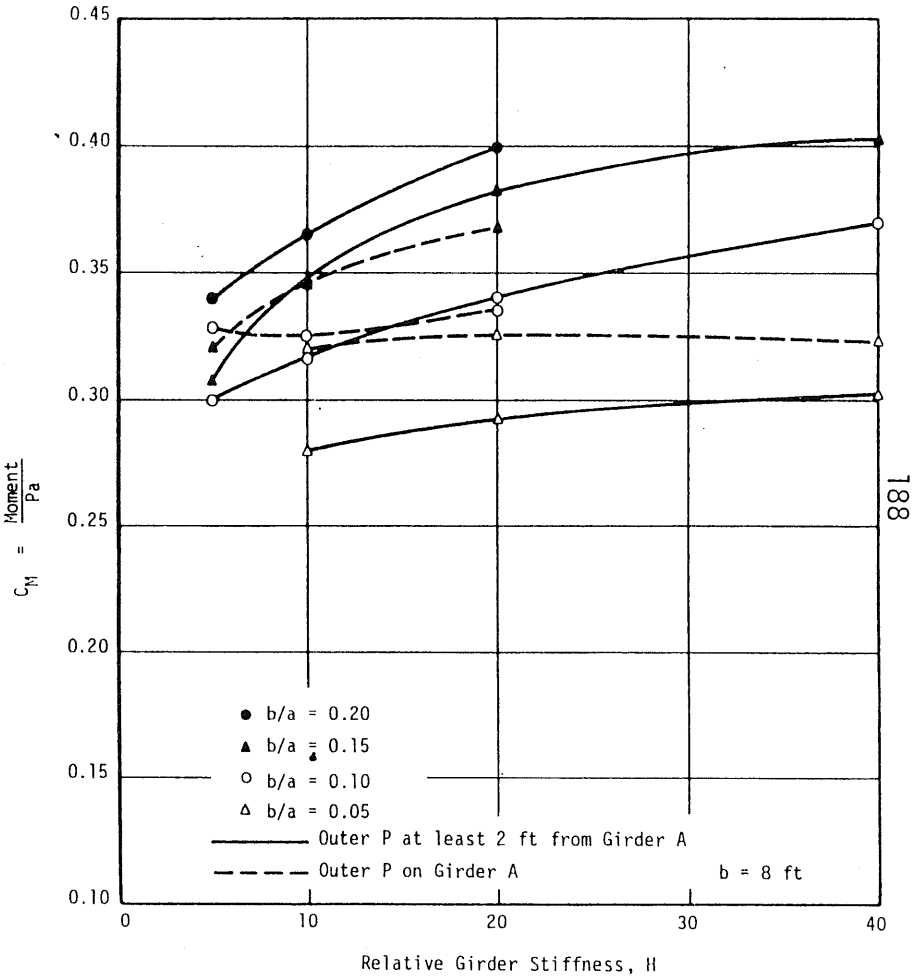
0.45
0.40
0.35
0.30
0.25
0.20
0.15
0.10
$C_M = \frac{\text{Moment}}{Pa}$
0
10
20
30
40
Relative Girder Stiffness, H
b/a = 0.20
b/a = 0.15
b/a = 0.10
b/a = 0.05
Outer P at least 2 ft from Girder A
Outer P on Girder A
b = 8 ft

FIG. 5.27 (Cont.)

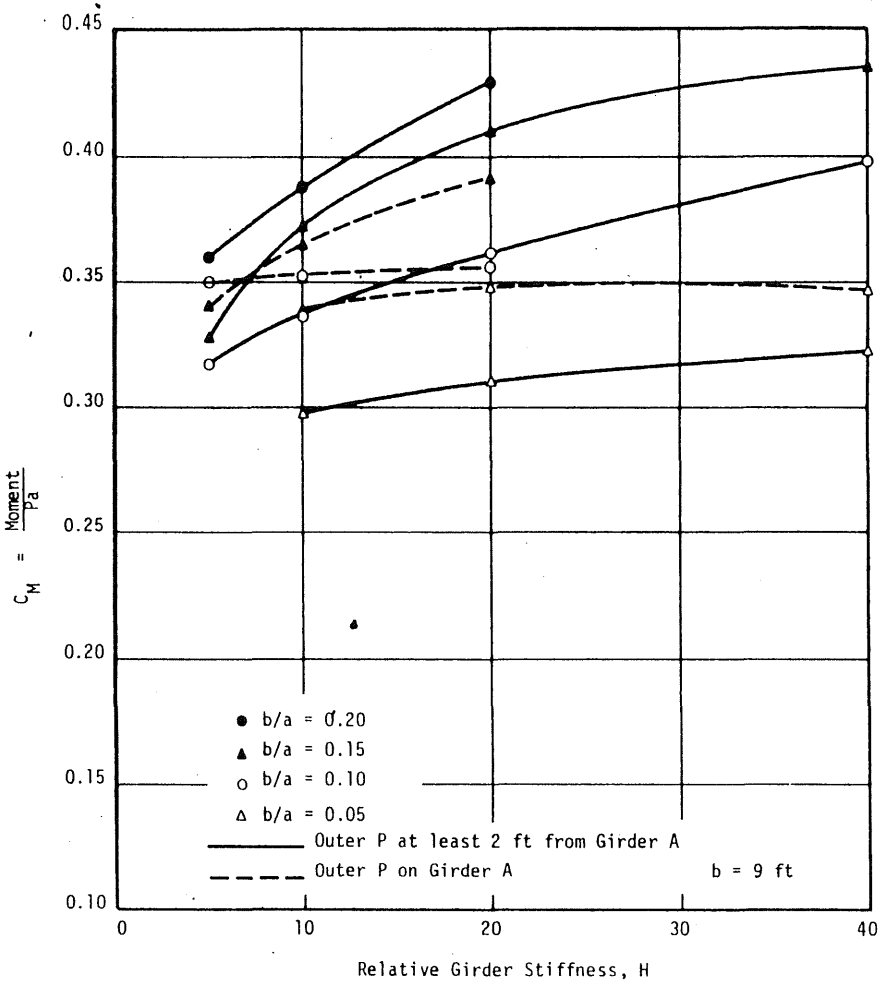
0.45
0.40
0.35
0.30
0.25
0.20
0.15
0.10
$C_M = \frac{\text{Moment}}{Pa}$
0
10
20
30
40
Relative Girder Stiffness, H
b/a = 0.20
b/a = 0.15
b/a = 0.10
b/a = 0.05
Outer P at least 2 ft from Girder A
Outer P on Girder A
b = 9 ft

FIG. 5.27 (Cont.)

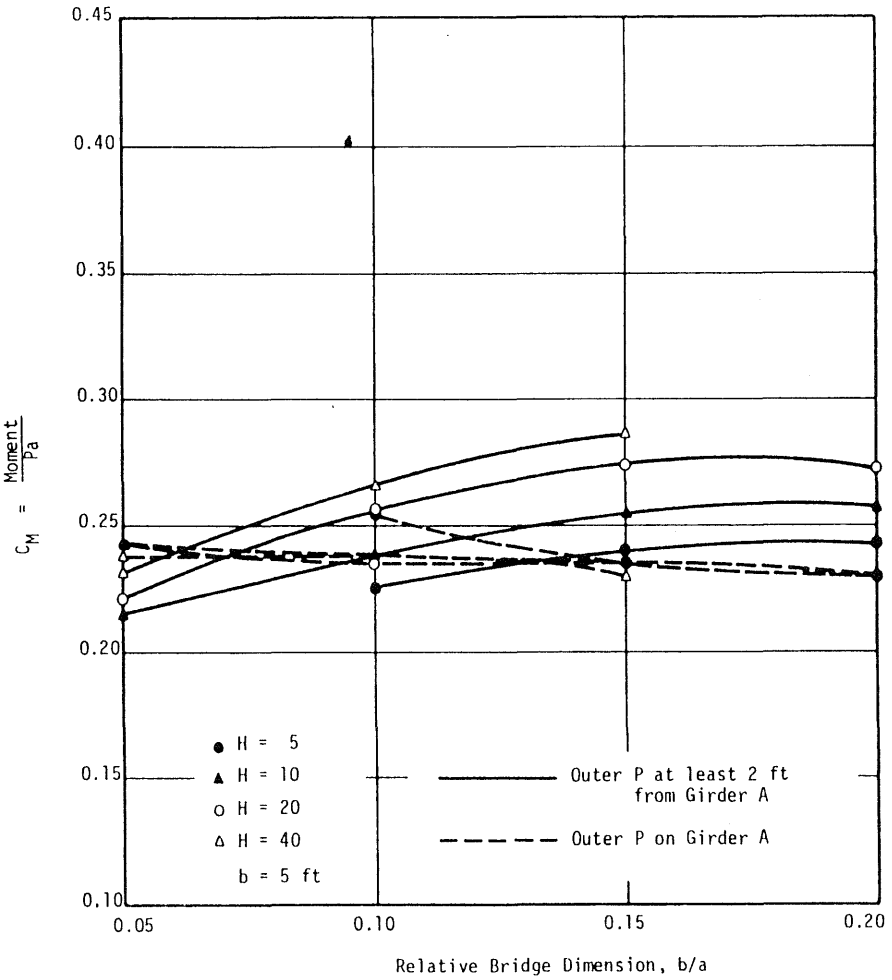

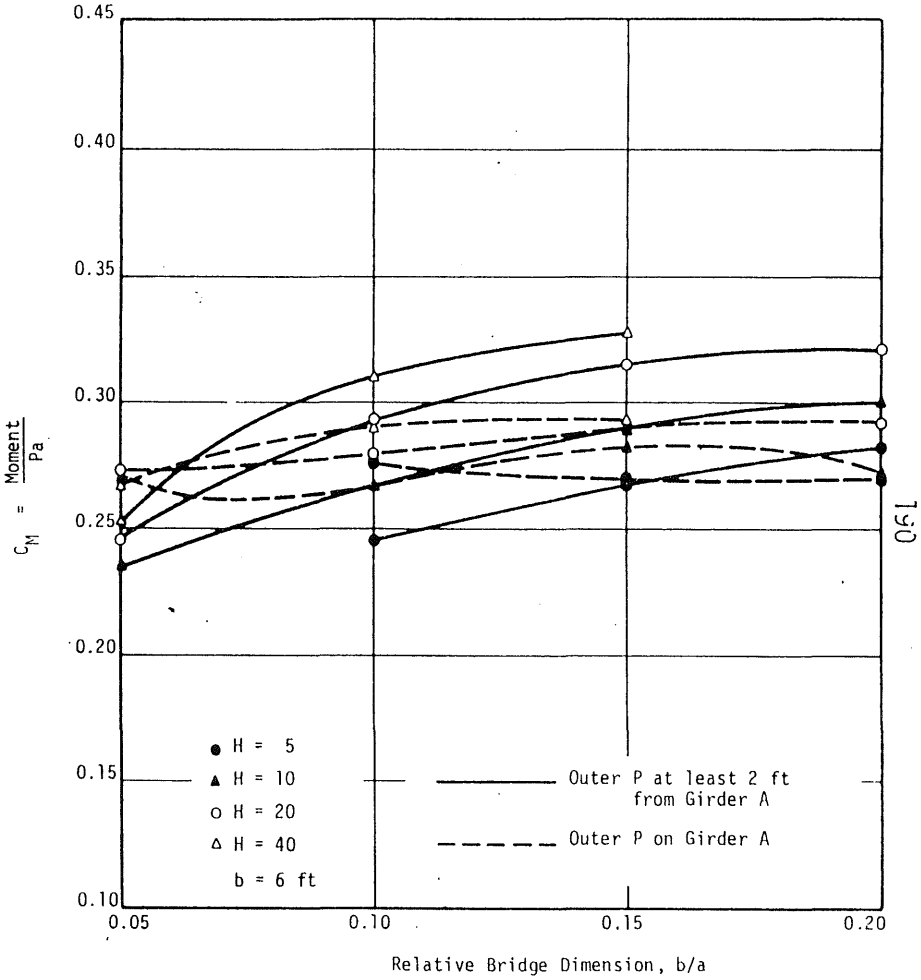

FIG. 5.28 RELATIONSHIP BETWEEN MAXIMUM MOMENT AT MIDSPAN DUE TO 4-WHEEL LOADING AT MIDSPAN AND RELATIVE BRIDGE DIMENSION, b/a

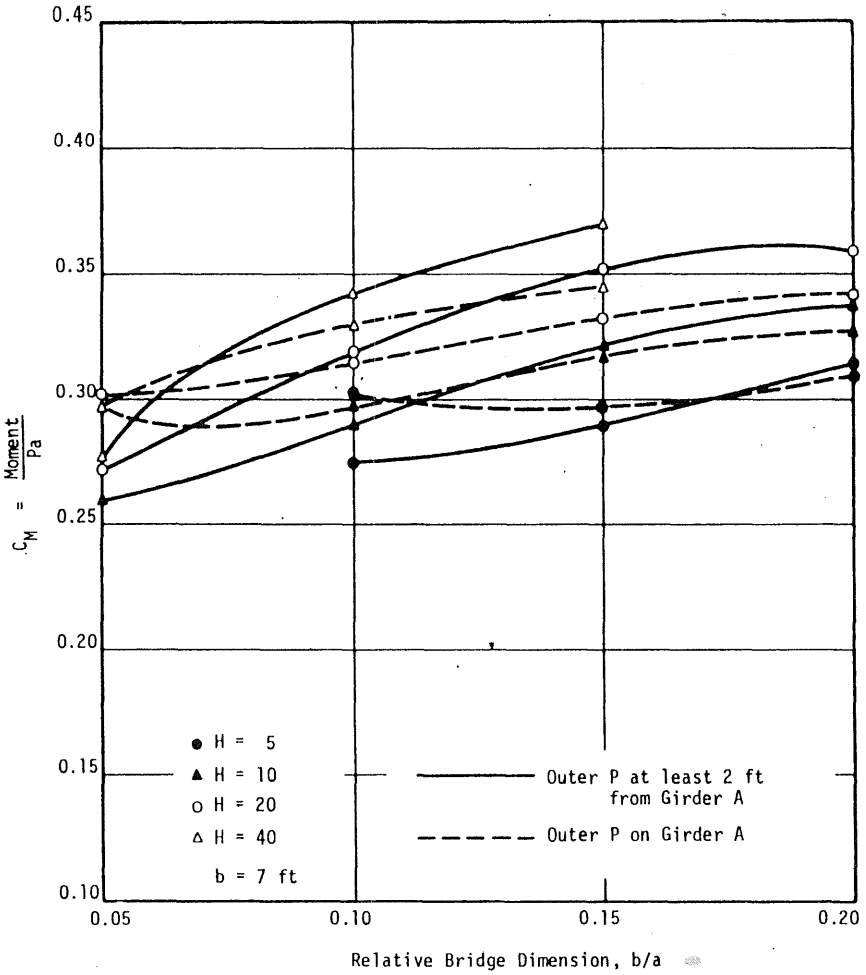
0.45
0.40
0.35
0.30
0.25
0.20
0.15
0.10
0.05
0.10
0.15
0.20
$C_M = \frac{\text{Moment}}{Pa}$
Relative Bridge Dimension, b/a
● H = 5
▲ H = 10
o H = 20
△ H = 40
b = 7 ft
Outer P at least 2 ft from Girder A
Outer P on Girder A

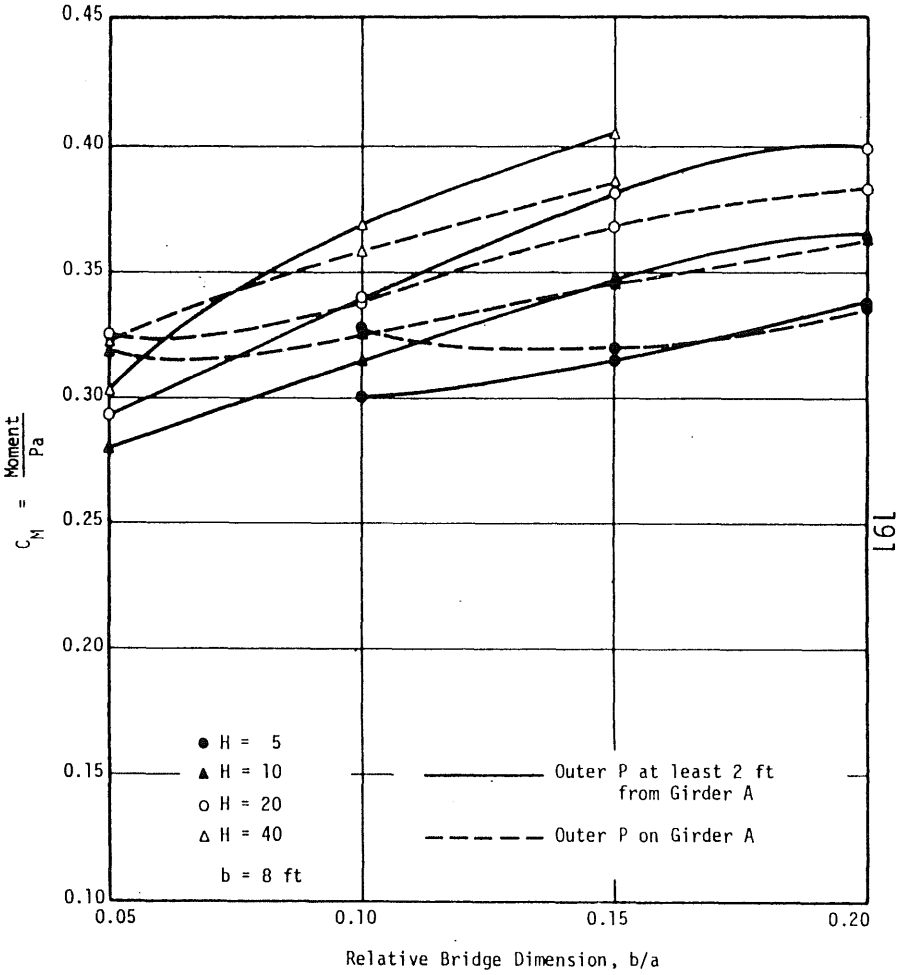
0.45
0.40
0.35
0.30
0.25
0.20
0.15
0.10
0.05
0.10
0.15
0.20
$C_M = \frac{\text{Moment}}{Pa}$
Relative Bridge Dimension, b/a
● H = 5
▲ H = 10
o H = 20
△ H = 40
b = 8 ft
Outer P at least 2 ft from Girder A
Outer P on Girder A

FIG. 5.28 (Cont.)

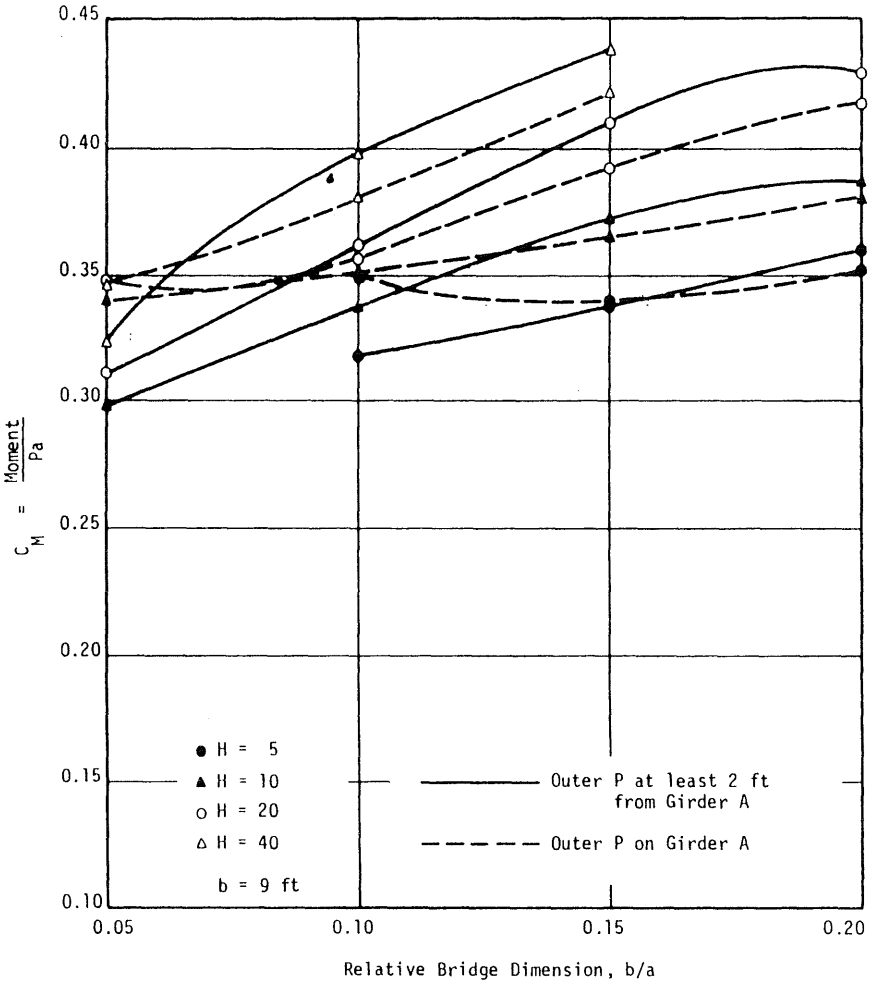
0.45
0.40
0.35
0.30
0.25
0.20
0.15
0.10
$C_M = \frac{\text{Moment}}{Pa}$
0.05
0.10
0.15
0.20
Relative Bridge Dimension, b/a
● H = 5
▲ H = 10
○ H = 20
△ H = 40
b = 9 ft
Outer P at least 2 ft from Girder A
Outer P on Girder A

FIG. 5.28 (Cont.)

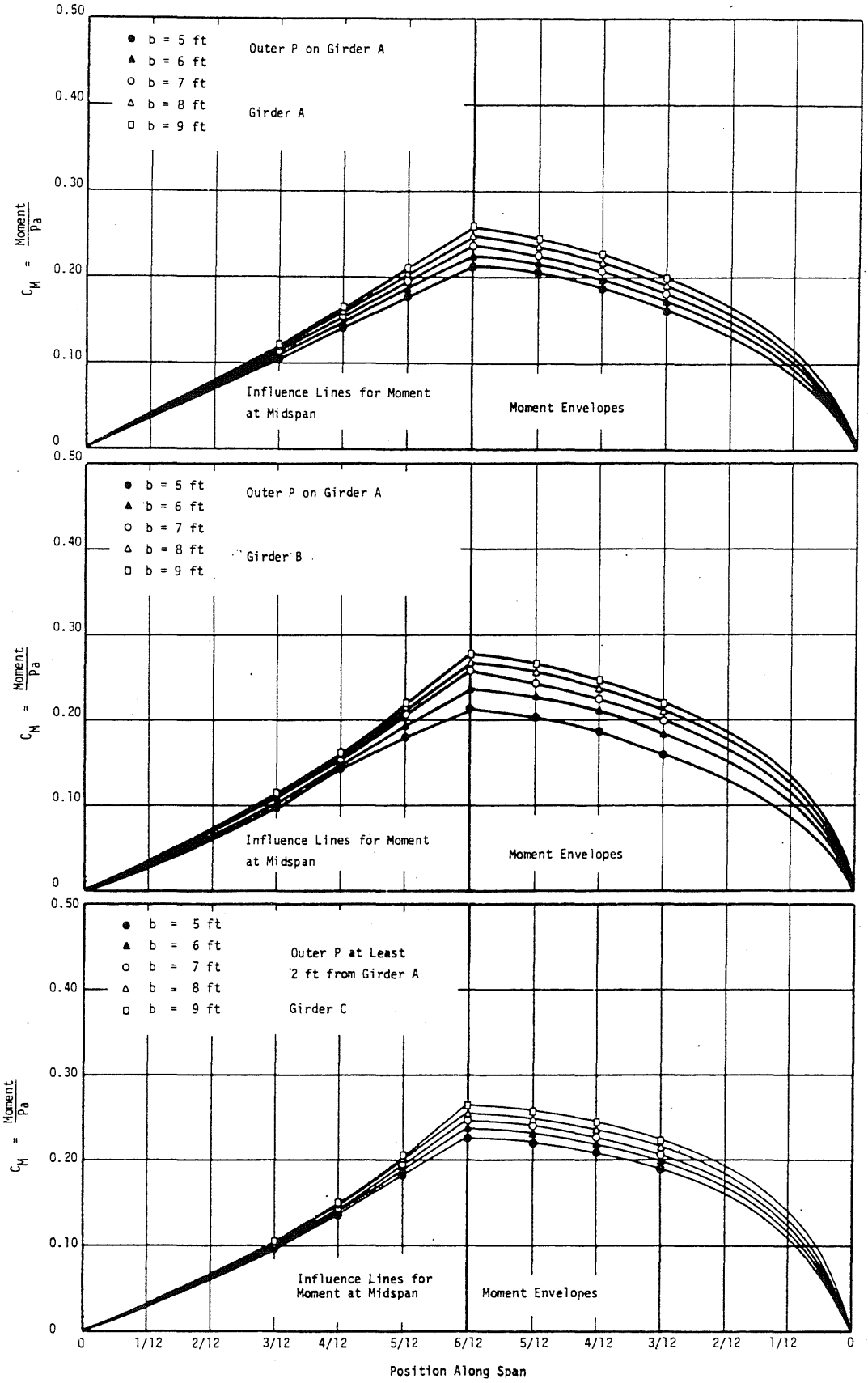

FIG. 5.29 INFLUENCE LINES FOR MAXIMUM MOMENT AT MIDSPAN AND MOMENT ENVELOPES OF GIRDER DUE TO 4-WHEEL LOADING MOVING ALONG SPAN OF BRIDGE: b/a = 0.10, H = 20, T = 1.0, WITHOUT DIAPHRAGMS

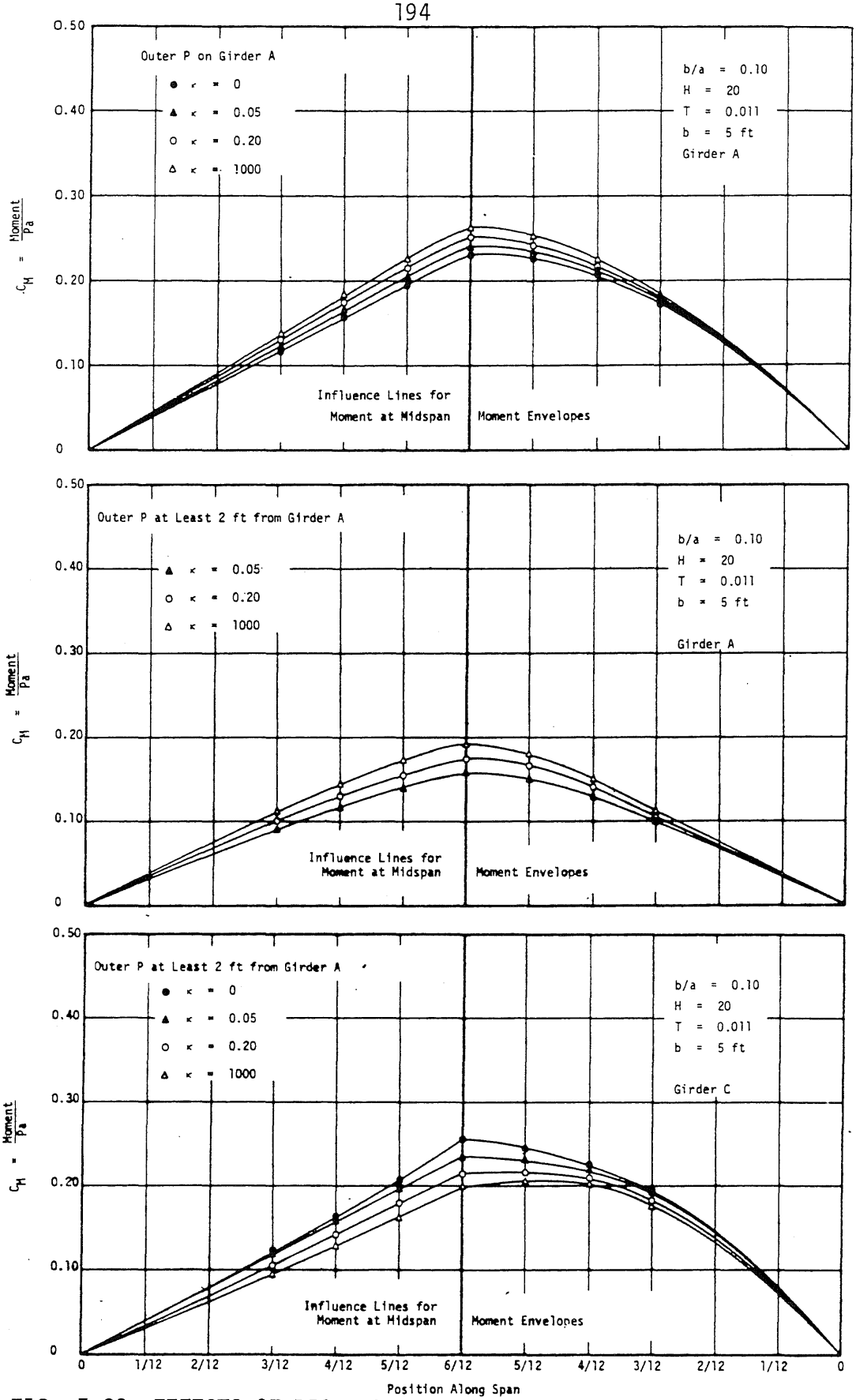

FIG. 5.30 EFFECTS OF DIAPHRAGMS ON INFLUENCE LINES FOR MAXIMUM MOMENT AT MIDSPAN AND MOMENT ENVELOPES OF STANDARD BRIDGE DUE TO 4-WHEEL LOADING MOVING ALONG SPAN; 1 DIAPHRAGM AT MIDSPAN

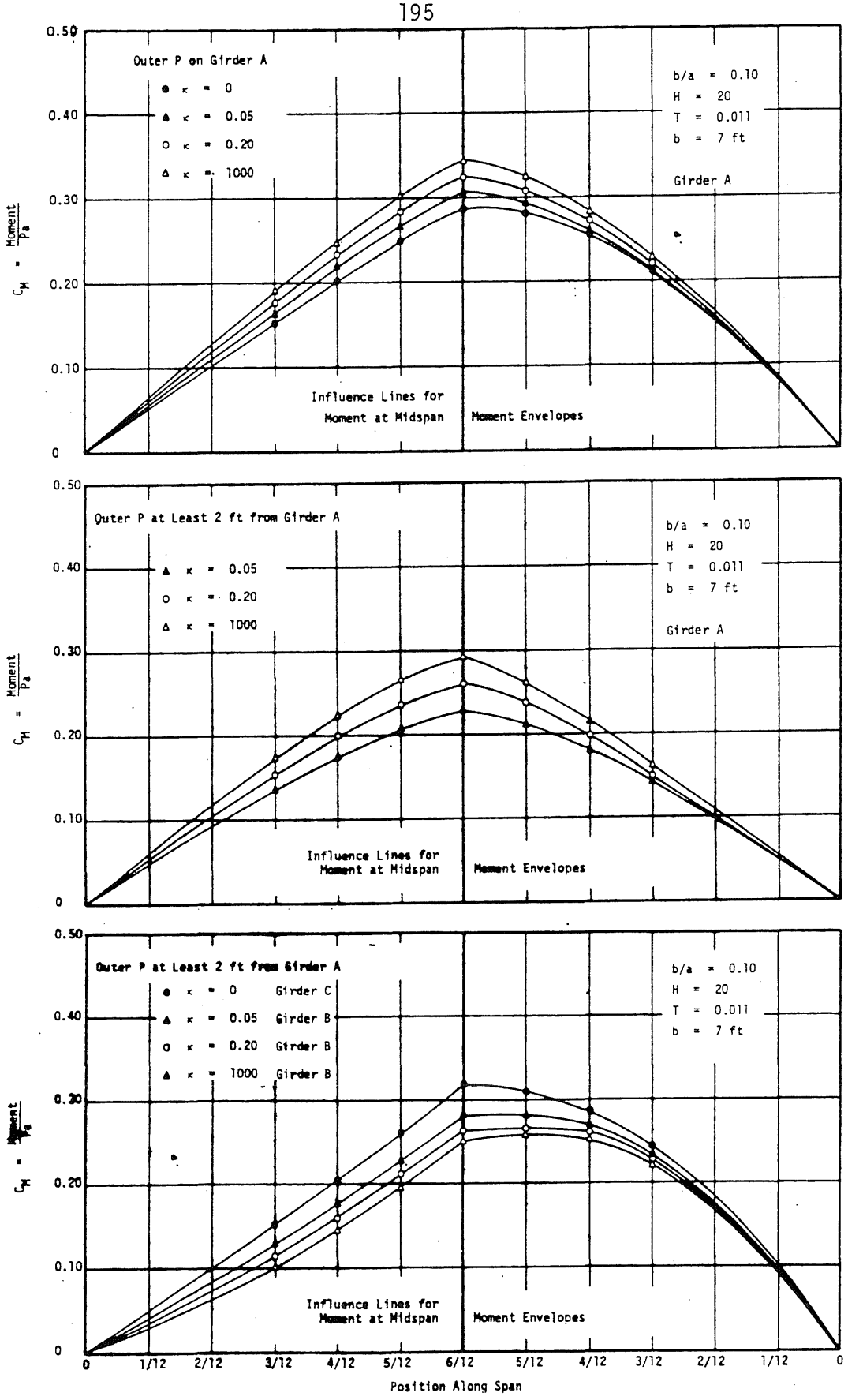
Outer P on Girder A
● κ = 0
▲ κ = 0.05
o κ = 0.20
Δ κ = 1000
b/a = 0.10
H = 20
T = 0.011
b = 7 ft
Girder A
Influence Lines for Moment at Midspan
Moment Envelopes
Outer P at Least 2 ft from Girder A
▲ κ = 0.05
o κ = 0.20
Δ κ = 1000
b/a = 0.10
H = 20
T = 0.011
b = 7 ft
Girder A
Influence Lines for Moment at Midspan
Moment Envelopes
Outer P at Least 2 ft from Girder A
● κ = 0 Girder C
▲ κ = 0.05 Girder B
o κ = 0.20 Girder B
▲ κ = 1000 Girder B
b/a = 0.10
H = 20
T = 0.011
b = 7 ft
Influence Lines for Moment at Midspan
Moment Envelopes
0.50
0.40
0.30
0.20
0.10
0
0 1/12 2/12 3/12 4/12 5/12 6/12 5/12 4/12 3/12 2/12 1/12 0
Position Along Span

FIG. 5.30 (Cont.)

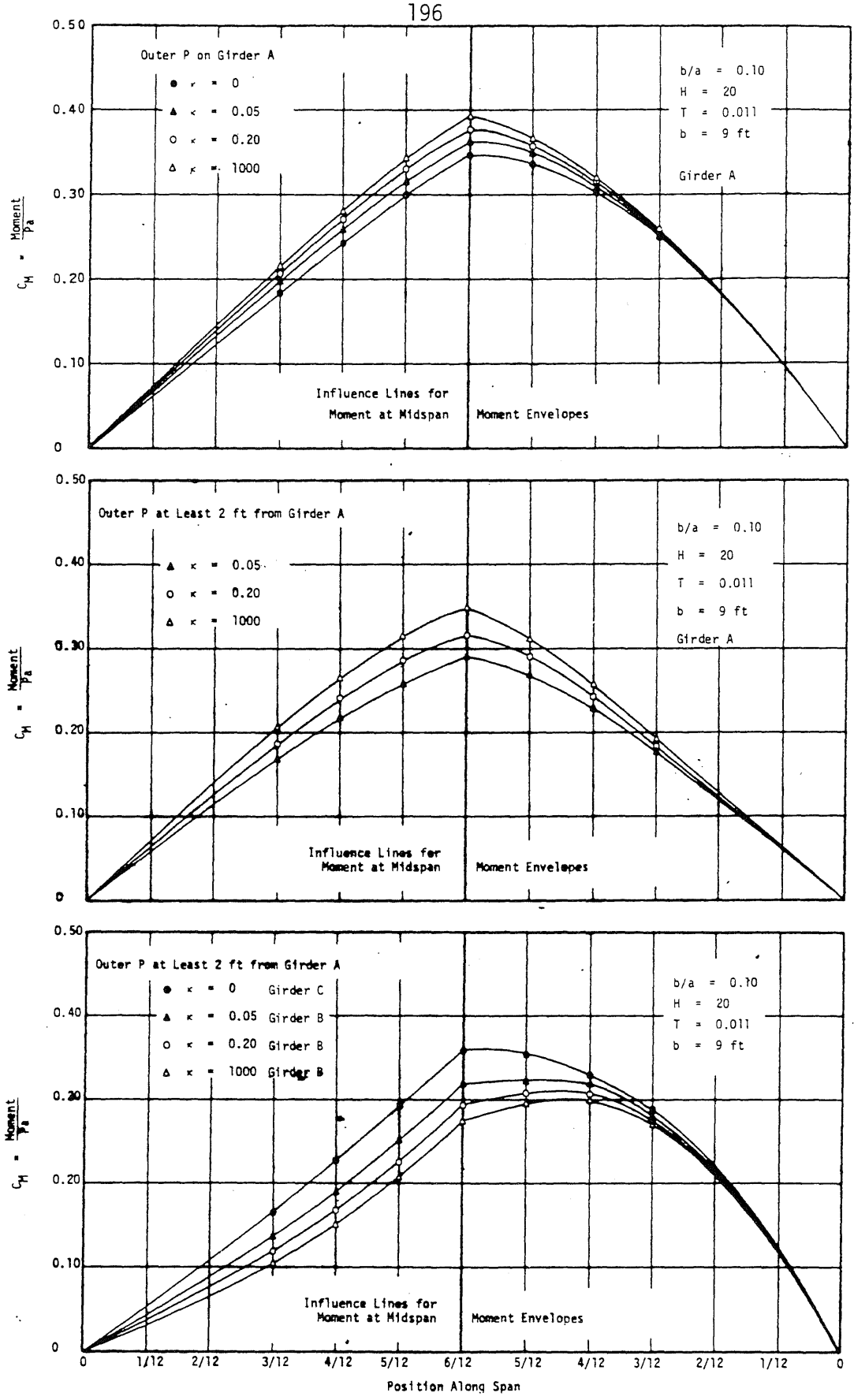
Outer P on Girder A
● κ = 0
▲ κ = 0.05
○ κ = 0.20
△ κ = 1000
b/a = 0.10
H = 20
T = 0.011
b = 9 ft
Girder A
Influence Lines for Moment at Midspan
Moment Envelopes
Outer P at Least 2 ft from Girder A
▲ κ = 0.05
○ κ = 0.20
△ κ = 1000
b/a = 0.10
H = 20
T = 0.011
b = 9 ft
Girder A
Influence Lines for Moment at Midspan
Moment Envelopes
Outer P at Least 2 ft from Girder A
● κ = 0 Girder C
▲ κ = 0.05 Girder B
○ κ = 0.20 Girder B
△ κ = 1000 Girder B
b/a = 0.10
H = 20
T = 0.011
b = 9 ft
Influence Lines for Moment at Midspan
Moment Envelopes
$C_H = \frac{\text{Moment}}{Pa}$
0.50
0.40
0.30
0.20
0.10
0
0 1/12 2/12 3/12 4/12 5/12 6/12 5/12 4/12 3/12 2/12 1/12 0
Position Along Span

FIG. 5.30 (Cont.)

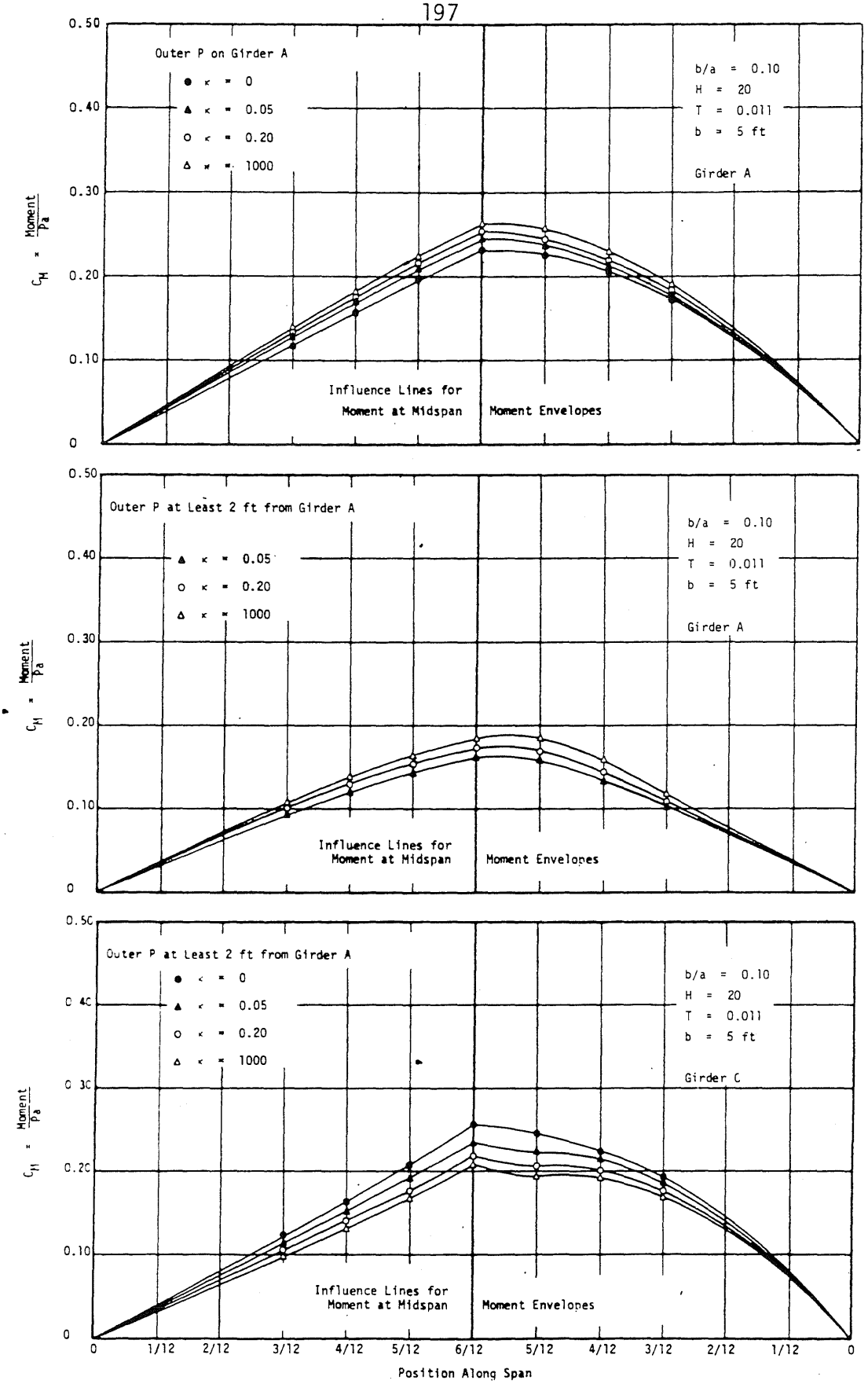

FIG. 5.31 EFFECTS OF DIAPHRAGMS ON INFLUENCE LINES FOR MAXIMUM MOMENT AT MIDSPAN AND MOMENT ENVELOPES OF STANDARD BRIDGE DUE TO 4-WHEEL LOADING MOVING ALONG SPAN; 2 DIAPHRAGMS AT 5/12 POINTS

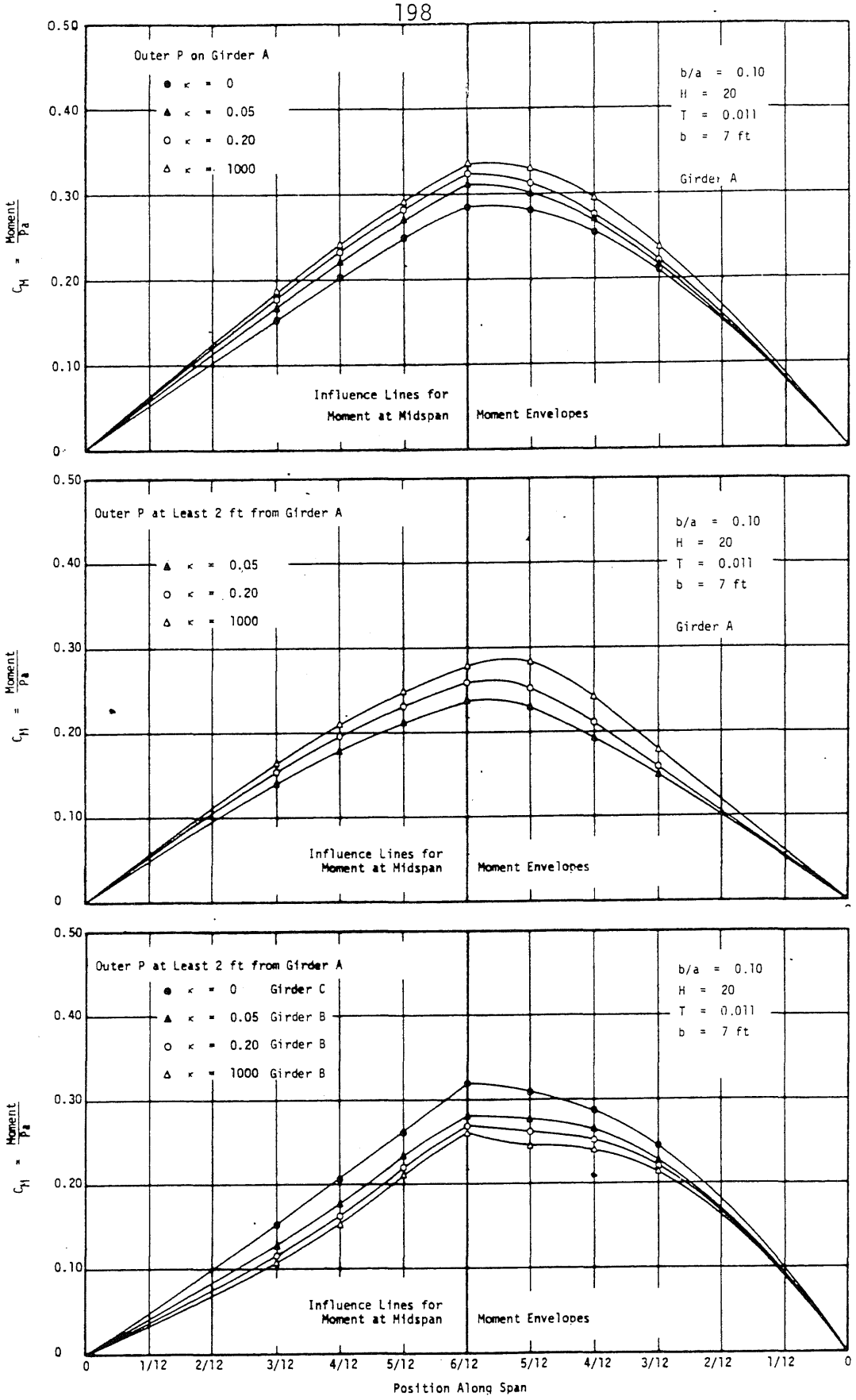
Outer P on Girder A
● κ = 0
▲ κ = 0.05
○ κ = 0.20
△ κ = 1000
b/a = 0.10
H = 20
T = 0.011
b = 7 ft
Girder A
Influence Lines for Moment at Midspan
Moment Envelopes
Outer P at Least 2 ft from Girder A
▲ κ = 0.05
○ κ = 0.20
△ κ = 1000
b/a = 0.10
H = 20
T = 0.011
b = 7 ft
Girder A
Influence Lines for Moment at Midspan
Moment Envelopes
Outer P at Least 2 ft from Girder A
● κ = 0 Girder C
▲ κ = 0.05 Girder B
○ κ = 0.20 Girder B
△ κ = 1000 Girder B
b/a = 0.10
H = 20
T = 0.011
b = 7 ft
Influence Lines for Moment at Midspan
Moment Envelopes
$C_M = \frac{\text{Moment}}{Pa}$
0.50
0.40
0.30
0.20
0.10
0
0 1/12 2/12 3/12 4/12 5/12 6/12 5/12 4/12 3/12 2/12 1/12 0
Position Along Span

FIG. 5.31 (Cont.)

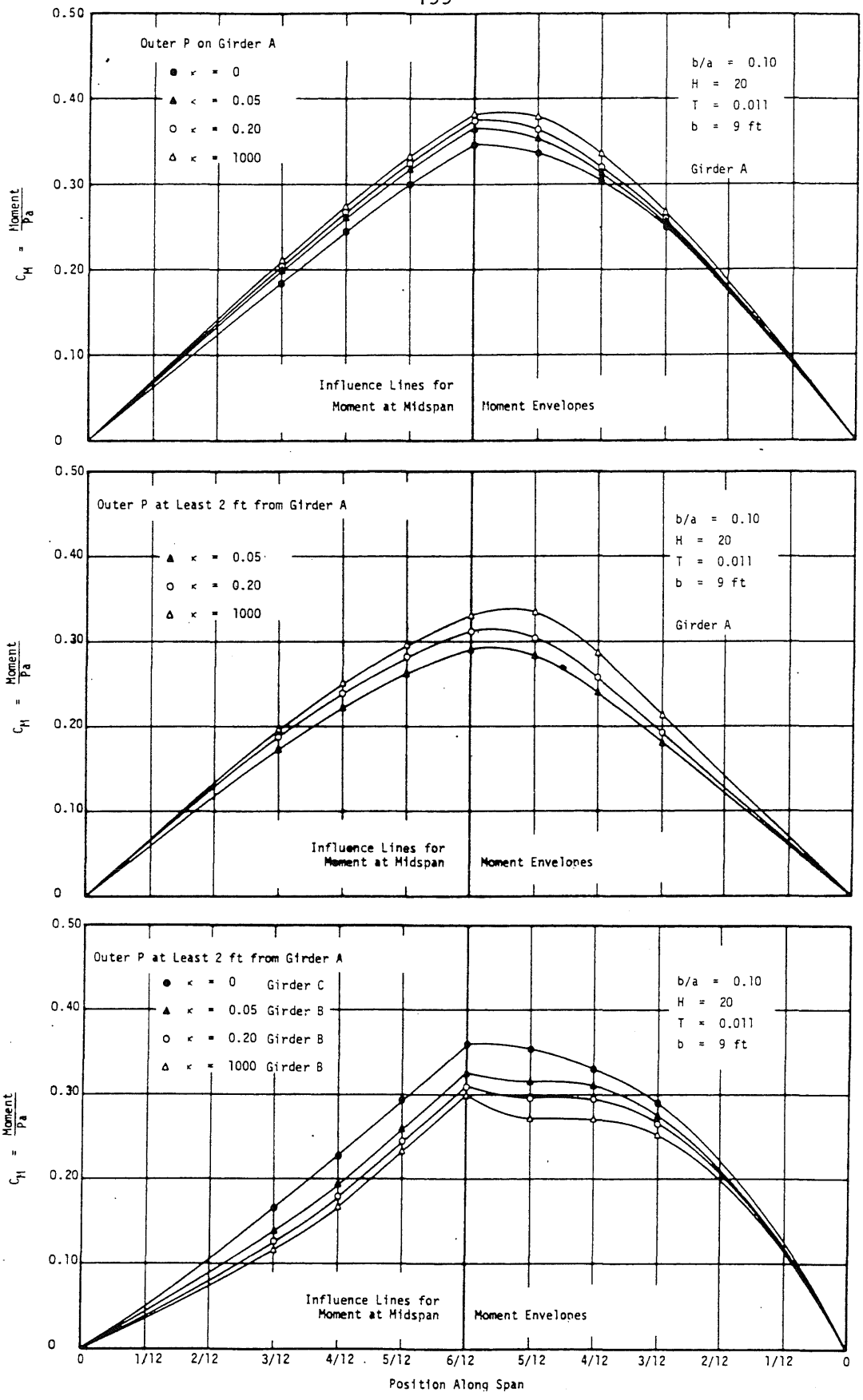
Outer P on Girder A
● κ = 0
▲ κ = 0.05
o κ = 0.20
Δ κ = 1000
b/a = 0.10
H = 20
T = 0.011
b = 9 ft
Girder A
Influence Lines for Moment at Midspan
Moment Envelopes
Outer P at Least 2 ft from Girder A
▲ κ = 0.05
o κ = 0.20
Δ κ = 1000
b/a = 0.10
H = 20
T = 0.011
b = 9 ft
Girder A
Influence Lines for Moment at Midspan
Moment Envelopes
Outer P at Least 2 ft from Girder A
● κ = 0 Girder C
▲ κ = 0.05 Girder B
o κ = 0.20 Girder B
Δ κ = 1000 Girder B
b/a = 0.10
H = 20
T = 0.011
b = 9 ft
Influence Lines for Moment at Midspan
Moment Envelopes
$C_M = \frac{\text{Moment}}{Pa}$
0.50
0.40
0.30
0.20
0.10
0
0 1/12 2/12 3/12 4/12 5/12 6/12 5/12 4/12 3/12 2/12 1/12 0
Position Along Span

FIG. 5.31 (Cont.)

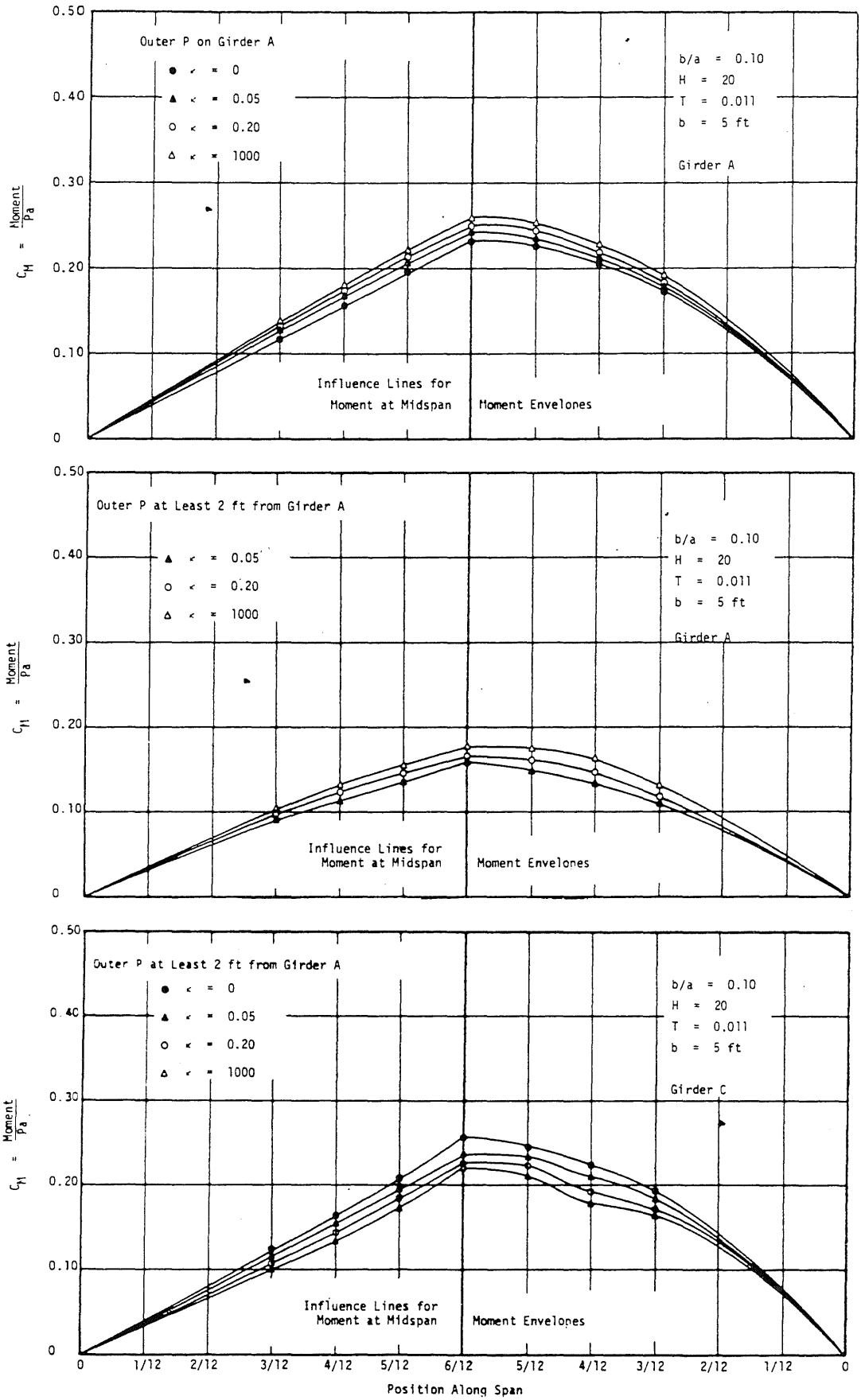

FIG. 5.32 EFFECTS OF DIAPHRAGMS ON INFLUENCE LINES FOR MAXIMUM MOMENT AT MIDSPAN AND MOMENT ENVELOPES OF STANDARD BRIDGE DUE TO 4-WHEEL LOADING MOVING ALONG SPAN; 2 DIAPHRAGMS AT THIRD-POINTS

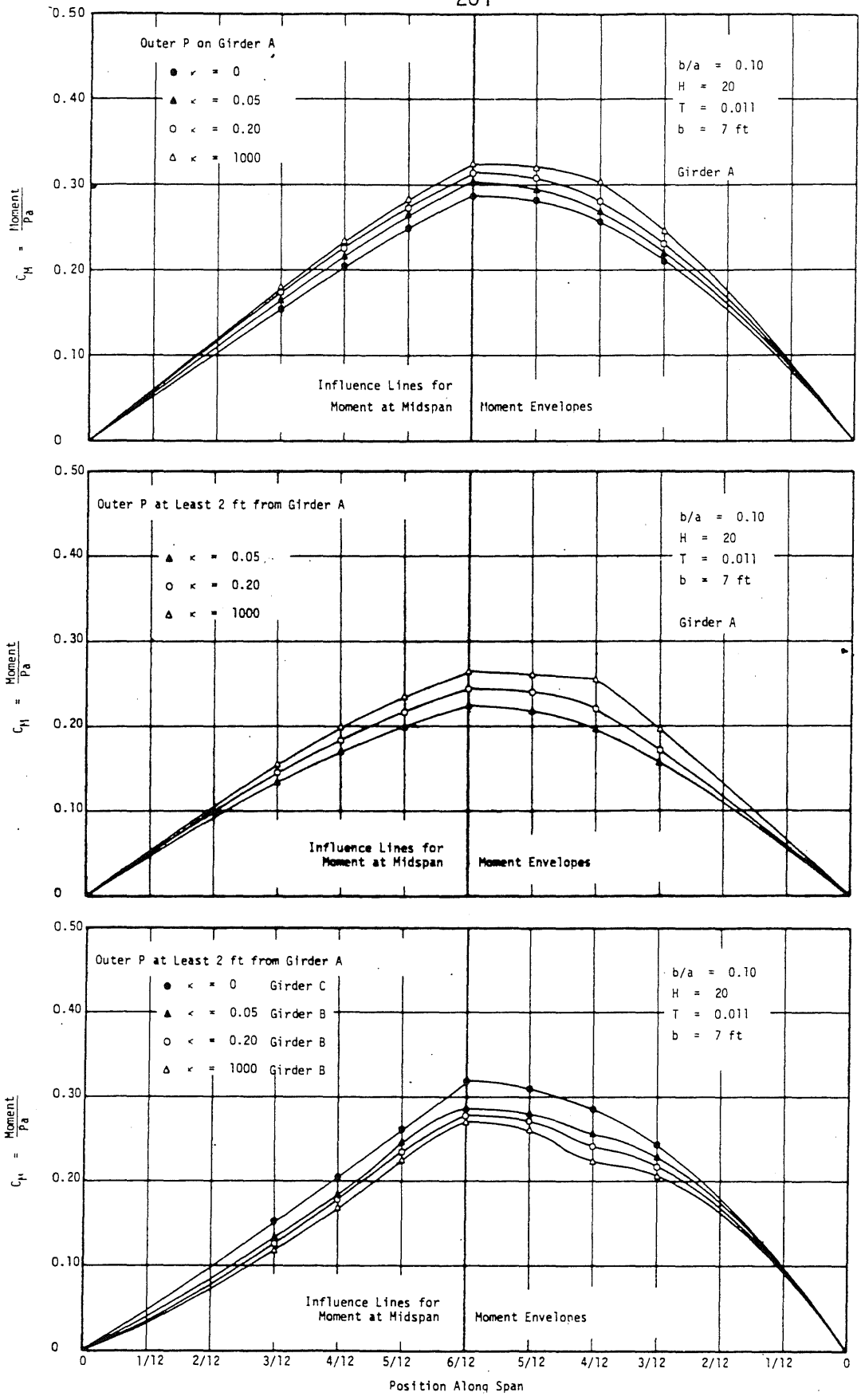
Outer P on Girder A
● κ = 0
▲ κ = 0.05
○ κ = 0.20
△ κ = 1000
b/a = 0.10
H = 20
T = 0.011
b = 7 ft
Girder A
Influence Lines for Moment at Midspan
Moment Envelopes
Outer P at Least 2 ft from Girder A
▲ κ = 0.05
○ κ = 0.20
△ κ = 1000
b/a = 0.10
H = 20
T = 0.011
b = 7 ft
Girder A
Influence Lines for Moment at Midspan
Moment Envelopes
Outer P at Least 2 ft from Girder A
● κ = 0 Girder C
▲ κ = 0.05 Girder B
○ κ = 0.20 Girder B
△ κ = 1000 Girder B
b/a = 0.10
H = 20
T = 0.011
b = 7 ft
Influence Lines for Moment at Midspan
Moment Envelopes
$C_M = \frac{\text{Moment}}{Pa}$
0.50
0.40
0.30
0.20
0.10
0
0 1/12 2/12 3/12 4/12 5/12 6/12 5/12 4/12 3/12 2/12 1/12 0
Position Along Span

FIG. 5.32 (Cont.)

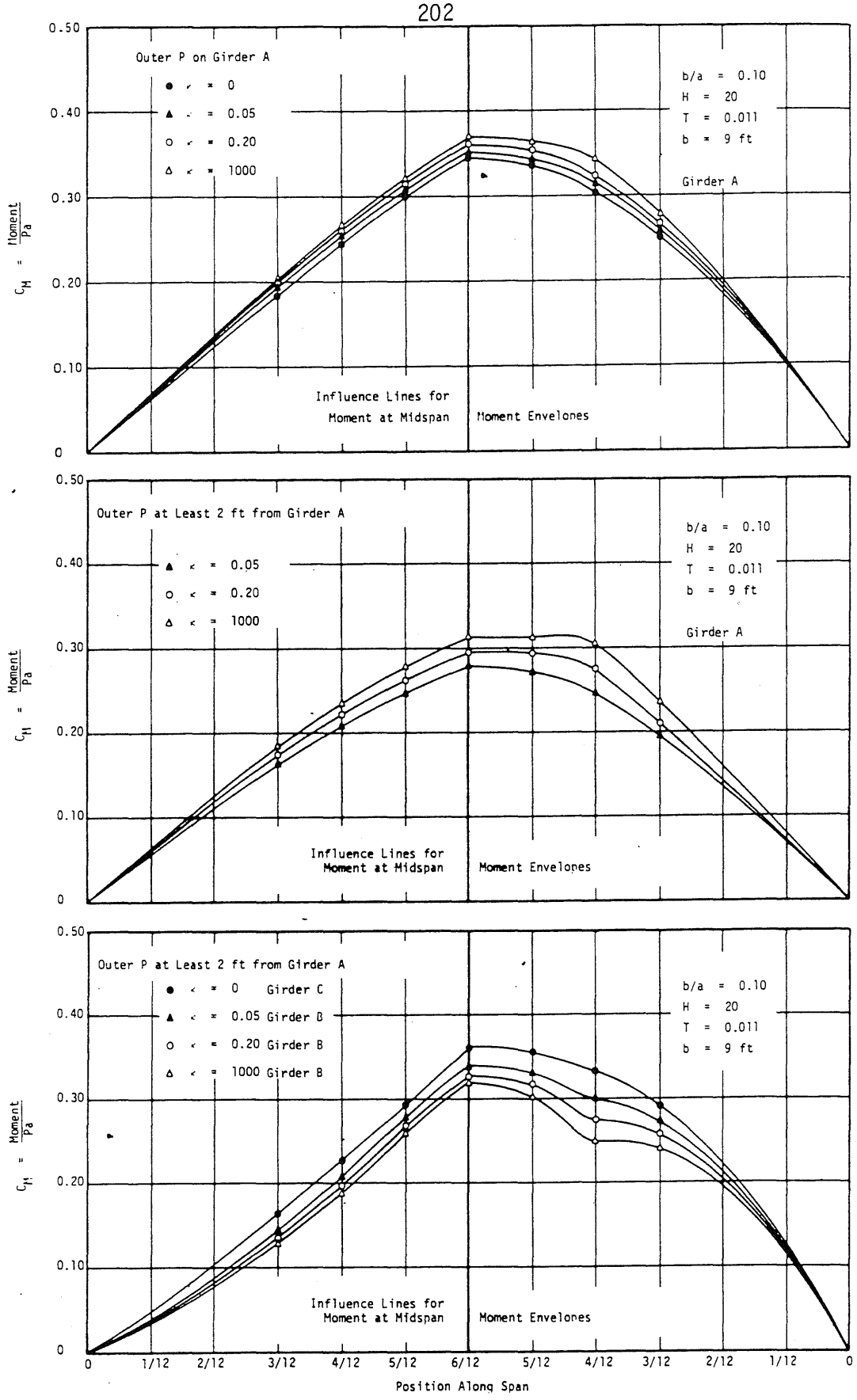
Outer P on Girder A
● κ = 0
▲ κ = 0.05
○ κ = 0.20
△ κ = 1000
b/a = 0.10
H = 20
T = 0.011
b = 9 ft
Girder A
Influence Lines for Moment at Midspan
Moment Envelopes
Outer P at Least 2 ft from Girder A
▲ κ = 0.05
○ κ = 0.20
△ κ = 1000
b/a = 0.10
H = 20
T = 0.011
b = 9 ft
Girder A
Influence Lines for Moment at Midspan
Moment Envelopes
Outer P at Least 2 ft from Girder A
● κ = 0 Girder C
▲ κ = 0.05 Girder B
○ κ = 0.20 Girder B
△ κ = 1000 Girder B
b/a = 0.10
H = 20
T = 0.011
b = 9 ft
Influence Lines for Moment at Midspan
Moment Envelopes
$C_M = \frac{\text{Moment}}{Pa}$
0.50
0.40
0.30
0.20
0.10
0
0 1/12 2/12 3/12 4/12 5/12 6/12 5/12 4/12 3/12 2/12 1/12 0
Position Along Span

FIG. 5.32 (Cont.)

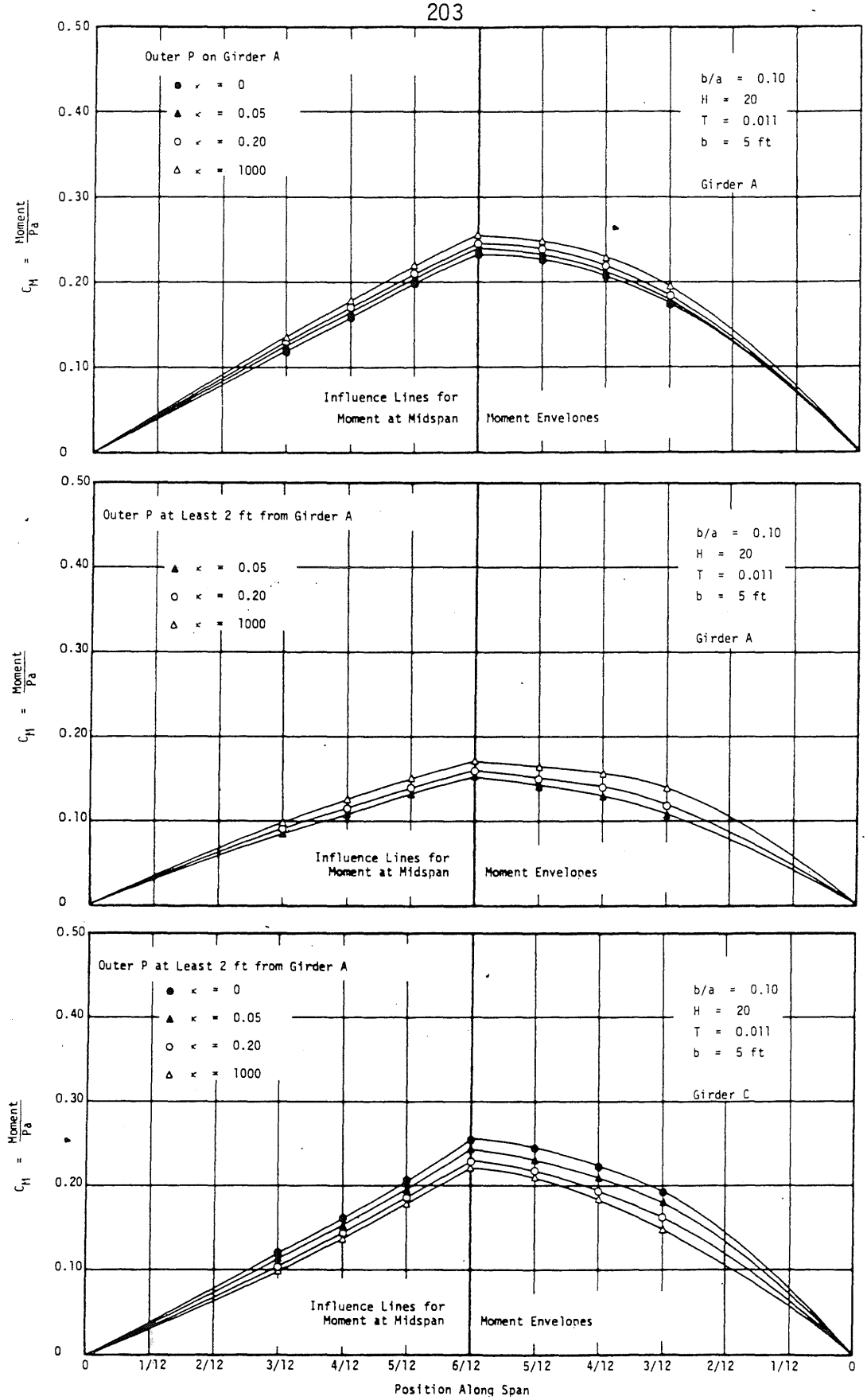

FIG. 5.33 EFFECTS OF DIAPHRAGMS ON INFLUENCE LINES FOR MAXIMUM MOMENT AT MIDSPAN AND MOMENT ENVELOPES OF STANDARD BRIDGE DUE TO 4-WHEEL LOADING MOVING ALONG SPAN; 2 DIAPHRAGMS AT QUARTER-POINTS

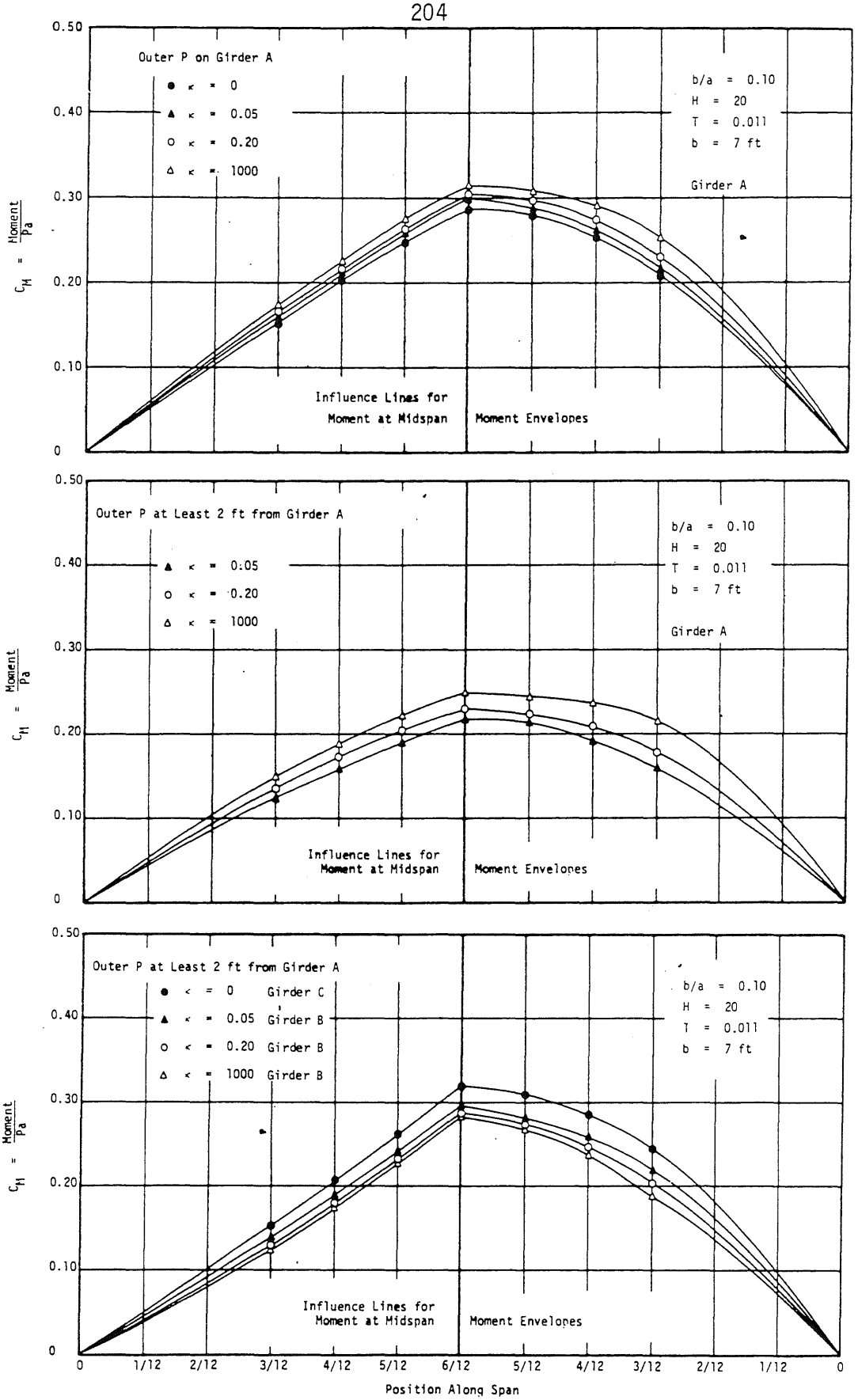
Outer P on Girder A
● κ = 0
▲ κ = 0.05
○ κ = 0.20
△ κ = 1000
b/a = 0.10
H = 20
T = 0.011
b = 7 ft
Girder A
Influence Lines for Moment at Midspan
Moment Envelopes
Outer P at Least 2 ft from Girder A
▲ κ = 0.05
○ κ = 0.20
△ κ = 1000
b/a = 0.10
H = 20
T = 0.011
b = 7 ft
Girder A
Influence Lines for Moment at Midspan
Moment Envelopes
Outer P at Least 2 ft from Girder A
● κ = 0 Girder C
▲ κ = 0.05 Girder B
○ κ = 0.20 Girder B
△ κ = 1000 Girder B
b/a = 0.10
H = 20
T = 0.011
b = 7 ft
Influence Lines for Moment at Midspan
Moment Envelopes
$C_M = \frac{\text{Moment}}{Pa}$
0.50
0.40
0.30
0.20
0.10
0
0 1/12 2/12 3/12 4/12 5/12 6/12 5/12 4/12 3/12 2/12 1/12 0
Position Along Span

FIG. 5.33 (Cont.)

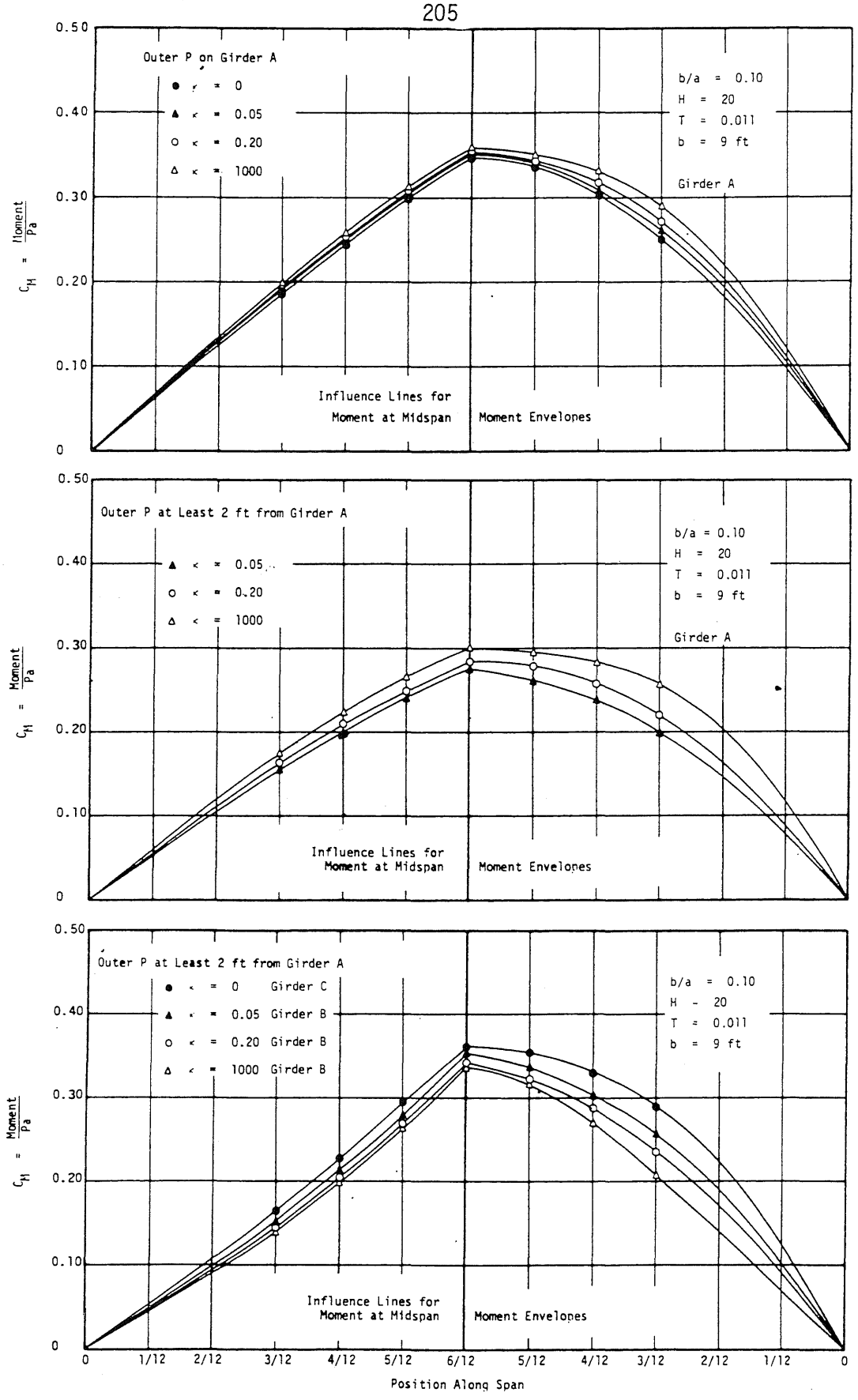
Outer P on Girder A
● κ = 0
▲ κ = 0.05
○ κ = 0.20
△ κ = 1000
b/a = 0.10
H = 20
T = 0.011
b = 9 ft
Girder A
Influence Lines for Moment at Midspan
Moment Envelopes
Outer P at Least 2 ft from Girder A
▲ κ = 0.05
○ κ = 0.20
△ κ = 1000
b/a = 0.10
H = 20
T = 0.011
b = 9 ft
Girder A
Influence Lines for Moment at Midspan
Moment Envelopes
Outer P at Least 2 ft from Girder A
● κ = 0 Girder C
▲ κ = 0.05 Girder B
○ κ = 0.20 Girder B
△ κ = 1000 Girder B
b/a = 0.10
H = 20
T = 0.011
b = 9 ft
Influence Lines for Moment at Midspan
Moment Envelopes
$C_M = \frac{\text{Moment}}{Pa}$
0.50
0.40
0.30
0.20
0.10
0
0 1/12 2/12 3/12 4/12 5/12 6/12 5/12 4/12 3/12 2/12 1/12 0
Position Along Span

FIG. 5.33 (Cont.)

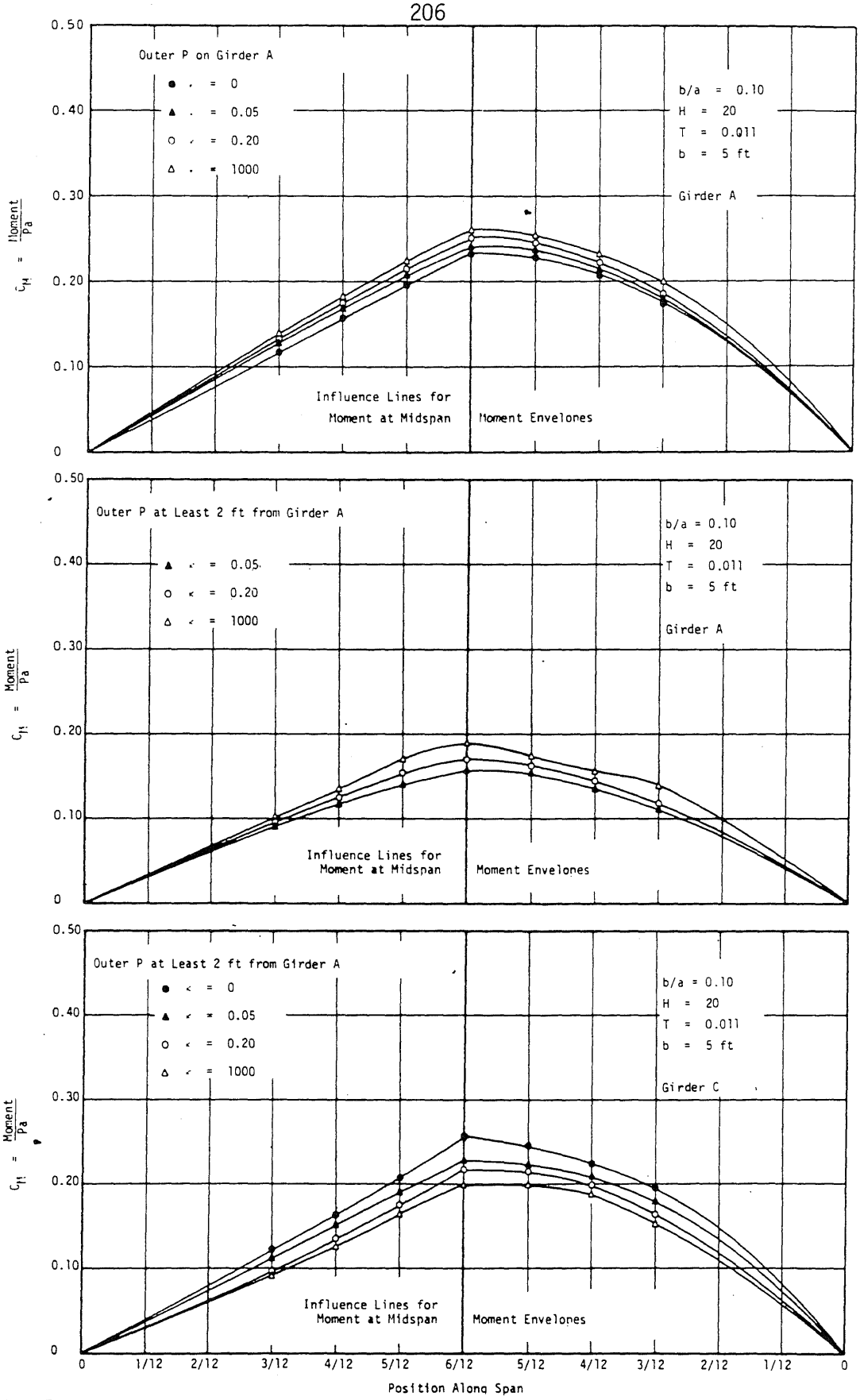

FIG. 5.34 EFFECTS OF DIAPHRAGMS ON INFLUENCE LINES FOR MAXIMUM MOMENT AT MIDSPAN AND MOMENT ENVELOPES OF STANDARD BRIDGE DUE TO 4-WHEEL LOADING MOVING ALONG SPAN; 3 DIAPHRAGMS AT QUARTER-POINTS AND MIDSPAN

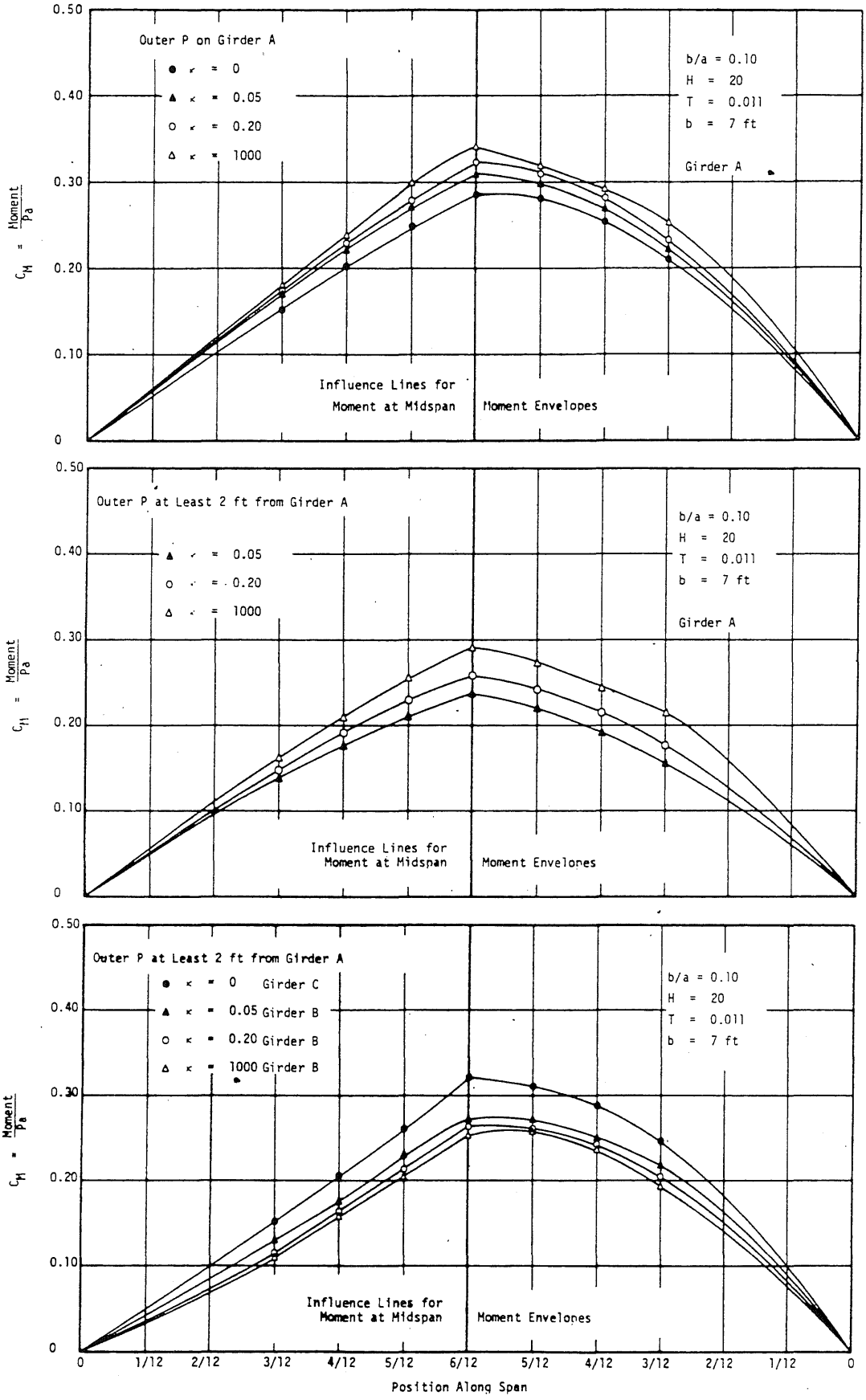
Outer P on Girder A
κ = 0
κ = 0.05
κ = 0.20
κ = 1000
b/a = 0.10
H = 20
T = 0.011
b = 7 ft
Girder A
Influence Lines for Moment at Midspan
Moment Envelopes
Outer P at Least 2 ft from Girder A
κ = 0.05
κ = 0.20
κ = 1000
b/a = 0.10
H = 20
T = 0.011
b = 7 ft
Girder A
Influence Lines for Moment at Midspan
Moment Envelopes
Outer P at Least 2 ft from Girder A
κ = 0 Girder C
κ = 0.05 Girder B
κ = 0.20 Girder B
κ = 1000 Girder B
b/a = 0.10
H = 20
T = 0.011
b = 7 ft
Influence Lines for Moment at Midspan
Moment Envelopes
$C_M = \frac{\text{Moment}}{Pa}$
0.50
0.40
0.30
0.20
0.10
0
0 1/12 2/12 3/12 4/12 5/12 6/12 5/12 4/12 3/12 2/12 1/12 0
Position Along Span

FIG. 5.34 (Cont.)

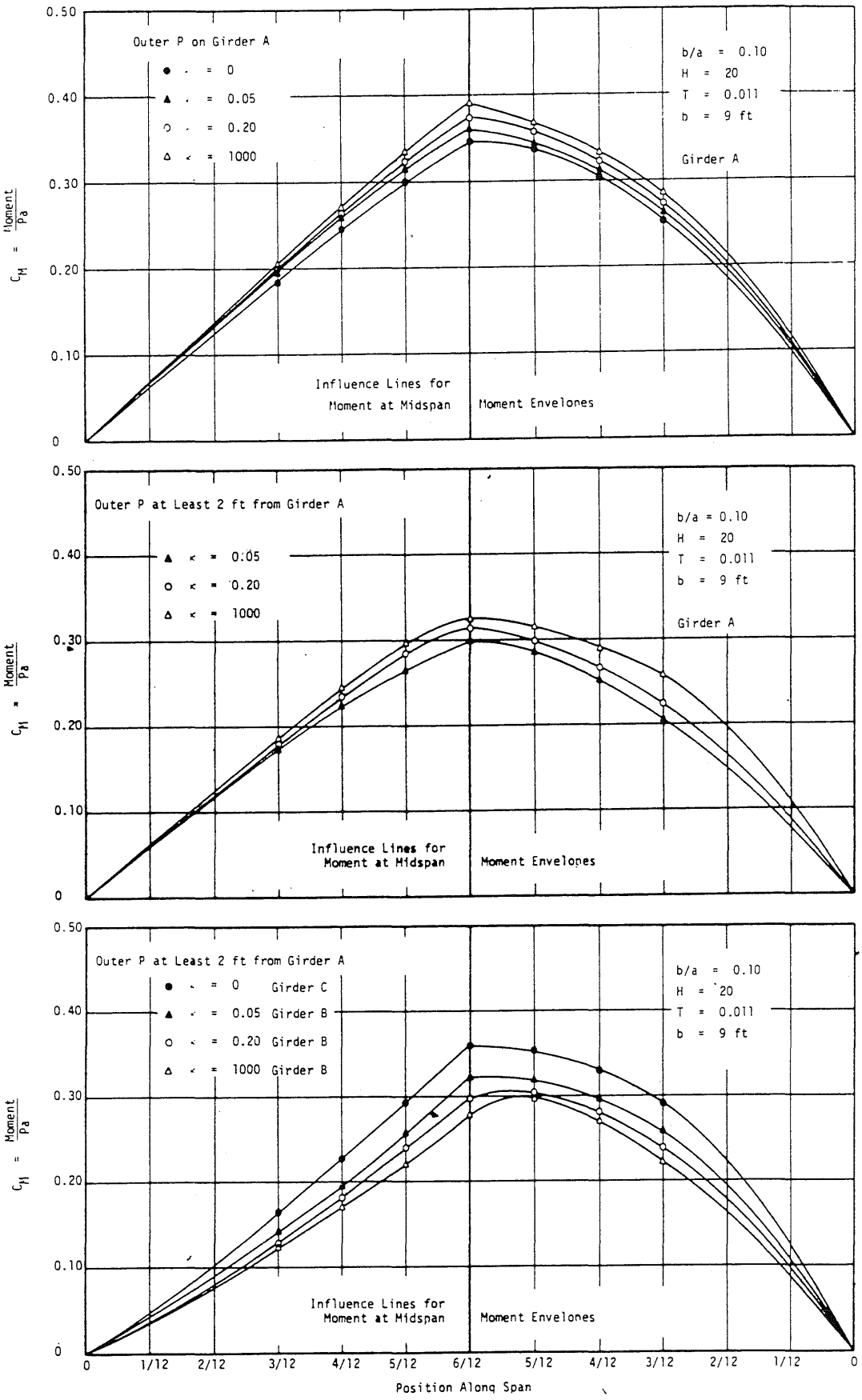
Outer P on Girder A
● κ = 0
▲ κ = 0.05
○ κ = 0.20
△ κ = 1000
b/a = 0.10
H = 20
T = 0.011
b = 9 ft
Girder A
Influence Lines for Moment at Midspan
Moment Envelopes
Outer P at Least 2 ft from Girder A
▲ κ = 0.05
○ κ = 0.20
△ κ = 1000
b/a = 0.10
H = 20
T = 0.011
b = 9 ft
Girder A
Influence Lines for Moment at Midspan
Moment Envelopes
Outer P at Least 2 ft from Girder A
● κ = 0 Girder C
▲ κ = 0.05 Girder B
○ κ = 0.20 Girder B
△ κ = 1000 Girder B
b/a = 0.10
H = 20
T = 0.011
b = 9 ft
Influence Lines for Moment at Midspan
Moment Envelopes
$C_M = \frac{\text{Moment}}{Pa}$
0.50
0.40
0.30
0.20
0.10
0
0 1/12 2/12 3/12 4/12 5/12 6/12 5/12 4/12 3/12 2/12 1/12 0
Position Along Span

FIG. 5.34 (Cont.)

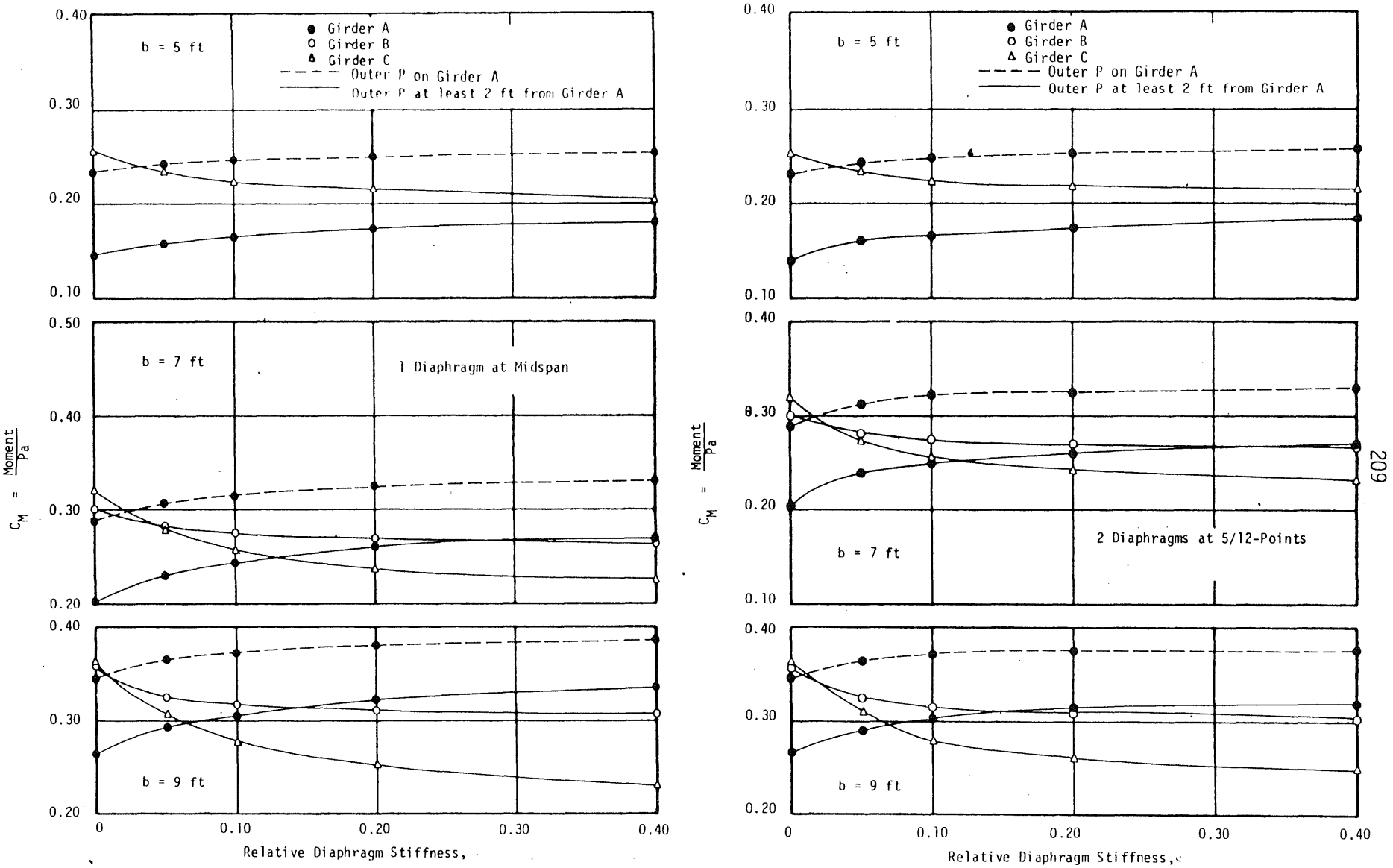

FIG. 5.35 MAXIMUM MOMENTS IN GIRDERS DUE TO 4-WHEEL LOADING VERSUS DIAPHRAGM STIFFNESS AND LOCATION; b/a = 0.10, H = 20, T = 0.011

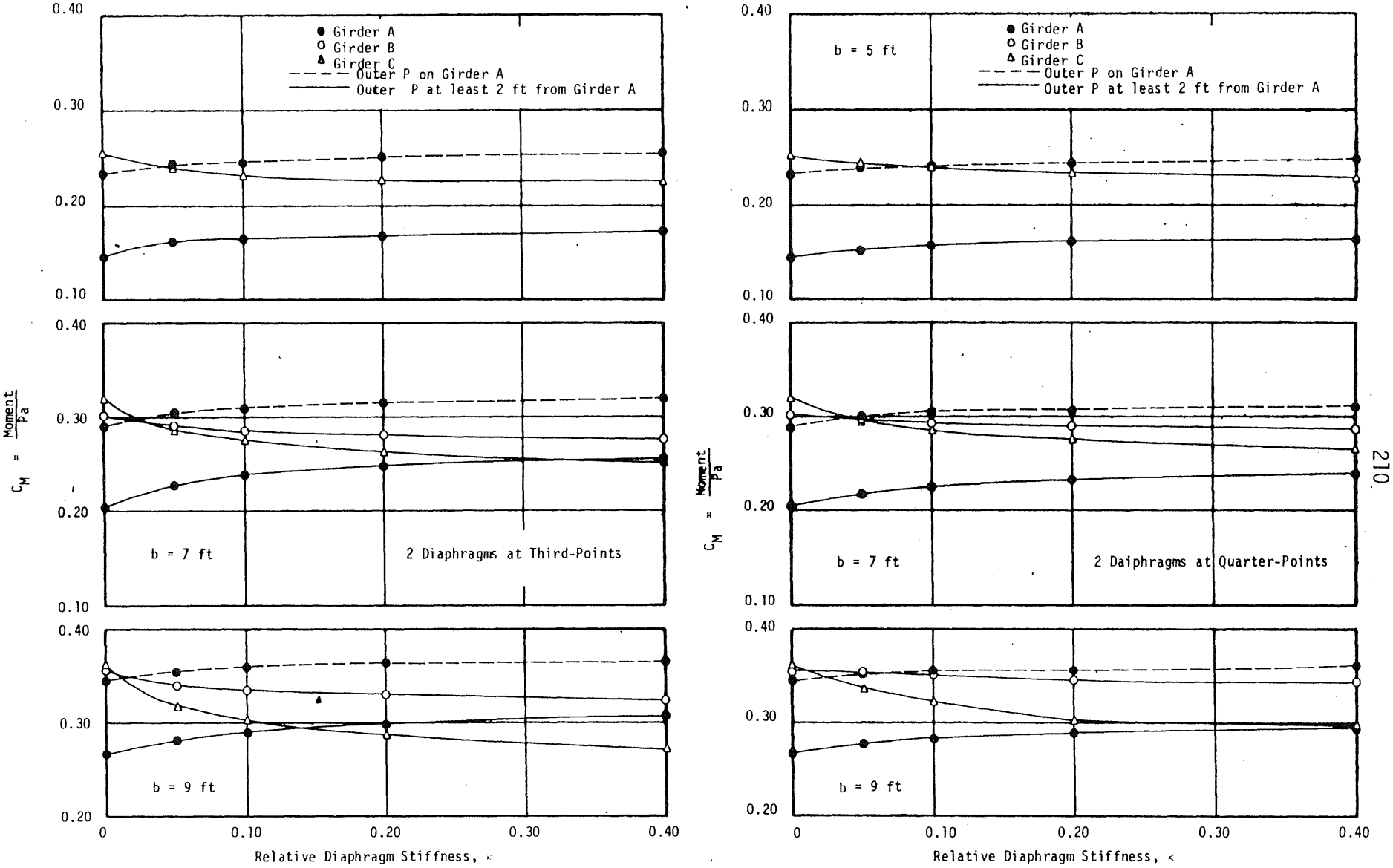
Girder A
Girder B
Girder C
Outer P on Girder A
Outer P at least 2 ft from Girder A
b = 5 ft
b = 7 ft
2 Diaphragms at Third-Points
2 Daiphragms at Quarter-Points
b = 9 ft
$C_M = \frac{\text{Moment}}{Pa}$
Relative Diaphragm Stiffness, κ
0.40
0.30
0.20
0.10
0
0.10
0.20
0.30
0.40

FIG. 5.35 (Cont.)

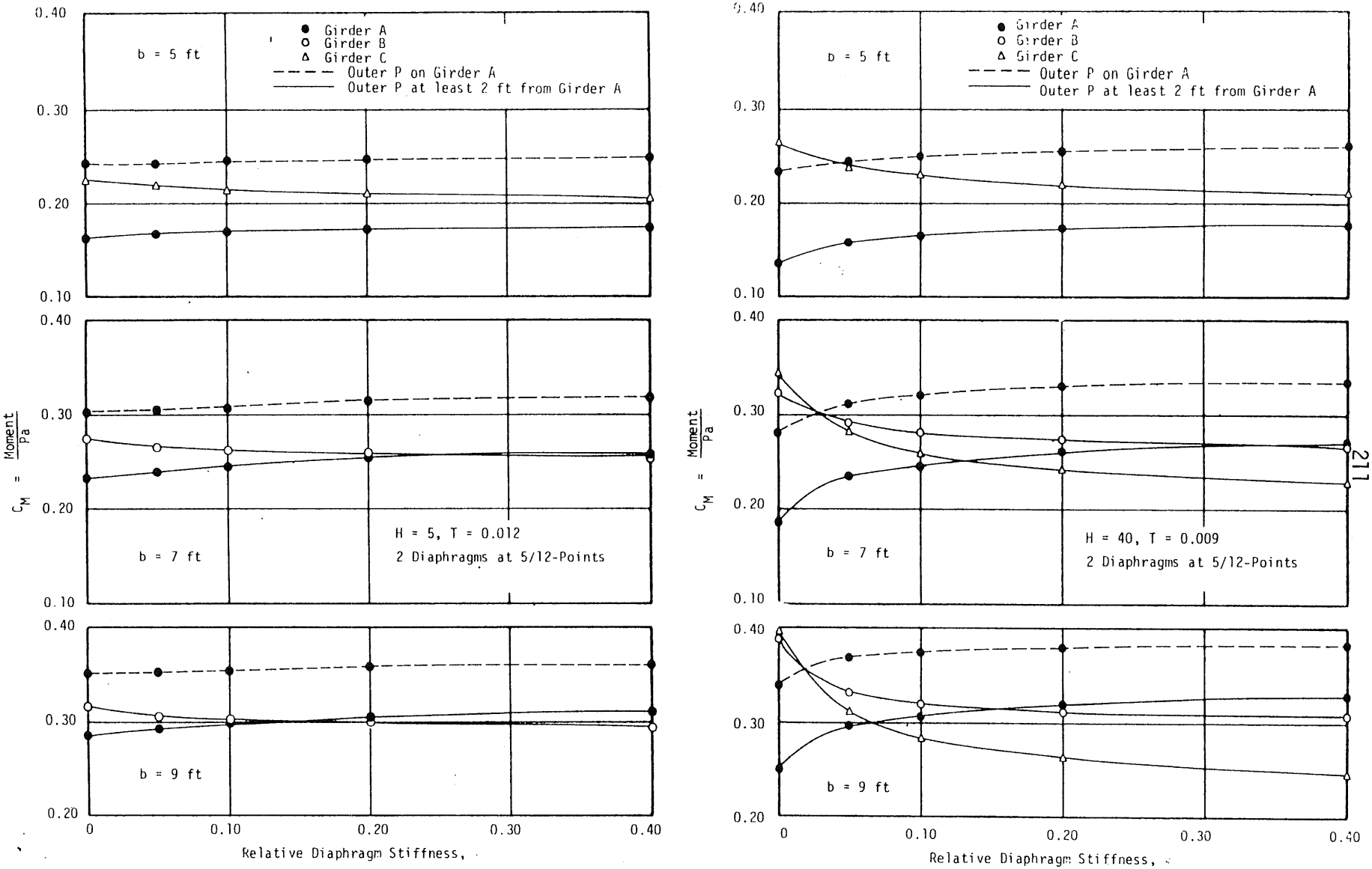

FIG. 5.36 MAXIMUM MOMENT IN GIRDERS DUE TO 4-WHEEL LOADING VERSUS DIAPHRAGM STIFFNESS AND LOCATION; b/a = 0.10

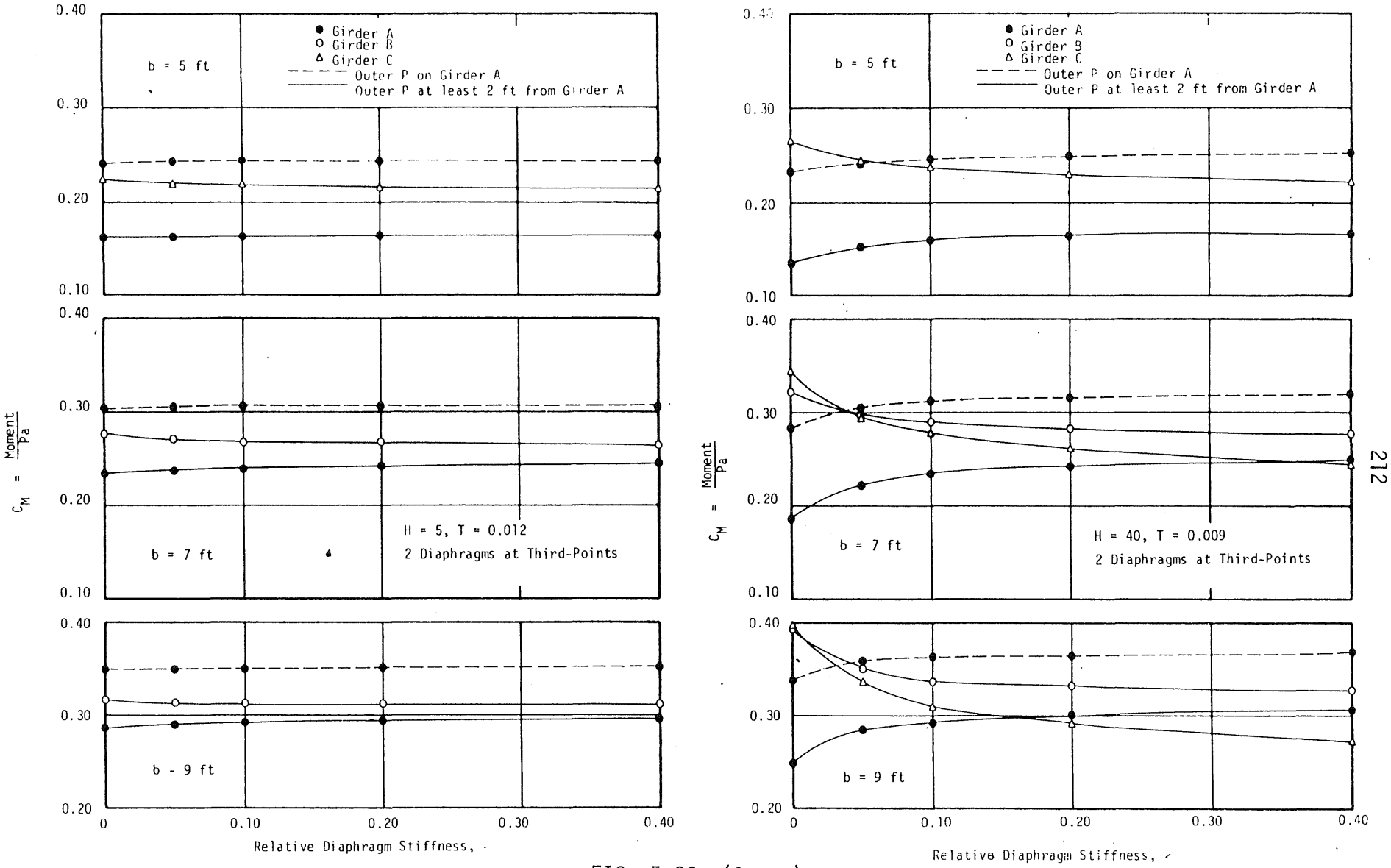
Girder A
Girder B
Girder C
Outer P on Girder A
Outer P at least 2 ft from Girder A
b = 5 ft
b = 7 ft
b = 9 ft
H = 5, T = 0.012
2 Diaphragms at Third-Points
H = 40, T = 0.009
2 Diaphragms at Third-Points
$C_M = \frac{\text{Moment}}{Pa}$
Relative Diaphragm Stiffness,
0.40
0.30
0.20
0.10
0
0.10
0.20
0.30
0.40

FIG. 5.36 (Cont.)

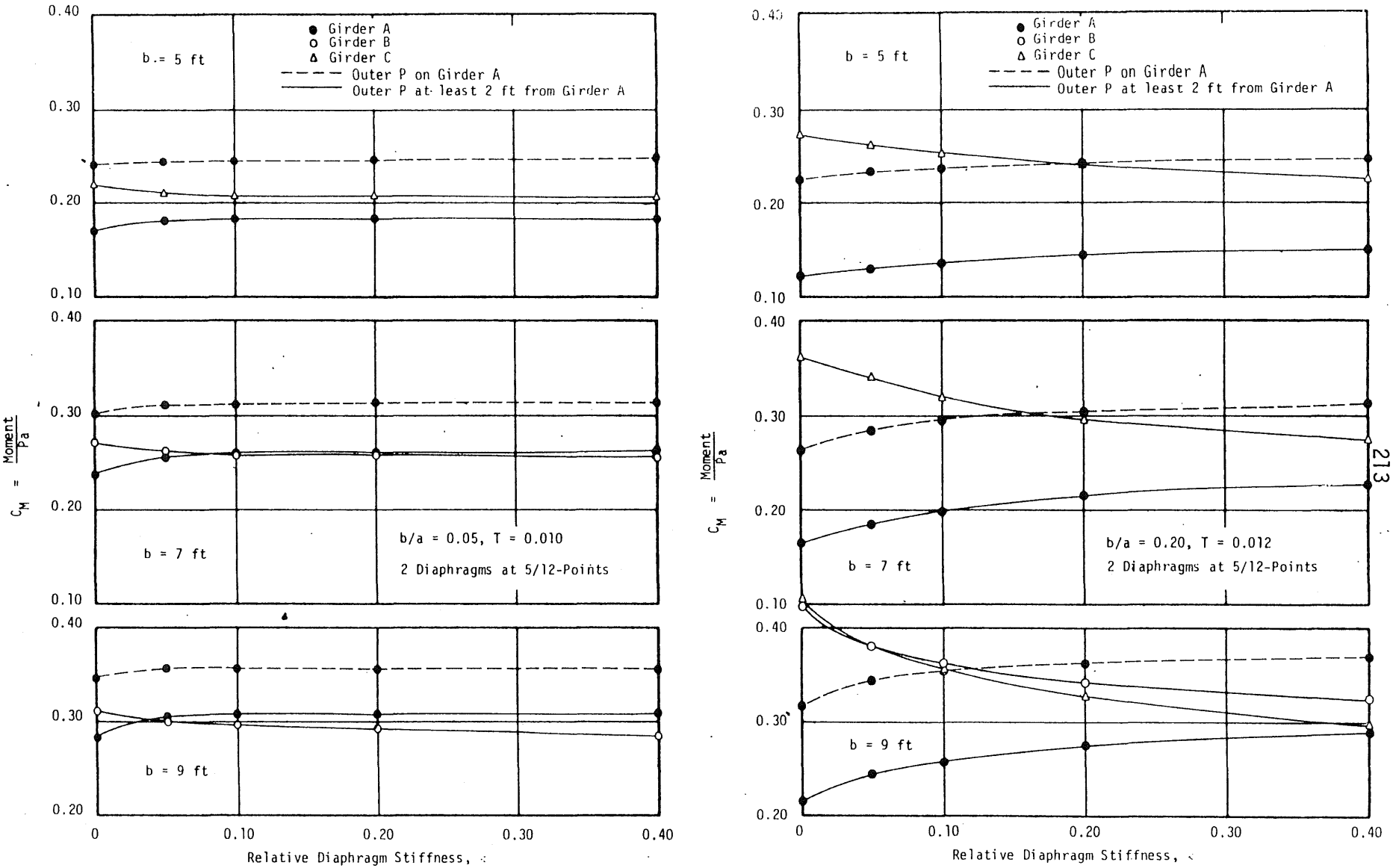

FIG. 5.37 MAXIMUM MOMENT IN GIRDERS DUE TO 4-WHEEL LOADING VERSUS DIAPHRAGM STIFFNESS AND LOCATION; H = 20

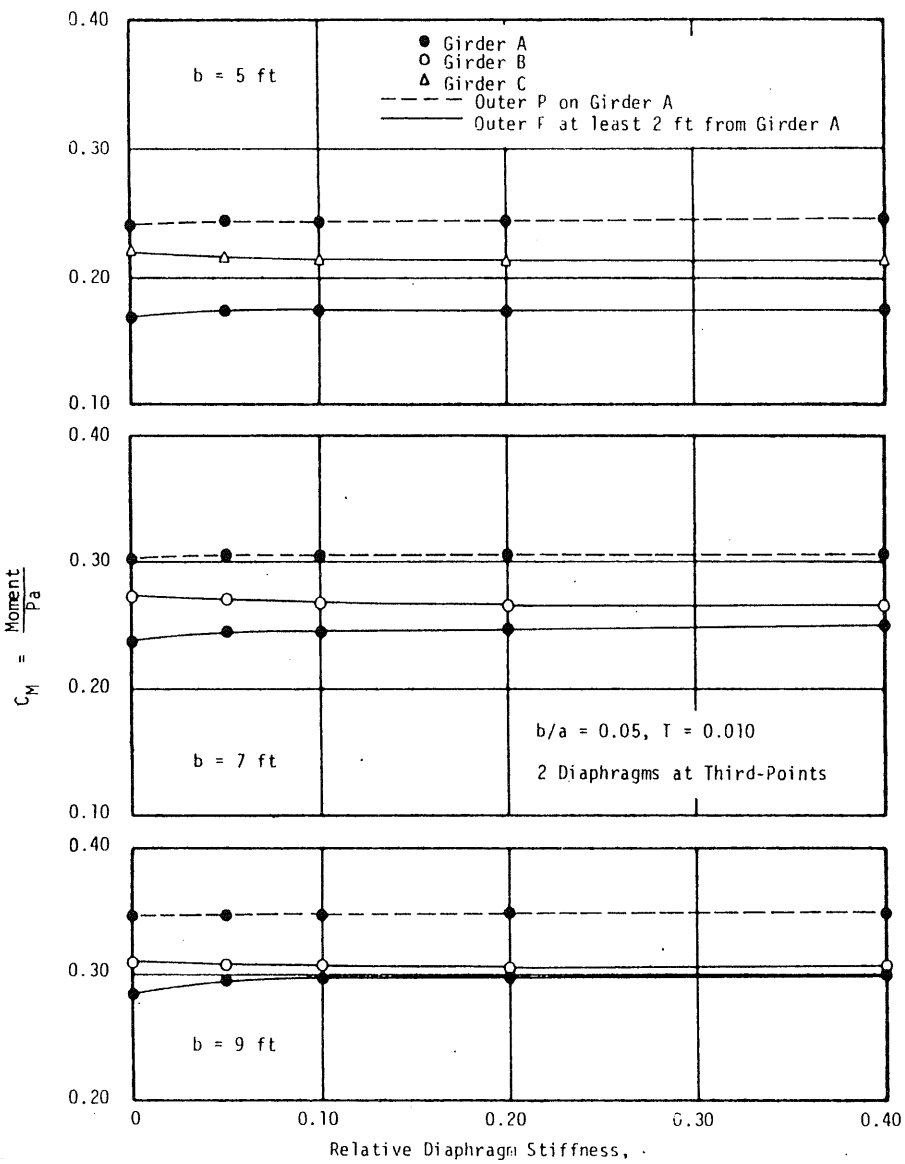
b = 5 ft
Girder A
Girder B
Girder C
Outer P on Girder A
Outer P at least 2 ft from Girder A
b = 7 ft
b/a = 0.05, T = 0.010
2 Diaphragms at Third-Points
b = 9 ft
$C_M = \frac{\text{Moment}}{Pa}$
Relative Diaphragm Stiffness,
0.40
0.30
0.20
0.10
0
0.10
0.20
0.30
0.40

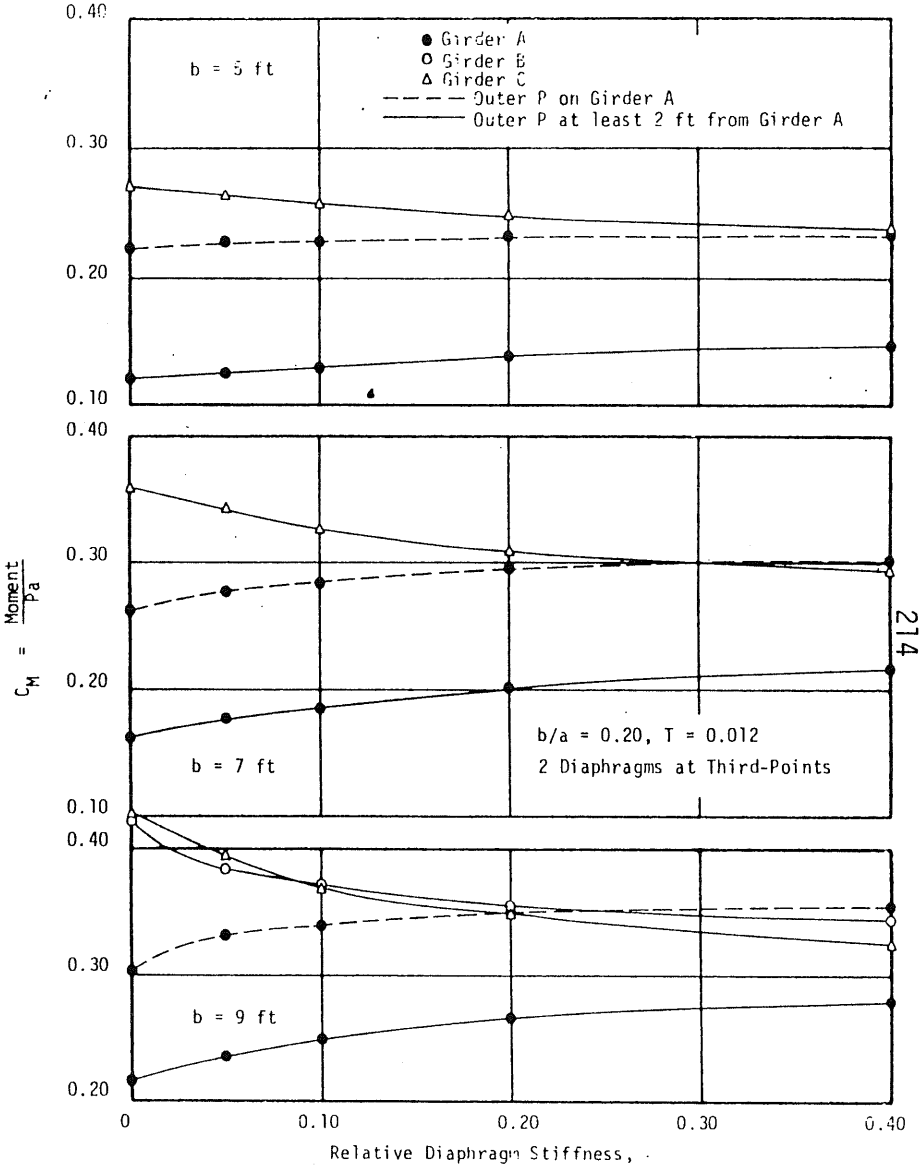
b = 5 ft
Girder A
Girder B
Girder C
Outer P on Girder A
Outer P at least 2 ft from Girder A
b = 7 ft
b/a = 0.20, T = 0.012
2 Diaphragms at Third-Points
b = 9 ft
$C_M = \frac{\text{Moment}}{Pa}$
Relative Diaphragm Stiffness,
0.40
0.30
0.20
0.10
0
0.10
0.20
0.30
0.40

FIG. 5.37 (Cont.)

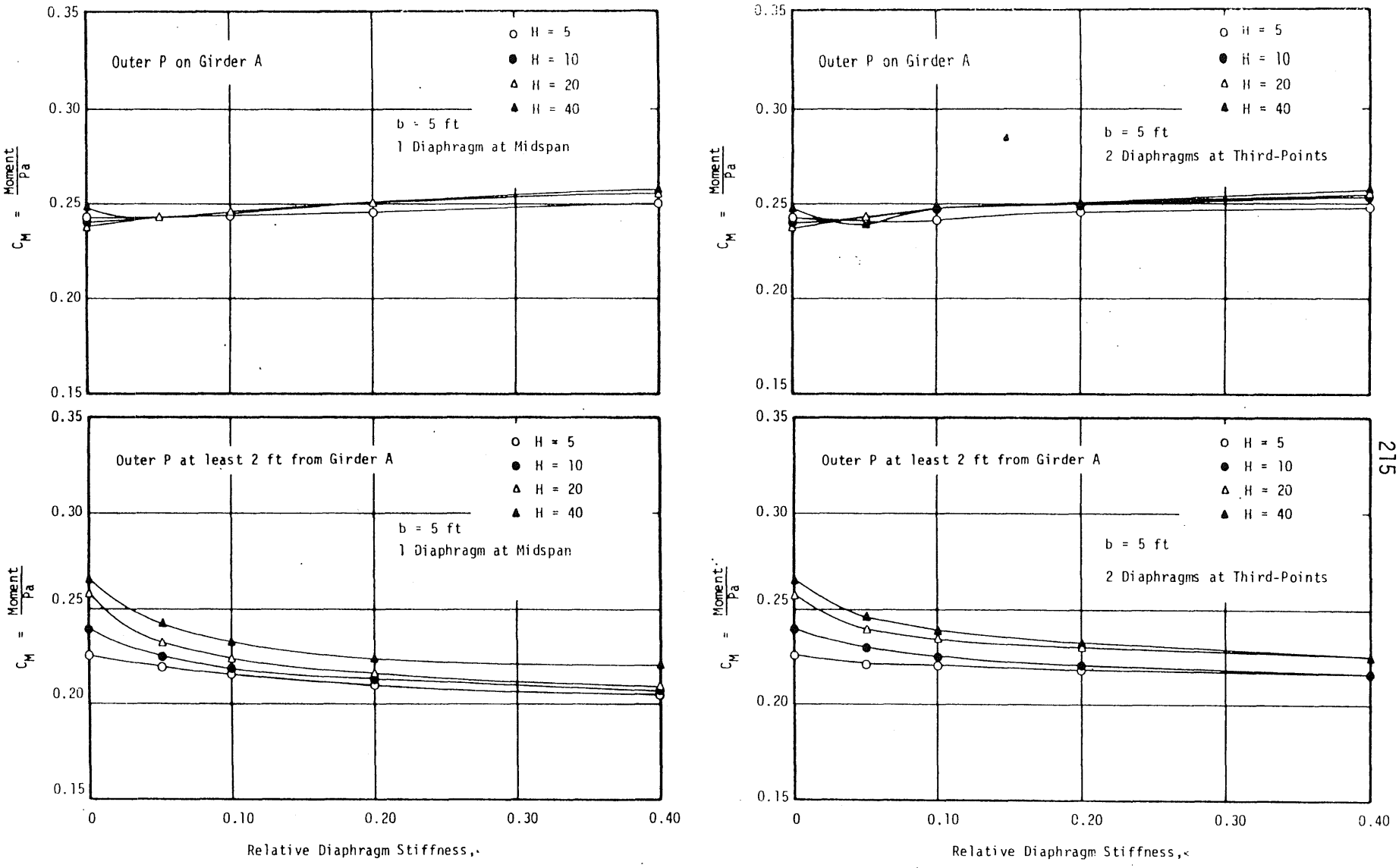

FIG. 5.38 MAXIMUM MOMENTS IN BRIDGES DUE TO 4-WHEEL LOADING VERSUS DIAPHRAGM STIFFNESS AND LOCATION; b/a = 0.10

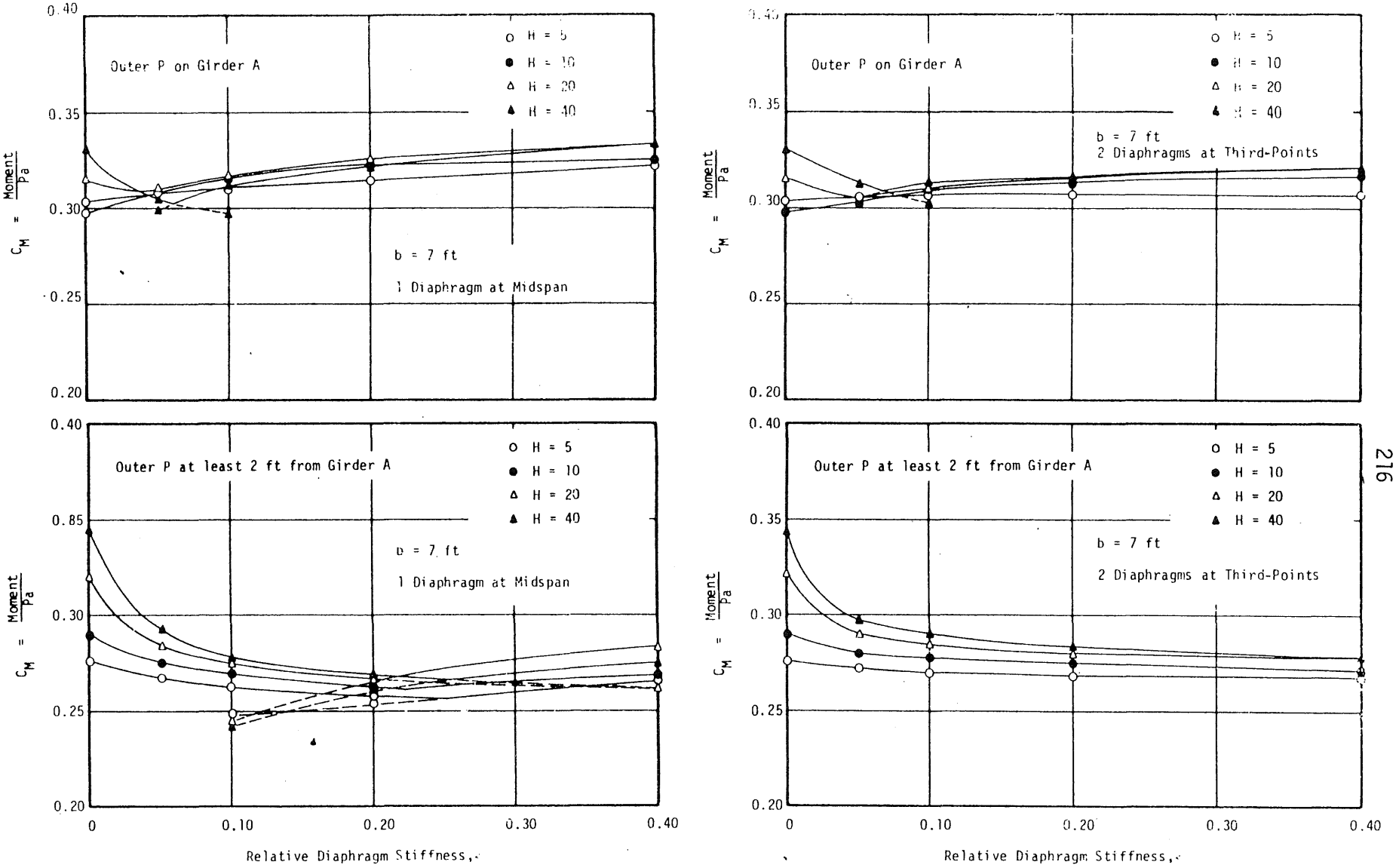
Outer P on Girder A
o H = 5
● H = 10
Δ H = 20
▲ H = 40
b = 7 ft
1 Diaphragm at Midspan
Outer P on Girder A
o H = 5
● H = 10
Δ H = 20
▲ H = 40
b = 7 ft
2 Diaphragms at Third-Points
Outer P at least 2 ft from Girder A
o H = 5
● H = 10
Δ H = 20
▲ H = 40
b = 7 ft
1 Diaphragm at Midspan
Outer P at least 2 ft from Girder A
o H = 5
● H = 10
Δ H = 20
▲ H = 40
b = 7 ft
2 Diaphragms at Third-Points
$C_M = \frac{\text{Moment}}{Pa}$
0.40
0.35
0.30
0.25
0.20
0.85
0
0.10
0.20
0.30
0.40
Relative Diaphragm Stiffness,

FIG. 5.38 (Cont.)

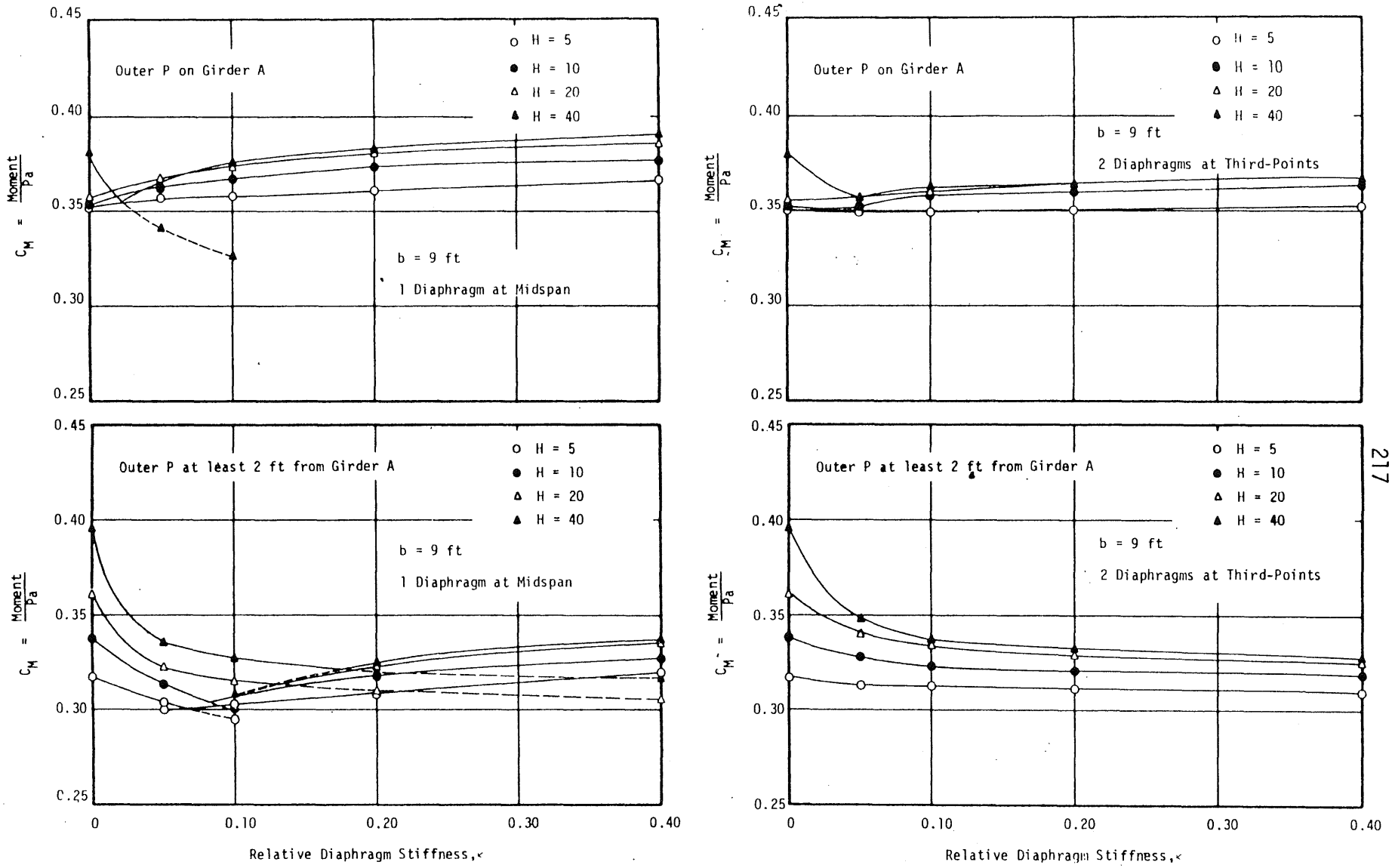
Outer P on Girder A
o H = 5
● H = 10
△ H = 20
▲ H = 40
b = 9 ft
1 Diaphragm at Midspan
Outer P on Girder A
o H = 5
● H = 10
△ H = 20
▲ H = 40
b = 9 ft
2 Diaphragms at Third-Points
Outer P at least 2 ft from Girder A
o H = 5
● H = 10
△ H = 20
▲ H = 40
b = 9 ft
1 Diaphragm at Midspan
Outer P at least 2 ft from Girder A
o H = 5
● H = 10
△ H = 20
▲ H = 40
b = 9 ft
2 Diaphragms at Third-Points
$C_M = \frac{\text{Moment}}{Pa}$
0.45
0.40
0.35
0.30
0.25
0
0.10
0.20
0.30
0.40
Relative Diaphragm Stiffness, κ

FIG. 5.38 (Cont.)

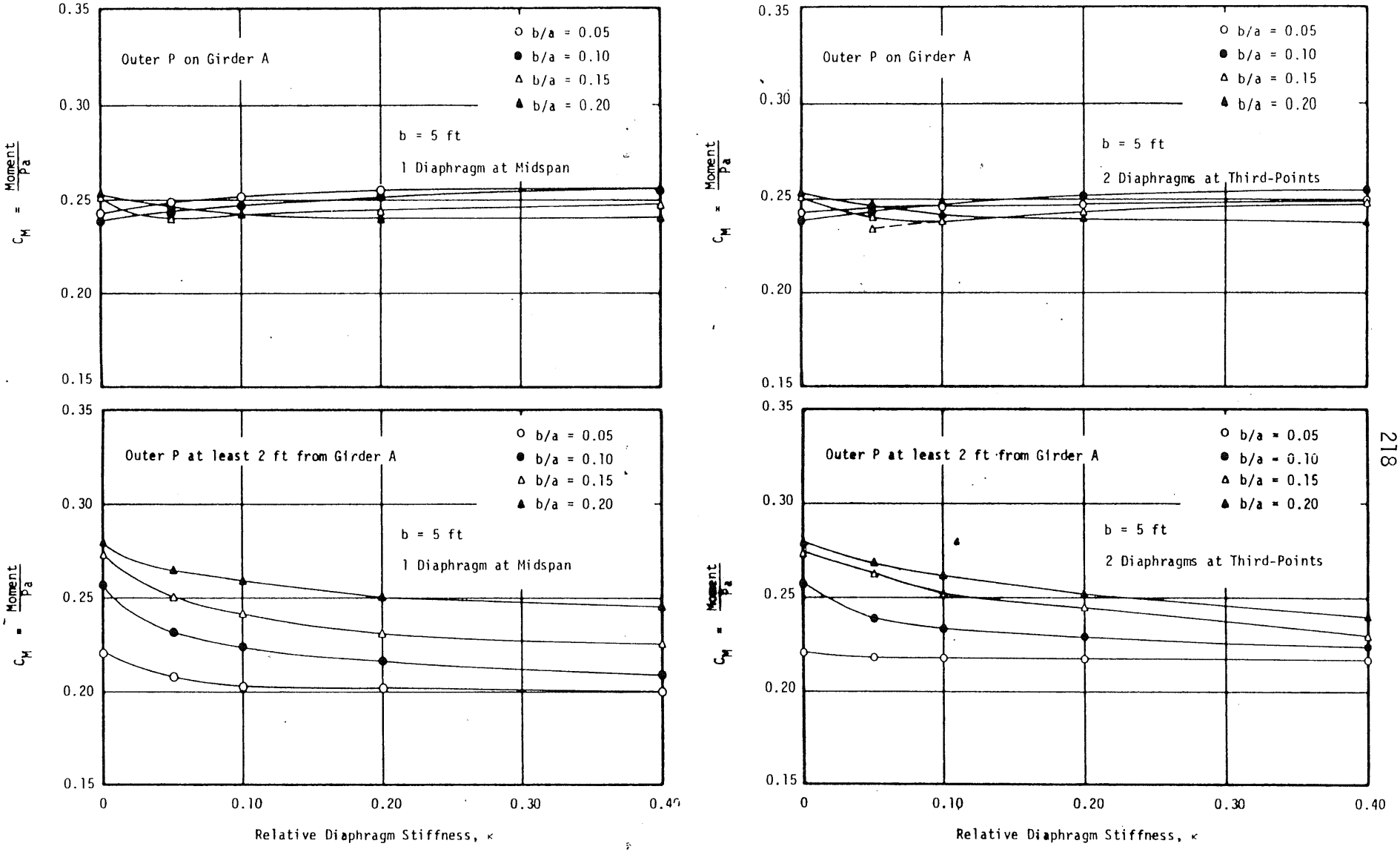

FIG. 5.39 MAXIMUM MOMENTS IN BRIDGES DUE TO 4-WHEEL LOADING VERSUS DIAPHRAGM STIFFNESS AND LOCATION; H = 20

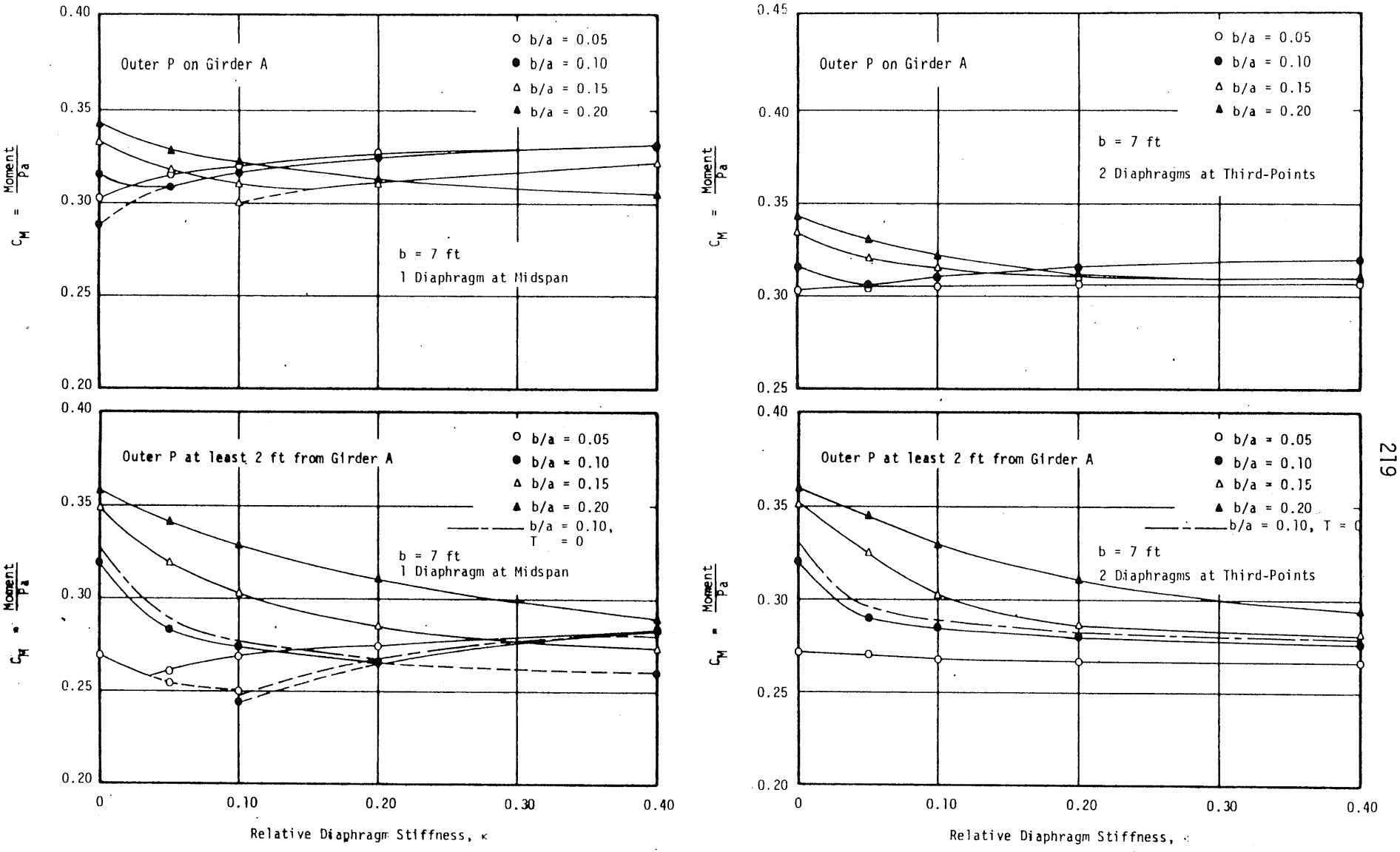
Outer P on Girder A
b/a = 0.05
b/a = 0.10
b/a = 0.15
b/a = 0.20
b = 7 ft
1 Diaphragm at Midspan
Outer P at least 2 ft from Girder A
b/a = 0.10, T = 0
2 Diaphragms at Third-Points
$C_M = \frac{\text{Moment}}{Pa}$
Relative Diaphragm Stiffness, κ
0.20
0.25
0.30
0.35
0.40
0.45
0
0.10
0.20
0.30
0.40

FIG. 5.39 (Cont.)

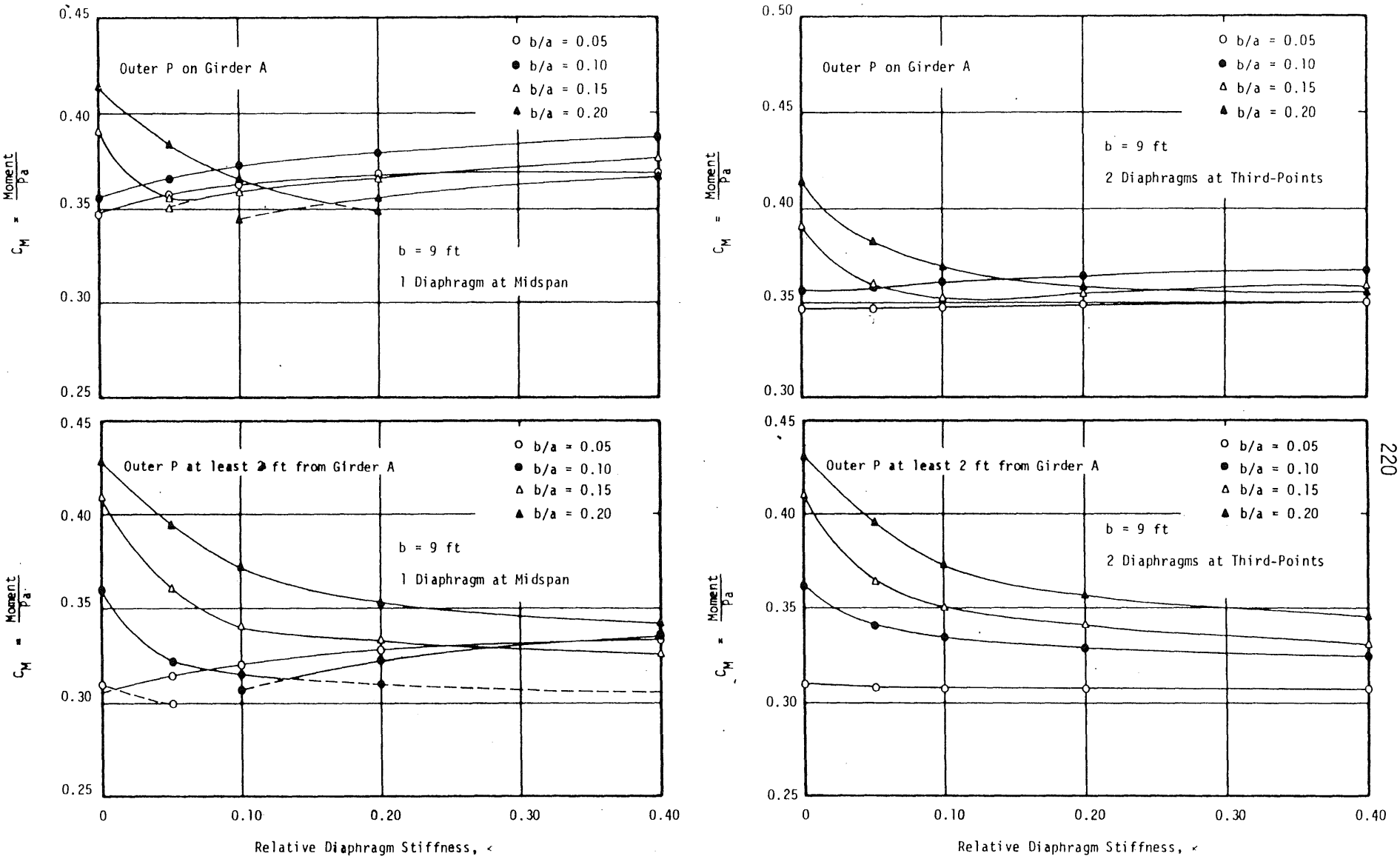
Outer P on Girder A
b = 9 ft
1 Diaphragm at Midspan
Outer P at least 2 ft from Girder A
b = 9 ft
1 Diaphragm at Midspan
Outer P on Girder A
b = 9 ft
2 Diaphragms at Third-Points
Outer P at least 2 ft from Girder A
b = 9 ft
2 Diaphragms at Third-Points
b/a = 0.05
b/a = 0.10
b/a = 0.15
b/a = 0.20
$C_M = \frac{\text{Moment}}{Pa}$
Relative Diaphragm Stiffness, κ

FIG. 5.39 (Cont.)

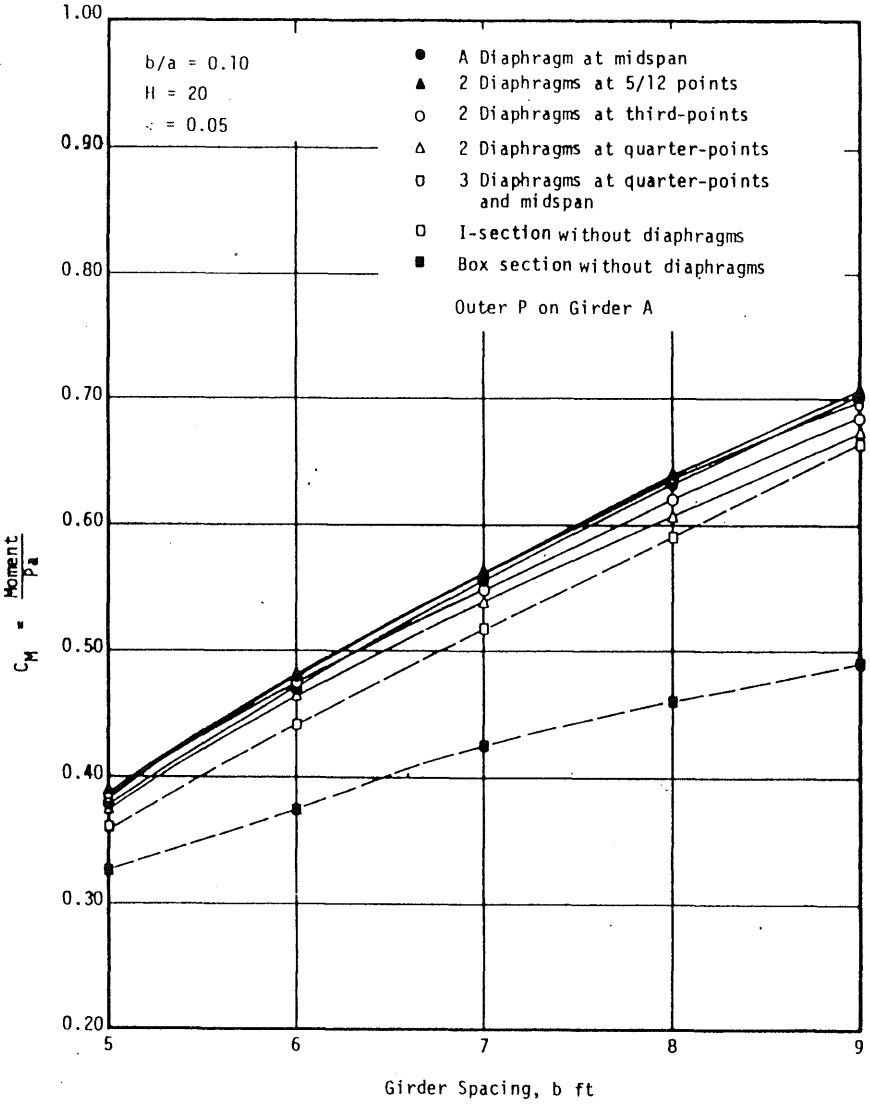

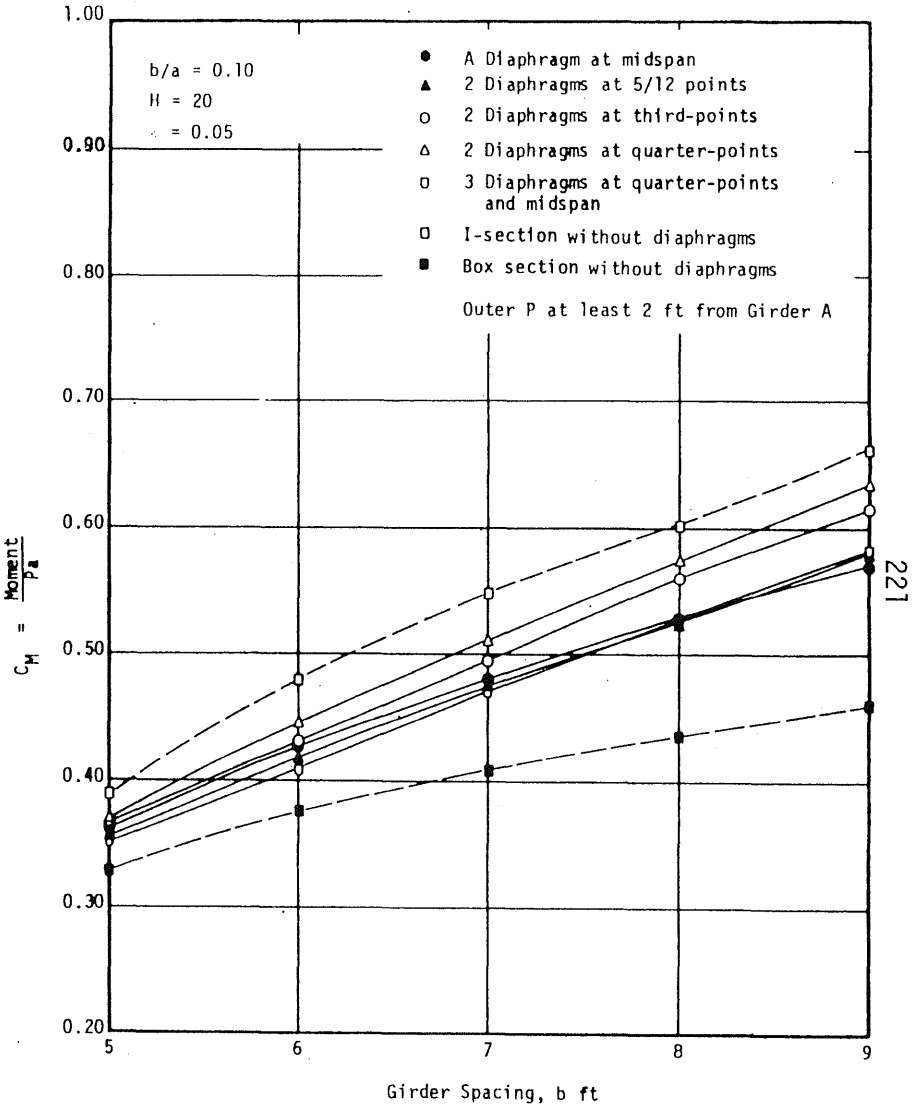

FIG. 5.40 EFFECTS OF DIAPHRAGMS ON MOMENTS IN BRIDGES SUBJECTED TO THREE-AXLE TRUCK LOADINGS

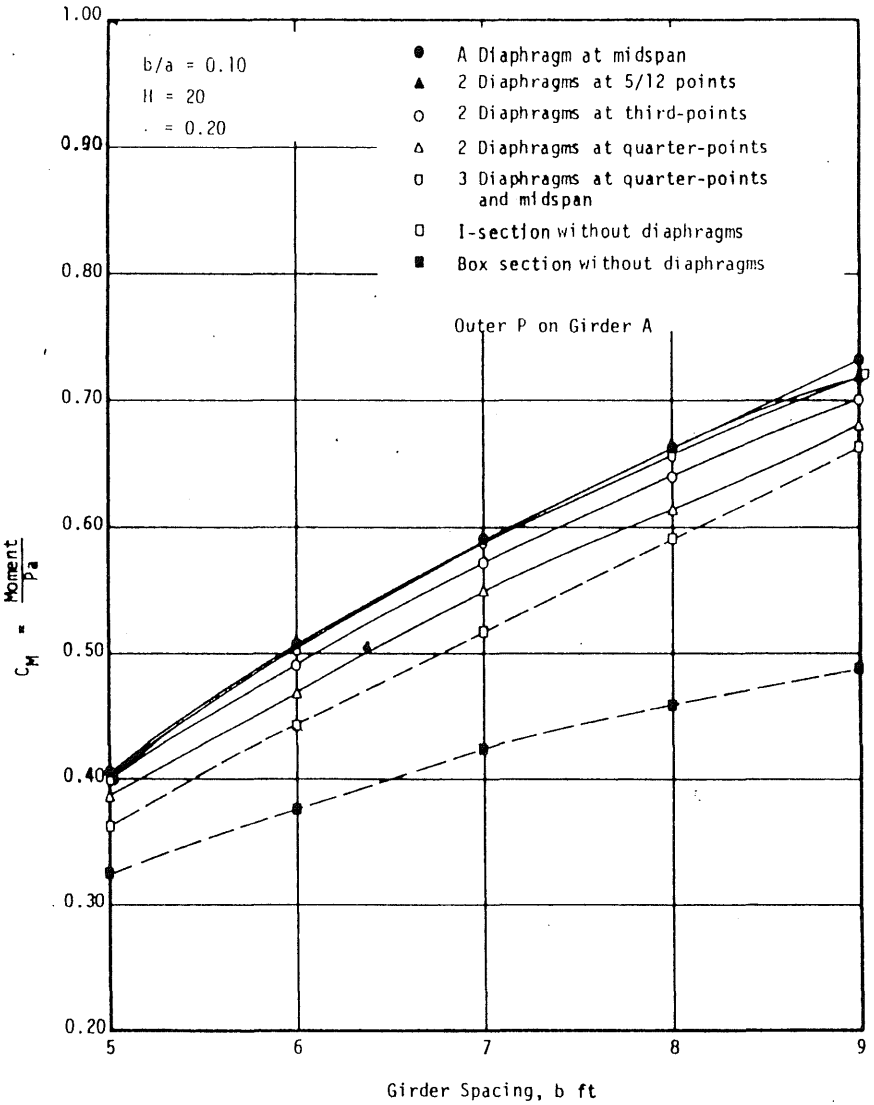
b/a = 0.10
H = 20
= 0.20
A Diaphragm at midspan
2 Diaphragms at 5/12 points
2 Diaphragms at third-points
2 Diaphragms at quarter-points
3 Diaphragms at quarter-points and midspan
I-section without diaphragms
Box section without diaphragms
Outer P on Girder A
$C_M = \frac{\text{Moment}}{Pa}$
1.00
0.90
0.80
0.70
0.60
0.50
0.40
0.30
0.20
5
6
7
8
9
Girder Spacing, b ft

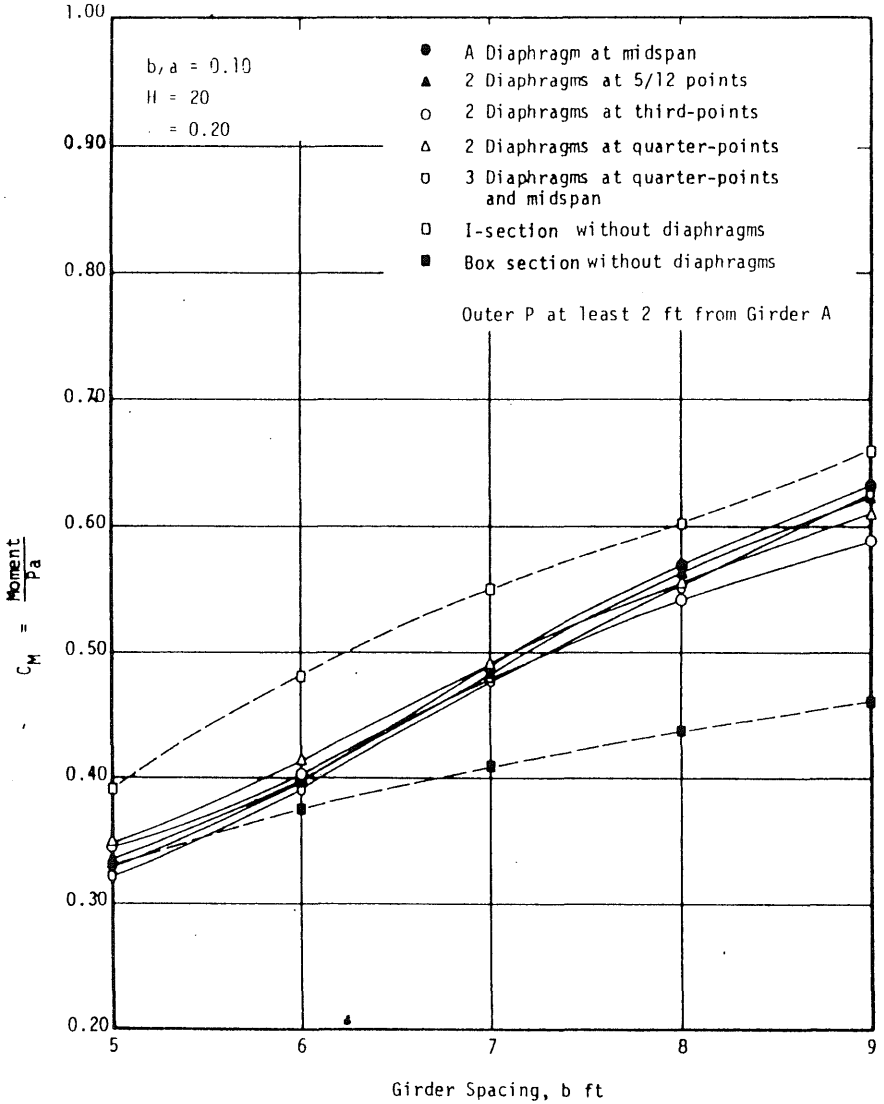
b/a = 0.10
H = 20
= 0.20
A Diaphragm at midspan
2 Diaphragms at 5/12 points
2 Diaphragms at third-points
2 Diaphragms at quarter-points
3 Diaphragms at quarter-points and midspan
I-section without diaphragms
Box section without diaphragms
Outer P at least 2 ft from Girder A
$C_M = \frac{\text{Moment}}{Pa}$
1.00
0.90
0.80
0.70
0.60
0.50
0.40
0.30
0.20
5
6
7
8
9
Girder Spacing, b ft

FIG. 5.40 (Cont.)

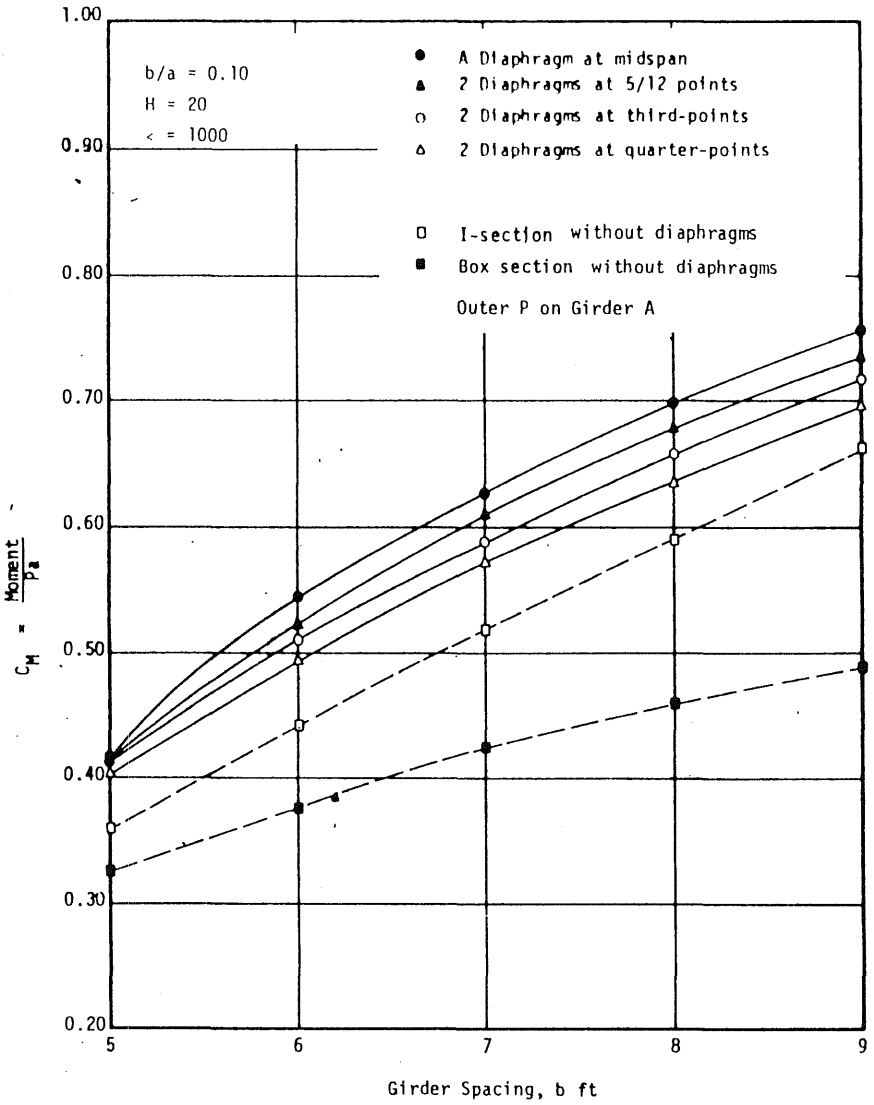
b/a = 0.10
H = 20
< = 1000
A Diaphragm at midspan
2 Diaphragms at 5/12 points
2 Diaphragms at third-points
2 Diaphragms at quarter-points
I-section without diaphragms
Box section without diaphragms
Outer P on Girder A
$C_M = \frac{\text{Moment}}{Pa}$
Girder Spacing, b ft

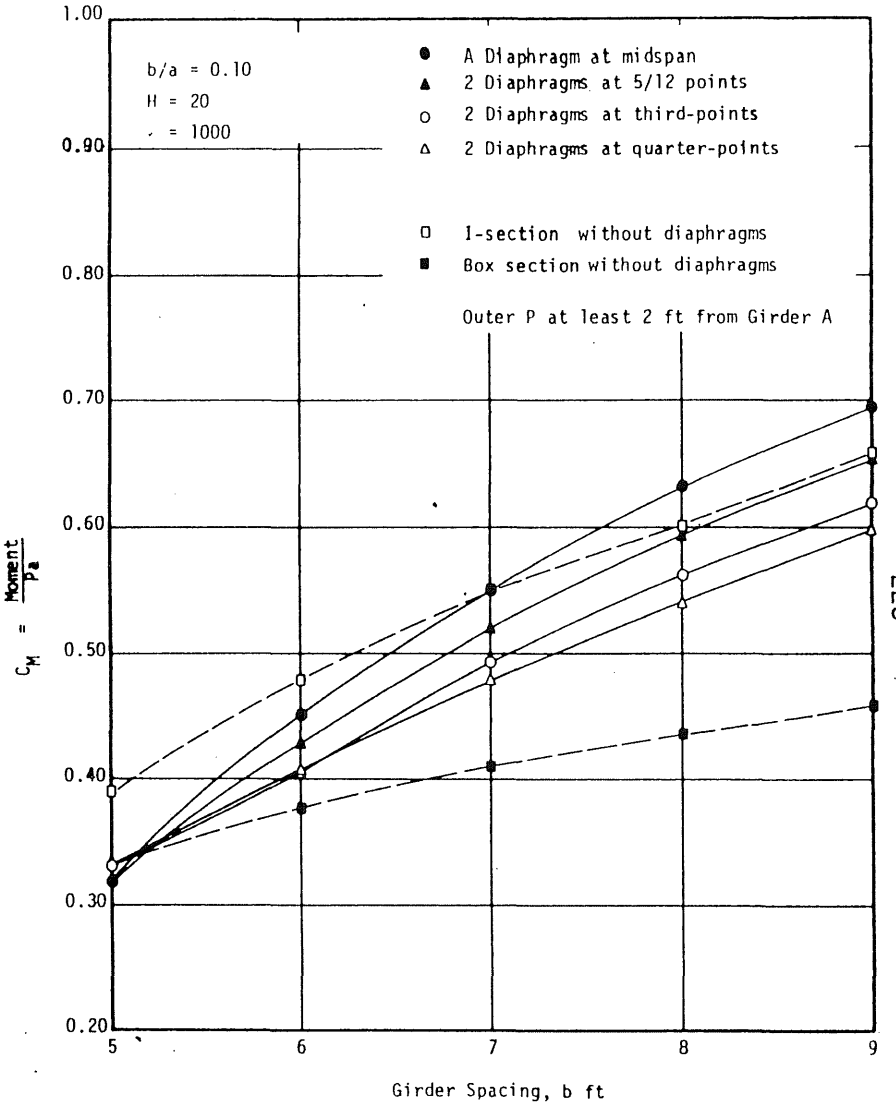
b/a = 0.10
H = 20
= 1000
A Diaphragm at midspan
2 Diaphragms at 5/12 points
2 Diaphragms at third-points
2 Diaphragms at quarter-points
I-section without diaphragms
Box section without diaphragms
Outer P at least 2 ft from Girder A
$C_M = \frac{\text{Moment}}{Pa}$
Girder Spacing, b ft

FIG. 5.40 (Cont.)

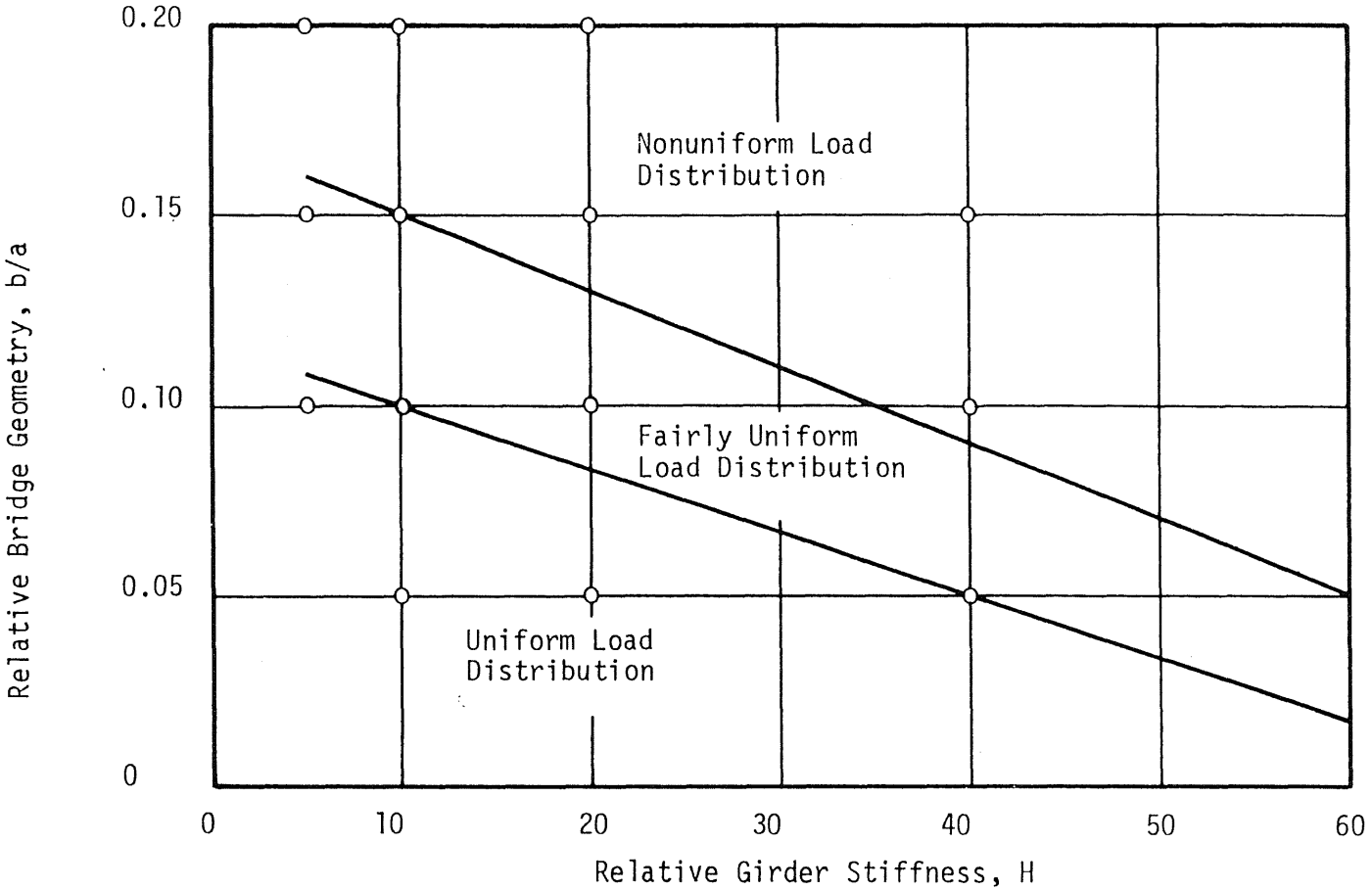

FIG. 6.1 DIAGRAM SHOWING APPROXIMATE CLASSIFICATIONS OF BRIDGES WITH PRESTRESSED CONCRETE I-SECTION GIRDERS

APPENDIX A

SUMMARY OF FUNDAMENTAL RELATIONS OF ORDINARY THEORY OF FLEXURE FOR SLABS AND DERIVATION OF FORMULAS

A.1 Fundamental Relations and Basic Assumptions

The basic assumptions for the ordinary theory of flexure of slabs are:

1. The material in the slab is homogeneous, elastic, and isotropic,
2. The slab is of uniform thickness,
3. The loads applied on the slab are normal to its plane. On any cross section, there is no resultant force in the direction of the plane of the slab, and
4. The flexural strains vary linearly through the depth of the slab.

The derivations of the fundamental equations are available in any books of plate theory. The necessary relations are summarized here.

The fundamental equation for the flexure of slabs is the governing differential equation:

$$\nabla^2(\nabla^2 w) = \frac{\partial^4 w}{\partial x^4} + 2\frac{\partial^4 w}{\partial x^2 \partial y^2} + \frac{\partial^4 w}{\partial y^4} = \frac{p}{D} \qquad (A.1)$$

where

w = slab deflection,

p = applied load, and

D = slab stiffness as given by the expression

$$D = \frac{E_s I_s}{1-\mu^2} = \frac{E_s h^3}{12(1-\mu^2)} \qquad (A.2)$$

where h = slab thickness.

The forces acting on cross-sections of the slab are shown in Fig. 1.4.

The relationships between the bending and twisting moments and the deflections, shears and deflections, and reactions on the edges and deflections, are:

For Moments

$$M_x = -D\left[\frac{\partial^2 w}{\partial x^2} + \mu \frac{\partial^2 w}{\partial y^2}\right]$$

$$M_y = -D\left[\frac{\partial^2 w}{\partial y^2} + \mu \frac{\partial^2 w}{\partial x^2}\right] \qquad \text{(A.3)}$$

$$M_{xy} = -D(1-\mu) \frac{\partial^2 w}{\partial x \partial y}$$

For Shears

$$V_x = -D \frac{\partial}{\partial x}\left[\frac{\partial^2 w}{\partial x^2} + \frac{\partial^2 w}{\partial y^2}\right]$$

$$V_y = -D \frac{\partial}{\partial y}\left[\frac{\partial^2 w}{\partial x^2} + \frac{\partial^2 w}{\partial y^2}\right] \qquad \text{(A.4)}$$

For Reactions

Reaction on an edge normal to the x-axis

$$R_x = -D\left[\frac{\partial^3 w}{\partial x^3} + (2-\mu) \frac{\partial^3 w}{\partial x \partial y^2}\right]$$

and on an edge normal to the y-axis (A.5)

$$R_y = -D\left[\frac{\partial^3 w}{\partial y^3} + (2-\mu) \frac{\partial^3 w}{\partial x^2 \partial y}\right]$$

A.2 General Solution of the Fundamental Equation for Slabs

Under certain conditions mentioned in Section A.1, the fundamental equation of the ordinary theory of flexure for slabs is:

$$\frac{\partial^4 w}{\partial x^4} + 2\frac{\partial^4 w}{\partial x^2 \partial y^2} + \frac{\partial^4 w}{\partial y^4} = \frac{p}{D}$$

The analysis of the slab problems involves the solution of the differential equation A.1 and satisfying the boundary conditions at the same time.

For a slab simply supported on two opposite edges, the solution may be in the form of a series:

$$w = \sum_{m=1}^{\infty} Y_m \sin \frac{m\pi x}{a} \tag{A.6}$$

For a rectangular slab shown in Fig. 3.3, with the sides x = 0 and x = a simply supported and the sides y = 0 and y = c restrained in some arbitrary manner, Eq. A.6 automatically satisfies the boundary condition of the first two sides.

With the notation

$$\alpha_m = \frac{m\pi}{a} \tag{A.7}$$

the slopes, moments, shears, and reactions given in Section A.1 may be written in terms of the deflection of Eq. A.6 and with the notation in A.7 as follows:

Slopes

$$\frac{\partial w}{\partial y} = \alpha_m Y_m' \sin \alpha_m x$$

$$\frac{\partial w}{\partial x} = \alpha_m Y_m \cos \alpha_m x \tag{A.8}$$

Moments

$$M_x = D\alpha_m^2 [Y_m - \mu Y_m''] \sin \alpha_m x$$

$$M_y = D\alpha_m^2 [-Y_m'' + \mu Y_m] \sin \alpha_m x \qquad (A.9)$$

$$M_{xy} = -D\alpha_m^2 (1-\mu) Y_m' \cos \alpha_m x$$

Shears

$$V_x = D\alpha_m^3 [Y_m - Y_m''] \cos \alpha_m x$$

$$V_y = D\alpha_m^3 [Y_m' - Y_m'''] \sin \alpha_m x \qquad (A.10)$$

Reactions

$$R_x = D\alpha_m^3 [Y_m - (2-\mu) Y_m''] \cos \alpha_m x$$

$$R_y = D\alpha_m^3 [(2-\mu) Y_m' - Y_m'''] \sin \alpha_m x \qquad (A.11)$$

Load

$$p = D\alpha_m^4 [Y_m - 2Y_m'' + Y_m''''] \sin \alpha_m x$$

Since the equations for slopes, moments, shears, and reactions all consist of sine curves or cosine curves in the x-direction and Y_m, which is in functions of y only, the solution of the problem lies in the determination of Y_m.

For further simplification of the solution, the deflection w in Eq. A.6 may be stated in two parts:

$$w = w_p + w_c \qquad (A.13)$$

where w_p is the solution for the loading for the particular value of m which satisfies Eq. A.1, but may not satisfy the boundary conditions. On the other hand, the function w_c, which is the complementary solution, does satisfy the boundary conditions without lateral load, i.e., w_c satisfies the differential equation

$$\frac{\partial^4 w_c}{\partial x^4} + 2\frac{\partial^4 w_c}{\partial x^2 \partial y^2} + \frac{\partial^4 w_c}{\partial y^4} = 0 \tag{A.14}$$

Therefore, the summation of these two functions satisfies all of the boundary conditions for the particular value of m.

The solution of Eq. A.14 is the same form as Eq. A.6 and may be written as:

$$w_c = Y_m \sin \alpha_m x \tag{A.15}$$

where Y_m is a function of y only. For a rectangular slab, shown in Fig. 3.3, with two edges parallel to the y-axis simply supported, and the other two restrained in any manner, Eq. A.15 automatically satisfies the boundary conditions of the first two edges. It is necessary to determine Y_m in such a form as to satisfy the boundary conditions of the other two edges.

By substituting the deflection, Eq. A.15, in the differential equation A.14

$$[\alpha_m^4 Y_m - 2\alpha_m^2 Y_m'' + Y_m''''] \sin \alpha_m x = 0 \tag{A.16}$$

the general form of Y_m can be found to be

$$Y_m = A_m \sinh \alpha_m y + B_m \cosh \alpha_m y + C_m \alpha_m y \sinh \alpha_m y + D_m \alpha_m y \cosh \alpha_m y \tag{A.17}$$

The four constants in Eq. A.17 are determined from the boundary conditions at the edges of the slab y = 0 and y = c. Its derivatives are:

$$
\begin{aligned}
Y_m' &= (B_m + C_m)\sinh \alpha_m y + (A_m + D_m)\cosh \alpha_m y + \\
&\quad D_m \alpha_m y \sinh \alpha_m y + C_m \alpha_m y \cosh \alpha_m y \\
Y_m'' &= (A_m + 2D_m)\sinh \alpha_m y + (B_m + 2C_m)\cosh \alpha_m y + \\
&\quad C_m \alpha_m y \sinh \alpha_m y + D_m \alpha_m y \cosh \alpha_m y \\
Y_m''' &= (B_m + 3C_m)\sinh \alpha_m y + (A_m + 3D_m)\cosh \alpha_m y + \\
&\quad D_m \alpha_m y \sinh \alpha_m y + C_m \alpha_m y \cosh \alpha_m y
\end{aligned}
\tag{A.18}
$$

A.3 Formulas for Flexibility Constants for a Panel of Slab

Consider the case of a sine wave of edge reaction acting at the edge y = c of the slab shown in Fig. 3.4, the edge y = 0 remaining free. The cross-section of the slab parallel to the y-axis is shown in Fig. 3.5(a). The boundary conditions for this case may be stated as follows:

At y = 0

$$
\begin{aligned}
R &= -D\left[\frac{\partial^3 w}{\partial y^3} + (2-\mu)\frac{\partial^3 w}{\partial x^2 \partial y}\right] = 0 \\
M &= -D\left[\frac{\partial^2 w}{\partial y^2} + \mu \frac{\partial^2 w}{\partial x^2}\right] = 0
\end{aligned}
\tag{A.19}
$$

At y = c

$$
\begin{aligned}
R &= -D\left[\frac{\partial^3 w}{\partial y^3} + (2-\mu)\frac{\partial^3 w}{\partial x^2 \partial y}\right] = R_{rm} \sin \alpha_m x \\
M &= -D\left[\frac{\partial^2 w}{\partial y^2} + \mu \frac{\partial^2 w}{\partial x^2}\right] = 0
\end{aligned}
\tag{A.20}
$$

Since there is no load on the slab, the complementary solution only is required; i.e., $w_p = 0$ and $w = w_c$.

With these four boundary conditions, the four constants A_m, B_m, C_m, and D_m of Eq. A.17 can be found as follows:

$$A_m = \frac{(1+\mu)}{(1-\mu)} D_m = \frac{(1+\mu)}{D\alpha_m^3}\left[\frac{\beta_m \sinh \beta_m}{(3+\mu)^2 \sinh^2 \beta_m - (1-\mu)^2 \beta_m^2}\right] R_{rm}$$

$$B_m = -\frac{2}{(1-\mu)} C_m = \frac{2}{(1-\mu) D\alpha_m^3}\left[\frac{(3+\mu) \sinh \beta_m + (1-\mu)\beta_m \cosh \beta_m}{(3+\mu)^2 \sinh^2 \beta_m - (1-\mu)^2 \beta_m^2}\right] R_{rm} \quad \text{(A.21)}$$

where

$$\beta_m = \alpha_m c = \frac{m\pi c}{a} \quad \text{(A.22)}$$

Since the deflections, and the slopes in the y-direction, are the function of the sine wave, the general expressions can be obtained by substituting the four constants in Eq. A.21 into Eq. A.17 and the first of Eqs. A.18, and multiplied by $\sin \alpha_m x$. Consequently, the deflections and the rotations at the edges can be determined by substituting the corresponding values of y for each edge. The results are:

At $y = 0$

$$w_1 = F_{rf} R_{rm} \sin \alpha_m x$$

$$\theta_1 = F_{cf} R_{rm} \sin \alpha_m x \quad \text{(A.23)}$$

At $y = c$

$$w_r = F_{rn} R_{rm} \sin \alpha_m x$$

$$\theta_r = F_{cn} R_{rm} \sin \alpha_m x \quad \text{(A.24)}$$

where

$$F_{rf} = \frac{2}{(1-\mu)D\alpha_m^3}\left[\frac{(3+\mu)\sinh\beta_m+(1-\mu)\beta_m\cosh\beta_m}{(3+\mu)^2\sinh^2\beta_m-(1-\mu)^2\beta_m^2}\right]$$

$$F_{cf} = \frac{2}{D\alpha_m^2}\left[\frac{\beta_m\sinh\beta_m}{(3+\mu)^2\sinh^2\beta_m-(1-\mu)^2\beta_m^2}\right]$$

$$F_{rn} = \frac{2}{(1-\mu)D\alpha_m^3}\left[\frac{(3+\mu)\sinh\beta_m\cosh\beta_m+(1-\mu)\beta_m}{(3+\mu)^2\sinh^2\beta_m-(1-\mu)^2\beta_m^2}\right] \qquad (A.25)$$

$$F_{cn} = \frac{1}{(1-\mu)D\alpha_m^2}\left[\frac{(1+\mu)(3+\mu)\sinh^2\beta_m-(1-\mu)^2\beta_m^2}{(3+\mu)^2\sinh^2\beta_m-(1-\mu)^2\beta_m^2}\right]$$

Now consider the case of a sine wave of edge moment acting at the same edge y = c of the slab shown in Fig. 3.4, the edge y = 0 remaining free. The cross section of the slab parallel to the simply supported edges is shown in Fig. 3.5(b). The boundary conditions for this case may be stated as follows:

At y = 0

$$R = -D\left[\frac{\partial^3 w}{\partial y^3} + (2-\mu)\frac{\partial^3 w}{\partial x^2 \partial y}\right] = 0$$
$$M = -D\left[\frac{\partial^2 w}{\partial y^2} + \mu\frac{\partial^2 w}{\partial x^2}\right] = 0 \qquad (A.26)$$

At y = c

$$R = -D\left[\frac{\partial^3 w}{\partial y^3} + (2-\mu)\frac{\partial^3 w}{\partial x^2 \partial y}\right] = 0$$
$$M = -D\left[\frac{\partial^2 w}{\partial y^2} + \mu\frac{\partial^2 w}{\partial x^2}\right] = M_{rm}\sin\alpha_m x \qquad (A.27)$$

Since there is no load on the slab, $w_p = 0$ and $w = w_c$.

The four constants of Eq. A.17 can be found as follows:

$$A_m = \frac{(1+\mu)}{(1-\mu)}D_m = -\frac{(1+\mu)}{(1-\mu)D\alpha_m^2}\left[\frac{(3+\mu)\sinh\beta_m - (1-\mu)\beta_m\cosh\beta_m}{(3+\mu)^2\sinh^2\beta_m - (1-\mu)^2\beta_m^2}\right]M_{rm} \qquad (A.28)$$

$$B_m = -\frac{2}{(1-\mu)}C_m = \frac{2}{D\alpha_m^2}\left[\frac{\beta_m\sinh\beta_m}{(3+\mu)^2\sinh^2\beta_m - (1-\mu)^2\beta_m^2}\right]M_{rm}$$

The deflections and the rotations at the edges can be found from Eqs. A.17, A.18 and the four constants in Eq. A.28 as follows:

At y = 0

$$w_1 = F_{cf}M_{rm}\sin\alpha_m x$$
$$\theta_1 = -F_{mf}M_{rm}\sin\alpha_m x \qquad (A.29)$$

At $y = c$

$$w_r = -F_{cn} M_{rm} \sin \alpha_m x$$
$$\theta_r = -F_{mn} M_{rm} \sin \alpha_m x \qquad \text{(A.30)}$$

where

F_{cf} and F_{cn} are given in Eq. A.25

$$F_{mf} = \frac{2}{(1-\mu)D\alpha_m}\left[\frac{(3+\mu)\sinh \beta_m-(1-\mu)\beta_m \cosh \beta_m}{(3+\mu)^2\sinh^2\beta_m-(1-\mu)^2\beta_m^2}\right]$$
$$F_{mn} = \frac{2}{(1-\mu)D\alpha_m}\left[\frac{(3+\mu)\sinh \beta_m \cosh \beta_m-(1-\mu)\beta_m}{(3+\mu)^2\sinh^2\beta_m-(1-\mu)^2\beta_m^2}\right] \qquad \text{(A.31)}$$

A.4 Formulas for Flexibility Constants Due to A Concentrated Load

It is necessary to determine the displacements at the edge $y = 0$ and $y = c$ for the slab shown in Fig. 3.3 due to a concentrated load P distributed in sine curves in x-direction

$$p = p_m \sin \alpha_m x \qquad \text{(A.32)}$$

on the line $y = y_p$, and

$$p_m = \frac{2P}{a} \sin \alpha_m x_p$$

Since a sine wave of loading produces a sine wave of edge deflection, and also since a sine wave of edge reaction produces a deflection with ordinates varying as a sine wave, Maxwell's theorem of reciprocal deflections can be applied to obtain the edge deflections.

With all quantities given as sine waves in the x-direction, the deflection in the slab on the line $y = y_p$ due to a unit reaction at the center of the edge $y = c$ when edge $y = 0$ is free, is equal to the deflection along the edge $y = c$ due to a unit load applied at the center of the line $y = y_p$.

These reciprocal relations may be written as follows:

$$R_r = R_{rm} \sin \alpha_m x = p = p_m \sin \alpha_m x$$
$$w = w_m \sin \alpha_m x = w_r = w_{rm} \sin \alpha_m x \tag{A.33}$$

The deflection of the slab subjected to the reaction at the edge $y = c$, the edge $y = 0$ remaining free, is treated in Section A.3 of this Appendix. The deflection of the slab due to the reaction

$$R_r = R_m \sin \alpha_m x$$

at the edge $y = c$, can be written in terms of the four constants in Eqs. A.21. With the reciprocal relations given in Eqs. A.33, the deflection at the edge $y = c$ due to this sinusoidal loading on the line $y = y_p$, can be formulated, with the quantity $\gamma_m = \alpha_m y_p$, as follows:

$$w_{rm} = F_{dr}\, p_m \tag{A.34}$$

where

$$F_{dr} = \frac{1}{D\alpha_m^3\{(3+\mu)^2 \sinh^2 \beta_m - (1-\mu)^2 \beta_m^2\}} [\beta_m \sinh \beta_m \{(1+\mu) \sinh \gamma_m + (1-\mu)\gamma_m \cosh \gamma_m\}$$
$$+ \{(3+\mu) \sinh \beta_m + (1-\mu)\beta_m \cosh \beta_m\}$$
$$\{(\frac{2}{1-\mu}) \cosh \gamma_m - \gamma_m \sinh \gamma_m\}] \tag{A.35}$$

The deflection at the edge $y = 0$ due to this load can be stated as follows:

$$w_{1m} = F_{d1}\, p_m \tag{A.36}$$

where F_{dl} can be obtained from substituting $\gamma_m' = \alpha_m(c-y_p)$ for $\quad_m$ in Eq. A.35.

$$F_{dl} = \frac{1}{D\alpha_m^3\{(3+\mu)^2 \sinh^2 \beta_m-(1-\mu)^2\beta_m^2\}}[\beta_m \sinh \beta_m\{(1+\mu) \sinh \gamma_m'+(1-\mu)\gamma_m' \cosh \gamma_m'\}$$
$$+ \{(3+\mu) \sinh \beta_m+(1-\mu)\beta_m \cosh \beta_m\}$$
$$\{(\frac{2}{1-\mu}) \cosh \gamma_m'-\gamma_m' \sinh \gamma_m'\}] \qquad (A.37)$$

In a manner similar to that used to determine the edge deflections, the rotation at the edge y = c of the slab shown in Fig. 3.3 due to a sinusoidal load

$$p = p_m \sin \alpha_m x$$

acting on the line $y = y_p$ is obtained from the case of the slab subjected to a sinusoidal edge moment at the edge y = c, the edge y = 0 remaining free, as treated in Section A.3 of this Appendix. The reciprocal relations of this case may be formulated as follows:

$$M_r = M_{rm} \sin \alpha_m x = -p = -p_m \sin \alpha_m x$$
$$w = w_m \sin \alpha_m x = \theta_r = \theta_{rm} \sin \alpha_m x \qquad (A.38)$$

from which the rotation at the edge y = c can be written as

$$\theta_{rm} = -F_{rr} p_m \qquad (A.39)$$

The minus sign is required by the sign convention.

The flexibility coefficient F_{rr} can be obtained from Eq. A.17 and four constants in Eqs. A.28, and may be formulated as follows:

$$F_{rr} = \frac{1}{D\alpha_m^2\{(3+\mu)^2 \sinh^2 \beta_m-(1-\mu)^2\beta_m^2\}} [\beta_m \sinh \beta_m\{2 \cosh \gamma_m-(1-\mu)\gamma_m \sinh \gamma_m\}$$
$$- \{(3+\mu) \sinh \beta_m-(1-\mu)\beta_m \cosh \beta_m\}$$
$$\{(\frac{1+\mu}{1-\mu}) \sinh \gamma_m - \gamma_m \cosh \gamma_m\}] \qquad (A.40)$$

The rotation at the edge y = 0 due to this load is

$$\theta_{1m} = F_{r1} p_m \qquad (A.41)$$

In a manner similar to that used to determine the edge deflection, the flexibility coefficient F_{r1} can be formulated with the quantity $\gamma_m' = \alpha_m(c-y_p)$ as follows:

$$F_{r1} = \frac{1}{D\alpha_m^2\{(3+\mu)^2 \sinh^2 \beta_m-(1-\mu)^2\beta_m^2\}} [\beta_m \sinh \beta_m\{2 \cosh \gamma_m'-(1-\mu)\gamma_m' \sinh \gamma_m'\}$$
$$- \{(3+\mu) \sinh \beta_m-(1-\mu)\beta_m \cosh \beta_m\}$$
$$\{(\frac{1+\mu}{1-\mu}) \sinh \gamma_m' - \gamma_m' \cosh \gamma_m'] \qquad (A.42)$$

APPENDIX B

SUMMARY OF FUNDAMENTAL RELATIONS OF PLANE STRESS THEORY OF ELASTICITY FOR SLABS AND DERIVATION OF FORMULAS

B.1 Fundamental Relations and Basic Assumptions

The basic assumptions for plane stress theory of elasticity are:

1. The slab is made of isotropic Hookian material,
2. The deformations of the structures are assumed small, and
3. End diaphragms prevent only vertical deflections at edges at x = 0 and x = a (Fig. 3.7).

The derivations of the fundamental equations can be found from any book about the theory of elasticity. The necessary relations, with the absence of body forces and temperature change, are summarized here.

The stresses acting on cross-sections of a slab are shown in Fig. 1.5.

Stress-Strain Relationships

$$\varepsilon_x = \frac{1}{E}[\sigma_x - \mu\sigma_y]$$

$$\varepsilon_y = \frac{1}{E}[\sigma_y - \mu\sigma_x] \qquad \text{(B.1)}$$

$$\gamma_{xy} = \frac{2(1+\mu)}{E}\tau_{xy}$$

Strain-Displacement Relationships

$$\varepsilon_x = \frac{\partial u}{\partial x}$$

$$\varepsilon_y = \frac{\partial v}{\partial y} \qquad \text{(B.2)}$$

$$\gamma_{xy} = \frac{\partial u}{\partial y} + \frac{\partial v}{\partial x}$$

Equilibrium Equations

In the x-direction

$$\frac{\partial \sigma_x}{\partial x} + \frac{\partial \tau_{xy}}{\partial y} = 0 \tag{B.3}$$

In the y-direction

$$\frac{\partial \tau_{xy}}{\partial x} + \frac{\partial \sigma_y}{\partial y} = 0$$

Compatability Equation

In terms of strain

$$\frac{\partial^2 \varepsilon_x}{\partial y^2} + \frac{\partial^2 \varepsilon_y}{\partial x^2} = \frac{\partial^2 \gamma_{xy}}{\partial x \partial y} \tag{B.4}$$

Boundary Conditions

$$\begin{aligned} \overline{X} &= l\sigma_x + m\tau_{xy} \\ \overline{Y} &= m\sigma_y + l\tau_{xy} \end{aligned} \tag{B.5}$$

The solution of the plane stress problem for an elastic slab reduces to the integration of the differential equations (Eq. B.3) and the compatibility equation (Eq. B.4) and satisfying the boundary conditions (Eq. B.5). The usual method of solving these equations is by using the stress function, Φ, which is introduced by G. B. Airy. Consequently, the following relations have been derived in terms of Φ, which is the function of x and y.

Stress-Φ Relationships

$$\sigma_x = \frac{\partial^2 \Phi}{\partial y^2}$$

$$\sigma_y = \frac{\partial^2 \Phi}{\partial x^2} \tag{B.6}$$

$$\tau_{xy} = -\frac{\partial^2 \Phi}{\partial x \partial y}$$

Strain-Displacement-Φ Relationships

$$\varepsilon_x = \frac{\partial u}{\partial x} = \frac{1}{E}\left[\frac{\partial^2 \Phi}{\partial y^2} - \mu \frac{\partial^2 \Phi}{\partial x^2}\right]$$

$$\varepsilon_y = \frac{\partial v}{\partial y} = \frac{1}{E}\left[\frac{\partial^2 \Phi}{\partial x^2} - \mu \frac{\partial^2 \Phi}{\partial y^2}\right] \tag{B.7}$$

$$\gamma_{xy} = \frac{\partial u}{\partial y} + \frac{\partial v}{\partial x} = \frac{-2(1+\mu)}{E} \frac{\partial^2 \Phi}{\partial x \partial y}$$

Compatibility Equation

$$\frac{\partial^4 \Phi}{\partial x^4} + 2 \frac{\partial^4 \Phi}{\partial x^2 \partial y^2} + \frac{\partial^4 \Phi}{\partial y^4} = 0 \tag{B.8}$$

B.2 General Solution of the Plane Stress for the Elastic Slab

Since the stress function, Φ, has the relations stated in Eq. B.6, it automatically satisfies the differential equations of equilibrium (Eq. B.3). Thus, the problem of the plane stress of the elastic slab is reduced to the solution of the differential equation of compatibility (Eq. B.8), which satisfies the boundary conditions (Eq. B.5).

It is noted that the differential equation of compatibility (Eq. B.8) is identical to the fundamental differential equation (Eq. A.14) of the ordinary theory of flexure of the slab with no load on it. Consequently, the solution of Eq. B.8 can be written in a form similar to Eq. A.15

$$\Phi = \Phi_m \sin \alpha_m x \tag{B.9}$$

where α_m is a function of y only, and $\alpha_m = \frac{m\pi}{a}$.

In the case of the rectangular slab with the coordinate axes taken parallel to the edges of the slab, the boundary conditions in Eq. B.5 can be simplified. For this particular problem, the span of the slab is in the direction of x-axis so that the normal $\overline{N}$ in Fig. 1.6 is parallel to the y-axis, hence the direction cosines, $l = 0$ and $m = \pm 1$. Equation B.5 then becomes

$$\begin{aligned} \overline{X} &= \pm\tau_{xy} \\ \overline{Y} &= \pm\sigma_y \end{aligned} \tag{B.10}$$

The positive signs of Eq. B.10 are taken when the normal $\overline{N}$ is in the positive direction of the y-axis and the negative signs for the opposite direction of $\overline{N}$.

The stresses, strains, and displacements in Section B.1 can be written in the following forms:

Stresses

$$\begin{aligned} \sigma_x &= \alpha_m^2 \Phi_m'' \sin \alpha_m x \\ \sigma_y &= -\alpha_m^2 \Phi_m \sin \alpha_m x \\ \tau_{xy} &= -\alpha_m^2 \Phi_m' \cos \alpha_m x \end{aligned} \tag{B.11}$$

Strains

$$\varepsilon_x = \frac{\alpha_m^2}{E} [\Phi_m'' + \mu\Phi_m] \sin \alpha_m x$$

$$\varepsilon_y = -\frac{\alpha_m^2}{E}\left[\Phi_m + \mu\,\Phi_m''\right]\sin\alpha_m x \qquad (B.12)$$

$$\gamma_{xy} = \frac{-2(1+\mu)}{E}\,\alpha_m^2\,\Phi_m'\cos\alpha_m x$$

Displacements

$$u = -\frac{\alpha_m}{E}\left[\Phi_m'' + \mu\,\Phi_m\right]\cos\alpha_m x + f_1(y)$$
$$v = -\frac{\alpha_m}{E}\left[\int\Phi_m\,dy + \mu\,\Phi_m'\right]\sin\alpha_m x + f_2(x) \qquad (B.13)$$

It is noted that, in a rectangular slab with two opposite edges parallel to the y-axis simply supported, the functions $f_1(y)$ and $f_2(x)$ are zero.

The equations for the displacements for this particular slab can be reduced to

$$u = -\frac{\alpha_m}{E}\left[\Phi_m'' + \mu\Phi_m\right]\cos\alpha_m x$$
$$v = -\frac{\alpha_m}{E}\left[\int\Phi_m\,dy + \mu\,\Phi_m'\right]\sin\alpha_m x \qquad (B.14)$$

The function Φ_m can be obtained in the same manner as the function Y_m in Section A. 2 of Appendix A. It may be stated as follows:

$$\Phi_m = a_m \sinh\alpha_m y + b_m \cosh\alpha_m y + c_m\alpha_m y \sinh\alpha_m y + d_m\alpha_m y \cosh\alpha_m y \qquad (B.15)$$

The four constants a_m, b_m, c_m, and d_m, in Eq. B.15 are determined from the four boundary conditions at the edges y = 0, and y = c. The derivatives of Φ_m are:

$$\Phi_m' = (b_m+c_m) \sinh \alpha_m y + (a_m+d_m) \cosh \alpha_m y + d_m \alpha_m y \sinh \alpha_m y + c_m \alpha_m y \cosh \alpha_m y$$

$$\Phi_m'' = (a_m+2d_m) \sinh \alpha_m y + (b_m+2c_m) \cosh \alpha_m y + c_m \alpha_m y \sinh \alpha_m y + d_m \alpha_m y \cosh \alpha_m y \tag{B.16}$$

$$\Phi_m''' = (b_m+3c_m) \sinh \alpha_m y + (a_m+3d_m) \cosh \alpha_m y + d_m \alpha_m y \sinh \alpha_m y + c_m \alpha_m y \cosh \alpha_m y$$

B.3 Formulas for Flexibility Constants for a Panel of Slab Due to In-Plane Forces

Consider the case of a sine wave of the in-plane edge force, N_r, applied at the edge y = c of the slab shown in Fig. 3.6, the edge y = 0 remaining free. A portion of the slab in the x-y plane is shown in Fig. 3.7(a). The boundary conditions for this case may be stated as follows:

At y = 0

$$\begin{aligned} \tau_{xy} &= 0 \; ; \quad -\alpha_m^2 \Phi_m' \cos \alpha_m x = 0 \; ; \quad \Phi_m' = 0 \\ \sigma_y &= 0 \; ; \quad -\alpha_m^2 \Phi_m \sin \alpha_m x = 0 \; ; \quad \Phi_m = 0 \end{aligned} \tag{B.17}$$

At y = c

$$\begin{aligned} \tau_{xy} &= 0 \; ; \quad -\alpha_m^2 \Phi_m' \cos \alpha_m x = 0 \; ; \quad \Phi_m' = 0 \\ \sigma_y &= N_r/h \; ; \quad -\alpha_m^2 \Phi_m \sin \alpha_m x = \frac{N_{rm}}{h} \sin \alpha_m x \end{aligned} \tag{B.18}$$

With these four boundary conditions, the four constants, a_m, b_m, c_m, and d_m, of Eq. B.15 can be found as follows:

$$a_m = -d_m = -\frac{1}{\alpha_m^2 h}\left[\frac{\sinh \beta_m + \beta_m \cosh \beta_m}{\sinh^2 \beta_m - \beta_m^2}\right] N_{rm}$$

$$b_m = 0 \qquad \text{(B.19)}$$

$$c_m = -\frac{1}{\alpha_m^2 h}\left[\frac{\beta_m \sinh \beta_m}{\sinh^2 \beta_m - \beta_m^2}\right] N_{rm}$$

where

$$\beta_m = \alpha_m c$$

The general expressions for the in-plane displacements u and v can be obtained by substituting the four constants in Eq. B.19 into Eqs. B.15 and B.16, then the results into Eq. B.14. Consequently, the displacements at the edges are determined by the substitution of the corresponding values of y for each edge. The results are:

At y = c

$$u_r = -F_{kn} N_{rm} \cos \alpha_m x$$

$$v_r = F_{nn} N_{rm} \sin \alpha_m x \qquad \text{(B.20)}$$

At y = 0

$$u_1 = F_{kf} N_{rm} \cos \alpha_m x$$

$$v_1 = F_{nf} N_{rm} \sin \alpha_m x \qquad \text{(B.21)}$$

where

$$F_{kn} = \frac{1}{E\alpha_m h}\left[\frac{(1-\mu) \sinh^2 \beta_m + (1+\mu) \beta_m^2}{\sinh^2 \beta_m - \beta_m^2}\right]$$

$$F_{nn} = \frac{2}{E\alpha_m h}\left[\frac{\sinh \beta_m \cosh \beta_m + \beta_m}{\sinh^2 \beta_m - \beta_m^2}\right] \qquad \text{(B.22)}$$

$$F_{kf} = \frac{2}{E\alpha_m h}\left[\frac{\beta_m \sinh \beta_m}{\sinh^2 \beta_m - \beta_m^2}\right]$$
$$F_{nf} = \frac{2}{E\alpha_m h}\left[\frac{\sinh \beta_m + \beta_m \cosh \beta_m}{\sinh^2 \beta_m - \beta_m^2}\right] \qquad (B.22)$$

Now consider the case of a cosine wave of in-plane edge shear, S_r, applied at the edge r, y = c, of the slab shown in Fig. 3.6, with the edge 1, y = 0, remaining free. A portion of the slab in the x-y plane is shown in Fig. 3.7(b). The boundary conditions for this case are:

At y = 0

$$\tau_{xy} = 0 ; \qquad -\alpha_m^2 \Phi_m' \cos \alpha_m x = 0 ; \qquad \Phi_m' = 0$$
$$\sigma_y = 0 ; \qquad -\alpha_m^2 \Phi_m \sin \alpha_m x = 0 ; \qquad \Phi_m = 0 \qquad (B.23)$$

At y = c

$$\tau_{xy} = S_r/h; \qquad -\alpha_m^2 \Phi_m' \cos \alpha_m x = \frac{S_{rm}}{h} \cos \alpha_m x$$
$$\sigma_y = 0 ; \qquad -\alpha_m^2 \Phi_m \sin \alpha_m x = 0; \qquad \Phi_m = 0 \qquad (B.24)$$

The four constants in Eq. B.15 can be found from the four boundary conditions in Eqs. B.23 and B.24, and may be stated as follows:

$$a_m = -d_m = \frac{1}{\alpha_m^2 h}\left[\frac{\beta_m \sinh \beta_m}{\sinh^2 \beta_m - \beta_m^2}\right]$$
$$b_m = 0 \qquad (B.25)$$
$$c_m = -\frac{1}{\alpha_m^2 h}\left[\frac{\sinh \beta_m - \beta_m \cosh \beta_m}{\sinh^2 \beta_m - \beta_m^2}\right]$$

And the in-plane displacements, u, v, at the edges are:

At y = c

$$u_r = F_{sn} S_{rm} \cos \alpha_m x$$
$$v_r = -F_{kn} S_{rm} \sin \alpha_m x \qquad (B.26)$$

At y = 0

$$u_1 = F_{sf} S_{rm} \cos \alpha_m x$$
$$v_1 = -F_{kf} S_{rm} \sin \alpha_m x \qquad (B.27)$$

where

$$F_{sn} = \frac{2}{E\alpha_m h}\left[\frac{\sinh \beta_m \cosh \beta_m - \beta_m}{\sinh^2 \beta_m - \beta_m^2}\right]$$
$$F_{sf} = \frac{2}{E\alpha_m h}\left[\frac{\sinh \beta_m - \beta_m \cosh \beta_m}{\sinh^2 \beta_m - \beta_m^2}\right] \qquad (B.28)$$

The expressions for F_{kn} and F_{kf} are the same as Eq. B.22. The minus sign is taken into account the sign conventions.

B.4 Flexibility Matrix Formulations for a Slab Panel

The flexibility constants of the deflections and slopes at the edge l and the edge r of the slab shown in Fig. 3.3, due to the edge reactions, the edge moments and the loading, were obtained by the ordinary theory of flexure for slab, as presented in Sections A.3 and A.4 of Appendix A. The flexibility constants of the in-plane displacements, u and v, at the edges of the slab due to the in-plane edge forces, as shown in Fig. 3.6, were

obtained by the plane stress theory of elasticity, as presented in Section B.3 of this appendix. The total results for each displacement due to the edge forces and loading can be determined by summing the displacement produced by each force. The flexibility constants may be presented in the matrix forms. The general equations for the edge displacements may be stated as follows:

At left edge, l

$$\begin{aligned} w_{LS} &= w_{Lm} \sin \alpha_m x \\ \theta_{LS} &= \theta_{Lm} \sin \alpha_m x \\ v_{LS} &= v_{Lm} \sin \alpha_m x \\ u_{LS} &= u_{Lm} \cos \alpha_m x \end{aligned} \tag{B.29}$$

At right edge, r

$$\begin{aligned} w_{RS} &= w_{Rm} \sin \alpha_m x \\ \theta_{RS} &= \theta_{Rm} \sin \alpha_m x \\ v_{RS} &= v_{Rm} \sin \alpha_m x \\ u_{RS} &= u_{Rm} \cos \alpha_m x \end{aligned} \tag{B.30}$$

These displacements at the edges and the edge forces may be stated in column matrices W_S and N_E, respectively. Thus,

$$W_S = \left\{ \begin{matrix} w_{Lm} \\ \theta_{Lm} \\ v_{Lm} \\ u_{Lm} \\ w_{Rm} \\ \theta_{Lm} \\ v_{Rm} \\ u_{Rm} \end{matrix} \right\}_{8 \times 1} \quad \text{and} \quad N_E = \left\{ \begin{matrix} R_{lm} \\ M_{lm} \\ N_{lm} \\ S_{lm} \\ R_{rm} \\ M_{rm} \\ N_{rm} \\ S_{rm} \end{matrix} \right\}_{8 \times 1} \tag{B.31}$$

The flexibility constants due to the unknown edge forces may be formulated in the matrix F_S, and the flexibility constants due to loading may be formulated in the column matrix, L_S. Thus,

$$F_S = \left[\begin{array}{cccc|cccc} -F_{rn} & -F_{cn} & 0 & 0 & F_{rf} & F_{cf} & 0 & 0 \\ F_{cn} & F_{mn} & 0 & 0 & F_{cf} & -F_{mf} & 0 & 0 \\ 0 & 0 & -F_{nn} & -F_{kn} & 0 & 0 & F_{nf} & -F_{kf} \\ 0 & 0 & -F_{kn} & -F_{sn} & 0 & 0 & F_{kf} & F_{sf} \\ \hline -F_{rf} & F_{cf} & 0 & 0 & F_{rn} & -F_{cn} & 0 & 0 \\ F_{cf} & F_{mf} & 0 & 0 & F_{cn} & -F_{mn} & 0 & 0 \\ 0 & 0 & -F_{nf} & -F_{kf} & 0 & 0 & F_{nn} & -F_{kn} \\ 0 & 0 & F_{kf} & -F_{sf} & 0 & 0 & -F_{kn} & F_{sn} \end{array}\right]_{8 \times 8} \tag{B.32}$$

Where the elements in the matrix were presented in the appendix as follows: F_{rn}, F_{rf}, F_{cn} and F_{cf} in Eq. A.25 of Appendix A; F_{mn}, F_{mf} in Eq. A.31 of Appendix A; F_{nn}, F_{nf}, F_{kn} and F_{kf} in Eq. B.22 of Appendix B; F_{sn} and F_{sf} in Eq. B.28 of Appendix B.

The flexibility matrix, F_S, may be partitioned into submatrices as follows:

$$F_S = \left[\begin{array}{c|c} F_{ll} & F_{lr} \\ \hline F_{rl} & F_{rr} \end{array}\right] \qquad (B.33)$$

The submatrix, F_{ll}, is the flexibility matrix of the left edge, l, of the slab due to forces acting on the left edge, and the submatrix, F_{lr}, is the flexibility matrix of the left edge due to forces acting on the right edge, r. On the other hand, the submatrix, F_{rl}, contains the flexibility constants of the right edge of the slab due to forces acting on the left edge, and the submatrix, F_{rr}, contains the flexibility constants of the right edge due to forces acting on the right edge of the slab.

$$L_S = \left\{\begin{array}{c} F_{dl} \\ F_{rl} \\ 0 \\ 0 \\ F_{dr} \\ F_{rr} \\ 0 \\ 0 \end{array}\right\}_{8 \times 1} \qquad (B.34)$$

The elements, F_{dl}, F_{rl}, F_{dr} and F_{rr} were given by Eqs. A.37, A.42, A.35 and A.40 of Appendix A.

The relationship between the displacements, edge forces, and applied loads may be written in the matrix forms as follows:

$$W_S = F_S N_E + pL_S \tag{B.35}$$

APPENDIX C

SUMMARY OF FUNDAMENTAL THEORIES OF AXIAL, BIAXIAL AND TORSIONAL BENDING OF BEAMS AND DERIVATION OF FORMULAS

C.1 Basic Assumptions

1. The material is homogeneous, elastic, and isotropic;
2. Stress varies linearly as strain;
3. The shear deformations and distortion of the cross-section are negligible; and
4. The girder is of uniform stiffness.

C.2 Internal and External Force Relationships

The girder is subjected to the transverse loading as well as the edge forces at the mid-depth of the slab and a moment about an axis parallel to the x-axis and passing through the shear center of the cross-section, S. A small element of the girder is shown in Fig. 3.8, with the x-axis parallel to the span length and through the centroid, O, of the cross-section. The y-axis is parallel to the simple supports and the z-axis is pointed downward. The positive directions of coordinates are shown in Fig. 3.8. The right-hand rules are used in this analysis.

The edge forces are R_l, M_l, N_l and S_l, with the magnitudes given by Eqs. 3.10 and 3.25, acting at the edge l; and R_r, M_r, N_r and S_r, with the magnitudes given by Eqs. 3.9 and 3.24, acting at the edge r. The magnitude of the load is given by Eq. 3.4, and the concentrated moment due to the diaphragm is given by

$$m_t = M_{dm} \sin \alpha_m x \qquad (C.1)$$

where

$$M_{dm} = \frac{2M_d}{a} \sin \frac{m\pi x_d}{a} \qquad (C.2)$$

in which M_d is the moment due to the diaphragm, with its coordinate in the direction of x-axis designated as x_d.

The positive directions of the load and external forces are shown in Fig. 3.8. The distances from the mid-depth of the slab to the centroid and the shear center are designated as h_o and h_s, respectively. The y- and z-coordinates of the shear center is y_s and z_s, and y_l and y_r are the y-coordinates of edge l and r, respectively.

The internal forces of the element may be resolved into six components. Three of them are forces, namely, F_x, F_y and F_z, in the directions of x-, y- and z-axes, respectively. The other three components are moments, namely, M_x, M_y and M_z, about x-, y- and z-axes, respectively. The positive directions of these internal forces are shown in Fig. 3.8.

The analysis is derived for the general case in which the cross-section of the girder may not be symmetrical. For example, the exterior girders, with the sidewalk taken into consideration, are not symmetrical about either axis. Since the girder is subjected to twisting moment about the axis through the shear center, the problem may be simplified by considering the axial force, F_x, and the bending moments, M_y and M_z, to be acting at the centroid, O, and the shearing forces F_y and F_z, and the twisting moment, M_x, to be acting at the shear center, S.

Consider the equilibrium of the element shown in Fig. 3.8. Six equilibrium differential equations are obtained in relating the internal forces to the external forces and loading. The first three equations are

obtained from the summation of forces in the directions of each axis equal to zero. The results are as follows:

$$\begin{aligned}
\frac{\partial F_x}{\partial x} &= (S_{lm} - S_{rm}) \cos \alpha_m x \\
\frac{\partial F_y}{\partial x} &= (N_{lm} - N_{rm}) \sin \alpha_m x \\
\frac{\partial F_z}{\partial x} &= (R_{lm} - R_{rm} - p_m) \sin \alpha_m x
\end{aligned} \tag{C.3}$$

The other three equations are obtained from the summation of the moments about each axis equal to zero. The results are as follows:

$$\begin{aligned}
\frac{\partial M_x}{\partial x} &= [(y_l - y_s)R_{lm} - M_{lm} + h_s N_{lm} - (y_r - y_s)R_{rm} + M_{rm} - \\
&\qquad h_s N_{rm} - (y_p - y_s)p_m - M_{dm}] \sin \alpha_m x \\
\frac{\partial M_y}{\partial x} &= h_o (S_{rm} - S_{lm}) \cos \alpha_m x + F_z \\
\frac{\partial M_z}{\partial x} &= (y_r S_{rm} - y_l S_{lm}) \cos \alpha_m x - F_y
\end{aligned} \tag{C.4}$$

By integrating Eqs. C.3 and C.4, the results are as follows:

$$\begin{aligned}
F_x &= \frac{1}{\alpha_m} (S_{lm} - S_{rm}) \sin \alpha_m x + c_1 \\
F_y &= \frac{1}{\alpha_m} (N_{rm} - N_{lm}) \cos \alpha_m x + c_2 \\
F_z &= \frac{1}{\alpha_m} (R_{rm} - R_{lm} + p_m) \cos \alpha_m x + c_3 \\
M_x &= \frac{1}{\alpha_m} M_T \cos \alpha_m x + c_4 \\
M_y &= \frac{1}{\alpha_m^2} (-R_{lm} - \alpha_m h_o S_{lm} + R_{rm} + \alpha_m h_o S_{rm} + p_m) \\
&\qquad \sin \alpha_m x + c_3 x + c_5
\end{aligned} \tag{C.5}$$

$$M_z = \frac{1}{\alpha_m^2}(N_{1m} - \alpha_m y_1 S_{1m} - N_{rm} + \alpha_m y_r S_{rm})$$

$$\sin \alpha_m x + c_2 x + c_6$$

where

$$M_T = [-(y_1-y_s)R_{1m} + M_{1m} - h_s N_{1m} + (y_r-y_s)R_{rm} -$$

$$M_{rm} + h_s N_{rm} + (y_p-y_s)p_m + M_{dm}] \qquad (C.6)$$

All constants in Eq. 3.5, except c_4, can be found from the boundary conditions as follows:

At x = 0 and x = a

$$F_x = M_y = M_z = 0$$

Thus,

$$c_1 = c_2 = c_3 = c_5 = c_6 = 0$$

The constant c_4 in the fourth of Eq. C.5 has to be determined from the boundary condition that the angles of twist at the supports are zero. The relation between the angle of twist and the torsional moment is stated by Timoshenko[23] in the form of a differential equation as follows:

$$M_x = GJ\frac{\partial \beta}{\partial x} - EC\frac{\partial^3 \beta}{\partial x^3} \qquad (C.7)$$

where

β = angle of twist

E = modulus of elasticity

G = shearing modulus of elastitiy

J = torsion constant

C = warping constant

Substitute the expression for M_x from Eq. C.5 into Eq. C.7 and differentiate with respect to x. The equation may be written as follows:

$$\frac{\partial^4 \beta}{\partial x^4} - \frac{GJ}{EC} \frac{\partial^2 \beta}{\partial x^2} = \frac{M_T}{EC} \sin \alpha_m x \tag{C.8}$$

The angle of twist, β, in Eq. C.8, may be stated in two parts

$$\beta = \beta_p + \beta_c \tag{C.9}$$

where β_p is the particular solution taking into account the loading, and β_c is the complementary solution taking into account the boundary conditions. The function, β_p, satisfies Eq. C.8, but may not satisfy the boundary conditions. The function, β_c, satisfies the differential equation:

$$\frac{\partial^4 \beta_c}{\partial x^4} - \frac{GJ}{EC} \frac{\partial^2 \beta_c}{\partial x^2} = 0 \tag{C.10}$$

The summation of β_c and β_p satisfies all the boundary conditions for a particular loading.

The solution of Eq. C.10 with the quantity $k = \frac{GJ}{EC}$, may be stated as follows:

$$\beta_c = A_1 \sinh kx + A_2 \cosh kx + A_3 x + A_4 \tag{C.11}$$

The constants, A_1, A_2, A_3 and A_4, can be obtained from the boundary conditions.

The particular solution, β_p, of Eq. C.8 may be stated as follows:

$$\beta_p = \frac{M_T}{(\alpha_m^4 EC + \alpha_m^2 GJ)} \sin \alpha_m x \tag{C.12}$$

$$\beta = \frac{M_T}{(\alpha_m^4 EC + \alpha_m^2 GJ)} \sin \alpha_m x + A_1 \sinh kx + A_2 \cosh kx + A_3 x + A_4 \qquad (C.13)$$

Consider the case of a girder in which cross-sections at the supports are prevented from twisting and in which the two flanges at the supports are free to rotate in their own planes. The boundary conditions of this girder may be stated as follows:

At $x = 0$ and $x = a$

$$\beta = 0 \quad \text{and} \quad \beta'' = 0$$

With these four boundary conditions, the four constants in Eq. C.13 are obtained. All constants are equal to zero.

$$A_1 = A_2 = A_3 = A_4 = 0$$

Thus, the final solution is

$$\beta = \frac{M_T}{(\alpha_m^4 EC + \alpha_m^2 GJ)} \sin \alpha_m x \qquad (C.14)$$

The twisting moment, M_x, can be obtained by substituting the functions, β, from Eq. C.14 into Eq. C.7.

The expressions for the internal forces and moments of the girder, with the cross-section shown in Fig. 3.8, can be summarized as follows:

Forces

$$F_x = F_{xm} \sin \alpha_m x$$

$$F_y = F_{ym} \cos \alpha_m x \qquad \text{(C.15)}$$

$$F_z = F_{zm} \cos \alpha_m x$$

Moments

$$M_x = M_{xm} \cos \alpha_m x$$

$$M_y = M_{ym} \sin \alpha_m x \qquad \text{(C.16)}$$

$$M_z = M_{zm} \sin \alpha_m x$$

in which

$$F_{xm} = \frac{1}{\alpha_m} (S_{lm} - S_{rm})$$

$$F_{ym} = \frac{1}{\alpha_m} (-N_{lm} + N_{rm}) \qquad \text{(C.17)}$$

$$F_{zm} = \frac{1}{\alpha_m} (-R_{lm} + R_{rm} + p_m)$$

$$M_{xm} = \frac{1}{\alpha_m} M_T$$

$$= \frac{1}{\alpha_m} [-(y_l - y_s)R_{lm} + M_{lm} + (y_r - y_s)R_{rm} - M_{rm} + (y_p - y_s)p_m + M_{dm}]$$

$$+ F_{ym} h_s$$

$$M_{ym} = \frac{1}{\alpha_m^2} (-R_{lm} - \alpha_m h_o S_{lm} + R_{rm} + \alpha_m h_o S_{rm} + p_m) \qquad \text{(C.18)}$$

$$= \frac{1}{\alpha_m} F_{zm} - F_{xm} h_o$$

$$M_{zm} = \frac{1}{\alpha_m^2} (N_{lm} - \alpha_m y_l S_{lm} - N_{rm} + \alpha_m y_r S_{rm})$$

C.3 Forces and Displacements Relationships

Consider the girder with the axial force F_x and bending moments M_y and M_z acting at the centroid O. The general expression for the axial stress at any point of the cross-section, with coordinates y and z, may be stated as follows:

$$\sigma_x = \frac{F_x}{A} + \frac{(M_y + M_z I_{yz}/I_z)z}{I_{my}} - \frac{(M_z + M_y I_{yz}/I_y)y}{I_{mz}} \qquad (C.19)$$

where

σ_x = axial stress in the x-axis at any point y, z

A = cross-sectional area

M_y = bending moment about y-axis

M_z = bending moment about z-axis

I_{my} = modified moment of inertia about y-axis

I_{mz} = modified moment of inertia about z-axis

In biaxial bending, the relations between moments and curvatures may be written as follows:

$$M_y = \frac{EI_y}{\rho_z} - \frac{EI_{yz}}{\rho_y}$$
$$M_z = \frac{EI_z}{\rho_y} - \frac{EI_{yz}}{\rho_z} \qquad (C.20)$$

And the modified moments of inertia are

$$I_{my} = I_y - \frac{I_{yz}^2}{I_z}$$
$$I_{mz} = I_z - \frac{I_{yz}^2}{I_y} \qquad (C.21)$$
$$I_{mo} = \frac{I_y I_z}{I_{yz}} - I_{yz}$$

where

$\frac{1}{\rho_z}$ = curvature in the z-direction

$\frac{1}{\rho_y}$ = curvature in the y-sirection

I_y = moment of inertia about y-axis

I_z = moment of inertia about z-axis

I_{yz} = product of inertia about y- and z-axes.

Equation C.20 may be written with the sign conventions in Fig. 3.8 as follows:

$$M_y = - EI_y \frac{\partial^2 w}{\partial x^2} - EI_{yz} \frac{\partial^2 v}{\partial x^2}$$

$$M_z = EI_z \frac{\partial^2 v}{\partial x^2} + EI_{yz} \frac{\partial^2 w}{\partial x^2} \qquad \text{(C.22)}$$

From Eq. C.22, the curvatures $\frac{\partial^2 w}{\partial x^2}$ and $\frac{\partial^2 v}{\partial x^2}$ may be obtained as follows:

$$\frac{\partial^2 w}{\partial x^2} = - \frac{1}{E} \left(\frac{M_y}{I_{my}} + \frac{M_z}{I_{mo}} \right)$$

$$\frac{\partial^2 v}{\partial x^2} = \frac{1}{E} \left(\frac{M_y}{I_{mo}} + \frac{M_z}{I_{mz}} \right) \qquad \text{(C.23)}$$

Since the girder is also subjected to the twisting moment M_x about the shear center S, the displacement at any point on the cross section, except the shear center S, are affected by M_x. However, Eq. C.23 gives the displacement of the shear center even though the girder is subjected to the twisting moment.

Let w_s and v_s be the displacements w and v of the shear center. With the Eq. C.16 for M_y and M_z, the curvatures for the shear center can be given as follows:

$$\begin{aligned} \frac{\partial^2 w_s}{\partial x^2} &= -\frac{1}{E}\left(\frac{M_{ym}}{I_{my}} + \frac{M_{zm}}{I_{mo}}\right)\sin \alpha_m x \\ \frac{\partial^2 v_s}{\partial x^2} &= \frac{1}{E}\left(\frac{M_{ym}}{I_{mo}} + \frac{M_{zm}}{I_{mz}}\right)\sin \alpha_m x \end{aligned} \qquad \text{(C.24)}$$

The displacements w and v due to biaxial bending can be obtained from the results of the integration of Eq. C.24 by satisfying the following boundary conditions:

at x = 0 and x = a

$$w = 0 \quad \text{and} \quad v = 0 \qquad \text{(C.25)}$$

The results are:

$$\begin{aligned} w_s &= \frac{1}{\alpha_m^2 E}\left(\frac{M_{ym}}{I_{my}} + \frac{M_{zm}}{I_{mo}}\right)\sin \alpha_m x \\ v_s &= \frac{-1}{\alpha_m^2 E}\left(\frac{M_{ym}}{I_{mo}} + \frac{M_{zm}}{I_{mz}}\right)\sin \alpha_m x \end{aligned} \qquad \text{(C.26)}$$

The girder is also subjected to a twisting moment M_x about an axis through the shear center S and parallel to the x-axis. The cross-section of the girder undergoes an angle of twist, β, about the shear center. Consequently, the displacements w and v of any point on the cross-section of the girder, except at the shear center, are affected by this rotation. The general expressions for the displacements w and v may be stated as follows:

$$w = \frac{1}{\alpha_m^2}\left[\frac{(y-y_s)M_T}{\alpha_m^2 EC + GJ} + \frac{M_{ym}}{EI_{my}} + \frac{M_{zm}}{EI_{mo}}\right] \sin \alpha_m x$$

$$v = \frac{-1}{\alpha_m^2}\left[\frac{(z-z_s)M_T}{\alpha_m^2 EC + GJ} + \frac{M_{ym}}{EI_{mo}} + \frac{M_{zm}}{EI_{mz}}\right] \sin \alpha_m x \qquad (C.27)$$

The displacement of the centroid in the x-direction is obtained from the first of Eqs. C.15.

$$u_o = \frac{-1}{\alpha_m EA} F_{xm} \cos \alpha_m x \qquad (C.28)$$

when u_o is the displacement at the centroid. The general displacement u is as follows:

$$u = u_o - y\frac{\partial v_s}{\partial x} - z\frac{\partial w_s}{\partial x}$$

$$u = \frac{1}{\alpha_m E}\left[\frac{-F_{xm}}{A} - z\left(\frac{M_{ym}}{I_{my}} + \frac{M_{zm}}{I_{mo}}\right) + y\left(\frac{M_{ym}}{I_{mo}} + \frac{M_{zm}}{I_{mz}}\right)\right]\cos \alpha_m x \qquad (C.29)$$

The rotation of the cross-section of the girder about x-axis is equal to the angle of twist β, thus

$$\theta = \frac{M_T}{\alpha_m^4 EC + \alpha_m^2 GJ} \sin \alpha_m x \qquad (C.30)$$

C.4 Formulas for Flexibility Constants of a Prismatic Girder

The final equations of the four components of displacements w, θ, v, and u at any points of the cross-section of the girder were obtained and were presented in Section C.3, Eqs. C.27, C.29, and C.30. Since the functions M_T, M_{ym}, M_{zm}, and F_{xm} are related to the unknown edge forces and the loading,

these displacements may also be expressed in terms of the edge forces and loading. Consequently, the displacements along the edges l and r of the girder can be determined by the substitution of the appropriate coordinates y and z for each edge.

It is more convenient to state the flexibility constants in the matrix form. The general expressions of the total results of each displacement due to the edge forces and loading may be written as follows:

At left edge, l

$$\begin{aligned} w_{LG} &= w_{LM} \sin \alpha_m x \\ \theta_{LG} &= \theta_{LM} \sin \alpha_m x \\ v_{LG} &= v_{LM} \sin \alpha_m x \\ u_{LG} &= u_{LM} \cos \alpha_m x \end{aligned} \qquad (C.31)$$

At right edge, r

$$\begin{aligned} w_{RG} &= w_{RM} \sin \alpha_m x \\ \theta_{RG} &= \theta_{RM} \sin \alpha_m x \\ v_{RG} &= v_{RM} \sin \alpha_m x \\ u_{RG} &= u_{RM} \cos \alpha_m x \end{aligned} \qquad (C.32)$$

Since all the forces along the edges l and r, joint forces, are unknowns and have to be determined, the flexibility constants should be divided into two matrices. The first matrix contains the flexibility constants due to the unknown edge forces. The second matrix contains the flexibility constants due to loading.

Let W_G (Eq. 3.38) be the displacement function matrix of the girder, and N_E be the edge force function matrix. Both matrices are column matrices and may be stated as follows:

$$W_G = \begin{Bmatrix} w_{LM} \\ \theta_{LM} \\ v_{LM} \\ u_{LM} \\ w_{RM} \\ \theta_{RM} \\ v_{RM} \\ u_{RM} \end{Bmatrix}_{8 \times 1} \qquad N_E = \begin{Bmatrix} R_{lm} \\ M_{lm} \\ N_{lm} \\ S_{lm} \\ R_{rm} \\ M_{rm} \\ N_{rm} \\ S_{rm} \end{Bmatrix}_{8 \times 1} \tag{C.33}$$

The forms of the flexibility matrices, F_G, L_G or C_G, are given as follows:

$$F_G = \left[\begin{array}{cccc|cccc} F_{11} & F_{12} & F_{13} & F_{14} & F_{15} & -F_{12} & -F_{13} & F_{18} \\ -F_{12} & F_{22} & F_{23} & 0 & F_{25} & -F_{22} & -F_{23} & 0 \\ F_{13} & -F_{23} & F_{33} & F_{34} & F_{35} & -F_{23} & -F_{33} & F_{38} \\ F_{14} & 0 & F_{34} & F_{44} & -F_{14} & 0 & -F_{34} & F_{48} \\ \hline -F_{15} & F_{25} & -F_{35} & F_{14} & F_{55} & -F_{25} & F_{35} & F_{18} \\ -F_{12} & F_{22} & F_{23} & 0 & F_{25} & -F_{22} & -F_{23} & 0 \\ F_{13} & -F_{23} & F_{33} & F_{34} & F_{35} & F_{23} & -F_{33} & F_{38} \\ -F_{18} & 0 & -F_{38} & F_{84} & F_{18} & 0 & F_{38} & F_{88} \end{array}\right]_{8 \times 8} \tag{C.34}$$

$$L_G = \begin{Bmatrix} L_1 \\ L_2 \\ L_3 \\ L_4 \\ L_5 \\ L_6 \\ L_7 \\ L_8 \end{Bmatrix}_{8 \times 1} \quad \text{and} \quad C_G = \begin{Bmatrix} C_1 \\ C_2 \\ C_3 \\ C_4 \\ C_5 \\ C_6 \\ C_7 \\ C_8 \end{Bmatrix}_{8 \times 1} \tag{C.35}$$

where

$$F_{11} = -\frac{(y_1-y_s)^2}{\alpha_m^4 EC + \alpha_m^2 GJ} - \frac{1}{\alpha_m^4 EI_{my}}$$

$$F_{12} = \frac{y_1-y_s}{\alpha_m^4 EC + \alpha_m^2 GJ}$$

$$F_{13} = -\frac{h_s(y_1-y_s)}{\alpha_m^4 EC + \alpha_m^2 GJ} + \frac{1}{\alpha_m^4 EI_{mo}}$$

$$F_{14} = -\frac{1}{\alpha_m^3}\left(\frac{h_o}{EI_{my}} + \frac{y_1}{EI_{mo}}\right)$$

$$F_{15} = \frac{(y_1-y_s)(y_r-y_s)}{\alpha_m^4 EC + \alpha_m^2 GJ} + \frac{1}{\alpha_m^4 EI_{my}}$$

$$F_{18} = \frac{1}{\alpha_m^3}\left(\frac{h_o}{EI_{my}} + \frac{y_r}{EI_{mo}}\right)$$

$$F_{22} = \frac{1}{\alpha_m^4 EC + \alpha_m^2 GJ}$$

$$F_{23} = -\frac{h_s}{\alpha_m^4 EC + \alpha_m^2 GJ}$$

$$F_{25} = \frac{y_r - y_s}{\alpha_m^4 EC + \alpha_m^2 GJ}$$

$$F_{33} = -\frac{h_s^2}{\alpha_m^4 EC + \alpha_m^2 GJ} - \frac{1}{\alpha_m^4 EI_{mz}}$$

$$F_{34} = \frac{1}{\alpha_m^3}\left(\frac{y_1}{EI_{mz}} + \frac{h_o}{EI_{mo}}\right)$$

$$F_{35} = \frac{h_s(y_r - y_s)}{\alpha_m^4 EC + \alpha_m^2 GJ} - \frac{1}{\alpha_m^4 EI_{mo}}$$

$$F_{38} = -\frac{1}{\alpha_m^3}\left(\frac{y_r}{EI_{mz}} + \frac{h_o}{EI_{mo}}\right)$$

$$F_{44} = -\frac{1}{\alpha_m^2}\left[y_1\left(\frac{y_1}{EI_{mz}} + \frac{h_o}{EI_{mo}}\right) + h_o\left(\frac{h_o}{EI_{my}} + \frac{y_1}{EI_{mo}}\right) + \frac{1}{EA}\right]$$

$$F_{48} = \frac{1}{\alpha_m^2}\left[y_1\left(\frac{y_r}{EI_{mz}} + \frac{h_o}{EI_{mo}}\right) + h_o\left(\frac{h_o}{EI_{my}} + \frac{y_r}{EI_{mo}}\right) + \frac{1}{EA}\right]$$

$$F_{55} = \frac{(y_r - y_s)^2}{\alpha_m^4 EC + \alpha_m^2 GJ} + \frac{1}{\alpha_m^4 EI_{my}}$$

$$F_{84} = -\frac{1}{\alpha_m^2}\left[y_r\left(\frac{y_1}{EI_{mz}} + \frac{h_o}{EI_{mo}} \right) + h_o\left(\frac{h_o}{EI_{my}} + \frac{y_1}{EI_{mo}} \right) + \frac{1}{EA} \right]$$

$$F_{88} = \frac{1}{\alpha_m^2}\left[y_r\left(\frac{y_r}{EI_{mz}} + \frac{h_o}{EI_{mo}} \right) + h_o\left(\frac{h_o}{EI_{my}} + \frac{y_r}{EI_{mo}} \right) + \frac{1}{EA} \right]$$

$$L_1 = \frac{(y_p-y_s)(y_1-y_s)}{\alpha_m^4 EC + \alpha_m^2 GJ} + \frac{1}{\alpha_m^4 EI_{my}}$$

$$L_2 = L_6 = \frac{(y_p-y_s)}{\alpha_m^4 EC + \alpha_m^2 GJ}$$

$$L_3 = L_7 = \frac{h_s(y_p-y_s)}{\alpha_m^4 EC + \alpha_m^2 GJ} - \frac{1}{\alpha_m^4 EI_{mo}}$$

$$L_4 = -F_{14}$$

$$L_5 = \frac{(y_p-y_s)(y_r-y_s)}{\alpha_m^4 EC + \alpha_m^2 GJ} + \frac{1}{\alpha_m^4 EI_{my}}$$

$$L_8 = F_{18}$$

and

$$C_1 = F_{12}$$

$$C_2 = C_6 = F_{22}$$

$$C_3 = C_7 = -F_{23}$$

$$C_4 = C_8 = 0$$

$$C_5 = F_{25}$$

The flexibility matrix F_G may be partitioned to form submatrices as follows:

$$F_G = \left[\begin{array}{c|c} F_{ll} & F_{lr} \\ \hline F_{rl} & F_{rr} \end{array}\right] \qquad (C.36)$$

The submatrix F_{ll} contains the flexibility constants of the left edge, l, due to forces acting on the left edge, and the submatrix F_{lr} contains the flexibility constants of the left edge due to forces acting on the right edge, r. The submatrix F_{rl} contains the flexibility constants of the right edge due to forces acting on the left edge, and submatrix F_{rr} contains the flexibility constants of the right edge due to forces acting on the right edge.

It is noted that, for the interior girders of the prestressed concrete I-section girder bridge, the following quantities vanish because of symmetry:

$$y_s = 0$$

$$I_{yz} = 0$$

$$y_l = -y_r = b_t/2$$

Thus,

$$I_{my} = I_y$$

$$I_{mz} = I_z$$

$$I_{mo} = \infty$$

Consequently, the following terms in the expressions for the flexibility constants also vanish:

$$\frac{1}{\alpha_m^4 EI_{mo}} = \frac{y_1}{EI_{mo}} = \frac{y_r}{EI_{mo}} = \frac{h_o}{EI_{mo}} = 0$$

and the flexibility constants can be simplified as follows:

$$F_{18} = -F_{14}$$

$$F_{25} = -F_{12}$$

$$F_{35} = F_{13}$$

$$F_{38} = F_{34}$$

$$F_{55} = -F_{11}$$

$$F_{84} = -F_{48}$$

$$F_{88} = -F_{44}$$

APPENDIX D

SUMMARY OF FORMULAS AND MATRIX FORMULATIONS FOR THE DETERMINATION OF THE EFFECTS OF DIAPHRAGMS

D.1 General Formulas for Deflections and Slopes of Diaphragms Due to Reaction Forces and Couples

Since the length of the individual pieces of the diaphragm is equal to the spacing of the gorders, b, the total span of the diaphragm, treated as a cross beam, is equal to $N_s b$ as shown in Fig. 4.4, where N_s is the number of spacings or slabs. For a bridge having N_G identical girders, the number of reaction forces is equal to N_G, the number of couples is also equal to N_G, and $N_s = N_G - 1$.

Let

g = girder number, 1, 2, . . . N_G

s = $g - 1$, slab number

I_d = moment of inertia of the diaphragm

E_d = modulus of elasticity of material in diaphragms

V_{ig} = reaction at the point of intersection of the diaphragm and the girder g, and

M_{ig} = couple of the point of intersection of the diaphragm and the girder g

Deflections and slopes along the span of the diaphragm, relative to line o-o shown in Fig. 4.3, produced by reaction forces and couples, may be obtained by using the Moment-Area or the Conjugate Beam method. The general formulas for computing the deflections and slopes produced by the reactions were obtained and stated as follows:

Deflections due to a load at a distance sb from the left support

$$w_y = V_{ig}(f_g^{II} y - \frac{1}{3} f_g^{III} y^3) \qquad (0 \le y \le sb)$$

$$w_y = V_{ig}[f_g^{II} y - f_g(y - \frac{2}{3} sb) - \frac{1}{3} f_g^{IV}(y - sb)^2\{2(N_s - s)b + (N_s b - y)\}]$$

$$(sb \le y \le N_s b) \qquad (D.1)$$

Slopes due to a load at a distance sb from the left support

$$\theta_y = V_{ig}(f_g^{II} - f_g^{III} y^2) \qquad (0 \le y \le sb)$$

$$\theta_y = V_{ig}[f_g^{II} - f_g - f_g^{IV}(y - sb)\{(N_s - s)b + (N_s b - y)\}]$$

$$(sb \le y \le N_s b) \qquad (D.2)$$

where

$$f_g = \frac{s^2(N_s - s)\, b^2}{2N_s\, E_d\, I_d}$$

$$f_g^I = \frac{s(N_s - s)^2\, b^2}{2N_s\, E_d\, I_d}$$

$$f_g^{II} = \frac{1}{3N_s}[f_g\{3(N_s - s) + s\} + 2f_g^I(N_s - s)]$$

$$f_g^{III} = \frac{N_s - s}{2N_s\, E_d\, I_d}$$

$$f_g^{IV} = \frac{s}{2N_s\, E_d\, I_d}$$

The general formulas for computing the deflections and slopes produced by the couples were also obtained and stated as follows:

Deflections due to a couple at a distance sb from the left support

$$w_y = M_{ig}(e_g^{II} y - \frac{1}{3} e_g^{III} y^3) \qquad (0 \le y \le sb)$$

$$w_y = M_{ig}\left[e_g^{II} y - e_g(y - \frac{2}{3} sb) + \frac{1}{3} e_g^{III}(y - sb)^2\{2(N_s - s)b + (N_s b - y)\}\right]$$

$$(sb \le y \le N_s b) \qquad (D.3)$$

Slopes due to a couple at a distance sb from the left support

$$\theta_y = M_{ig}(e_g^{II} - e_g^{III} y^2) \qquad (0 \le y \le sb)$$

$$\theta_y = M_{ig}\left[e_g^{II} - e_g + e_g^{III}(y - sb)\{N_s - s)b + (N_s b - y)\}\right]$$

$$(sb \le y \le N_s b) \qquad (D.4)$$

where

$$e_g = \frac{s^2 b}{2N_s E_d I_d}$$

$$e_g^I = \frac{(N_s - s)^2 b}{2N_s E_d I_d}$$

$$e_g^{II} = \frac{1}{3N_s}\left[e_g\{3(N_s - s) + s\} - 2 e_g^I(N_s - s)\right]$$

$$e_g^{III} = \frac{1}{2N_s E_d I_d b}$$

With the appropriate values of y, the deflections and slopes at the points of intersection of the diaphragm and the girders can be obtained from Eqs. D.1 and D.2, produced by the reactions, Eqs. D.3 and D.4, produced by the couples. The total deflections and slopes caused by all

reactions and couples are determined by summing up the results produced by each individual reaction and couple.

It is noted that the deflections, at the points y = 0 and y = $N_s b$ (exterior girders), due to each reaction and couple are zero. Thus, two equations formed by the deflection compatibility at these two points cannot be obtained. In order to solve the problem, two more equations are needed. Since the diaphragm is in equilibrium, the summations of the reaction forces and the moments about the right support (Fig. 4.4) are zero. Thus

$$V_{i,1} + V_{i,2} + \ldots + V_{i,g} + \ldots + V_{i,N_g} = 0$$

$$(N_s b)V_{i1} + (N_s - 1)bV_{i2} + \ldots + (b)V_{i,N_G - 1} + M_{i1} + M_{i2} + \ldots + M_{i,N_G} = 0 \qquad (D.5)$$

Equations D.5 may be written as follows:

$$\sum_{g=1}^{N_G} V_{ig} = 0$$

$$\sum_{g=1}^{N_G} (N_s - s)bV_{is} + \sum_{g=1}^{N_G} M_{ig} = 0 \qquad (D.6)$$

D.2 Deflections and Slopes of a Bridge with Diaphragm

Consider a bridge with diaphragms, with the cross-section shown in Fig. 4.2(a). The diaphragms are replaced by reaction forces and concentrated moments as shown in Fig. 4.2(b). The displacements at the points of intersection of one of the diaphragms and the girders, such as midspan diaphragm, caused by all unknown reactions and moments, and external load, are shown in Fig. 4.3. The displacements are:

$\Delta'_{i,1}, \Delta'_{i,2}, \Delta'_{i,g}, \ldots, \Delta'_{i,N_G}$ = deflections caused by all forces and loadings, measured from the original line $o' - o'$

$\theta'_{i,1}, \theta'_{i,2}, \ldots, \theta'_{i,g}, \ldots, \theta'_{i,N_G}$ = rotations caused by all forces and loadings, measured from the original line $o' - o'$

$\Delta_{i,1}, \Delta_{i,2}, \ldots, \Delta_{i,g}, \ldots, \Delta_{i,N_G}$ = deflections caused by all forces and loadings, measured from a line o - o passing through the points of intersection of the diaphragm and the deflected edge girders, and

$\theta_{i,1}, \theta_{i,2}, \ldots, \theta_{i,g}, \ldots, \theta_{i,N_G}$ = rotations caused by all forces and loadings, measured from a line o - o passing through the points of intersection of the diaphragm and the deflected edge girders

The first subscript refers to the location of diaphragm, i.e., $i = 1, 2, \ldots, N_D$. The second subscript refers to the points of intersection of the diaphragm and the girders, i.e., $g = 1, 2, \ldots, N_G$.

$\theta_{1,o}, \theta_{2,o}, \theta_{i,o}, \ldots, \theta_{N_D,o}$ = slopes of the line o - o at the locations of the diaphragms 1, 2, ..., N_D, respectively, measured from the original line $o' - o'$, and

N_D = number of diaphragms, i.e., $N_D = 1$ for one diaphragm at midspan, and so on.

The slope of the reference line o - o may be given by the equation

$$\theta_{i,o} = \frac{\Delta'_{i,N_G} - \Delta'_{i,1}}{N_s b} \tag{D.7}$$

The deflections $\Delta_{i,1}, \Delta_{i,2}, \ldots, \Delta_{i,N_G}$, the rotations $\theta_{i,1}, \theta_{i,2}, \ldots, \theta_{i,N_G}$, may be stated in terms of the deflections $\Delta'_{i,1}, \Delta'_{i,1}, \Delta'_{i,2}, \ldots, \Delta'_{i,N_G}$ and the rotations $\theta'_{i,1}, \theta'_{i,2}, \ldots, \theta'_{i,N_G}$, as follows:

$$\Delta_{i,g} = \Delta'_{i,g} - \Delta'_{i,1} + \frac{s}{N_s}(\Delta'_{i,1} - \Delta'_{i,N_G}) \tag{D.8}$$

and

$$\theta_{i,g} = \theta_{i,o} + \theta'_{i,g} \tag{D.9}$$

D.3 Flexibility Matrices of Bridge and Diaphragm

The unknown forces and displacements of the bridge at the point of intersection of diaphragms and girders, relative to the line o' - o', may be stated in column matrices N_U and W'_B, respectively. Thus

$$N_U = \begin{Bmatrix} N_1 \\ N_2 \\ \vdots \\ N_i \\ \vdots \\ N_{N_D} \end{Bmatrix}_{K_D,1} \qquad W'_B = \begin{Bmatrix} W'_{B,1} \\ W'_{B,2} \\ \vdots \\ W'_{B,i} \\ \vdots \\ W'_{B,N_D} \end{Bmatrix}_{K_D,1} \tag{D.10}$$

where K_D is the order of the matrix and equal to the number of displacements at the points of intersection of diaphragms and girders. Thus

$$K_D = 2N_D N_G \tag{D.11}$$

Each term in the column matrices, given by Eq. D.10, is a submatrix defining the forces and displacements at the points of intersection of the bridge girders with a diaphragm. Thus, the submatrices, N_i and $W'_{B,i}$, which represent the forces and the displacements of the intersection points between girders and the diaphragm i, may be stated as follows:

$$N_i = \left\{ \begin{matrix} V_{i,1} \\ V_{i,2} \\ \vdots \\ V_{i,N_G} \\ M_{i,1} \\ M_{i,2} \\ \vdots \\ M_{i,N_G} \end{matrix} \right\}_{K_G,1} \qquad W'_{B,i} = \left\{ \begin{matrix} \Delta'_{i,1} \\ \Delta'_{i,2} \\ \vdots \\ \Delta'_{i,N_G} \\ \theta'_{i,1} \\ \theta'_{i,2} \\ \vdots \\ \theta'_{i,N_G} \end{matrix} \right\}_{K_G,1} \tag{D.12}$$

where K_G is the order of the submatrix $W'_{B,i}$ and equal to the number of displacements at the points of intersection of the diaphragm i and the girders. Thus

$$K_G = 2N_G \tag{D.13}$$

The force-displacement relationship of the points of intersection of the diaphragm i and the girders can be written as follows:

$$W'_{B,i} = (B'_{i,1}\ B'_{i,2} \cdots B'_{i,i} \cdots B'_{i,N_D})N_U + P\ell'_i \qquad (D.14)$$

in which $B'_{i,1}$, $B'_{i,2}$, ..., $B'_{i,i}$, ..., B'_{i,N_D} are flexibility submatrices of the displacement submatrix $W'_{B,i}$ with respect to the unknown forces acting at the points of intersection of the girders and diaphragms 1, 2, ..., i, ..., N_D, respectively. Thus the submatrix $B'_{i,i}$ can be stated as follows:

$$B'_{i,i} = \left[\begin{array}{cccccc|cccc}
\delta^{i,i}_{1,1} & \delta^{i,i}_{1,2} & \cdots & \delta^{i,i}_{1,g} & \cdots & \delta^{i,i}_{1,N_G} & \delta^{i,i}_{1,N_G+1} & \delta^{i,i}_{1,N_G+2} & \cdots & \delta^{i,i}_{1,2N_G} \\
\delta^{i,i}_{2,1} & \delta^{i,i}_{2,2} & \cdots & \delta^{i,i}_{2,g} & \cdots & \delta^{i,i}_{2,N_G} & \delta^{i,i}_{2,N_G+1} & \delta^{i,i}_{2,N_G+2} & \cdots & \delta^{i,i}_{2,2N_G} \\
\vdots & \vdots & & \vdots & & \vdots & \vdots & \vdots & & \vdots \\
\delta^{i,i}_{N_G,1} & \delta^{i,i}_{N_G,2} & \cdots & \delta^{i,i}_{N_G,g} & \cdots & \delta^{i,i}_{N_G,N_G} & \delta^{i,i}_{N_G,N_G+1} & \delta^{i,i}_{N_G,N_G+2} & \cdots & \delta^{i,i}_{N_G,2N_G} \\
\hline
\omega^{i,i}_{1,1} & \omega^{i,i}_{1,2} & \cdots & \omega^{i,i}_{1,g} & \cdots & \omega^{i,i}_{1,N_G} & \omega^{i,i}_{1,N_G+1} & \omega^{i,i}_{1,N_G+2} & \cdots & \omega^{i,i}_{1,2N_G} \\
\omega^{i,i}_{2,1} & \omega^{i,i}_{2,2} & \cdots & \omega^{i,i}_{2,g} & \cdots & \omega^{i,i}_{2,N_G} & \omega^{i,i}_{2,N_G+1} & \omega^{i,i}_{2,N_G+2} & \cdots & \omega^{i,i}_{2,2N_G} \\
\vdots & \vdots & & \vdots & & \vdots & \vdots & \vdots & & \vdots \\
\omega^{i,i}_{N_G,1} & \omega^{i,i}_{N_G,2} & \cdots & \omega^{i,i}_{N_G,g} & \cdots & \omega^{i,i}_{N_G,N_G} & \omega^{i,i}_{N_G,N_G+1} & \omega^{i,i}_{N_G,N_G+2} & \cdots & \omega^{i,i}_{N_G,2N_G}
\end{array}\right]_{K_G,K_G} \qquad (D.15)$$

where δ and ω are the deflection and the rotation, respectively, due to a unit reaction or moment. The first superscript defines the deflections or rotations at the points corresponding to the particular location of diaphragm. The second superscript defines the unit reactions or moments at the points

corresponding to a particular location of diaphragm. The first subscript defines the deflections or rotations at the points corresponding to the girder. The second subscript defines the unit reaction or moment action at the points corresponding to the girder. The submatrix $B'_{i,i}$ may be partitioned into four submatrices as shown in Eq. D.15.

The submatrix ℓ'_i is the column flexibility matrix defining the displacements of the girders caused by the external concentrated load on the bridge. It may be written as follows:

$$\ell'_i = \begin{Bmatrix} \delta^i_{1,P} \\ \delta^i_{2,P} \\ \vdots \\ \delta^i_{N_G,P} \\ \omega^i_{1,P} \\ \omega^i_{2,P} \\ \vdots \\ \omega^i_{N_G,P} \end{Bmatrix}_{K_G,1} \qquad (D.16)$$

where $\delta^i_{1,P}$, $\delta^i_{2,P}$, ..., $\delta^i_{N_G,P}$ are the deflections of the girders at the points of intersection with the diaphragm i, cuased by a unit load on the bridge. The displacements which are represented by the column matrix W'_B may be stated as follows:

$$W_B' = F_B' N_U + PL_B' \tag{D.17}$$

where F_B' is the flexibility matrix of the bridge, relative to line $o' - o'$, and can be presented as follows:

$$F_B' = \begin{bmatrix} B_{1,1}' & B_{1,2}' & \cdots & B_{1,i}' & \cdots & B_{1,N_D}' \\ B_{2,1}' & B_{2,2}' & \cdots & B_{2,i}' & \cdots & B_{2,N_D}' \\ \vdots & \vdots & & \vdots & & \vdots \\ B_{i,1}' & B_{i,2}' & & B_{i,i}' & & B_{i,N_D}' \\ \vdots & \vdots & & \vdots & & \vdots \\ B_{N_D,1}' & B_{N_D,2}' & & B_{N_D,i}' & & B_{N_D,N_D}' \end{bmatrix}_{K_D \times K_D} \tag{D.18}$$

and L_B' is the flexibility matrix of the bridge subjected to the external load P, and refer to line $o' - o'$. Thus

$$L_B' = \begin{Bmatrix} \ell_1' \\ \ell_2' \\ \vdots \\ \ell_i' \\ \vdots \\ \ell_{N_D}' \end{Bmatrix}_{K_D,1} \tag{D.19}$$

The displacements of diaphragms, the displacements of the girders of the bridge, at their intersection points which refer to the lines o - o, may be stated in column matrices W_D and W_B, respectively. Thus

$$W_D = \begin{Bmatrix} W_{D,1} \\ W_{D,2} \\ \vdots \\ W_{D,i} \\ \vdots \\ W_{D,N_D} \end{Bmatrix}_{K_D,1} \qquad W_B = \begin{Bmatrix} W_{B,1} \\ W_{B,2} \\ \vdots \\ W_{B,i} \\ \vdots \\ W_{D,N_D} \end{Bmatrix}_{K_D,1} \tag{D.20}$$

where each term in the column matrices in Eqs. D.20 is a submatrix defining the displacements of a certain diaphragm and the girders of the bridge at their intersection points. However, it has been mentioned in Sections D.1 and D.2 that the deflections at the points of intersection of the diaphragms and the deflected exterior girders are zero. Thus, the submatrices $W_{D,i}$ and $W_{B,i}$, which represent the displacements of the diaphragm i and the girders of the bridge, respectively, at the points of their intersection, may be written as follows:

$$W_{D,i} = \begin{Bmatrix} 0 \\ \Delta^D_{i,2} \\ \Delta^D_{i,3} \\ \cdot \\ \cdot \\ \cdot \\ \Delta^D_{i,N_G-1} \\ 0 \\ \theta^D_{i,1} \\ \theta^D_{i,2} \\ \cdot \\ \cdot \\ \cdot \\ \theta^D_{i,N_G} \end{Bmatrix}_{K_G,1} \qquad W_{B,i} = \begin{Bmatrix} 0 \\ \Delta^B_{i,2} \\ \Delta^B_{i,3} \\ \cdot \\ \cdot \\ \cdot \\ \Delta^B_{i,N_G-1} \\ 0 \\ \theta^B_{i,1} \\ \theta^B_{i,2} \\ \cdot \\ \cdot \\ \cdot \\ \theta^B_{i,N_G} \end{Bmatrix}_{K_G,1} \tag{D.21}$$

The force-displacement relationships of the diaphragms and the bridge may be stated as follows:

$$W_D = F_D N_U$$

$$W_B = F_B N_U + PL_B \tag{D.22}$$

in which F_D and F_B are flexibility matrices of all diaphragms and the bridge, respectively. The L_B is the flexibility matrix for the bridge without diaphragms, subjected to external unit loads, relative to line o - o. These matrices may be written as follows, assuming all diaphragms have the same properties:

$$F_D = \begin{bmatrix} B^D & & & & \\ & B^D & & & \\ & & B^D & & \\ & & & \ddots & \\ & & & & B^D \end{bmatrix}_{K_D, K_D} \tag{D.23}$$

and

$$F_B = \begin{bmatrix} B_{1,1} & B_{1,2} & \cdots & B_{1,i} & \cdots & B_{1,N_D} \\ B_{2,1} & B_{2,2} & \cdots & B_{2,i} & \cdots & B_{2,N_D} \\ \vdots & \vdots & & \vdots & & \vdots \\ B_{i,1} & B_{i,2} & \cdots & B_{i,i} & \cdots & B_{i,N_D} \\ \vdots & \vdots & & \vdots & & \vdots \\ B_{N_D,1} & B_{N_D,2} & \cdots & B_{N_D,i} & \cdots & B_{N_D,N_D} \end{bmatrix}_{K_D, K_D} \tag{D.24}$$

$$L_B = \left\{ \begin{matrix} \ell_1 \\ \ell_2 \\ \vdots \\ \ell_i \\ \vdots \\ \ell_{N_D} \end{matrix} \right\}_{K_{D,1}} \tag{D.25}$$

The submatrix B^D is the flexibility matrix for each individual diaphragm and may be written as follows:

$$
{}_{B}{}^{D} = \left[\begin{array}{ccccc|ccccc}
1 & 1 & 1 & 1 & 1 & 0 & 0 & 0 & 0 \\
0 & f_{2,2} & \cdots f_{2,g} & \cdots f_{2N_G-1} & 0 & f_{2,N_G+1} & f_{2,N_G+2} & \cdots f_{2,N_G+g} & \cdots f_{2,2N_G} \\
\vdots & \vdots & \vdots & \vdots & \vdots & \vdots & \vdots & \vdots & \vdots \\
0 & f_{g,2} & \cdots f_{g,g} & \cdots f_{g,N_G-1} & 0 & f_{g,N_G+1} & f_{g,N_G+2} & \cdots f_{g,N_G+g} & \cdots f_{g,2N_G} \\
\vdots & \vdots & \vdots & \vdots & \vdots & \vdots & \vdots & \vdots & \vdots \\
0 & f_{N_G-1,2} & \cdots f_{N_G-1,g} & \cdots f_{N_G-1,N_G-1} & 0 & f_{N_G-1,N_G+1} & f_{N_G-1,N_G+2} & \cdots f_{N_G-1,N_G+g} & \cdots f_{N_G-1,2N_G} \\
N_s b & (N_s-1)b & \cdots (N_s-s)b & \cdots b & 0 & 1 & 1 & \cdots 1 & \cdots 1 \\
\hline
0 & f_{N_G+1,2} & \cdots f_{N_G+1,g} & \cdots f_{N_G+1,N_G-1} & 0 & f_{N_G+1,N_G+1} & f_{N_G+1,N_G+2} & \cdots f_{N_G+1,N_G+g} & \cdots f_{N_G+1,2N_G} \\
0 & f_{N_G+2,2} & \cdots f_{N_G+2,g} & \cdots f_{N_G+2,N_G-1} & 0 & f_{N_G+2,N_G+1} & f_{N_G+2,N_G+2} & \cdots f_{N_G+2,N_G+g} & \cdots f_{N_G+2,2N_G} \\
\vdots & \vdots & \vdots & \vdots & \vdots & \vdots & \vdots & \vdots & \vdots \\
0 & f_{2N_G,2} & f_{2N_G,g} & \cdots f_{2N_G,N_G-1} & 0 & f_{2N_G,N_G+1} & f_{2N_G,N_G+2} & \cdots f_{2N_G,N_G+g} & \cdots f_{2N_G,2N_G}
\end{array}\right]_{K_G,K_G}
$$

(D.26)

The elements in the submatrix B^D are deflections and rotations due to unit reactions or moments. The deflections are in rows 2 to $N_G - 1$ and can be obtained from Eqs. D.1 and D.3. The rotations are in rows $N_G + 1$ to $2N_G$ and can be obtained from Eqs. D.2 and D.4. The elements in columns 1 to N_G are deflections and rotations due to unit reactions and can be found from Eqs. D.1 and D.2, the elements in columns $N_G + 1$ to $2N_G$ are deflections and rotations due to unit moments and can be found from Eqs. D.3 and D.4. Those elements in rows 1 and N_G are the coefficients of the equilibrium Eqs. D.5.

The flexibility matrix of the bridge F_B with respect to line o - o is related to the flexibility matrix of the bridge F_B' which relates to line $o' - o'$. Each submatrix in the matrix F_B can be obtained from the corresponding submatrix in the matrix F_B'. For example, by using Eqs. D.7, D.8, and D.9, the submatrix $B_{i,i}$ can be found from the submatrix $B_{i,i}'$ and is presented as follows:

$$
B_{i,i} = \left[\begin{array}{cccc|cccc}
0 & 0 & \cdots 0 & \cdots 0 & 0 & 0 & \cdots 0 & \cdots 0 \\
b^{i,i}_{2,1} & b^{i,i}_{2,2} & \cdots b^{i,i}_{2,g} & \cdots b^{i,i}_{2,N_G} & b^{i,i}_{2,N_G+1} & b^{i,i}_{2,N_G+2} & \cdots b^{i,i}_{2,N_G+g} & \cdots b^{i,i}_{2,2N_G} \\
\vdots & \vdots & \vdots & \vdots & \vdots & \vdots & \vdots & \vdots \\
b^{i,i}_{N_G-1,1} & b^{i,i}_{N_G-1,2} & b^{i,i}_{N_G-1,g} & b^{i,i}_{N_G-1,N_G} & b^{i,i}_{N_G-1,N_G+1} & & b^{i,i}_{N_G-1,N_G+g} & b^{i,i}_{N_G-1,2N_G} \\
0 & 0 & 0 & 0 & 0 & & 0 & 0 \\
\hline
b^{i,i}_{N_G+1,1} & b^{i,i}_{N_G+1,2} & & \cdots b^{i,i}_{N_G+1,N_G} & b^{i,i}_{N_G+1,N_G+1} & & & \cdots b^{i,i}_{N_G+1,2N_G} \\
\vdots & \vdots & & \vdots & \vdots & & & \vdots \\
b^{i,i}_{2N_G,1} & b^{i,i}_{2N_G,2} & & \cdots b^{i,i}_{2N_G,N_G} & b^{i,i}_{2N_G,N_G+1} & & & \cdots b^{i,i}_{2N_G,2N_G}
\end{array}\right]_{K_G,K_G}
$$

(D.27)

The elements in rows 1 to N_G of Eq. D.27 are obtained by applying Eq. D.8 to the elements in rows 1 to N_G of the submatrix $B'_{i,i}$. The elements in rows $N_G + 1$ to $2N_G$ of Eq. D.27 are obtained by applying Eq. D.7 to the elements in rows 1 and N_G, and Eq. D.9.

In the same manner the column matrix L_B due to the external load can be obtained from the column matrix L'_B. A typical submatrix ℓ_i may be stated as follows:

$$\ell_i = \begin{Bmatrix} 0 \\ b^i_{2,P} \\ b^i_{3,P} \\ \vdots \\ b^i_{N_G-1,P} \\ 0 \\ b^i_{N_G+1,P} \\ \vdots \\ b_{2N_G,P} \end{Bmatrix}_{K_G,1} \qquad \text{(D.28)}$$

For the particular cases of the arrangements of diaphragms as shown in Fig. 4.5, the matrix F_B in Eq. D.24 may be simplified as follows:

Case 1: Bridge with one diaphragm of midspan

$$F_B = B_{11} \qquad \text{(D.29)}$$

Case 2: Bridge with two diaphragms at symmetrical positions with respect to midspan

$$F_B = \begin{bmatrix} B_{11} & B_{12} \\ B_{12} & B_{11} \end{bmatrix} \tag{D.30}$$

Case 3: Bridge with three diaphragms, one at midspan and two at symmetrical positions with respect to midspan

$$F_B = \begin{bmatrix} B_{11} & B_{12} & B_{12} \\ B_{12} & B_{22} & B_{23} \\ B_{12} & B_{23} & B_{22} \end{bmatrix} \tag{D.31}$$